

TECHNISCHE UNIVERSITÄT MÜNCHEN
Lehrstuhl für Proteomik und Bioanalytik
MAX-PLANCK-INSTITUT FÜR BIOCHEMIE
Abteilung Molekularbiologie

Targets and Off-Targets of Kinase Inhibitors in Diabetes

Zoltán Órfi

Vollständiger Abdruck der von der Fakultät Wissenschaftszentrum Weihenstephan für Ernährung, Landnutzung und Umwelt der Technischen Universität München zur Erlangung des akademischen Grades eines

Doktors der Naturwissenschaften

genehmigten Dissertation.

Vorsitzender: Univ.-Prof. Dr. K. Schneitz

Prüfer der Dissertation: 1. Univ.-Prof. Dr. B. Küster,
2. Hon.-Prof. Dr. Dr. h.c. A. Ullrich
(Eberhard-Karls-Universität Tübingen)

Die Dissertation wurde am 17.12.2014 bei der Technischen Universität München eingereicht und durch die Fakultät Wissenschaftszentrum Weihenstephan für Ernährung, Landnutzung und Umwelt der Technischen Universität München am 02.03.2015 angenommen.

ABSTRACT

ABBREVIATIONS

1	INTRODUCTION	1
1.1	Diabetes	
1.1.1	Type I diabetes	
1.1.2	Type II diabetes	
1.2	General mechanisms of insulin secretion in beta cells	2
1.3	Medicaments used in the therapy of diabetes	6
1.3.1	Insulin secretagogues	
1.3.1.1	<i>Sulfonylureas (SU)</i>	
1.3.1.2	<i>Meglitinides</i>	
1.3.2	Insulin sensitizers	7
1.3.2.1	<i>Biguanides</i>	
1.3.2.2	<i>Thiazolidinediones (TZD)</i>	
1.3.2.3	<i>Dual PPAR agonists</i>	8
1.3.3	Incretin-based therapies	9
1.3.4	Alpha-glucosidase inhibitors	
1.3.5	DPP-4 inhibitors	10
1.3.6	SGLT2 inhibitors	
1.4	Preclinical developments for the treatment of diabetes	11
1.4.1	G protein-coupled receptors (GPCRs)	
1.4.2	FGF21 and its analog LY2405319	
1.4.3	Glucokinase activators (GKA)	
1.4.4	11beta-hydroxysteroid dehydrogenase type 1 (11 β -HSD-1) inhibitors	12
1.4.5	Glycogen phosphorylase inhibitors (GPIs)	
1.5	Roles of sunitinib and other kinase inhibitors in diabetes	13
2	AIMS AND SCOPE	15
3	MATERIALS AND METHODS	16
3.1	Cell lines	
3.1.1	Differentiation of 3T3-L1 cells	
3.2	Insulin ELISA	17
3.3	CellTiter-Glo assay	
3.4	IC₅₀ and EC₅₀ determination	
3.5	MTT assay	
3.6	Protein concentration determination	18
3.7	Calcium influx measurements	
3.7.1	Calcium influx measurement by FACS	
3.7.2	Calcium influx measurement on Flexstation	19
3.7.3	Calcium influx measurement by spinning disc confocal microscopy	

3.8	Patch clamp experiments	
3.9	2-NBDG (glucose analog) uptake	20
3.10	Intracellular cAMP determination	
3.11	Gene silencing	21
3.11.1	siRNA resuspension protocol	
3.11.2	Accell siRNA transfection	
3.11.3	Transfection with DharmaFECT ON-TARGETplus	
3.12	Preparation of affinity matrices for MS experiment	22
3.13	Binding and competition pre-experiments	24
3.14	SILAC labeling of RIN-5AH cells for mass spectrometry (MS) experiments	
3.15	Cellular Target Profiling by MS	25
3.16	Kinase affinity experiments	26
3.17	Real-time QPCR (RT-PCR)	27
3.18	Western Blot	28
3.19	Excel macro for the analysis of more than 2 sets of protein targets	29
3.20	In silico prediction of ADME properties of the compounds	
3.21	Buffers and solutions	
4	RESULTS	31
4.1	A phenotype-based drug and target discovery project	
4.2	Results of the primary screen of insulin secretion in RIN-5AH cells	32
4.2.1	Efficient compounds	
4.2.2	In vitro toxicity studies	33
4.2.3	Clustering the hits into different core structures	34
4.2.3.1	<i>Highlighted Core structures and structure-activity relationships (SAR)</i>	36
4.2.4	Insulinotropic action of some marketed kinase inhibitors in RIN-5AH cells	39
4.3	Glucose sensitivity of different beta cell lines	40
4.4	Characterization of the most effective compounds	41
4.5	Selected best compounds were more selective than sunitinib	45
4.6	MS affinity chromatography using RIN-5AH cell lysate	48
4.6.1	Pre-experiments for MS- based target deconvolution	
4.6.1.1	<i>VCC350485:02 (Styryl-quinazoline)</i>	49
4.6.1.2	<i>Sunitinib (Oxindoles)</i>	
4.6.1.3	<i>VCC512891:01 (Amino pyrimidines I.)</i>	50
4.6.1.4	<i>VCC124075:02 (Amino pyrimidines II.)</i>	51
4.6.2	Target deconvolution results	52
4.6.3	Selection of common kinase hits	55
4.7	Designing a pool of targets from affinity screen results and MS target deconvolution	56

4.8	Validation of potentially negatively regulating kinases of insulin secretion by siRNA	59
4.9	Other potential non-kinase hits	61
4.9.1	Effect of PDE4 and PDE5 inhibitors in RIN-5AH and TC6 cells	63
4.10	Insulin secretion and GDIS in different beta cells	65
4.11	Elevated cAMP levels can be a possible mechanism of action for some compounds	67
4.12	Increased Ca²⁺ influx is another mechanism of action for some compounds	68
4.12.1	Validation experiments with patch clamp for VCC981125	73
4.13	Combination treatments with ion channel modulators suggest different mechanism of actions for certain compounds	76
4.14	Compounds can increase glucose analog (2-NBDG) uptake in different cells	78
4.15	Pathway analysis in RIN-5AH beta cells	81
5	DISCUSSION	86
	SUMMARY	95
	ZUSAMMENFASSUNG	96
	ACKNOWLEDGEMENTS	97
	REFERENCES	98
	APPENDIX	119
	Toxic compounds	
	Supplementary info for knockdown experiments	121
	Efficient quinoline derivatives in BRIN-BD11 cells	122
	Thieno-pyrimidines supplementary data	123
	Altered K_{ATP} expression levels in different beta cell lines and the correlation with GBA sensitivity	124
	Western blot supplementary info	125
	ADME QikProp (Schrödinger)	126
	Kinase affinity assay results	129
	Cellular Target Profiling results (MS-affinity chromatography)	142
	Excel macro for the analysis of overlapping targets	147

ABSTRACT

Various tyrosine kinase inhibitors (TKIs) developed for the treatment of cancer have been reported to exert a protective effect in diabetic patients, which manifested in improved glycemic control and insulin sensitivity, favorable regulation of lipid metabolism and increased insulin secretion. In our studies we focused on the insulinotropic property of sunitinib and inspired by the TKI associated clinical investigations our aim was to discover kinase targets and better compound analogues that on one hand can help us to understand the mechanism how these TKIs induce insulin secretion, furthermore could open a new field for the development of anti-diabetic therapy. We assembled a library of 558 compounds for a phenotypic screen in order to look for candidates having insulinotropic effect. The members of this compound library were rationally picked and built upon similarity with the target profile of sunitinib. By insulin ELISA assay we could identify 55 compounds that effectively stimulated insulin secretion in RIN-5AH beta cells. These compounds could be clustered into different core structure families and for some of them we were able to set up qualitative structure activity relationships (SAR). Ten active compounds with 8 different core structures were profiled for their kinase affinities and screened on a kinase panel of 392 kinases. Four of these compounds were validated by affinity chromatography followed by mass spectrometry, wherein RIN-5AH beta cell lysates and special linker derivatives of the active compounds coupled to affinity matrices were employed. We hypothesized that there are common targets for these compounds which upon inhibition can induce insulin secretion. We identified three kinases by siRNA that induced insulin release in RIN-5AH and INS-1E beta cell lines. The compounds were also investigated for other potential mechanisms, including cAMP or Ca²⁺ level upregulation, membrane potential changes and related pathways. We have found and characterized interesting candidate compounds, furthermore based on the available SAR and assay results we could conclude that kinase inhibitor molecules can be optimized for insulinotropic effect. These observations also support the fact that we should not ignore the blood glucose lowering effect of some small molecule kinase inhibitors used in cancer therapy.

ABBREVIATIONS

2-NBDG	2-(N-(7-Nitrobenz-2-oxa-1,3-diazol-4-yl)amino)-2-deoxyglucose
ACS	Acyl Coenzyme Synthase
ADME	Absorption Distribution Metabolism Excretion
AMPK	5'-AMP - Activated Protein Kinase
ATP	Adenosine Triphosphate
AUC	Area Under The Curve
BCA	Bicinchoninic Acid
BOC	Tert-Butyloxycarbonyl
CAMK2	Calcium/Calmodulin-Dependent Protein Kinase II
cAMP	Cyclic Adenosine Monophosphate
CC	Current Clamp
CPD	Compound
CPT-1	Carnitine-Palmitoyl Transferase
CREB	Camp Responsive Element Binding Protein
CSNK2A1	Casein Kinase 2, Alpha 1 Polypeptide Pseudogene
DAO	Diazoxide
DNTP	Deoxynucleotide Triphosphates
DPP-4	Dipeptidyl Peptidase-4
DTT	Dithiothreitol
EC ₅₀	Median Effective Concentration
ECL	Enhanced Chemiluminescence
EFD	Efonidipine
ELISA	Enzyme-Linked Immunosorbent Assay
ERK	Extracellular Signal-Regulated Kinase, Mitogen-Activated Protein Kinase
FACS	Fluorescence Activated Cell Sorting
FADH ₂	Flavin Adenine Dinucleotide
FFA	Free Fatty Acid
FLT3	Fms-Related Tyrosine Kinase 3
G6PASE	Glucose 6-phosphatase
GBA	Glibenclamide
GDH	Glutamate Dehydrogenase
GDIS	Glucose Dependent Insulin Secretion
GIP	Glucose-Dependent Insulinotropic Polypeptide
GLP-1	Glucagon-Like Peptide-1
GLUT	Glucose Transporter
GPCR	G Protein-Coupled Receptor
GSIS	Glucose Stimulated Insulin Secretion
HBSS--	Hank'S Balanced Salt Solution Without Ca ²⁺ And Mg ²⁺
HBSS++	Hank'S Balanced Salt Solution With Ca ²⁺ And Mg ²⁺
HFD	High Fat Diet
HRP	Horseradish Peroxidase
IBMX	3-Isobutyl-1-methylxanthine

IC ₅₀	Median Inhibition Concentration
IP3R	IP3 receptor
JNK2	Mapk9 - Mitogen-Activated Protein Kinase 9, Jun Kinase
KATP	Potassium Atp Channel
KRBH	Krebs Ringer Buffer With Hepes
MARK2	Map/Microtubule Affinity-Regulating Kinase 2
MAST1	Microtubule Associated Serine/Threonine Kinase 1
MCF	Metabolic Coupling Factor
MEK	Mapk Kinase
MOA	Mode Of Action / Mechanism Of Action
MS	Mass Spectrometry
MTOR	Mechanistic Target Of Rapamycin
MTT	Thiazolyl Blue Tetrazolium Bromide
NADH	Nicotinamide Adenine Dinucleotide
NaOV	Sodium Orthovanadate
NDP	Nifedipine
NHS	N-Hydroxysuccinimide
ON	Overnight
PDE	Phosphodiesterase
PEPCK	Phosphoenolpyruvate Carboxykinase
PIN	Pinacidil
PKA	Protein Kinase A
PKC	Protein Kinase C
PMSF	Phenylmethylsulfonyl Fluoride
PPAR	Peroxisome Proliferator-Activated Receptor
ROS	Reactive Oxygen Species
RT	Room Temperature
SAR	Structure Activity Relationship
SGLT-2	Sodium-Glucose Cotransporter 2
SLK	Ste20-Like Kinase
STK16	Serine/Threonine Kinase 16
T1D/T1DM	Diabetes Type I
T2D/T2DM	Diabetes Type II
TBST	Tris-Buffered Saline With Tween 20
TG	Thapsigargin
TI	Therapeutic Index
TKI	Tyrosine Kinase Inhibitor
TUM	Technical University München
TZD	Thiazolidinedione
VC	Voltage Clamp
VDCC	Voltage Dependent Calcium Channel
VER	Verapamil

1 INTRODUCTION

1.1 Diabetes

Diabetes is a chronic disease and it shows an increasing incidence in the world. There are 347 million people worldwide diagnosed with diabetes¹ and globally 6% of deaths are caused by diabetes². The causes that result in diabetes are that either the beta cells can't produce enough insulin or the body can't use the hormone efficiently. Untreated diabetes can lead to serious side effects and consequences including increased risk of heart failure and stroke, retinopathy, nephropathy and neuropathy. Diabetes onset can be prevented or delayed with regular physical activity, healthy diet and maintaining normal body weight³.

1.1.1 Type I diabetes

Type I diabetes (insulin-dependent diabetes or juvenile diabetes, T1D) is an autoimmune disease, where beta cells are destroyed and insulin cannot be produced anymore. Typical symptoms of type I diabetes are: excessive thirst and hunger, unusually high levels of urination, extreme fatigue, body weight loss, and blurry vision. The first sign of development of autoimmunity is the presence of any of these antibodies associated with the disease: IA-2Ab, IAA, GAD65Ab, and ZnT8Ab. Later on the decrease of these antibodies may indicate the progression of T1D. The treatment of T1D is currently possible by insulin only.

1.1.2 Type II diabetes

Type II diabetes (non-insulin-dependent or adult-onset diabetes, T2D) occurs in 90% of the people diagnosed with diabetes. T2D is the result of ineffectively utilized insulin in the body. Symptoms are similar to T1D but the diagnosis can be more difficult because of the slow progression of the disease. Medically uncontrolled diabetes can lead to severe complications including neuropathy, ketoacidosis, nephropathy, high blood pressure, stroke and complication on skin and eyes. Therefore it is necessary to recognize the symptoms as early as possible. Oral glucose tolerance test (OGTT) is one of the possibilities to diagnose pre-diabetes or diabetes. The pre-diabetic state may indicate a risk for the development of T2D, which later on leads to beta cell dysfunction. Factors that can contribute to the progressive deterioration of the beta cells and insulin resistance include genetic⁴⁻⁶ and acquired (glucotoxicity, lipotoxicity, alterations in GLP-1 and GIP, small membrane permeant islet amyloid polypeptide formation,

pro-inflammatory cytokines) causes⁷⁻¹². Reactive oxygen species (ROS) are produced when cells are chronically exposed to glucose or fat, and their excessive accumulation can damage beta cells. This phenomenon often occurs in diabetes. Nevertheless ROS are necessary to maintain physiological function of beta cells as well. Not surprisingly it was also observed that the levels of antioxidant enzymes in pancreatic islets were lower compared to other tissues¹³. It is also proposed that not only the excessive ROS generation, but the insufficient oxidative redox potential and therefore decreased S-S bond formation can contribute to the development of T2D¹⁴. It is interesting to notice that in contrary to the inhibitory effect of physiological ROS scavenger proteins, the small molecule polyphenolic flavonoid antioxidants can activate Ca^{2+} channels and induce insulin release. These flavonoids may also improve beta cell health by regulating the expression of important survival genes in beta cells^{15,16}. Although there are a big variety of medicines available for the treatment of T2D, notwithstanding every therapy has its side effects and contraindications or inconvenience. Antidiabetic medication needs to be customized for every patient and combinations of drugs are sometimes necessary to sustain normoglycemia. Currently insulin secretagogues, insulin sensitizers and some other medications (alpha glucosidase inhibitors, incretin-based therapy, DPP-4 inhibitors and SGLT2 inhibitors) including insulin products are available for the treatment of type II diabetes.

1.2 General mechanisms of insulin secretion in beta cells

Beta cells are important fuel sensors of the body. Under normal physiological circumstances insulin secretion is regulated by the metabolism of carbohydrates, fatty acids and amino acids (*Figure 1.4.1*). During the process different metabolic coupling factors (MCFs) are produced (e.g. ATP, cAMP, NADH, Acyl-CoA, glutamate) that take part in the regulation of insulin secretion. The ATP is one of the most important that can directly modulate the activity of ATP dependent potassium channels (K_{ATP} channels) in beta cells. Pancreatic K_{ATP} channels have crucial role in the regulation of insulin secretion and membrane potential. They consist of a hetero-octamer structure, where four Kir6.2 pore forming units and four SUR1 regulatory subunits connect each other¹⁷. At elevated ATP concentration K_{ATP} channels are inhibited by binding ATPs at the Kir6.2 subunits and as a result it induces a shift in the membrane potential ($\Delta\Psi$)¹⁸⁻²⁰. This gives rise to the opening of voltage dependent calcium channels (VDCC) which leads to an increased intracellular calcium level, that stimulates exocytosis of insulin vesicles²¹. Besides inactivation of K_{ATP} channels, other factors and ion channels e.g. TRP channels might be involved to reach the necessary rate of membrane potential shift required for exocytosis^{22,23}. It is important to mention that glucose can also increase insulin secretion independently from

K_{ATP} channels. This is often referred as metabolic amplifying pathway and could be linked to the second phase of insulin secretion²⁴⁻²⁶. ATP is also needed for the generation of cAMP that is catalyzed by the adenylyl cyclase (AC) enzyme. AC can be stimulated by the activation of some G protein (G_s) coupled receptors (GPCRs) that are found in beta cells (e.g. GLP-1 receptor, beta adrenergic receptor, GPR119) or inhibited by G_i coupled GPCRs (e.g. ADRA2A, GALR1, SSTR)²⁷⁻²⁹, additionally other regulators of AC (e.g. glucose, CAMK2) also exist³⁰⁻³². The negative regulation and degradation of cAMP is mediated by the phosphodiesterase (PDE) enzymes. The increased intracellular cAMP level potentiates exocytosis through its effector molecules, PKA and Epac2. PKA can phosphorylate various substrates related to exocytosis (e.g. phosphorylation of SNAP-25, Snapin, K_{ATP} , and VDCC). Epac can initiate the Epac-Rap-1-Raf-MEK-ERK pathway, furthermore it probably activates small GTPases such as Cdc42 and Rac which regulate cytoskeleton realignment therefore promote vesicle transport. Similarly to PKA it is also connected to intracellular calcium mobilization through IP3R. Sulphonylureas may also act in an Epac sensitive way; however the direct mechanism is not clarified yet³³⁻³⁷. Free fatty acids (FFA) enter the cells by diffusion and they are converted to long chain acyl-CoA in the cytosol. Accumulation of long chain acyl-CoA in the cytoplasm can acutely stimulate Ca^{2+} influx and insulin exocytosis, furthermore may assist secretory vesicle fusion with the plasma membrane³⁸⁻⁴⁰. During beta-oxidation (fasting state) it is degraded to acetyl-CoA, NADH and FADH2 in the mitochondria. The generated NADH and FADH2 will be used in the electron transport chain (oxidative phosphorylation) to generate ATPs, while the acetyl CoA can join the TCA cycle, where additional NADH is generated. Glycolysis and lipid signaling can intercross (FA-CoA and G3-P) and send further exocytotic related signals (FFA, Munc13-1 activation, PKC, PKD)⁴¹. It is worth to mention that a loss function of HADH (Hydroxyacyl-CoA, the enzyme in beta oxidation that catalyzes the transformation of hydroxyacyl-CoA to ketoacyl-CoA) is associated with hyperinsulinemia⁴²⁻⁴⁵. FFAs can also stimulate GPR40, hence induce IP3/DAG/PKC pathway which also leads to the release of insulin^{46,47}. In the case of amino acid induced secretion, glutamine is transported into the cell and converted to glutamate, then to α -ketoglutarate (by glutamate dehydrogenase, GDH). Afterwards α -ketoglutarate enters TCA cycle and participates in the generation of NADH. The importance of this process was confirmed by inspecting the gain of function mutations of GDH in animal models and in patients harboring the mutant form, which caused hyperinsulinemic hypoglycemic syndrome, triggered by protein meals⁴⁸⁻⁵⁰. Leucine induced insulin secretion can happen due to activation of GDH and the production of its metabolite, α -ketoisocaproate which enters TCA cycle as well. Reportedly, Leu induced hypoglycemia was only observed in patients

harboring HADH mutations, but not in the control group⁵¹⁻⁵³. Arginine as it has a cationic character at physiological pH, after entering the cell, it induces insulin secretion directly through membrane depolarization. It is also often used as a control substance in clinics to test beta cell function and capacity^{54,55}. Alanine and glycine induced insulin secretion can be attributed to the co-transport with Na⁺ and the consequent changes in membrane potential similarly to arginine⁵⁶⁻⁵⁸.

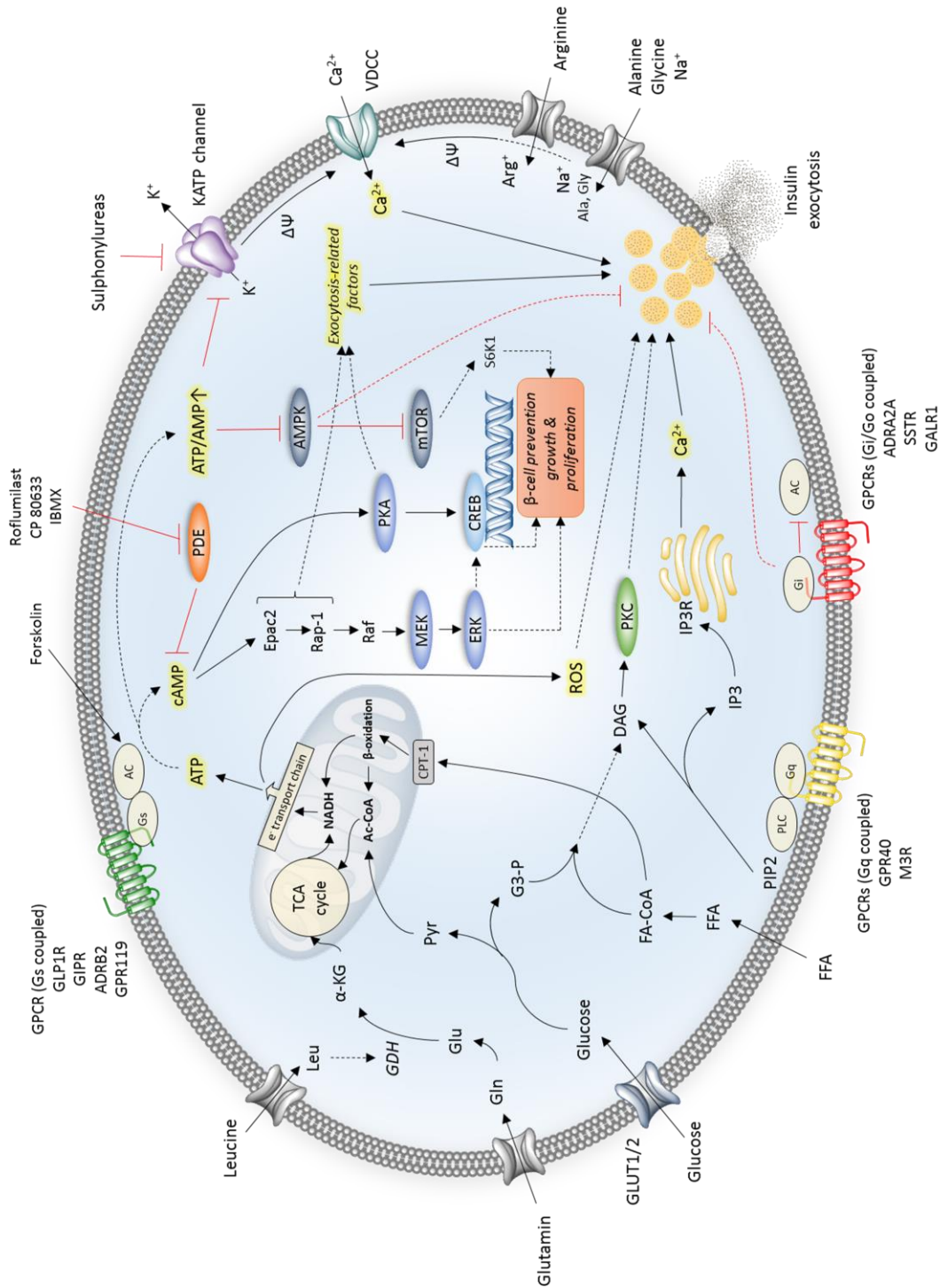


Figure 1.4.1 Schematic view of a beta cell, including metabolic pathways and some investigated elements related to insulin secretion. Effector molecules are highlighted with yellow. Please find the detailed description in the text. α -KG (α -ketoglutarate); ADRA2A (α adreneg receptor); ADRA2A (α adreneg receptor); DAG (diacyl-glycerol); FFA (free fatty acid); FA-CoA (fatty acid CoA); G3-P (glycerol-3P); GALR1 (Galanin receptor); GDH (Glutamate dehydrogenase); Gln (glutamine); GLP1R (GLP-1 receptor); Glu (glutamate); GLUT1/2 (glucose transporters GLUT1 in human, GLUT2 in rodents); IP3 (inositol 1,4,5-trisphosphate); M3R (muscarinic acetylcholine receptor); PDE (Phosphodiesterase); Phosphatidylinositol 4,5-bisphosphate (PIP2); Pyr (Pyruvate); ROS (reactive oxygen species); TCA cycle (citric acid cycle/Krebs cycle); VDCC (Voltage dependent Ca²⁺ channel); $\Delta\Psi$ (membrane potential)

1.3 Medicaments used in the therapy of diabetes

1.3.1 Insulin secretagogues

1.3.1.1 *Sulfonylureas (SU)*

The insulin secretagogue sulfonylurea drug family inhibits K_{ATP} channels found in beta cells (Kir6.2/SUR1) by binding with high affinity to SUR1 regulatory subunit. Nevertheless they have a low affinity binding site on Kir6.2 subunit as well. Blocking K_{ATP} channels induces membrane depolarization which promotes Ca^{2+} influx into the cells. The increased intracellular Ca^{2+} level stimulates the exocytosis of insulin vesicles. Interestingly certain SU may also directly activate Epac2, an important protein that senses cAMP level and regulate PKA independent insulin secretion⁵⁹. By application of these drugs there is an increased risk of hypoglycemia, therefore it is advised to take them during meal. Weight gain is also associated with the long term usage of these medicaments. Some SU might be potentially teratogenic. Chronic treatment with SU can be associated with apoptosis and therefore loss of beta cell mass⁶⁰. First generation SU-s are chlorpropamide, tolbutamide, tolazamide. They are not recommended and rarely used because of more side effects compared to newer SU. Second generation (glipizide, glibenclamide/glyburide, gliquidone, glyclopyramide) and third generation (glimepiride) SU-s are still widely used for the treatment of type II diabetes.

1.3.1.2 *Meglitinides*

Repaglinide, nateglinide and mitiglinide belong to the meglitinide drug family. They promote insulin secretion by the same mechanism as SU-s. However they have a shorter effect (they act quickly within 30 min, but their effect can last for several hours) and hypoglycemia is less frequent compared to the treatment with SU-s. Another mechanism by which they increase insulin secretion is the activation of ryanodine receptors (RyR). Side effects are weight gain, headache, muscle and joint ache and sinus infections.

1.3.2 Insulin sensitizers

1.3.2.1 *Biguanides*

Metformin is often prescribed as initial or combination therapy (with insulin or SU/glinides). It lowers blood glucose level by decreasing the glucose production in the liver. This is often a preferred therapy because of several benefits. There is no risk of hypoglycemia, low side effect profile; furthermore some anticancer effects are also reported during the treatment of metformin. It is currently under investigation in clinical trials and used in neoadjuvant therapy, it may also selectively kill cancer stem cells. Confirmation is needed for whether it can enhance the treatment outcome of various cancer types⁶¹⁻⁶³. Metformin can suppress appetite and compared to other members of the family it does not cause lactic acidosis. Metformin blocks the synthesis of NfkB which is responsible for inflammatory processes, furthermore activates Nrf2, a transcription factor that regulates many antioxidant enzymes. These enzymes can stop the activity of reactive oxygen species, thus may prevent the destruction of pancreatic beta cells⁶⁴. Metformin indirectly activates AMPK (AMP-activated protein kinase) by targeting and inhibiting the complex I of the respiratory chain in the mitochondria. As a result it is lowering the mitochondrial ATP/AMP ratio that's sufficient for activation of AMPK⁶⁵. AMPK has a central role in the regulation of metabolism, some of its function will be discussed later⁶⁶.

1.3.2.2 *Thiazolidinediones (TZD)*

Thiazolidinediones (pioglitazone, rosiglitazone) are peroxisome proliferator-activated receptor- γ (PPAR γ) agonists and are approved for the treatment of type II diabetes (T2D). PPARs are nuclear receptors that are mainly expressed in brown adipose tissue and play a decisive role in the development of adipocytes, therefore weight gain can be a substantial side effect of PPAR γ activation^{67,68}. After activation, it forms a heterodimer with the retinoid receptor (RXR), and exerts antidiabetic effects by binding to DNA and regulating genes which are involved in glucose homeostasis and lipid metabolism^{69,70}. TZDs have a complex effect that in overall leads to an improved insulin sensitivity of muscle and fat cells, increased lipolysis and reduced FFA secretion⁷¹. It also stimulates the translocation of GLUT4 transporters to the membrane, thus promoting glucose uptake from blood⁷². TZDs can improve the inflammatory state of fat cells in T2D by inhibiting the expression of cytokines (TNF α)^{73,74}. Furthermore they induce adiponectin secretion that is an important hormone responsible for fatty acid oxidation and can reverse hyperglycemic effects^{75,76}. A recent study suggests that they also act by increasing the expression level of GPR40⁷⁷. In spite of these, safety issues raised big concerns by application of these drugs. According to some studies, the treatment with rosiglitazone can be associated

with increased risk of getting heart attack and stroke, however this correlation was not significant in another analysis⁷⁸. Rivoglitazone, a new TZD under development has a greater potential compared to pioglitazone, however it produced serious adverse effects (cardiovascular events, renal failures)⁷⁹. Another drawback of the TZDs is that they can induce osteoporosis under some circumstances⁸⁰. Patients who can't take metformin because of renal insufficiency may take TZDs^{81,82}. INT-131, a new non-TZD PPAR agonist is under development and it is expected to be better tolerable and less harmful for the cardiovascular system compared to available TZDs⁸³⁻⁸⁵.

1.3.2.3 Dual PPAR agonists

Saroglitazar, the first compound of a new class of drugs is approved for the treatment of diabetic dyslipidemia. It acts on both PPAR α and PPAR γ , therefore an improved, joint effect is expected from this group of compounds that might also lower the cardiovascular risks caused by TZDs^{67,86-91}.

1.3.3 Incretin-based therapies

The physiologically acting incretin hormones, glucagon like peptide-1 (GLP-1) and gastric inhibitory peptide or glucose dependent insulintropic polypeptide (GIP) are produced by the intestinal K and L cells. They both act on G-protein coupled receptors (GPCRs) and exert their effects in a glucose dependent manner. Therefore patients treated with incretin analogues (exenatide, liraglutide, lixisenatide, albiglutide and the recently approved dulaglutide) are less affected by hypoglycemia. For reaching their final effect, activation of MEK/ERK1/2 pathway and Ca²⁺ influx through L-type Ca²⁺ channels is necessary⁹². Exenatide shows 50% homology with human GLP-1. It slows down the gluconeogenesis, slows stomach emptying and regulates hunger. Since it causes weight loss as well this is a suitable treatment for patients who are overweight^{93,94}. In some cases severe side effects can develop by the treatment of incretin-based therapies, however the incidence was low. Hemorrhagic or necrotizing pancreatitis were reported in some patients and currently there is a big discussion and several studies ongoing about comparing the benefits and disadvantages of this therapy⁹⁵⁻¹⁰¹. An additional benefit could be the protective effect produced on the heart. However this might be negligible according to a study, because of the more dangerous and damaging effect produced in the pancreas¹⁰². Liraglutide also possess cardio-protective effect¹⁰³. It was however reported to increase the risk of development of thyroid cancer in rats and mice, but this couldn't be confirmed in humans yet¹⁰⁴⁻¹⁰⁶. Incretin analogues are administered subcutaneously either daily (exenatide, liraglutide) or weekly (albiglutide, dulaglutide).

1.3.4 Alpha-glucosidase inhibitors

Acarbose and miglitol inhibit the alpha glucosidase enzyme that breaks down oligosaccharides. They slow down the digestion of starch and other carbohydrates which helps to keep the blood glucose level low. They do not cause hypoglycemia, weight gain and have only minor side effects (flatulence). It must be taken after the first bite during meal.

1.3.5 DPP-4 inhibitors

Inhibition of dipeptidyl peptidase-4 (DPP-4) leads to decreased degradation of glucagon-like peptide-1 (GLP-1). It significantly reduces HbA1c level, there is no induction of weight gain and there is only a low risk of hypoglycemia under the treatment of these medicines. The first FDA approved drug in this class is sitagliptine, so far 8 derivatives are available in the market (Sitagliptin, Vildagliptin, Saxagliptin, Linagliptin, Anagliptin, Tenzeligliptin, Alogliptin, Gemigliptin). However many studies and meta-analyses revealed that there are no increased risks for cardiovascular events, pancreatic cancer and pancreatitis for this class of drugs¹⁰⁷⁻¹¹⁰, according to a recent study, sitagliptin was highlighted for increased risk of heart failure compared to other members of DPP4 inhibitors. The adverse cardiovascular effects of sitagliptine might be due to the reduced level of a cardio active GLP-1 metabolite and increased level of the native, intact GLP-1¹¹¹. Further studies raised concerns for Saxagliptin and Alogliptin, which are now under FDA investigation¹¹²⁻¹¹⁴.

1.3.6 SGLT2 inhibitors

This new class of diabetes medication lowers blood glucose level through inhibition of sodium-glucose co-transporter 2 (SGLT-2) that is located in the proximal tubule of kidneys. It is a low affinity and high capacity glucose transporter, which is responsible for 90% of the reabsorption. Inhibiting the SGLT-2 will lower blood glucose level by facilitating the renal glucose excretion. This new mechanism of action further improves glucose control by increasing the glucose sensitivity and the glucose uptake in the muscle cells, decrease gluconeogenesis in liver and improve insulin release from beta cells. So far no serious side effects (no cardiovascular risk) were observed by treatment of these drugs, however there is an increased risk of getting urinary and genital infections, nasopharyngitis and mycotic infections for people who are taking it^{115,116}. The medication is not indicated in type 1 diabetes and it is also not recommended for patients with severe renal impairment, but recent studies suggest that they might improve glycemic control in combination with insulin in T1DM as well^{117,118}. Currently dapagliflozin and canagliflozin are approved by FDA, ipragliflozin approved in Japan and empagliflozin completed phase III in Dec 2013.

1.4 Preclinical developments for the treatment of diabetes

1.4.1 G protein-coupled receptors (GPCRs)

The GPCR family consists of around 1000 members and they are targeted by approximately 50% of the available drugs today. They regulate many of the most important physiological processes and are good targets because they show different expression patterns in various tissues and organs as well (e.g. adrenergic receptors). There are GPCRs in beta cells which main roles are the potentiation and regulation of glucose stimulated insulin release (GSIS). Targeting these receptors could be a big advantage compared to other available medications that often cause hypoglycemia. Therefore proper agonist and antagonist development for these receptors is currently a quickly emerging field giving hope for a novel therapy against diabetes with a potentially reduced risk of getting hypoglycemia from the treatment^{27,34}. From numerous targetable GPCRs I would highlight the GPR119, but there are many other candidates as well¹¹⁹⁻¹²⁷. Several GPR119 agonists were studied in preclinical and clinical experiments, unfortunately with poor outcomes yet. The main handicaps associated to them are tachyphylaxis and therefore low potency of glucose lowering effect in vivo^{128,129}.

1.4.2 FGF21 and its analog LY2405319

The fibroblast growth factor family consists of 22 members. FGF21 is known to induce favorable metabolic effects in rodents and in humans as well. Its serum level is significantly increased after exercise in humans¹³⁰. In vitro it increased glucose uptake and upregulated GLUT1 in 3T3-L1 cells. In vivo it lowers blood glucose level and it was free of the common side effects of insulin therapy, like increased weight gain and hypoglycemia. However FGF21 activates FGFR related pathways, it does not bind to FGFR directly. It requires the co-receptor β Klotho (KLB) to exert its action via phosphorylation of FRS2 and activation of MAPK pathway. LY2405319 is an improved and more stable analog of FGF21. In clinical trials it decreased serum triglyceride, LDL, insulin levels in consequence reduced body weight was observed as well. Importantly adiponectin level – a protein hormone secreted by adipose tissue, which regulates glucose level and fatty acid oxidation - was elevated after treatment.¹³¹⁻¹³⁴

1.4.3 Glucokinase activators (GKA)

The principle of mechanism of action of these drugs is that they activate the glucokinase (GK), an enzyme that facilitates glucose metabolism by phosphorylating glucose. Presumably they lower blood glucose level by two mechanisms: by increasing insulin secretion from beta cells and by increasing glucose uptake and modulating its metabolism in hepatocytes¹³⁵⁻¹³⁷. They

might also have a protective effect on beta cells¹³⁸. There were many clinical trials conducted with GK activators, but most of them were terminated in phase I, some of them reached phase II: AZD1656¹³⁹ (Japan, phase I), LY2608204, LY2599506 (Eli Lilly, phase I); ZYGK1 (Zyduz Cadila, India, phase I); HMS5552 (Hua Medicine Limited, China, phase I); ARRY-403 (Array BioPharma / Amgen, phase II); MK-0941¹⁴⁰ (Merck Sharp & Dohme Corp., phase II); GK Activator (2) (Hoffmann-La Roche, phase II). The cause of discontinuation of these trials might be due to their potential side effects including hyperlipidemia, hypoglycemia and fatty liver¹⁴¹.

1.4.4 11beta-hydroxysteroid dehydrogenase type 1 (11 β -HSD-1) inhibitors

Overexpression of 11 β -HSD-1 in adipose tissues can lead to the development of metabolic syndrome and obesity. The enzyme catalyzes the conversion of inactive cortisone to active cortisol, which primary function is to increase gluconeogenesis. Thus it has been proposed to have a potential benefit for T2DM patients, since it significantly reduced haemoglobin A1c (HbA1c) levels. INCB013739 (Incyte Corporation, phase II), P2202 (Piramal Enterprises Limited, terminated).

1.4.5 Glycogen phosphorylase inhibitors (GPIs)

Hepatic glycogenolysis is the physiological process that forms glucose-6-phosphate from glycogen, by this blood glucose level raises. Glycogen phosphorylase catalyzes the formation of glucose-1-phosphate from glycogen which is converted later into glucose-6-phosphate. Two endogenous hormones that can induce glycogenolysis are adrenalin and glucagon. They are produced in response to stress or low blood glucose level. Theoretically as these physiological compensatory mechanisms are present, hypoglycemia can also be prevented by application of GPIs. So far there were only a few studies with low success in this field: GSK1362885 (GlaxoSmithKline, phase I); CP-91149 and CP-316819 (Pfizer, preclinical studies).

1.5 Roles of sunitinib and other kinase inhibitors in diabetes

Sunitinib and imatinib both were able to reverse type 1 diabetes in nonobese diabetes (NOD) mice model. The study is based on previously observed positive outcomes achieved with imatinib in the treatment of different autoimmune diseases and underlines its anti-inflammatory effect. The possible mechanisms of imatinib and sunitinib treatments were investigated and found that on-set prevention could be linked to the neutralization of PDGFR. It was also concluded that c-Kit, c-Fms or Lck was not associated with this effect¹⁴². For demonstration of this principle in human, a clinical trial has been started recently which purpose is to study the potential role of short-term therapy with imatinib to induce T1DM remission^{143,144}. Additional evidences confirm that tyrosine kinase inhibitors (TKIs) might have beneficial effects in T2DM patients as well, such as normoglycemia upon treatment, increased insulin secretion, favorable regulation of lipid metabolism and improved insulin sensitivity. Templeton et al. reported an interesting case of a patient with renal cell carcinoma (RCC) who received sunitinib treatment. The patient got diabetes therefore needed insulin treatment, but this could be gradually reduced and later on completely stopped during the administration of sunitinib. Interestingly sunitinib was able to sustain normoglycemia even after terminating the therapy as well¹⁴⁵. A follow-up clinical study conducted on more patients with both RCC and T2D receiving sunitinib treatment, ended with similar results. Sunitinib induced remission in T2D patients and lowered blood glucose level. In addition it should be noted that blood glucose level was not dropped significantly in non-diabetic patients, so it cannot be excluded that the effect of sunitinib is glucose dependent¹⁴⁶. VEGFR, PDGFR, c-Kit, Flt3, RET, CSF-1R are considered as main targets for sunitinib but apart from these, it is binding to many kinases and may inhibit others as well¹⁴⁷. A recent review about TKIs proposed some mechanisms and theories for the general action of them in diabetes and insulin resistance. These involve the following effects: reversing adipose tissue macrophage phenotype from M1 to the non-inflammatory M2 type (PD153035); reducing ER stress and JNK/IRS1 Ser307 phosphorylation (imatinib); inhibiting c-Abl that can prevent beta cell death. Additionally erlotinib, nilotinib, pazopanib, dasatinib and sorafenib treated patients were also reported to produce lowered fasting plasma glucose level^{148,149}. In overall the TKIs seem to be able to reduce beta cell apoptosis as well in T1D and T2D^{150,151}. A recent study performed on rabbits revealed that sunitinib was able to reduce plasma glucose level in this model as well. The drop in the plasma glucose level was higher in diabetic animals, which seems to correlate with the plasma level of sunitinib. This could be attributed to the decreased function of CYP3A4 in diabetes, therefore allowing the drug to act longer and produce a stronger effect¹⁵². Sunitinib could also prevent beta cell loss and cure hyperglycemia

in spontaneously diabetic Torii rats¹⁵³. Although TKIs are proposed to carry out their anti-diabetic actions mostly by improving insulin resistance and preventing beta cell failure, in our experiments we demonstrated that sunitinib was able to increase insulin secretion from different beta cell lines. The mechanism of this process was not studied by others yet, therefore we hypothesized that some of the “off-target kinases” or potentially other proteins may negatively regulate the insulin release in their active form, which can be inhibited by TKIs, including sunitinib. This hypothesis has been partly proven previously by an siRNA-based target discovery screening in beta-TC6 cells¹⁵⁴.

2 AIMS AND SCOPE

Our main goal was to use a diverse compound library as a tool to identify targets based on a phenotypic screening method, which are likely responsible for negative regulation of insulin secretion. Furthermore we were looking for less toxic compounds with comparable or better insulinotropic effect than sunitinib. The mechanisms of action of these compounds were further studied in *in vitro* systems.

3 MATERIALS AND METHODS

3.1 Cell lines

Culture medium and supplements were purchased from Life Technologies. RIN-5AH insulinoma beta cell line and the BRIN-BD11 were cultured in RPMI 1640 supplemented with 10% FBS, 2mM glutamine. For propagation of the glucose responsive INS-1E cells the same RPMI 1640 medium was used, further supplemented with 10mM HEPES, 1mM Sodium pyruvate and 50µM beta-mercaptoethanol. The Beta-TC-6 cells were grown in DMEM (glucose: 4.5g/l) with 15% FBS, 2mM glutamine and 1mM pyruvate. C2C12 mouse myoblast cells were cultured in high glucose DMEM (4.5g/l) with 10% FBS, 2mM glutamine. 3T3-L1 adipocytes were propagated in low glucose DMEM (1g/l) supplemented with 10% NBS and 2mM glutamine. All culture medium contained 1x Penicillin-Streptomycin. Cells were grown on 15cm culture plates in 37°C, 5% CO₂ in a high humidity atmosphere.

CELL lines and culture media						
<i>Cell line</i>	RIN-5AH	TC-6	BRIN-BD11	INS-1E	C2C12	3T3-L1
<i>Description</i>	rat beta cell line	mouse beta cell line	primary beta cells- RINm5F hybrid	glucose sensitive rat beta cell line	mouse myoblasts	mouse adipocytes
<i>Origin</i>		ATCC	PHE	Kindly provided by prof. Claes Wollheim	ATCC	ATCC
<i>Medium</i>	RPMI 1640	DMEM Hi	RPMI 1640	RPMI 1640	DMEM Hi	DMEM Lo
<i>Serum</i>	FBS 10%	FBS 15%	FBS 10%	FBS 10%	FBS 10%	NBS 10%
<i>Glutamine</i>	2mM	2mM	2mM	2mM	2mM	2mM
<i>Pen/Strep</i>	1x	1x	1x	1x	1x	1x
<i>Pyruvate</i>		1mM		1mM		
<i>β-mercaptoethanol</i>				50uM		
<i>HEPES</i>				10mM		
<i>Splitting</i>	2x10 ⁶ / 15cm plate	2x10 ⁶ / 15cm plate	1,5x10 ⁶ / 15cm plate	1,5x10 ⁶ / 15cm plate	0,4x10 ⁶ / 15cm plate or 1 to 10	1 to 5-8

INS-1E cells were kindly provided by prof. Claes Wollheim and Pierre Maechler (Department of Cell Physiology and Metabolism, University of Geneva, Geneva, Switzerland)

ATCC - American Type Culture Collection

PHE – Public Health England

3.1.1 Differentiation of 3T3-L1 cells

100.000 cells were seeded in 12 well plates and incubated for 1-2 days at 37°C, 5% CO₂. Medium was carefully removed and replaced with differentiation medium I (10% NCS in high glucose DMEM containing 500µM IBMX, 1µM Dexamethasone and 1µg/ml insulin). After 2 days of incubation, medium was changed for differentiation medium II (high glucose DMEM supplemented with 10% NCS and 1µg/ml insulin). Then after further incubation for 2-4 days

in differentiation medium II cells were ready for the experiment. Differentiation medium II was changed every second day if necessary.

3.2 Insulin ELISA

To determine the insulin level from the cell supernatants we used the insulin ELISA kits from Millipore or Merckodia. Cells were seeded in 96 well or 12 well plates and grown overnight (RIN-5AH, TC-6 cells) or for 2 days (INS-1E, BRIN-BD11). They never reached more than 80% confluency before treatment. Cells were either washed 1x with PBS (RIN-5AH, TC-6, and BRIN-BD11) or preincubated for 40min in KRBH containing 1mM glucose (INS-1E cells) before treatment. Cells were treated in medium or KRBH buffer with 1mM or 11mM glucose (INS-1E cells) for 2 hours and 5uM if otherwise not stated. Samples were assayed immediately or stored at -20°C until measurement. Dilutions were made if necessary then ELISA was performed according to the user's manual. Plates were read on BioTek Elx800 Absorbance reader at 450 or 490nm.

3.3 CellTiter-Glo assay

Cells were plated on flat bottom white 96 well plates (Costar). Treatment was performed after overnight incubation for the desired time. CellTiter-Glo component (Promega) was added in a 1:1 volume ratio to the wells and then plate was incubated at RT in dark for 15min. Luminescence intensity was measured on TECAN Evolution microplate reader.

3.4 IC₅₀ and EC₅₀ determination

IC₅₀ values for viability were determined with CellTiter-Glo and treatment was performed for 72h. EC₅₀ values for insulin secretion were determined with insulin ELISA kit and normalized to the 2h treatment MTT absorbance value. Values were calculated in GraphPad Prism using four parameters fit. Top and Bottom constrains were set to 100 and 0. IC₅₀ values were calculated for curves with R²>0.85.

3.5 MTT assay

After 2h treatment of RIN-5AH beta cells, their viability was checked by MTT assay in order to normalize their insulin secretion capacity. A stock solution of 5mg/ml of Thiazolyl Blue Tetrazolium Bromide (MTT, Sigma, M5655) was prepared in PBS and filtered. MTT reagent was added in 1:5 ratio to the wells and incubated in 37°C for 45min. Later on 1:1 stop solution (200ml 10% SDS; 12ml iso-butanol; 1.3ml 2N HCl) was added and incubated overnight in dark at RT. Absorbance reading was done on BioTek Elx800 plate reader at 570nm.

3.6 Protein concentration determination

Protein concentrations were determined by BCA assay kit in 96 well plates (Thermo Scientific, 23225). This method was used to measure the protein concentrations for western blot experiments and for normalizing the insulin secretion data to protein amount of INS-1E cells as well. Assay was performed according to the manual, using 5 – 12.5µl sample amounts. After 30min - 1h incubation time absorbance was read at 570nm on BioTek Elx800 plate reader.

3.7 Calcium influx measurements

For Fluo-4 AM (molecular probes, F14201) staining a 3µM stock solution was prepared in HBSS with Ca²⁺ and Mg²⁺ (HBSS++) with addition of a final amount of 0.02% Pluronic-F127 (molecular probes, P6867). Probenecid was not necessary for loading and displayed toxicity on cells as well. Cells were incubated with the dye for 1h at 37°C, in 5% CO₂. They were washed 2x with Ca²⁺ and Mg²⁺ free HBSS (HBSS--) (Gibco, 14170) before moving to the next step of the protocol (see below). Washing steps could be reduced for Fluo-4 Direct (molecular probes, F10471) and Calcium-6 (Molecular Devices, R8194) staining, since these formulas contain a secondary masking dye that does not enter the cell and quenches the unspecific signal of residual extracellular calcium indicators. These dyes were used when performing the calcium measurements on Flexstation plate reader. Moreover it does not disturb the fluorescent read-out as they have different excitation and emission wavelengths.

3.7.1 Calcium influx measurement by FACS

Similar protocols were already described using this method for Ca²⁺ influx determination¹⁵⁵⁻¹⁵⁷. RIN-5AH, TC-6, INS-1E (30.000 cells/well) or C2C12 cells (80.000 cells/well) were plated in 12 well plates and incubated ON at 37°C, 5% CO₂. After washing with HBSS--, cells were trypsinized for 3min, at 37C, 5% CO₂. Then diluted with HBSS-- and centrifuged for 3min at 1200 rpm. Cells were suspended in 1ml of HBSS++ or HBSS-- before starting the measurement. Base fluorescent signal was recorded for 30s, afterwards treatments with the various compounds were done, by quickly suspending them into FACS tubes, while the acquiring was not interrupted. Final DMSO concentration did not exceed 0.1%. Then samples were measured continuously for the desired time and all measurements completed within 40 min. Unstained cells were used as negative controls for each treatment. Compounds used in the calcium influx experiments were purchased from various sources (Chloroquine diphosphate - Sigma, C6628; Quinidine - Sigma, Q3625; Verapamil - Santa Cruz, sc-3590A; Efonidipine HCl monoethanolate - Sigma, E0159; NNC 55-0396 - Sigma, N0287; Glibenclamide - Santa Cruz, sc-200982; Nickel(II) chloride hexahydrate - Sigma, N6136; Gatifloxacin - Santa Cruz, sc-

204762; Levofloxacin HCl - Santa Cruz, sc-202693; Thapsigargin - Serva, 36000; A23187 Calcium ionophore - Sigma, C7522; Ryanodine - Santa Cruz, sc-201523; Caffeine - Sigma, C0750; 4-Chloro-3-methylphenol - Sigma, C55402; 9-Phenanthrol - Sigma, 211281). Data were acquired on BD-FACSCalibur flow cytometer from at least 15.000 cells, data visualizations were prepared by FlowJo software.

3.7.2 Calcium influx measurement on Flexstation

The increased throughput capacity of the Flexstation (Molecular Devices) made it available to test more compounds with more replicates. Further advantages of this system were that using the built in pipetting system 8 samples could be treated and measured almost at the same time. RIN-5AH cells were seeded (50.000 cells/200µl/well) and incubated overnight at 37°C, 5% CO₂ then loaded either with Fluo-4 Direct or Calcium-6 (100µl/well). Buffer was replaced with 200µl of HBSS++ and plates were stored at RT in dark for max. 30 minutes until measurement. Plates were treated by adding 50µl of 5x stock solution of compounds prepared in the appropriate buffer to each well using the built in pipetting system. Measurements were performed with Flexstation 3 in FLEX mode using the shortest reading interval time. Evaluation and calculation of AUC values were made with SoftMax Pro 5.4.5 software.

3.7.3 Calcium influx measurement by spinning disc confocal microscopy

RIN-5AH cells were plated (30.00 cells) in 35mm u-Dishes (IBIDI, 80136) and incubated overnight at 37°C, in 5% CO₂. Cells were loaded with Fluo-4 AM and washed 2x with HBSS-. Volume was adjusted with HBSS++ to 1200µl / dish. Base fluorescence signal was recorded for 30s and treatment was done by using a perfusion pump (Ismatec) with a final concentration of 5µM for VCC981125:09, VCC673193:01, VCC718565:01 and 250µM for glibenclamide. Monitoring and recording of fluorescence intensity was carried out on an UltraVIEW Vox spinning disk microscope system (PerkinElmer), which was attached to a HAMAMATSU ImagEM camera (cooled down to -80°C). Calculation of results was done by Volocity software (PerkinElmer).

3.8 Patch clamp experiments

In order to confirm the calcium influx results for the quinoline molecule VCC981125:09, whole cell patch clamp experiments were carried out under the supervision and kind help of Dr. Jana Hartmann from TUM (Institute for Neurosciences).

RIN-5AH cells were trypsinized and suspended in medium. Cells were transferred into the recording chamber and allowed to settle down before beginning a slow perfusion with the

external buffer. Cells were sealed and patched by the application of a gentle negative pressure. Holding membrane potential was set up to -70mV for voltage clamp experiments. After patching the cells, either 10s or 20s of base signal was recorded for both voltage clamp and current clamp measurements. External stimulation of cells was done by using Picospritzer II instrument (Parker) with 5psi for 30s. Total recording time was set to 2-4 minutes. AUC of the curves were analyzed in GraphPad Prism Software.

3.9 2-NBDG (glucose analog) uptake

The 2-(N-(7-Nitrobenz-2-oxa-1,3-diazol-4-yl)amino)-2-deoxyglucose (2-NBDG) is a fluorescent analogue of D-glucose, commonly used for monitoring glucose uptake in in vitro experiments.

C2C12 cells (80.000 cells/well) and RIN-5AH cells (300.000 cells/well) were seeded in 12w plates and incubated overnight (ON) at 37°C, in 5% CO₂. 3T3-L1 cells were first differentiated before starting the experiment. Medium was removed and cells were washed 1x with PBS. Treatment was done with various compounds at 5µM for 1h or 3h in glucose free medium or in medium containing 100µM 2-NBDG (molecular probes, N13195). Cells were washed 1x with PBS and trypsinized for 3min, then the volume was completed to 1ml with cold PBS and centrifuged at 4°C, 1400 rpm for 3min. Cells were resuspended in cold PBS with 5% FBS and stored at 4°C until measurement. Acquisition was done with BD-FACSCalibur flow cytometer from at least 15.000 cells. Data were analyzed with FlowJo software (Tree Star Inc.). Glucose uptake rate was normalized for all samples according to the following equation:

$$I_{1-wo} / I_{2-wo} * I_{2-w} / I_{1-w}$$

I_{1-wo}: cells in glucose free medium treated with vehicle

I_{2-wo}: cells in glucose free medium treated with compound

I_{2-w}: cells in 2-NBDG medium treated with compound

I_{1-w}: cells in 2-NBDG medium treated with vehicle

3.10 Intracellular cAMP determination

RIN-5AH (25.000 cells/well) were seeded in U-shaped bottom 96 well plates (Nunc, 163320) and incubated for 2 days at 37°C, in 5% CO₂. Cells were washed with KRBH without glucose and treatment was performed in medium (RIN-5AH) or in KRBH (INS-1E) supplemented with 11.1mM glucose. Supernatant was taken for insulin assays, then cells were lysed in 140µl of 0.1N HCl + 0.5% Triton-X for 10min at RT. Samples were centrifuged and stored at -20°C or assayed immediately by using the acetylation method described in the protocol of cAMP Complete ELISA kit (Enzo, ADI-900-163).

3.11 Gene silencing

In all experiments for each target, specific siRNA pools (pool of 3-4 siRNA sequences) were used and purchased from Dharmacon.

3.11.1 siRNA resuspension protocol

The siRNAs were resuspended and stored as described in the basic siRNA resuspension protocol of GE Dharmacon. Briefly, tubes were centrifuged and siRNA were resuspended in 1x siRNA buffer (Dharmacon, Cat. #B-002000-UB-100) to a convenient stock concentration (100 μ M for Accell siRNA and 5 μ M for DharmaFECT ON-TARGETplus protocol). The siRNA stocks were aliquoted and stored at -20°C or -80°C.

3.11.2 Accell siRNA transfection

RIN-5AH cells were seeded in 96 well (12.000 cells/well) or 12 well (100.000 cells/well) plates and incubated for 24h allowing them to attach well to the surface. Medium was removed and cells were transfected with 1 μ M of Accell siRNAs in 1:1 RPMI/Accell Delivery medium (Thermo, Cat #B-005000) mixture supplemented with 1% FBS, without antibiotics. Knock-down efficiency and insulin release was determined after 72 hours of incubation.

3.11.3 Transfection with DharmaFECT ON-TARGETplus

The siRNAs and DharmaFECT 4 reagent were incubated separately in serum and antibiotic free medium for 5min then the 1:1 ratio of siRNA:transfection reagent was incubated for 20 minutes at RT. 20-20 μ l of siRNA:transfection reagent mixture were pipetted into the wells of a 96 well plate then 80 μ l of RIN-5AH cells (12.000 cells/well) and INS-1E cells (20.000 cells/well) were added. Knock-down efficiency was determined by RT-PCR and insulin release was checked after 48h-72h KD by washing the cells and replacing the medium or buffer for 2h. Results are displayed in normalized values to protein amount or MTT absorbance.

3.12 Preparation of affinity matrices for MS experiment

Phenotypically active linker derivatives with primary amino groups were dissolved in the appropriate coupling buffers. They were then covalently bound to NHS- or EPOXY-activated sepharose beads (GE Healthcare, 17-0906-01; GE Healthcare, 17-0480-01). According to our theory, choosing the proper beads can be a critical point. Subsequently upon coupling compounds to the matrix, the altered basicity may change the binding properties of the immobilized compound to the proteins (*Figures 3.1 and 3.2*). The beads were washed 1x with water and 1x with coupling buffer. Compounds in coupling buffer were incubated with the beads in 2:1 ratio overnight on a rotating wheel at RT in dark. NHS-beads in coupling buffer were used as negative and EAH-beads (GE Healthcare, 17-0569-01) in coupling buffer with compounds as positive control. Supernatants were taken and coupling efficiencies were determined by recording the UV-absorbance maximums of NHS-coupled and EAH control samples. Coupling efficiency was normalized to the signal of free NHS by the following equation:

$$\text{NHS normalized coupling efficiency} = (1 - ((\text{ABS.SMPL} - \text{ABS.NHS}) / \text{ABS.EAH})) * f * c$$

ABS.SMPL = max. absorbance of the compound in the supernatant of NHS beads+compound

ABS.EAH = max. absorbance of the compound in the supernatant of EAH beads+compound

ABS.NHS = max. absorbance of NHS in the supernatant of NHS beads+coupling buffer

f = dilution factor = 2 (beads:coupling solution ratio = 1:2)

c = concentration equals the conc. used in the coupling solution in mM

Beads were then washed 1x with water, and 1x with coupling buffer. After that 1M ethanolamine (Aldrich, 411000) in coupling buffer was added and incubation was continued for 6h at RT in order to block unreacted sites on NHS-beads. Then beads were washed 1x with DMSO (or DMF) / ethanol (50-50%), 1x with water and 1x with NaCl. The affinity matrices were then stored in 20% ethanol (1:1) at 4°C until use. The coupling densities were calibrated as described in chapter 3.13. and the optimized affinity matrices were used in MS experiments (*Table 3.1*).

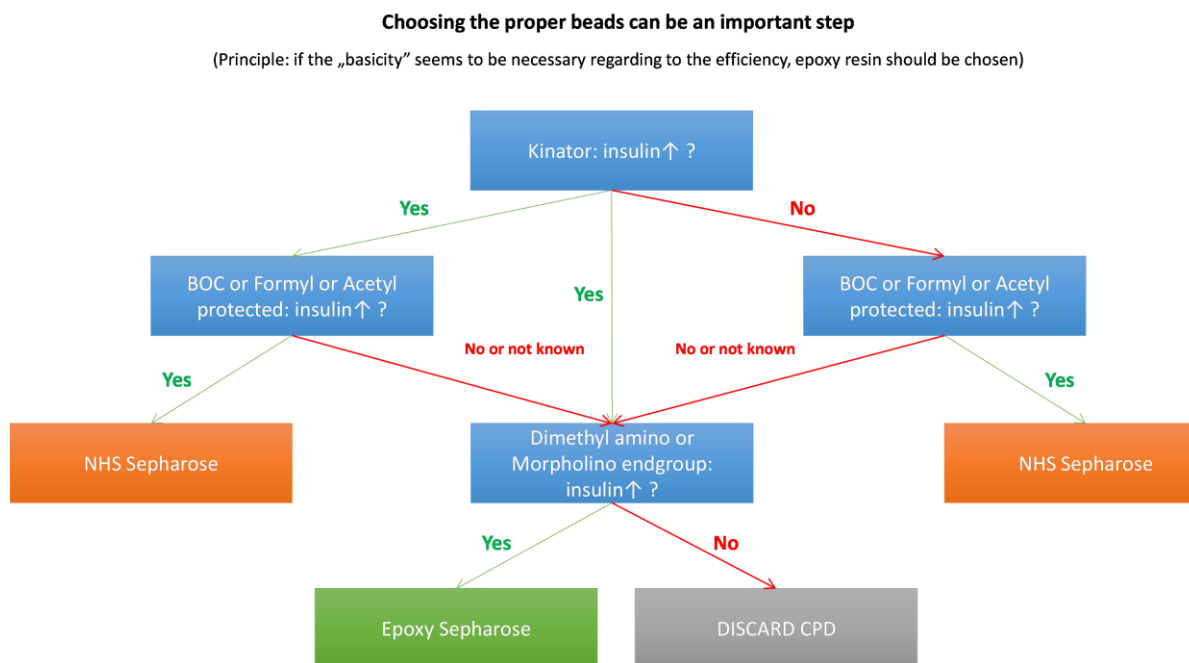


Figure 3.1 All linkers have their amino protected derivate for the purpose of modelling the coupled compound in the cellular assay. If BOC, Formyl or Acetyl protected cpd is active in the insulin ELISA assay, NHS beads can be chosen. If compound with dimethyl or morpholino endgroup is effective and no BOC/Formyl/Acetyl derivate was available, epoxy beads should be chosen.

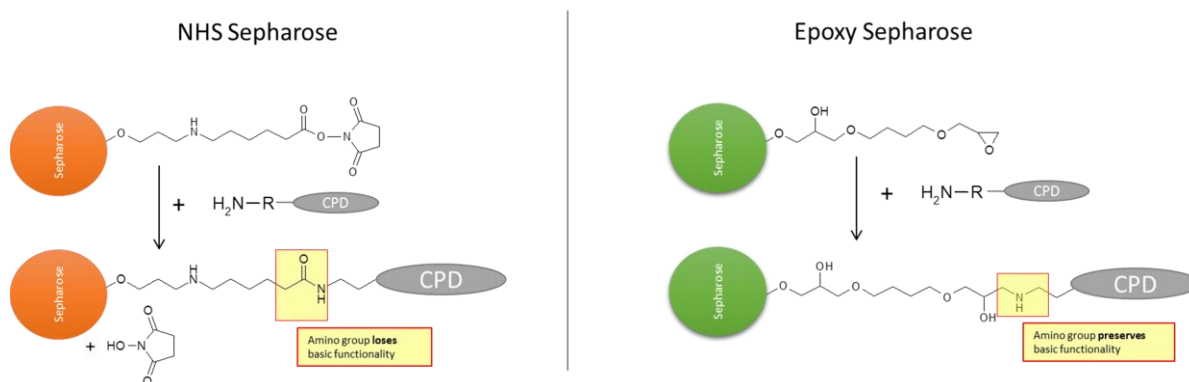


Figure 3.2 Linker derivatives and their amino protected versions were tested for insulin release before coupling. Based on the protective group, different beads should be chosen.

3.13 Binding and competition pre-experiments

The coupling densities were optimized for the final experiments by preparing affinity matrices with different coupling concentrations. After that samples were run on SDS gel and silver staining was employed to detect specific protein-matrix interactions.

For binding experiments 30µl beads were washed 2x with HEPES lysis buffer then 750µl of RIN-5AH cell lysate (4mg/ml) at 4°C for 2.5h at 4°C on a rotating wheel. For pull-down experiments (competition) prior to the 2.5h incubation, 30-100µM compound was mixed with lysate then incubated for 30min at 4°C, on a rotating wheel. (*Figure 3.3*)

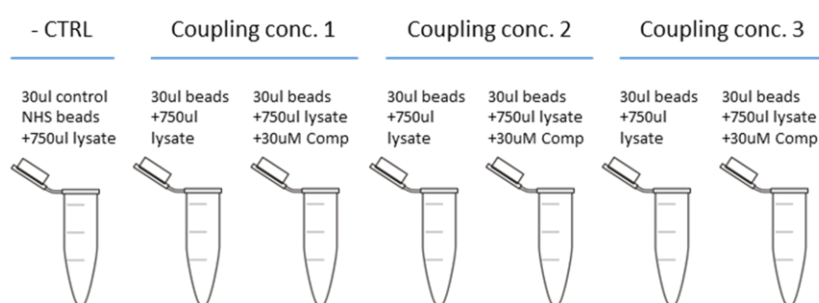


Figure 3.3 Example layout for binding/competition experiments.

After incubation beads were washed 3x with HEPES lysis buffer and residual supernatants were carefully removed from the top. 40µl LDS sample buffer (Invitrogen, NP0007) was added to the samples and boiled for 3min at 95°C. 5µl of eluates and 3-5µg of total cell lysates were loaded in SDS-PAGE gel. Gels were run in MES buffer (life technologies, NP0002) at 150V for 1h then silver-stained according to the user's manual (Invitrogen, LC6070).

3.14 SILAC labeling of RIN-5AH cells for mass spectrometry (MS) experiments

Cells were metabolically labeled with Arg and Lys isotopes in SILAC (Stable Isotope Labeling with Amino Acids in Cell Culture) medium. The advantage of this technique is that the differentially labeled samples could be mixed and analyzed together by LC-MS/MS. The peptide peaks can be quantified very accurately relative to each other to determine the peptide and protein ratios^{158,159}. SILAC RPMI 1640 medium (Thermo, 89984) supplied with 10% dialyzed FCS and penicillin streptomycin was prepared. For triple labeling of cells, three different compositions were prepared with the addition of the proper amino acid isotopes (Sigma, L8662; CIL, DLM-2640-0; Isotec, 608041; Sigma, A6969; CIL, CLM-2265-0; CIL, CNLM-539-0). For light labeled cells: Arg0/Lys0, for medium labeled cells: Arg6/Lys4 and

for heavy labeled cells: Arg10/Lys8 was employed. The concentrations used were: 42mg/l of Arg0 and 72mg/l of Lys0 and the molarity of all amino acids were equal. For efficient labeling of cells (>97% incorporation of amino acid isotopes) 14 days of culturing was necessary, which equals to ~10 doublings. Cells were then harvested by trypsinization, washed 2x with cold PBS and pellets were snap frozen in liquid nitrogen, then transferred to -80°C for long term storage.

3.15 Cellular Target Profiling by MS

We obtained the specific Kd_{free} values of each target protein that are present in the proteome of RIN-5AH cells by employing the Cellular Target Profiling technology¹⁶⁰. This method combines chemical proteomics with SILAC-based quantitative MS^{161,162}. The LC/MS-MS measurements and proteomics analysis were done in collaboration with Evotec AG (Martinsried). The generated affinity matrices were used to capture potential target proteins from the cell lysate in a dose-dependent manner by using a serial dilution of affinity matrices. Thus binding constants (Kd_{imm}) specific to immobilized compound could be determined. These specifically enriched proteins were competed off by the free compound (mother compound) with 6 different concentrations (up to 30µM) and the concentration at 50% competition (CC_{50}) was determined. Kd_{free} for each interacting protein target were then calculated by the Cheng-Prusoff equation, based on the Kd_{imm} , the CC_{50} and the known concentration of the immobilized compound (C_{comp})¹⁶³:

$$Kd_{free} = \frac{Kd_{imm}}{Kd_{imm} + C_{comp}} * CC_{50}$$

Specifically bound and competed proteins were filtered by a specific algorithm, among others: at least two fold higher protein enrichment on affinity matrix compared to negative control beads. At least a twofold difference between bound and competed proteins was considered as specific interaction partner for the free compound. Furthermore a ratio of 5h and 2.5h incubation time was used, where 5h/2.5h should be > 0.7 for further gating of relevant targets. Other criteria were taken into account as well, including reasonable number of peptide numbers identified in the measurements (sequence coverage >20%) and number of bound proteins should be more than in total lysate. Samples were analyzed in an LTQ-Orbitrap system.

Four target deconvolution experiments were performed:

Linker derivative	Mother compound	Competition type	Beads	Coupling buffer	Coupling density used
VCC938609:01 (Styryl quinazolines)	VCC350485:02	-	NHS-Sepharose	50mM NaHCO ₃ +DMSO (50-50%)	2mM
VCC757274:08 (Oxindoles)	sunitinib VCC512891:01	Direct Indirect	NHS-Sepharose	50mM NaHCO ₃ +DMSO (50-50%)	2.5mM
VCC607440:01 (2-Amino-pyrimidines I.)	VCC512891:01 sunitinib	Direct Indirect	EPOXY-Sepharose	50mM Na ₂ CO ₃ +DMSO (50-50%)	4.2mM
VCC124075:02 (2-Amino-pyrimidines II.)	VCC124075:02	Direct	NHS-Sepharose	50mM NaHCO ₃ +DMSO (50-50%)	8mM

Table 3.1 Linker derivatives were covalently coupled to sepharose beads with the indicated coupling densities. Competition type refers to the core structure difference between the linker compound and the mother compound. Direct competition means that the core structure is identical to its linker derivative, in turn indirect competition means that compounds do not belong to the same structure class.

3.16 Kinase affinity experiments

Ten active compounds in the insulin ELISA were selected and tested for their binding affinity to kinases in a full kinome panel assay. The service was provided by DiscoverX¹⁶⁴. The screen was performed against 451 kinases (total of 392 non-mutant kinases) at 5μM. Briefly, the unknown test compounds were used to compete with immobilized control ligands against DNA labeled kinases. The identification of hits is based on detecting DNA-labeled kinases by qPCR, where lower signal intensity means that targets are bound and competed off by the test compound. The exact calculation for each target was:

$$\frac{\text{test cpd signal} - \text{positive ctrl signal}}{\text{negative ctrl signal} - \text{positive ctrl signal}} \times 100$$

test cpd signal = compounds submitted for testing

negative ctrl = DMSO (100% control)

positive ctrl = positive control compound (0% control)

Selectivity scores are calculated by dividing the number of kinases that compounds bind to by the total number of distinct kinases tested, excluding mutant variants:

$$S = (\text{number of non-mutant kinases with \%Ctrl} < 35) / (\text{number of non-mutant kinases tested})$$

3.17 Real-time QPCR (RT-PCR)

Total RNA was isolated using RNeasy Mini kit (Qiagen, 74104) including a DNase digestion step according to the user's manual. The cDNA was transcribed from RNA based on the following protocol:

1-1µl of "K1" annealing primer (5'-AAGCAGTGGTATCAACGCAGAGTACT(30)V N-3' where N = A, C, G, or T; V = A, G, or C) was added to 9µl of 3-5µg RNA (mix1) and heated at 65°C for 2min, then incubated at RT for 5min and 20s on ice. Mix2 was prepared: 4µl RT-puffer (Roche, 11 465 368 001); 2µl dNTPs (10mM); 1.5µl AMV Reverse transcriptase (Roche, 10 109 118 001); 1.5 µl DTT (0.1M); 1µl RNase inhibitor (Fermentas, EO0381) and added to mix1, then incubated for 2h at 42°C. Reaction was stopped by incubating the sample at 95°C for 2minutes. The cDNA was purified using the QIAquick PCR Purification Kit (Qiagen, 28104).

PCR reaction mix was prepared as follows: 6.25µl Fast SYBR® Green Master Mix (Life Technologies, 4385612) + 2.5µl primer mix (1.5µl+1.5µl of 100pmol stocks in 100µl water) + 3.75µl of cDNA (20ng). PCR reaction was run for 40 cycles on Abi StepOnePlus™.

Primers used in RT-PCR:

SUR1_Fw	CAGGACCAAGAGCTGGAGAAGGA	Cyclophilin B_Rev	GCCAAATCCTTCTCTCCTGTAGC
SUR1_Rev	CATCCAGCAGAAGGCCATCTCTT	MAST1_Fw	TACCTAGGTGCCTCGTCACA
SUR2A_Fw	GGAGTGCGATACTGGTCCAAACCT	MAST1_Rev	TGTAGTTTCGGTGACAGCCC
SUR2A_Rev	CCCgatgcagagaacgagacact	STK16_Fw	TTCAAGAGAGGTACTACTGTGGAATG
SUR2B_Fw	CATAGCTCATCGGGTTCACACCATT	STK16_Rev	TTCAGGTCCTGTGTGCATAAC
SUR2B_Rev	GCATCGAGACACAGGTGCTGTTGT	CSNK2A1_Fw	CCAAGGTTCTGGGAACGGAA
Kir6.1_Fw	AGCTGGCTGCTCTTCGCTATCA	CSNK2A1_Rev	TTACGGGAGTGTCTGCCCAA
Kir6.1_Rev	CCCTCCAAACCAATGGTCACT	AAK1_Fw	AAGTTTTCTCGACTCCAGGCGG
Kir6.2_Fw	CAACGTCGCCCCACAAGAACATC	AAK1_Rev	GACGAGAGCGAATCCACCTTC
Kir6.2_Rev	CCAGCTGCACAGGAAGGACATG	SLK_Fw	ATCTTCAAGTTGGGGAGCGAG
β-Actin_Fw	CCTCTATGCCAACACAGTGCTGTCT	SLK_Rev	CTCCTTATTCTGGGCCTTATACACT
β-Actin_Rev	GCTCAGGAGGAGCAATGATCTTGA	MARK2_Fw	TAAGTCCAACATGCTGCGGG
GAPDH_Fw	AGACAGCCGCATCTTCTGTG	MARK2_Rev	ACAGCTACTCTTTCCCGTC
GAPDH_Rev	TGATGGCAACAATGTCCACT	JNK2_Fw	TGGGCTACAAGGAGAATGTTGA
Cyclophilin B_Fw	CTCCGTGGCCAACGATAAGAA	JNK2_Rev	AACTCTGCGGATGGTGTTC

3.18 Western Blot

Cells were lysed in CellLytic M (Sigma, C2978) lysis buffer supplemented with aprotinin (4µg/ml), NaF (10mM), PMSF (1mM), NaOV (1mM), Phosphatase inhibitor cocktail 2 (Sigma, P5726) and using cell scrapers lysate was collected and centrifuged at 4°C, 12.000 rpm for 20 minutes. 15-20µg protein was loaded in 8-10% SDS-gels. Gel electrophoresis was performed at 150V for 1h. Proteins were then transferred onto nitrocellulose membrane (GE) for 1.5 h at 0.8 mA/cm² using transblot-SD buffer and semi dry blotting technique. Afterwards, protein bands were stained on the membrane with Ponceau S (2 g/L in 2 % TCA) if necessary. The membrane was destained in TBST or NET-gelatine and blocked in the appropriate buffer containing 5% milk or 5% BCA for 1h at RT. Then antibody was diluted according to the manufacturer's instruction and added to the membrane for overnight incubation at 4 °C. On the following day HRP-conjugated secondary antibody was applied for 1h at RT. Luminescent signal was developed with Enhanced ChemiLuminescent (ECL) Kit (PerkinElmer/NEN, Köln, NEL104001EA) before detecting signal on Hyperfilm TM MP (Amersham Pharmacia, Freiburg). Between steps membrane was washed 3x15min with TBST or NET-Gelatine. Membranes were stripped (strip buffer, 50°C, 1h) and checked for sample loading accuracy with α -tubulin antibody. The following antibodies were used: p-AMPK- α (2531); p-CREB (9196); p-PKAc (4781); p-mTOR (2971); p-MEK1/2 (9154); p-ERK1/2 (9101); p-PKC-pan (9371); p-PKC α / β II (Thr638/641) (9375); p-PKC ζ / λ (Thr410/403) (9378); p-Tyr (9411); p-Thr (9381) from Cell Signaling; pSer (804-164-C100) from Alexis; Goat Anti-Mouse IgG secondary Ab (115-035-003) from Jackson Immuno Research; Goat Anti-Rabbit IgG Ab (172-1019) from Biorad.

3.19 Excel macro for the analysis of more than 2 sets of protein targets

As it was planned to perform 6 target deconvolutions, I have prepared an excel macro to compare more than two sets of targets. By this method the overlapping target hits for each compound could be quickly identified using their UniProt identifiers. The full macro code (MS Excel 2010) is included in *Appendix*.

3.20 In silico prediction of ADME properties of the compounds

In silico Pharmacokinetic (PK) and ADME parameters were predicted with the Schrödinger software package Qikprop in cooperation with F. Baska (Vichem Chemie Ltd.). Predicted descriptor values and ranges are included in *Appendix*.

3.21 Buffers and solutions

Coupling solutions for preparation of affinity matrices: depending on the solubility of linker derivatives, either DMSO or DMF was used mixed with 50mM NaHCO₃ (pH=8.5-9 for NHS beads) or Na₂CO₃ (pH=12-13 for Epoxy beads) in 1:1 ratio. In certain cases EtOH/DMF or EtOH/DMSO pH adjusted with TMEA (tetramethylammonium hydroxide, Acros Organics, AC42053) was used as coupling solution.

Extracellular solution for patch clamping: 138.0 mM; NaCl; 5.6 mM KCl; 11.1 mM Glucose; 1.2 mM; MgCl₂; 2.6 mM CaCl₂; 10.0 mM HEPES

HEPES Lysis Buffer for MS experiments and pre-experiments: 50mM HEPES (pH 7.5); 150mM NaCl; 0.5 % Triton X-100; 1mM EDTA; 1mM EGTA; 10mM NaF; 2.5mM Na₃VO₄; 1% Phosphatase Inhibitor Cocktail 3 (Sigma, P0044); 1 cComplete Protease Inhibitor Cocktail Tablet (Roche,) / 50ml ; 10µg/ml aprotinin; 10µg/ml leupeptin; 1mM PMSF

Intracellular solution for patch clamp experiments: 185 mM Potassium-gluconate (Sigma); 13 mM HEPES; 13 mM NaCl; 1 mM MgCl₂; 1 mM ATP (Sigma); 1 mM GTP (Sigma)

Krebs Ringer Buffer (KRBH): 134mM NaCl; 3.5mM KCl; 1.2mM KH₂PO₄; 0.5mM MgSO₄; 1.5mM CaCl₂; 5mM NaHCO₃; 10mM HEPES; 0.05% BSA (Sigma)

Laemmli buffer (3x): 100 mM Tris/HCl pH 6.8; 3 % SDS; 45 % Glycerol; 0.01 % Bromphenol blue; 7.5 % beta-mercaptoethanol

MTT stop solution: 9.5 % SDS; 5 % 2-Butanol; 0.012 M HCl

NET-gelatine: 50 mM Tris/HCl pH 7.4; 5 mM EDTA; 0.05 % Triton X-100; 150 mM NaCl

PBS: 137 mM NaCl; 27 mM KCl; 81 mM Na₂HPO₄; 1.5 mM KH₂PO₄

Running buffer for western blot: 25 mM Tris/HCl pH 7.5; 200 mM Glycine; 0.1 % SDS

Strip buffer: 62.5 mM Tris/HCl pH 6.8; 2 % SDS; 100 mM beta-mercaptoethanol

TBST: 24.2g Tris HCl; 80g NaCl; pH adjusted to 7.6 with HCl and total volume to 1000ml;
+0.05% Tween 20

Transblot SD: 50 mM Tris/HCl pH 7.5; 40 mM Glycine; 20 % Methanol; 0.004 % SDS

4 RESULTS

4.1 A phenotype-based drug and target discovery project

Out of the several beneficial effects of kinase inhibitors observed in diabetes, we focused on the insulin secretagogue effect of sunitinib. We tested sunitinib in different beta cell lines and found that it induced insulin secretion. With this object a compound library (558 members) was prepared by Vichem Chemie Ltd. (D. Erős). Their kinase inhibitor profiles were predicted to be analogous/overlapping with that of sunitinib, however they were structurally diverse and different. A semi-high throughput insulin ELISA assay was set up to start a phenotypic compound screening, looking for candidates with strong insulinotropic effect. Nevertheless many of them are derived from known cores of approved drugs, modifications in their structures (side group replacement, position change, extension or simplification of the structures) led to significant changes in their target profiles and phenotypic effects. For our primary screen we used the RIN-5AH rat insulinoma beta cell line. In further experiments other rodent derived beta cell lines (BRIN-BD11, INS-1E, TC6) were also included. These models are often used to study beta cell functions, since there are no immortalized human beta cell lines available yet. However recently a few human hybrid beta cell lines were established and some of them are stated to produce insulin¹⁶⁵. The steps of our target discovery strategy are displayed in *Figure 4.1*.



Figure 4.1 Steps of phenotypic based drug discovery. Sunitinib increased insulin secretion in different beta cells lines and insulin dosing could be eliminated in diabetic patients. Based on this observation we selected 558 compounds to use them as tools to identify common targets and/or mechanisms responsible for insulin secretion.

4.2 Results of the primary screen of insulin secretion in RIN-5AH cells

Since initial experiments were conducted with RIN-5AH (and beta-TC6) cell lines¹⁵⁴, therefore RIN-5AH was selected to screen compounds for insulin secretion. Insulin ELISA was used for the measurement of insulin secretion of an initial library consisting of 558 compounds. Treatment was performed at 5 μ M & for 2h.

4.2.1 Efficient compounds

An excellent hit rate of ~10% was observed in the assay. Some compounds induced insulin release from the beta cells (there were 128 compounds with higher than 20% insulin secretion) and some of them showed a negative effect, which could be either due to toxicity or because of negative modulation of insulin secretion (*Figure 4.2.1*). The *Figure 4.2.2* displays hit distributions. From this set of compounds we have chosen the best 80 candidates for further confirmation. 55 compounds could be confirmed and finally clustered into different core structure families (Chapter 4.4).

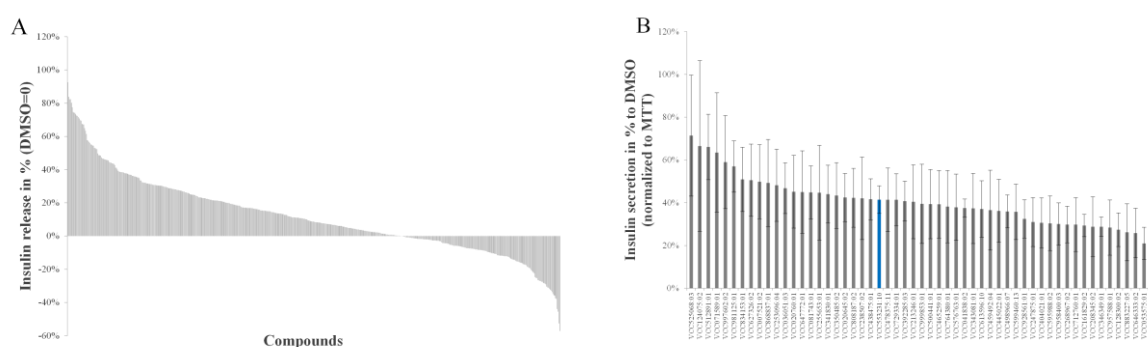


Figure 4.2.1 **A.** Displaying the effect on insulin secretion of 558 compounds. Sunitinib has an effect of ~60%. Compounds with more than 20% percent of insulin secretion were considered active. **B.** 55 compounds were confirmed later on for insulin secretion. Sunitinib is highlighted with blue color. (n=4)

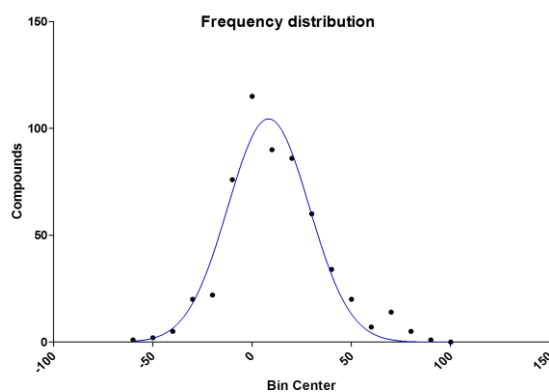


Figure 4.2.2

Gaussian distribution displays the efficiency (insulinotropic action) of compounds. The median of the curve is slightly shifted to the direction of higher insulin secretion (x-axis, median = 8,6), which reflects to the relatively high hit rate in the assay. Moreover since many of the compounds were originally designed to inhibit kinases and the median of the curve is positive, it is also likely that kinases are playing role in the mechanism of action.

4.2.2 In vitro toxicity studies

Cell viabilities were checked either by MTT assay (after treatment with compounds for 2h at 5 μ M) or with CellTiter-Glo for longer incubation times. In the primary screen we ruled out 40 highly toxic compounds (out of 558) that showed decreased MTT activity after 2h and 5 μ M treatment. These compounds have reduced cell viability in CellTiterGlo assay by at least 30%. We found some structure-activity relationships responsible for “acute toxicity” in some of the core structure groups (see Appendix). The 24h treatment revealed additional 2 toxic compounds (*Figure 4.2.3*) It should be noted that since MTT assay readout is proportional with mitochondrial activity and with functional NADPH oxidoreductase enzymes¹⁶⁶⁻¹⁶⁸, diminished reduction of the dye is associated with decreased metabolism of the cell, which in turn could also affect glucose metabolism not only viability. Similar is the mechanism for CellTiter-Glo assay, which detects the ATP level.

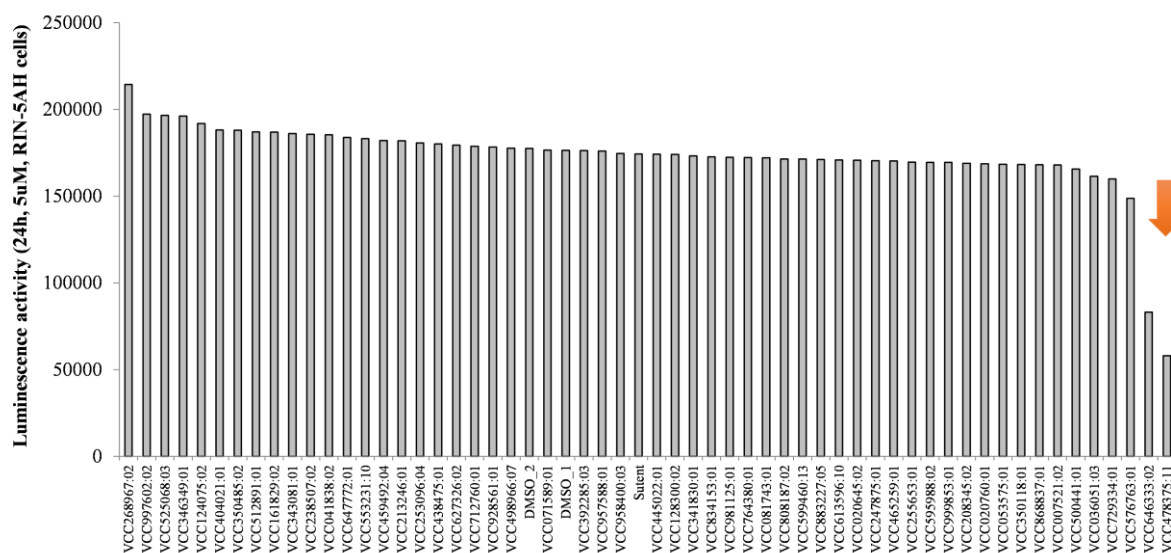
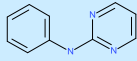
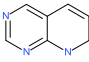
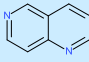
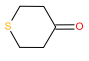
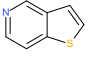
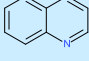
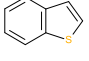
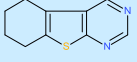
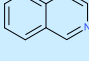
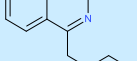


Figure 4.2.3 CellTiter-Glo. Most of the “55 efficient compounds” did not decrease the viability after 24h, 5 μ M treatment in RIN-5AH cells. Two, probably toxic compounds are indicated with the arrow.

4.2.3 Clustering the hits into different core structures

The most efficient compounds were clustered and their core structures are summarized in *Table 4.2.1*. The initial compound library of 558 compounds was extended with additional members from the styryl-quinazoline, quinoline and thieno-pyrimidine groups in order to set up qualitative structure-activity relationships.

	Core structure family	Core structure	Insulin release >25 %	Insulin release <25% or probably toxic	Total No. Of tested cpds	Hit rate
1	N-phenylpyrimidin-2-amine		20	22	42	47,6%
2	7,8-dihydropyrido[2,3-d]pyrimidine		5	20	25	20,0%
3	1,6-naphthyridine		5	11	16	31,3%
4	tetrahydrothiopyran-4-one		0	3	3	0,0%
5	thieno[3,2-c]pyridine		1	1	2	50,0%
6	quinoline		25	22	47	53,2%
7	benzothiophene		3	16	19	15,8%
8	5,6,7,8-tetrahydrobenzothiopheno[2,3-d]pyrimidine ("Thieno-pyrimidine")		29	46	75	38,7%
9	quinazoline		3	12	15	20,0%
10	4-quinazolin-4-ylbutyl ("Styryl quinazoline")		51	3	54	94,4%

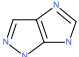
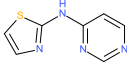
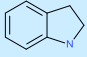
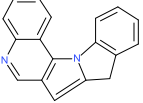
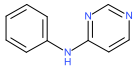
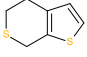
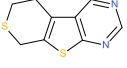
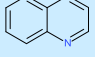
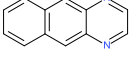
11	1,6-dihydroimidazo[4,5-c]pyrazole		1	1	2	50,0%
12	N-pyrimidin-4-ylthiazol-2-amine		0	1	1	Dasatinib
13	indoline (including "oxindols")		17	14	31	54,8%
14	Misc. 1		1	0	1	100,0%
15	N-phenylpyrimidin-4-amine		4	22	26	15,4%
16	5,7-dihydro-4H-thieno[2,3-c]thiopyran		1	1	2	50,0%
17	Misc. 2		2	7	9	22,2%
18	quinoxaline		7	8	15	46,7%
19	benzo[g]quinoxaline		2	22	24	8,3%
20	+Other misc. structures					

Table 4.2.1 Example core structures of insulin secretion inducer compounds including the highlighted core structures. Compounds with these core structures (highlighted in blue) were more extensively studied later on.

4.2.3.1 Highlighted Core structures and structure-activity relationships (SAR)

Based on the confirmation of 55 efficient compounds, we clustered the hits and highlighted the most promising core structures: oxindoles, thieno-pyrimidines, styryl-quinazolines, other quinazolines, quinolines, quinoxalines, 1,6-naphthyridines, 2-amino-pyrimidines, and some additional efficient compounds were included in miscellaneous structural groups. We established qualitative structure activity relationships in quinoline, thieno-pyrimidine and styryl-quinazoline groups (Figures 4.2.4a-c).

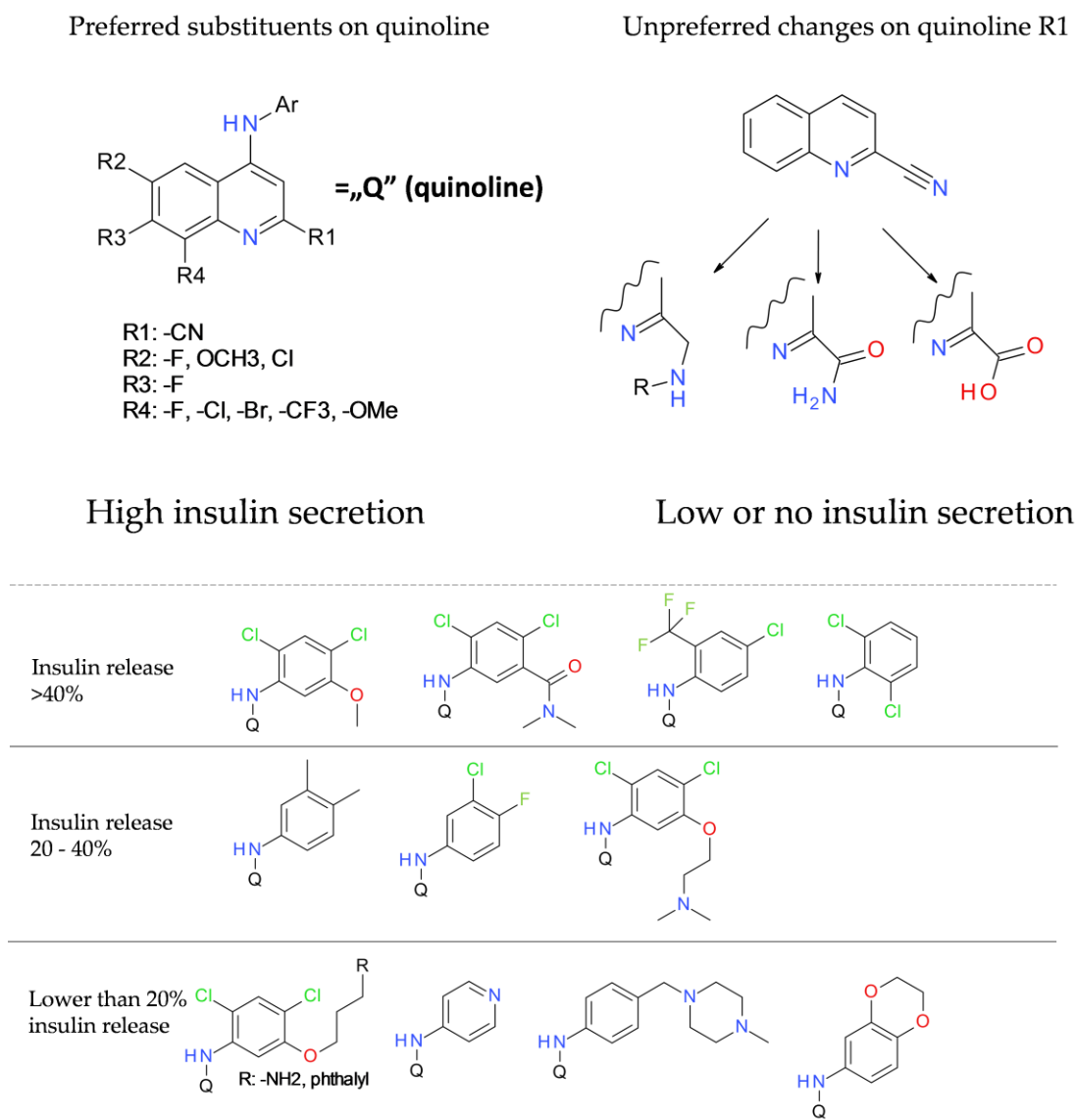


Figure 4.2.4a *Quinoline SAR. Core structure is displayed separately for the quinoline (top) and aryl (bottom) ring of the molecule. Preferred and unpreferred substituents and the rate of insulin secretion in RIN-5AH beta cells are displayed.*

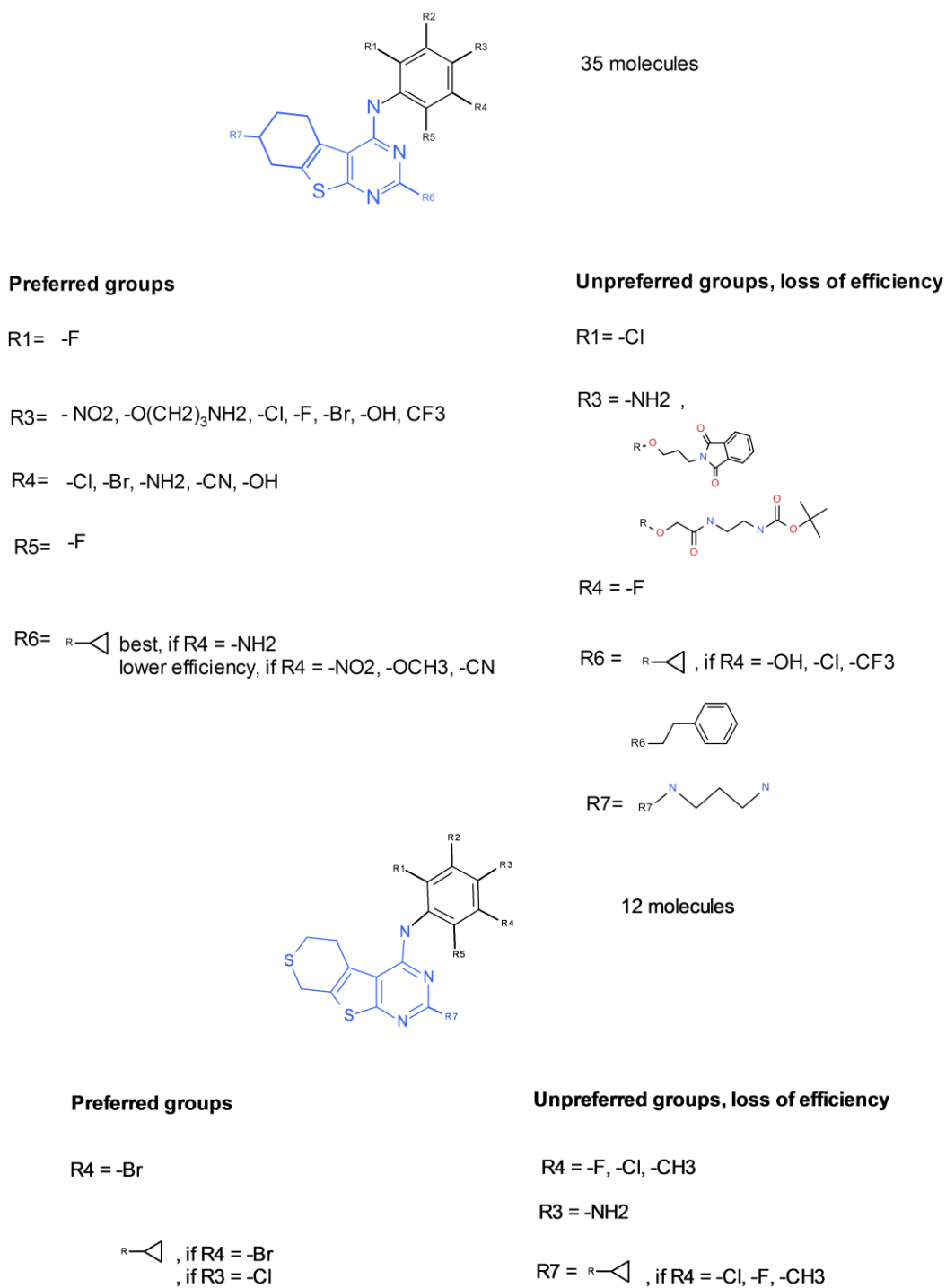


Figure 4.2.4b Thieno-pyrimidine SAR. The core structures and functional groups are displayed where SAR could be defined. Preferred substituents produced >20% insulin secretion in RIN-5AH cells.

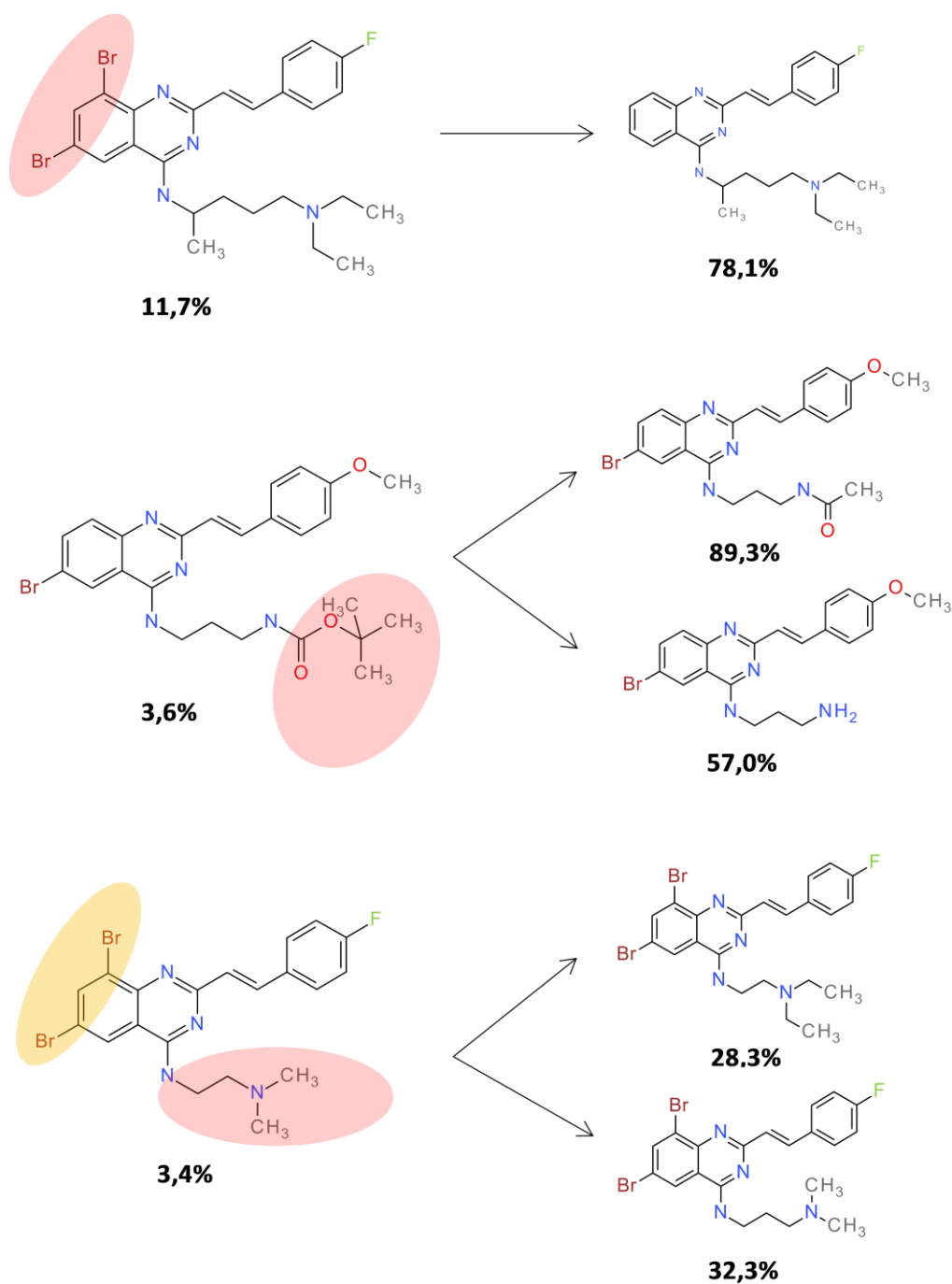


Figure 4.2.4c Styryl-quinazoline SAR. 3 ineffective compounds were found out of total 54 tested derivatives. Removing the 6,8 positioned Br substituents from the quinazoline ring significantly improves the efficiency of the compound (up), as well as removing BOC group from the aliphatic primer amino part of the molecule increases the insulinotropic effect (middle). A slight improvement in insulin secretion could be achieved when modifying the aliphatic part of the molecule (bottom). The insulin secretion in RIN-5AH cells is displayed in % under the structures.

4.2.4 Insulinotropic action of some marketed kinase inhibitors in RIN-5AH cells

Several clinically approved kinase inhibitors were also included in our ELISA screen as reference compounds. Based on the results of the primary screen we found no correlation between general kinase inhibitor property and insulin release. In our assay sunitinib and the imatinib derivate, missing the “magic methyl group” had stable insulinotropic property. This methyl group on the diaminophenyl ring serves also as a selectivity switch for PKC or Bcr-Abl kinases^{169,170} and probably it regulates the overall selectivity as well. Further kinase inhibitors showing weak or no insulinotropic effect in the primary screen were: dasatinib, sorafenib, tivantinib (*Figure 4.2.5*). Besides sunitinib, the small molecular inhibitors imatinib, dasatinib and sorafenib were also reported to have glycemic effects in clinical patients^{149,171,172}.

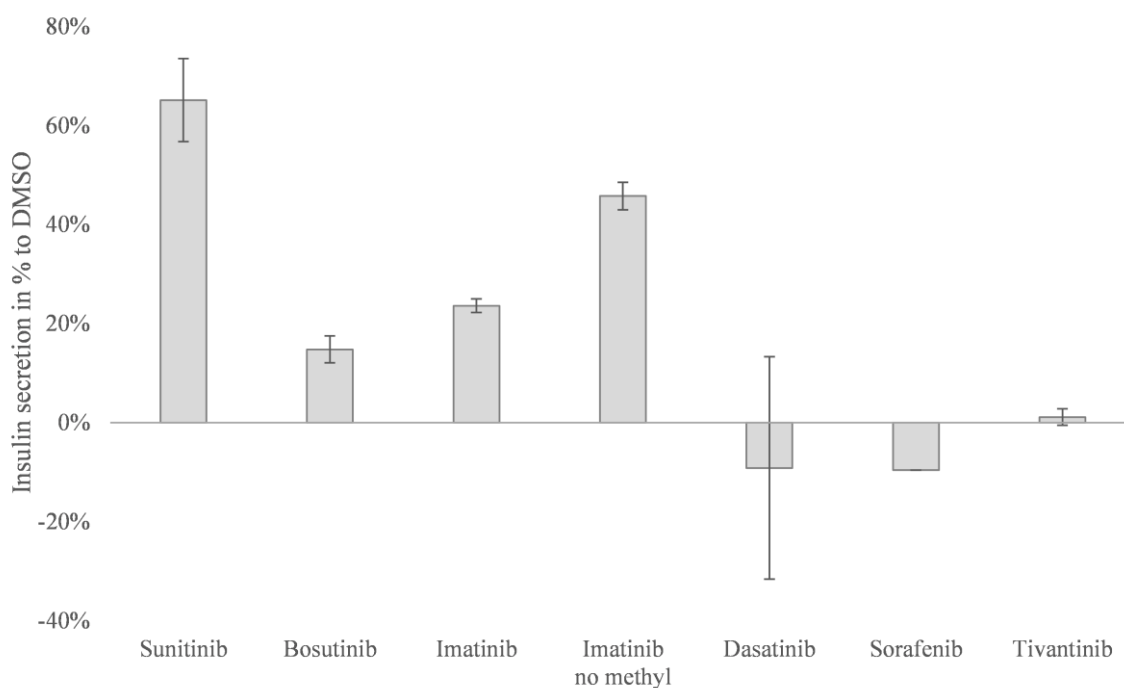


Figure 4.2.5 Some commercially available kinase inhibitors were included in the primary screen. It is worth to note that the derivative of imatinib lacking the methyl group was more active in insulin ELISA assay.

4.3 Glucose sensitivity of different beta cell lines

Glucose stimulated insulin secretion (GSIS) is one of the main physiological regulation mechanisms of insulin secretion, therefore it was important to include a cell line that secrete insulin in a glucose concentration dependent manner in our in vitro experiments. INS-1E cells proved to be the most sensitive and reliable model for testing GSIS¹⁷³. In other cells lines (RIN-5AH, beta-TC6, BRIN-BD11) GSIS was not observed, however BRIN-BD11 is also claimed to have this property^{174,175}. GSIS of different cell lines was tested in medium or KRBH buffer and the increase of insulin release was glucose dependent only in INS-1E cells (*Figure 4.3.1*).

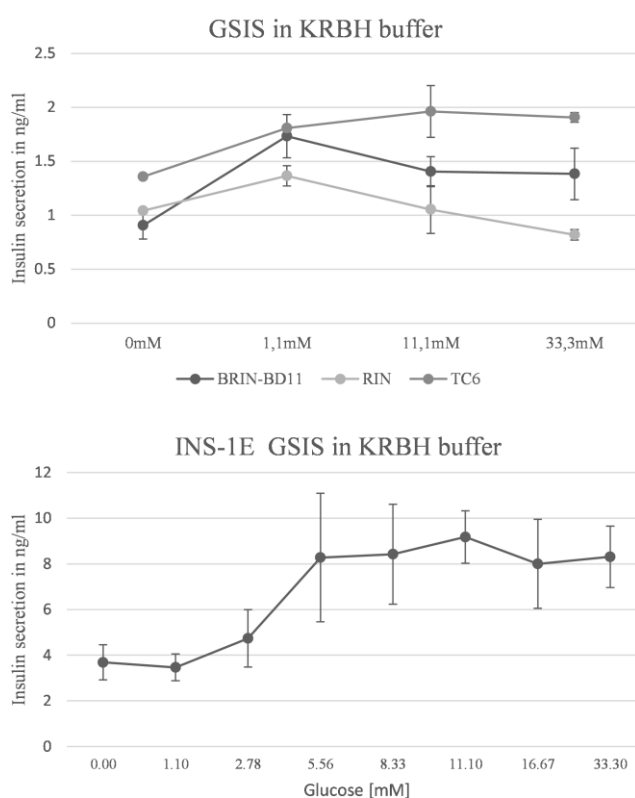


Figure 4.3.1 GSIS in different beta cell lines. Only INS-1E seems to be sensitive to GSIS, the RIN-5AH, TC6 and BRIN-BD11 didn't show any difference in insulin secretion between 1mM and higher concentrations of glucose.

4.4 Characterization of the most effective compounds

Altogether 12 compounds (including sunitinib) were selected as best hit compounds, at least one from each structure family. Compounds from this list were more extensively studied later on (*Table 4.4.1*). They increased insulin secretion in a concentration dependent manner and showed >25% insulin secretion in RIN-5AH cells. EC₅₀ values were calculated for the best candidates (*Figure 4.4.1*). Cell viability was determined after 72h treatment with the compounds in RIN-5AH cells and an “in vitro therapeutic index” (TI) was calculated, which reflects the relatively lower toxicity of the compounds compared to sunitinib (*Table 4.4.2a*). The TI was above 2 for most of the compounds, the highest TIs were observed for VCC036051:03 (8.54) and VCC981125:009 (6.19). The compounds were tested for in vitro toxicity in different cell lines as well (*Table 4.4.2b*). None of the compounds showed any decrease in viability up to 10µM treatment in C2C12 cells. Some compounds had a lower than 5µM IC₅₀ value in 3T3-L1, HepG2 and TC6 cells (VCC512178:08, sunitinib and VCC346349:01), however only one compound proved to be more toxic than sunitinib (VCC512178:08).

<i>Core structures</i>	<i>Compound ID</i>	<i>Insulin</i>	<i>properties already known / drugs with same core</i>
<i>Oxindoles</i>	sunitinib	55.9%	broad spectrum affinity to kinases
<i>Thieno pyrimidines</i>	VCC341830:01	38.6%	Selective EGFR inhibitor
	VCC834153:01	77.7%	
<i>Styryl-quinazolines</i>	VCC350485:02	40.5%	Derivative is a p53 inducer in HCT116 cells
<i>Other quinazolines</i>	VCC036051:03	35.7%	Contains core structure of erlotinib, gefitinib, lapatinib
	VCC981125:09	71.9%	Contains core structure of bosutinib, quinidine, chloroquine
<i>Quinolines</i>	VCC718565:01	101.4%	
	VCC673193:01	92.8%	
	VCC225733:01	72.7%	
<i>Bis-quinolines</i>	VCC405984:01	46.3%	
<i>Quinoxalines</i>	VCC958400:03	38.5%	
<i>1,6-Naphthyridines</i>	VCC459492:04	31.2%	
	VCC124075:02	32.7%	
<i>2-Amino-pyrimidines I.</i>	VCC512891:01	53.3%	Contains core structure of imatinib
	VCC346349:01	48.2%	
<i>2-Amino-pyrimidines II.</i>	VCC525068:03	82.4%	Inhibits PKC
	VCC161829:02	59.3%	Inhibits PAK
	VCC512178:08	72.2%	Inhibits PAK

Table 4.4.1 List of compounds that were selected for further research. Compounds in bold: kinase affinity profile is available. Insulin release is displayed in % to DMSO, 5 μ M and 2h treatment in RIN-5AH cells.

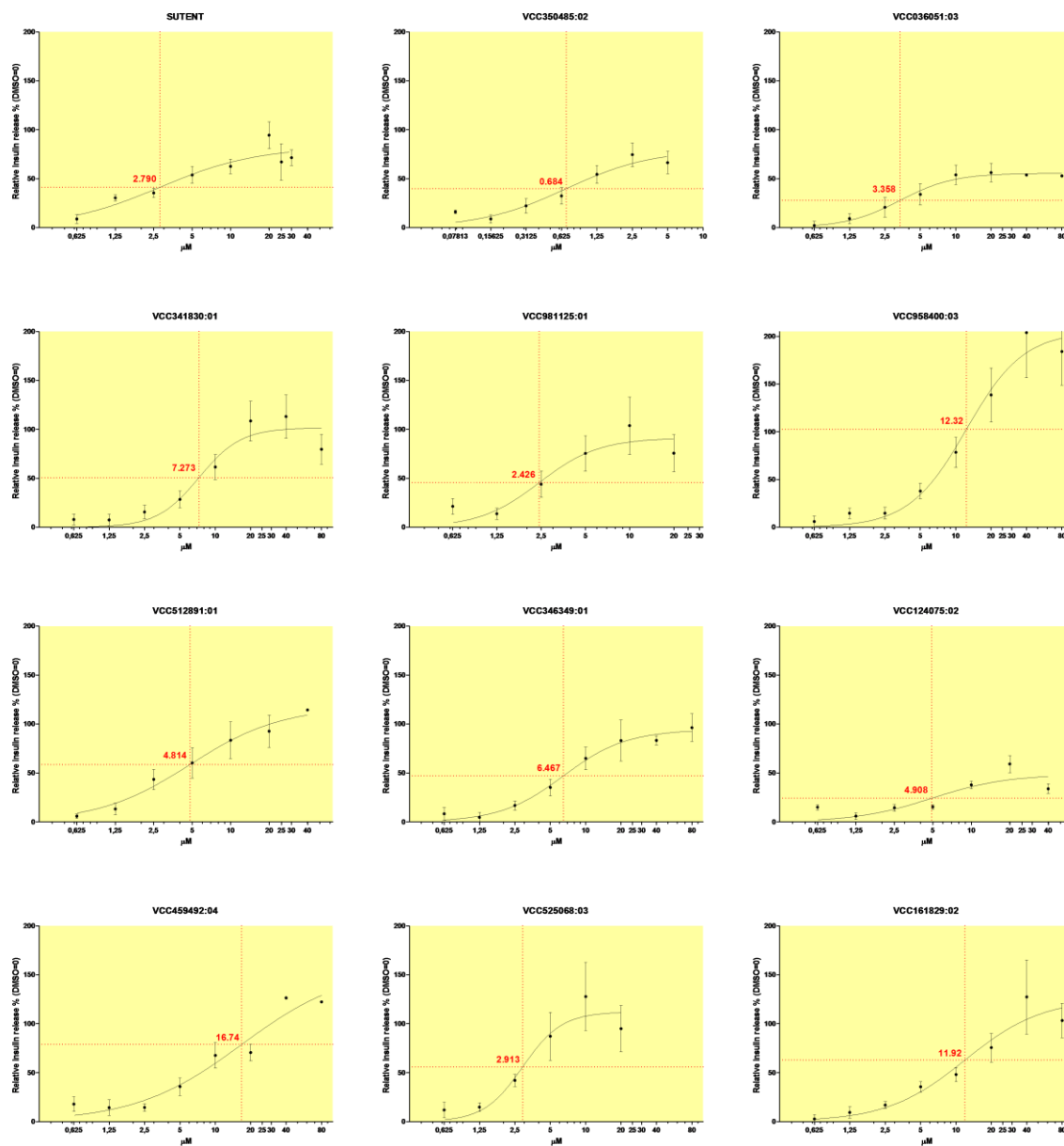


Figure 4.4.1 Concentration dependent effect on insulin secretion. EC50 values are displayed on the graphs for each compound. It is worth to mention that the total activity where the plateau is reached is different for the compounds.

Compound	EC50	IC50	"In vitro" TI
SUTENT	2.79	6.43	2.30
VCC350485:02	0.68	2.96	4.32
VCC036051:03	3.36	>20	8.54
VCC341830:01	9.84	>20	2.84
VCC981125:09	2.43	15.02	6.19
VCC958400:03	12.32	>20	>1.67
VCC512891:01	4.81	12.08	2.51
VCC346349:01	6.47	13.99	2.16
VCC124075:02	5.58	>20	4.60
VCC459492:04	16.74	>20	3.13
VCC525068:03	3.59	12.22	3.40
VCC161829:02	11.92	>20	>1.67

Table 4.4.2a Summarized EC₅₀ for insulin release, IC₅₀ viability values for 72h CellTiterGlo experiments and calculated "in vitro therapeutic indexes" (TI) values for RIN-5AH cells.

Compound	3T3-L1	C2C12	HepG2	TC6
VCC350485:02	5.942	>10	5.65	5.403
VCC036051:03	>10	>10	>10	>10
VCC834153:01	>10	>10	14.39	14.54
VCC341830:01	>10	>10	>10	11.9
VCC981125:09	>10	>10	>10	>10
VCC958400:03	>10	>10	>10	>10
VCC512891:01	6.802	>10	12.27	10.02
SUTENT	2.138	>10	5.742	6.056
VCC346349:01	7.734	>10	>10	3.99
VCC124075:02	6.286	>10	10.9	10.34
VCC459492:04	>10	>10	>10	>10
VCC525068:03	13.11	>10	>10	8.326
VCC512178:08	3.469	>10	3.979	2.288

Table 4.4.2b CellTiterGlo. IC₅₀ values (uM) of compounds are shown on different cell lines for 72h treatment. IC₅₀ values <5uM are highlighted in bold.

4.5 Selected best compounds were more selective than sunitinib

Since these compounds were originally designed as kinase inhibitors, their affinity and selectivity were tested against 392 kinases¹⁶⁴. The service was provided by DiscoverX. Most of the compounds were more selective than sunitinib and had better (VCC981125:09) but at least comparable impact on insulin secretion in RIN-5AH cells (*Figure 4.5.1*). The VCC124075:02 was the least selective of all compounds beside sunitinib ($S > 0.5$). The VCC512891:01, VCC346349:01 and VCC459492:04 shared moderate selectivity ($0.5 > S > 0.1$). The VCC350485:02, VCC036051:03 and VCC341830:01 were highly selective ($S < 0.1$). The VCC350485:02 binds FLT3 kinase and its numerous mutant forms selectively with high affinity (%Ctrl <20). It binds other kinases as well but with much lower affinity: CSNK1A1, RIOK3, GAK ($35 > \%Ctrl > 20$). VCC341830:01 is highly specific for EGFR, HER2, MKNK2 and KIT (%Ctrl <20) and binds several other kinases with lower affinity ($35 \geq \%Ctrl > 20$; IRAK3, RIPK2, GAK, TYK2, LTK). The VCC036051:03 binds two kinases selectively but with relatively low affinity ($30 < \%Ctrl < 40$; BMPR1B, MAP3K1). The VCC981125:01 and VCC958400:03 seemed to have no affinity to kinases (no hits at %Ctrl <35). The full profiling data is available in the *Appendix* separately for each compound.

Regarding to our main hypothesis that compounds probably share common kinase targets which can induce insulin secretion upon their inhibition, we planned to create a pool of overlapping kinase hits, but first, these targets had to be validated by MS to get information also about their presence in the RIN-5AH cell lysate (Chapter 4.6).

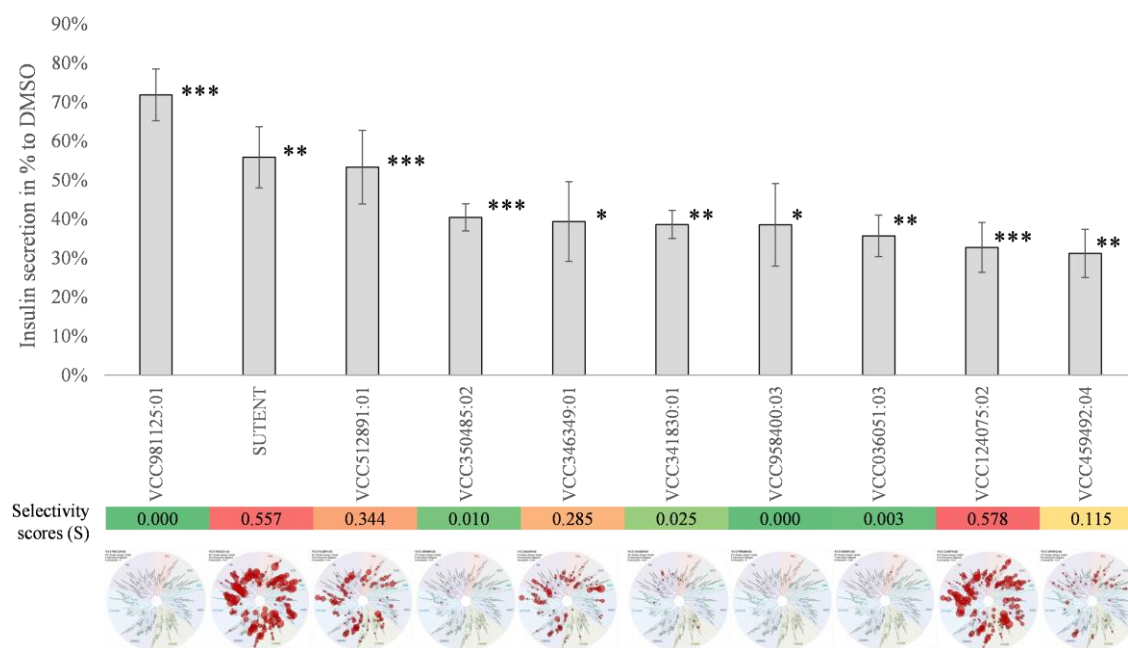
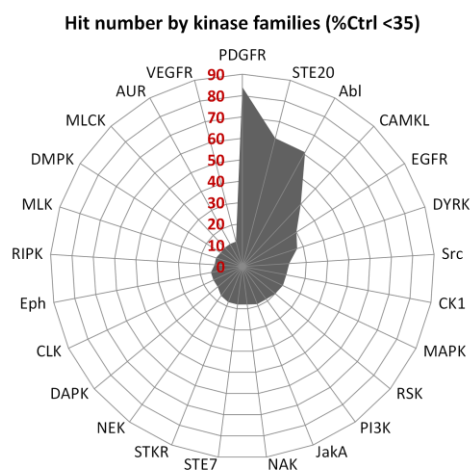
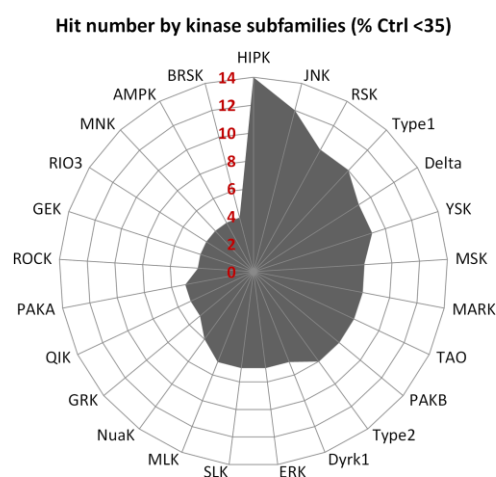


Figure 4.5.1 Insulin secretion is displayed on the diagram in % to DMSO in RIN-5AH cells ($n=4$; $*p<0.01$; $**p<0.005$; $***p<0.001$). Selectivity scores and kinome-trees are displayed under the bars (service by DiscoverX). Selectivity score (S) = (number of non-mutant kinases with %Ctrl < 35) / (392 non-mutant kinases tested)

The following figures highlight the kinase families and subfamilies that were most frequently hit by the compounds in the kinase affinity screen, however it does not mean that they are responsible for insulin secretion, indeed we think that off-targets (not main targets of the compound) or a combination of targets are more important in the matter of enhanced insulin secretion.



Frequent hits for all compounds were sorted by *kinase families*. 25 kinase families with most hits are shown (most hits were found in the PDGFR family = 84 kinases).



Frequent hits for all compounds were sorted by *kinase subfamilies*. 25 kinase subfamilies with most hits are shown (most hits were found in the HIPK subfamily = 14 kinases).

4.6 MS affinity chromatography using RIN-5AH cell lysate

Using the MS-based target deconvolution we could confirm targets from kinase affinity assay and their expression in the RIN-5AH cells. This technique is based on the binding affinity of compounds to protein targets which is independent of ATP concentration, therefore we can identify compounds with different binding modes. Altogether 20 amino-linker derivatives (“kinators”) were prepared and according to the criteria (see materials and methods) some of them were selected to perform the coupling experiments. Compounds were synthesized for oxindole, thieno-pyrimidine, styryl-quinazoline, quinoline, quinoxaline, 1,6-naphthyridine, amino-pyrimidine and misc. families (for some core structures more linker derivatives were available with distinct linker positions on the molecule). Four candidates were selected and analyzed by MS in the final experiments. These compounds showed specific binding or specific competition (target pull-down) in the pre-experiments as well.

4.6.1 Pre-experiments for MS- based target deconvolution

Linker derivatives and their amino-protected versions were tested for insulin secretion (5 μ M, 2h) and then affinity matrices were generated so far as the derivatized compounds remained active. Affinity matrices were incubated with protein lysate and free compound, after that samples were run in SDS gel and silver staining was performed as described in materials and methods.

4.6.1.1 VCC350485:02 (Styryl-quinazoline)

Its acetyl-protected derivative and the unprotected kinator were also effective in RIN-5AH cells. Different coupling densities were tested (2mM, 6mM and 10mM) and based on these results, 2mM was chosen for the final experiment. At higher densities the chance of unspecific binders is increased. Specific binders could be detected with silver-staining, however apparently no proteins could be competed off from the matrix (*Figure 4.6.1*)

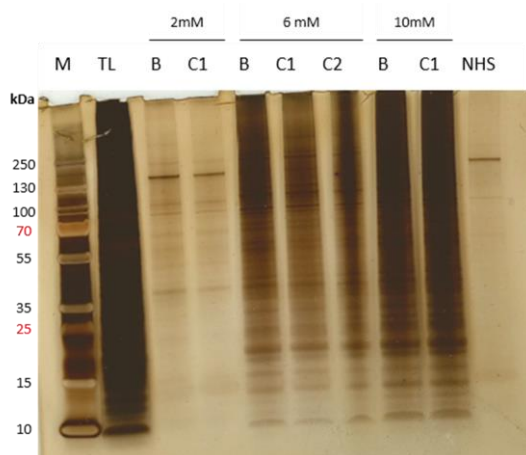


Figure 4.6.1

Silver gel staining of protein targets for VCC350485:02 matrix (2mM, 6mM and 10mM coupling densities).

M: Protein marker (Fermentas, #26619)

TL: Total lysate

B: Binders to the affinity matrix

C1: Competition with 50uM VCC350485:02

C2: Competition with 50uM Sunitinib

NHS: Empty NHS beads blocked with ethanolamine

No protein could be competed off that was visible by eye, however specific binders were detected.

4.6.1.2 Sunitinib (Oxindoles)

Acetyl protected derivative and kinator with the free primary amino group were effective (20%) but not the BOC protected. Reduced efficiency of the linker variant can be explained due its altered membrane permeability properties. This hypothesis is also supported by Schrödinger QikProp measurements using different prediction algorithms for testing pharmaceutically relevant properties of the compound structures, including Caco-permeability test, octanol/water logP, logS values. According to the Caco test, the linker derivative was ~4-fold less permeable (*See Appendix*). We assume that the binding affinity is changing because BOC is a “bulky group”, therefore it can strongly affect binding because of sterical hindrance. The effect of the kinator itself plays less importance in the cellular assay, because of its free amino group, its properties differ very much compared to the original lead molecule and the beads-coupled one. Linker derivative was tested in different coupling densities (2mM, 6mM and 8mM), for final experiment 2.5mM density was chosen (NHS beads). After silver staining, specific binders and competed off targets were also observed for sunitinib. Compounds possessing different core structures apparently did not compete off any proteins from the matrix, probably because of their binding modes or affinities are different (*Figure 4.6.2*).

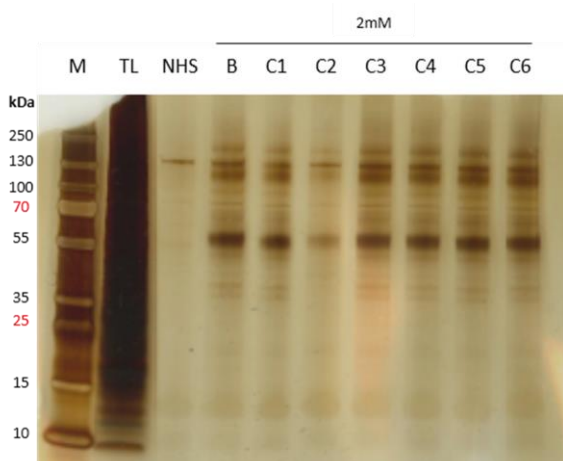


Figure 4.6.2

Silver gel staining of protein targets for Sunitinib affinity matrix (2mM coupling density) Direct and indirect pulldowns with different compounds.

M: Marker
TL: Total lysate
NHS: Empty NHS beads blocked with ethanolamine
B: Binders to affinity matrix of Sunitinib
C1: Competition with 50uM VCC341830:01
C2: Competition with 50uM Sunitinib (disappearing bands)
C3: Competition with 50uM VCC981125:01
C4: Competition with 50uM VCC346349:01
C5: Competition with 30uM VCC036051:03
C6: Competition with 50uM VCC350485:02

4.6.1.3 VCC512891:01 (Amino pyrimidines I.)

The protected amino derivative was effective in RIN-5AH cells (27%), weaker effect can be explained due to its lower permeability compared to the free linker derivative (see Appendix). After silver staining of gels specific protein enrichment and competition could be observed (Figure 4.6.3) Different coupling densities were tested on NHS beads (1.5mM, 3mM and 6mM) and 4.2mM density on epoxy beads. Coupling density used for final experiment was 4.2mM (epoxy beads).

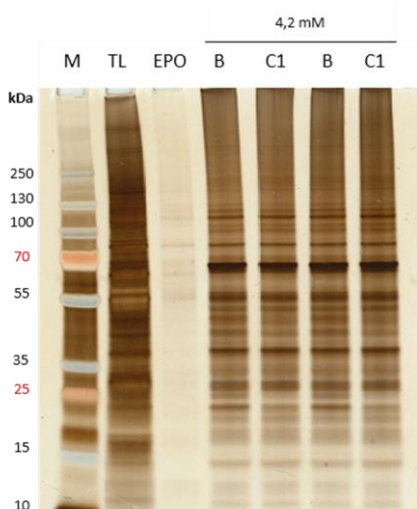


Figure 4.6.3

Silver gel staining of protein targets for epoxy coupled VCC512891:01 affinity matrix (4.2mM density).

M: Marker
TL: Total lysate
EPO: empty epoxy beads blocked with ethanolamine
B: Binders to affinity matrix of VCC512891:01
C1: Competition with 50uM VCC512891:01

Targets competed off at ~45kDa and ~25kDa

4.6.1.4 VCC124075:02 (Amino pyrimidines II.)

Formyl protected derivative was effective (23.8%) for insulin release, therefore NHS beads were used for coupling. Specific protein enrichment (binders) and competed targets were observed on silver stained gels (Figure 4.6.4). Coupling densities tested: 2mM, 4mM and 8mM. Coupling density used for final experiment was 8mM.

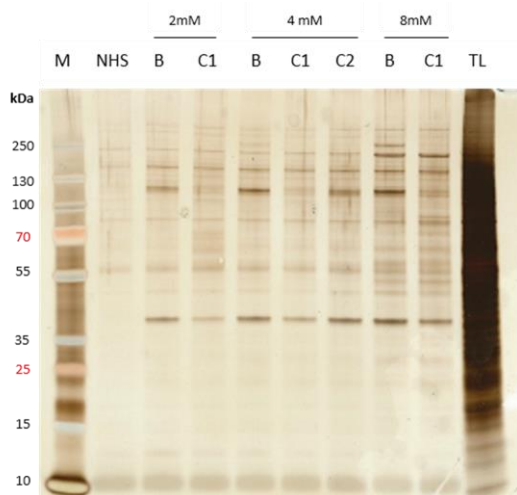


Figure 4.6.4

Silver staining of protein targets for VCC124075:02 matrix (densities: 2mM, 4mM, 8mM).

M: Marker

NHS: Empty NHS beads blocked with ethanolamine

B: Binders to affinity matrix

C1: Competition with 50uM VCC124075:02

C2: Competition with 50uM Sunitinib

TL: Total lysate

Targets competed off at ~120kDa, ~40kDa, ~250kDa

4.6.2 Target deconvolution results

The results and targets displayed in this chapter were selected by their $K_{d_{free}}$ and $K_{d_{imm}}$ values. The LC/MS-MS analysis and K_d values were calculated by an algorithm developed by Evotec AG.

VCC350485:02 linker derivative. Unfortunately no targets were competed off from the matrix, therefore $K_{d_{free}}$ values could not be determined. However specifically enriched binders ($K_{d_{imm}}$) were found which can still give a hint about the real targets of the mother compound. Hits with $K_{d_{imm}} < 90 \mu\text{M}$, peptide numbers ≥ 2 and sequence coverage $> 20\%$ were chosen. The main kinase target FLT3, from the kinase affinity screen was not enriched on the affinity matrix, probably because of its relatively low expression level in beta cells. FLT3 is mainly expressed in hematopoietic cells, thymus, lymph nodes, brain and gonads¹⁷⁶. We were focusing mainly on kinases but it is worth to mention other possibilities as well. Theoretically possible mechanisms and pathways related to insulin secretion were analyzed using the IPA software from Ingenuity, Qiagen, which is based on available literature findings. These potential targets include glycolytic enzymes (e.g.: aldolase A and pyruvate kinase) as well and were also described in a study to associate with K_{ATP} channels. Patch clamp measurements also showed that upon stimulation with their substrates (phosphoenolpyruvate or fructose-1,6-bisphosphate) K_{ATP} channel could be reversibly blocked¹⁷⁷, which in effect led to insulin secretion (*more detail in Figure 4.6.5*).

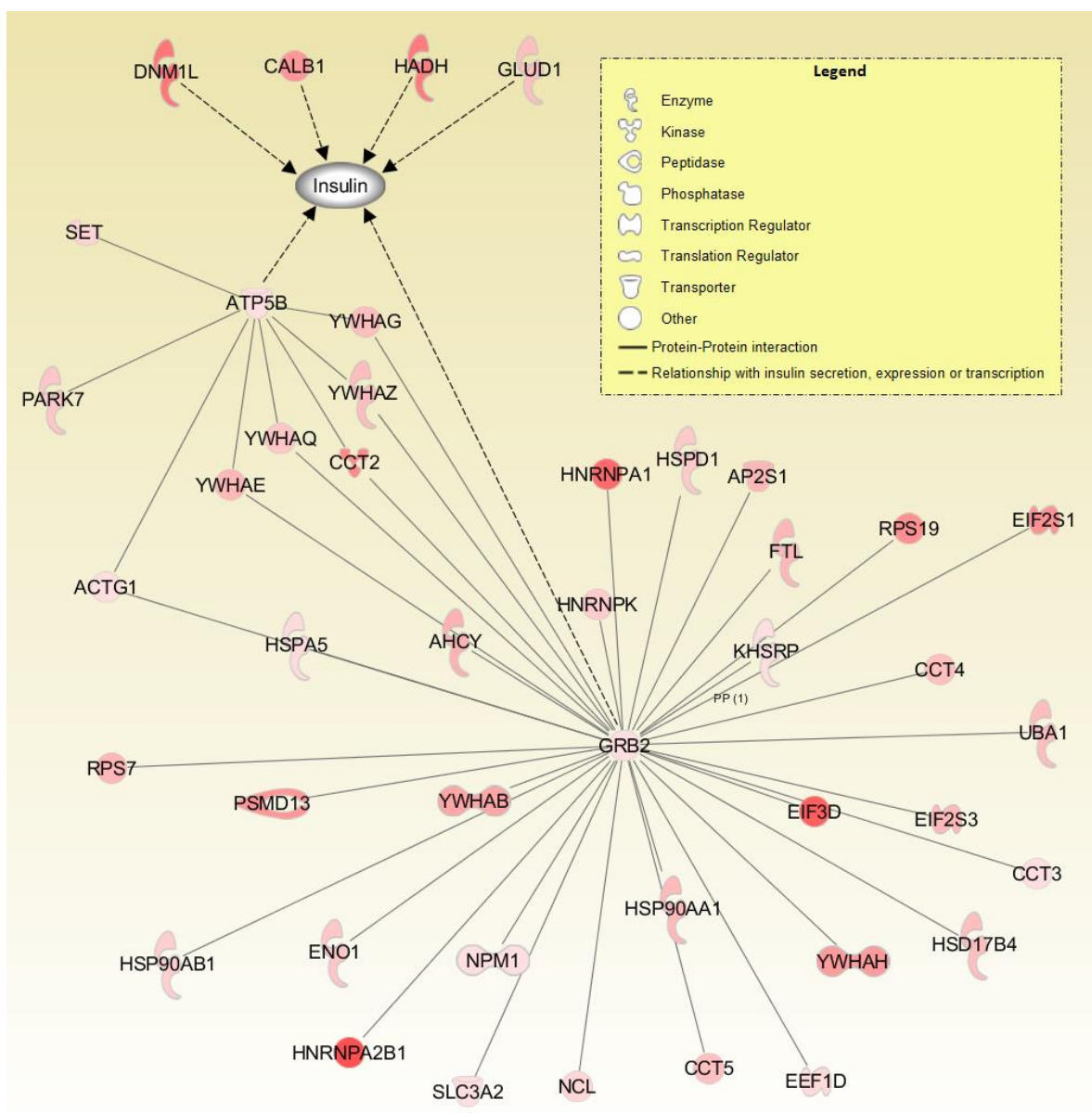


Figure 4.6.5 IPA Ingenuity pathway analysis (Qiagen). Binders for VCC350485 matrix and their relationship to insulin are depicted in the picture. Six targets were found by IPA analysis to play a role in the regulation of insulin secretion and are marked with dashed lines. Dominant negative mutant of DNM1L (Dynamin-1-like protein) was found to decrease GSIS insulin secretion in INS-1E cells¹⁷⁸; Calb1 (Calbindin) overexpression increased insulin mRNA level in RIN 1046-38 cells¹⁷⁹, another study showed that in knockout mice it induced insulin secretion¹⁸⁰; HADH (mitochondrial hydroxyacyl-coenzyme A dehydrogenase) was described to negatively regulate insulin secretion in INS832/13 β -cells and its loss of function mutation is associated with hyperinsulinemia⁴²⁻⁴⁵. In mice harboring the dysfunctional mutant an increased insulin level in blood was observed due to activation of glutamate dehydrogenase (GDH; GLUD1)¹⁸¹⁻¹⁸⁴. GDH stimulates glutamate conversion to α -ketoglutarate and as a consequence ATP is generated, which can induce insulin secretion⁴⁸. Interestingly GDH was also enriched on the matrix. Its activation promotes insulin secretion, conversely the knockdown reduces the effect. GRB2 and ATP5B is a binding partner of many other protein hits as well, therefore it seems that they are prone to form complexes thus they might not directly interact with the compound.

For the other compounds stronger evidence is available, since targets competed by the free compound could be identified. These targets were then compared to kinase affinity screen results.

Sunitinib. 124 targets were competed off (see $K_{d_{free}}$ values in the Appendix) from the sunitinib matrix and 70 of them are overlapping with the kinase affinity assay hits (Table 4.6.1). Threshold for kinase affinity screen were set to %Ctrl<55 and these potential targets were pooled together to compare the two methods and find the overlaps between them. The indirect competition with linker free derivate of sunitinib and VCC607440:01 matrix (VCC512891:01 linker derivative) resulted 49 hits. By comparing the direct and indirect competition experiments, 23 overlaps were found.

<i>Aak1</i>	<i>Camk2b</i>	<i>Gsk3b</i>	<i>Map3k15</i>	<i>Mek2</i>	<i>Pctk3</i>	<i>Src</i>
<i>Abl1</i>	<i>Camk2d</i>	<i>Insr</i>	<i>Map3k2</i>	<i>Mek5</i>	<i>Pdpk1</i>	<i>Stk16</i>
<i>Ampk1</i>	<i>Camkk2</i>	<i>Irak4</i>	<i>Map3k3</i>	<i>Melk</i>	<i>Phkg2</i>	<i>Tbk1</i>
<i>Ampk2</i>	<i>Chek1</i>	<i>Jak1</i>	<i>Map4k3</i>	<i>Plk3</i>	<i>Pip5k2c</i>	<i>Tlk2</i>
<i>Aurka</i>	<i>Csnk1a1</i>	<i>Jak2</i>	<i>Map4k5</i>	<i>Mst1</i>	<i>Plk4</i>	<i>Tnik</i>
<i>Aurkb</i>	<i>Csnk1d</i>	<i>Jnk2</i>	<i>Mark1</i>	<i>Mst2</i>	<i>Rps6ka4</i>	<i>Tnk1</i>
<i>Bike</i>	<i>Fak</i>	<i>Kit</i>	<i>Mark2</i>	<i>Mst3</i>	<i>Rps6ka5</i>	<i>Trka</i>
<i>Bmpr2</i>	<i>Fer</i>	<i>Lats1</i>	<i>Mark3</i>	<i>Nek2</i>	<i>Rsk1</i>	<i>Tyk2</i>
<i>Brsk2</i>	<i>Fes</i>	<i>Lyn</i>	<i>Mast1</i>	<i>Pak4</i>	<i>Rsk2</i>	<i>Ulk3</i>
<i>Camk2a</i>	<i>Gak</i>	<i>Map3k1</i>	<i>Mek1</i>	<i>Pak7</i>	<i>Slk</i>	<i>Yes</i>

Table 4.6.1

VCC512891:01. With this compound both direct and indirect competition was performed. We found 84 hits by competing off targets indirectly from the sunitinib matrix. Direct competition from its matrix analogue resulted 88 hits (see $K_{d_{free}}$ values in Appendix) and 25 of them overlapped with kinase affinity screen hits (Table 4.6.2). Targets from the kinase affinity screen were pooled where %Ctrl<55. Again, by indirect pull-down, the identified targets were different and only 12 overlaps have been found. This incoherence can be explained by the different affinities of sunitinib and VCC512891:01 to the proteins. Probably the binding modes of the two compounds also differ from each other.

<i>Aak1</i>	<i>Csnk2a1</i>	<i>Gsk3b</i>	<i>Map4k3</i>	<i>Pip5k1a</i>	<i>Slk</i>	<i>Taok3</i>
<i>Aurka</i>	<i>Dapk3</i>	<i>Jnk1</i>	<i>Mark2</i>	<i>Pip5k2b</i>	<i>Src</i>	
<i>Camk1</i>	<i>Fyn</i>	<i>Jnk2</i>	<i>Mast1</i>	<i>Pip5k2c</i>	<i>Stk16</i>	
<i>Camk2a</i>	<i>Gak</i>	<i>Limk2</i>	<i>Mink</i>	<i>Rock1</i>	<i>Syk</i>	

Table 4.6.2

VCC124075:02. We found 28 hits by directly competing off targets from its matrix analogue (see $K_{d\text{free}}$ values in Appendix), 14 of them overlapped with kinase affinity screen results (Table 4.6.3). Targets from the kinase affinity screen were pooled where %Ctrl<55.

<i>Aak1</i>	<i>Aurka</i>	<i>Gsk3b</i>	<i>Jnk1</i>	<i>Map3k1</i>	<i>Mark2</i>	<i>Sik</i>
<i>Ampk1</i>	<i>Gak</i>	<i>Hipk3</i>	<i>Jnk2</i>	<i>Mark1</i>	<i>Mark3</i>	<i>Stk16</i>

Table 4.6.3

4.6.3 Selection of common kinase hits

I have used an excel macro to analyze the big datasets of the MS experiments (Appendix). This made it possible to compare up to 10 different sets of protein IDs and at the end an arbitrary number of intersections could be selected and visualized. When pooling together all hits from the five MS competition experiments (see materials and methods) we got a list of overlapping targets wherein all the directly or indirectly found ones were included (Table 4.6.4). We hypothesized that some of these common kinase targets are involved in the negative regulation of insulin secretion.

Aak1	Aurka	Gsk3b	Jnk2
Prkab1	Azi2	Mark2	Stk16
Prkag1	Epha7	Mark3	
Prkaa1	Gak	Mast1	

Table 4.6.4

Overlapping hits from MS experiments. Common targets of 4 (regular) or of 5 (**bold**) competition experiments.

A few direct correlations were found in the literature that describes the roles of these kinases in the regulation of insulin secretion in beta cells. GSK3b was described to phosphorylate MARK2¹⁸⁵, therefore assuming a direct interaction it might be also possible that MARK2 and GSK3b were enriched in a complex form on the compound matrices. Selective knockdown of GSK3b in skeletal muscle cells in mice model decreased blood glucose and insulin level, while insulin sensitivity increased¹⁸⁶. Furthermore loss of GSK3b preserved beta cell mass in *Irs2*^{-/-} mice¹⁸⁷. MARK2 null mice became insulin hypersensitive and resistant to high fat-induced weight gain, while insulin level decreased¹⁸⁸. Another study also identified MARK2 as a potential target in diabetes, as it blocks TORC2/CREB activity, which is critical for beta cell survival¹⁸⁹. MARK3 null mice showed different phenotype to MARK2 null mice (protection against high-fat diet-induced obesity and improved glycemic control, but glycogen synthase level was increased)¹⁹⁰. The AMPK constitutes of three subunits (Prkab1, Prkag1, Prkaa1) that form a heterotrimer, where Prkag1 is essential for the activity of the enzyme¹⁹¹. AMPK1, which activity depends on the cytoplasmic ratio of AMP/ATP has a negative regulator role in insulin

secretion. This was observed in a study where constitutively active AMPK1 (Prkaa1) could inhibit insulin secretion^{192,193}. Nevertheless it is worth to mention that AMPK is activated by metformin in other tissues and has a capital role in the metabolism of fatty acids, cholesterol and triglycerides and it also improves glucose uptake in muscle cells and adipocytes^{194,195}. Insulin secretion could also be stimulated by the AMPK activator AICAR however it develops its effect likely through an AMPK independent pathway¹⁹⁶. In overall, recent knowledge suggests that the objective in the treatment of diabetes is rather AMPK activation than inhibition¹⁹⁷, although its deactivation may promote insulin secretion.

4.7 Designing a pool of targets from affinity screen results and MS target deconvolution

To summarize the target discovery results acquired by MS and kinase affinity assays, we took overlapping targets from both experiments and selected 14 kinase hits (*Table 4.7.1*). By processing the data the following rules were applied: the threshold was set to %Ctrl<55 and compound overlaps \geq 3 in the kinase affinity screen; from the MS data the best 57 targets were selected by applying the Excel macro on 5 datasets. These 57 targets are hits for at least 3 compounds (out of 5). These 14 kinase hits that were selected, unite the targets from MS experiments mentioned in the previous chapter (GAK, JNK2, MARK1, MARK2, MAST1 and STK16) and additional hits due to the increased threshold (overlaps for 5,4 or 3 competition experiments were also included, thus the list was extended with the following kinases: AAK1, AURKA, CAMK2A, CSNK1D, CSNK2A1, MAP3K1, MAP4K3 and SLK) furthermore it includes kinases that were identified in the kinase affinity screen. Hits highlighted in bold were selected for siRNA validation.

AAK1	CAMK2A	CSNK2A1	JNK2	MAP4K3	MARK2	SLK
AURKA	CSNK1D	GAK	MAP3K1	MARK1	MAST1	STK16

Table 4.7.1 Overlapping targets from MS and kinase affinity screen experiments

AAK1 is associated with clathrin-dependent endocytosis by phosphorylating the mu subunit of AP-2 adaptor protein¹⁹⁸⁻²⁰⁰, which triggers vesicle formation. Insulin is also stored in clathrin coated vesicles, however clathrin does not stimulate the formation or exocytosis of the granules, but it likely decreases protease activity in rat beta cells²⁰¹. GAK is probably another component of the clathrin coated vesicle, since its structure is homologous to auxilin, a protein that mediates the disassembly of the complex^{202,203}. CSNK2A1 is the alpha subunit of casein kinase II (CK2). CK2 is known to regulate insulin secretion and carbohydrate metabolism furthermore its inhibition by quinalizarin led to elevated insulin level in pancreatic beta cells^{204,205}. This target is used as a positive reference in the siRNA experiments. CK2 also plays an important role in cancer, cell viability and invasion due to its high expression level in rapidly proliferating cells, therefore it is a potentially new target against cancer. Additionally CK2 has an angiogenic effect as well. Two CK2 inhibitors are already in clinical trials for cancer treatment²⁰⁶⁻²⁰⁸. SLK is a microtubule associated protein and it belongs to the STE-20 kinase subfamily and transduces proapoptotic signal. It mediates apoptosis, adhesion, cell-component localization and migration²⁰⁹⁻²¹¹. Since it is a microtubule associated protein it might also regulate movement of secretory vesicles, i.e. vesicles loaded with insulin. Interestingly its activity can be down-regulated by CK2, in the course of direct phosphorylation²¹². The role of MARK2 in insulin level regulation was described previously, nevertheless it is also a possible target in tauopathies (e.g. Alzheimer disease). It regulates cell polarity and overexpression can be assigned with negative qualities in different cell types²¹³. MAST1 seems to be a recurrent partner of gene fusions in breast cancer^{214,215}. It includes a PDZ domain, which participates in organizing signaling complexes and anchoring transmembrane proteins to the cytoskeleton. In general these motifs bind to the C-terminus of other proteins²¹⁶. The well-studied JNK2 that is a member of the MAP kinase family and was also identified as hit of some compounds. It is involved in cell proliferation, differentiation, migration and programmed cell death. After stress stimuli the SAP/JNK2 pathway gets activated, which in turn activates transcription factor components of the AP-1 complex, such as c-Jun and ATF^{217,218}. JNK2 also promotes cell apoptosis by directly phosphorylating p53 at Ser6 and YAP1 protein^{219,220}. Activation of different isoforms of JNKs is also observed in insulin resistance and obesity models, for instance stimulation with fatty acids and high concentration of glucose and can be associated with apoptosis or increased level of proapoptotic genes in INS-1 beta cells²²¹. Consequently overexpression of dominant-negative JNK in adipose tissue and selective suppression of both JNK1 and JNK2 have a protective effect in preventing obesity, apoptosis and insulinitis in different models²²²⁻²²⁴. Deactivation of JNK resulted in increased insulin-stimulated glucose

uptake in skeletal muscles, furthermore decreased mRNA levels of PEPCK and G6Pase (enzymes responsible for gluconeogenesis) were observed, therefore glucose production was also reduced in dominant-negative HFD mice models compared to lean controls²²². The exact function of STK16 is not defined yet, but it is known that it undergoes myristylation and palmitoylation which is one of the important events regulating the subcellular localization of proteins. These changes in the protein structures can influence and regulate signaling pathways inside the cell. The acetylation by fatty acids of other proteins and enzymes (Ras, Src families, heterotrimeric G proteins and GRK6) were also shown to be important for their function^{225,226}. STK16 is a Golgi-resident protein and its structure and function is conserved amongst different species²²⁷. Env7, a strongly homologous protein to the human STK16 in yeast negatively regulates membrane/vacuole fusion^{227,228}. Regarding to these observations STK16 likely has an important role in the regulation and organization of the endomembrane structure in cells (ER, Golgi, endosomes, lysosomes and plasma membrane). A few studies revealed its involvement in different secretory events as well²²⁹⁻²³¹. The calmodulin-dependent kinase 2 (CAMK2) mediate the effects of Ca²⁺ in the cells. It takes part in the regulation of insulin exocytosis, as many insulin secretagogue can activate the kinase and thus induce insulin secretion^{232,233}. Furthermore a recent study reported that CAMK2 modulates insulin secretion by inhibiting K_{ATP} channels²³⁴ but it is also claimed to reduce the adenylyl cyclase III activity (AC-III) as well and by this it may downregulate cAMP level, albeit these studies were done not in beta cells^{32,235,236}. AC-III is expressed in beta cells and can induce the generation of cAMP²³⁷. A recent study showed that, under diabetic conditions the activation of hepatic CAMK2 can be associated with insulin resistance²³⁸. In overall CAMK2 exerts a complex regulatory effect in different tissues and its uncontrolled functioning can lead to phenotypical changes.

4.8 Validation of potentially negatively regulating kinases of insulin secretion by siRNA

The role of CK2 (CSNK2A1) in the negative regulation of insulin secretion is already known from some publications. This property of CSNK2A1 seems to exist in RIN-5AH and INS-1E cells too. Other kinases such as AAK1, GAK and STK16 are thought to modulate vesicle formation or trafficking, but their direct role in insulin secretion was not investigated yet by others. The function of MAST1 and SLK in insulin release was not studied yet either. MARK2 was described to have favorable impacts on insulin resistance in knockout mice, however its targeted knockdown was not tested in beta cells. The results achieved with ON-TARGETplus siRNAs show that knockdown of STK16, CSNK2A1 and MARK2 shows an increased insulin secretion in RIN-5AH cells (*Figure 4.8.1*). In INS-1E cells by silencing MAST1 and JNK2 an increased insulin secretion was observed besides knockdown of STK16, CSNK2A1 and MARK2 (*Figure 4.8.2*). However at 72h knockdown of MARK2 showed a reduced effect (*See Appendix*). By using Accell siRNAs, a different assay method to generate knockdown models, reasonable efficiencies that correlated with an increased insulin release could only be determined for STK16 and MAST1 samples. The stimulatory effects and results of the Accell siRNA experiments are displayed in *Appendix*.

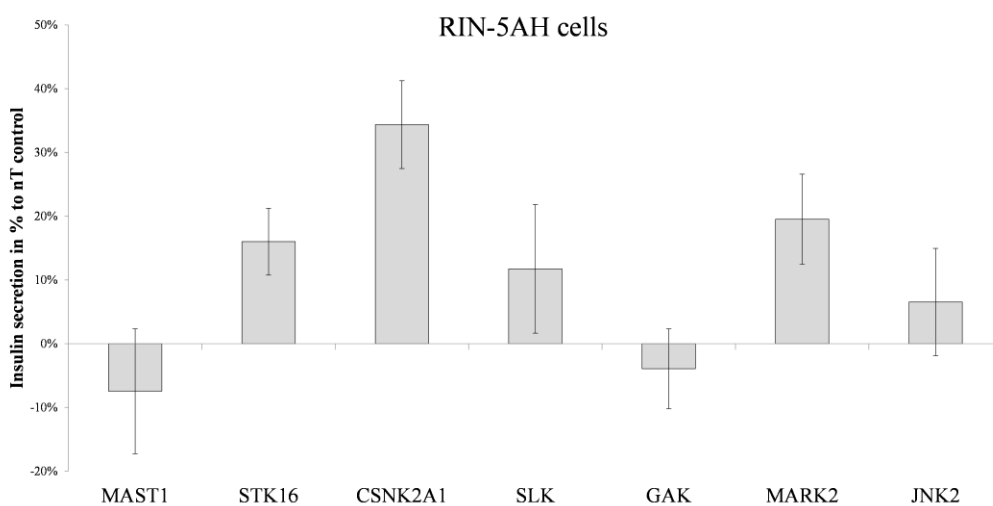


Figure 4.8.1 Knockdown effect on insulin secretion in RIN-5AH cells using Dharmacon ON-TARGETplus SMARTpool siRNAs. Cells were reverse transfected for 48h and insulin level was checked after 2h by replacing the medium (n=5)

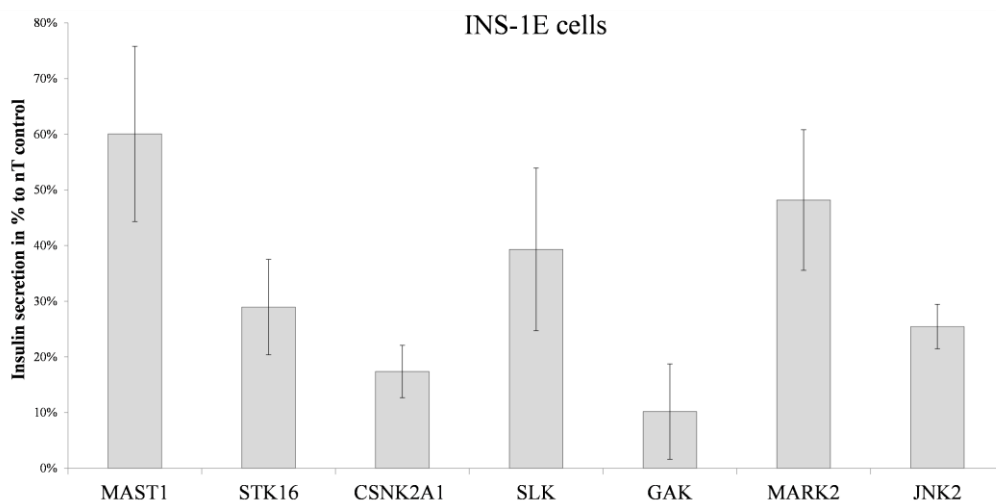


Figure 4.8.2 Knockdown effect on insulin secretion in INS-1E cells. Cells were reverse transfected for 48h and insulin level was measured after replacing the medium to KRBH and 11mM glucose (n=4)

4.9 Other potential non-kinase hits

Basically it is possible that the selected tool compounds induce insulin secretion through other pathways and targets than kinases. It is also assumed that they are acting on multiple targets and the observed result is an outcome of a complex effect. Many proteins other than kinases were described in the literature to have negative (or positive) key regulatory effect in insulin release, including G-proteins, PDEs, metabolic enzymes, ATPases and other proteins. Some non-kinase additional hits were identified by MS affinity chromatography pull-down or binding experiments, including enzymes participating in glucose metabolism, ATPases, PDEs, SNARE building elements and GDIs (GDP-dissociation inhibitors) (*Table 4.9.1*). The role of PDEs were further investigated later. However they are not validated compound targets, but can be possible intervention points for the regulation of secretion and can contribute to the MOA of compounds. Several G proteins were also found (mostly only binding and not pulled down) by MS approach (in collaboration with Evotec AG), which might encroach into GPCR signaling. A recent publication discovered the important role of MST1 kinase in beta cell apoptosis and insulin secretion as well²³⁹. In the kinase affinity assay MST1 was identified as a binding partner for sunitinib with high affinity, while other compounds did not bind it. Probably another interesting family is SGK, which main properties are that they regulate many different ion channels²⁴⁰⁻²⁴⁸ which could interfere with insulin secretion as well. SGK1 was identified as hit in kinase affinity assay for VCC124075, VCC346349, VCC512891 and sunitinib. Because of lack of validation, these two additional hits should be considered only as hints, furthermore we do not know anything about the nature of the compound-protein interaction yet.

	Bound to affinity matrix				Competed from affinity matrix			
	VCC350485:02	VCC553231:08 (SU)	VCC512891:01	VCC124075:08	VCC350485:02	VCC553231:08 (SU)	VCC512891:01	VCC124075:08
Negative modulators of Insulin release and Glucose metabolism								
AMPK (5-AMP activated kinase) ^{193,249}		X	X	X		X	X	X
Cpt-1a (Carnitine O-palmitoyltransferase 1) ²⁵⁰		X						
G6PC3 (Glucose-6-phosphatase 3) ²⁵¹		X						
HADH (Long chain 3-hydroxyacyl-CoA dehydrogenase) ^{51,252,253}	X	X	X	X				
IDH1 (Isocitrate dehydrogenase [NAD] cytoplasmic) ^{254,255}	X	X						
IDH2 or IDH3 (Isocitrate dehydrogenase [NAD] mitochondrial)	X	X	X	X				
Other regulators of metabolism								
ATPases – influence the amount of ATP								
Vcp	X	X	X	X				
Atp6v1e1	X	X						
Atp6v1b2	X	X		X				
Ola1			X	X				
Atp1a1		X						
Ahsa1		X						
Atp2a2		X		X				
Atp6v1a		X						
Psm13	X	X						
Psm11		X						
Psm6		X						
Psm1		X	X	X				
Atp9a		X						
Psm2		X	X	X				
Psm8		X						
Psm7		X						
Cyclic nucleotide phosphodiesterases (PDEs) ²⁵⁶⁻²⁶¹								
PDE2A				X				X
PDE1B				X				X
PDE10A				X				
PDE4C		X	X			X	X	
SNAREs - required for vesicle fusion and exocytosis ²⁶²								
Vti1b (Vesicle transport through interaction with t-SNAREs homolog 1B)				X				X
Ckap5 (Cytoskeleton-associated protein 5)		X						
G protein regulators responsible for secretion ^{263,264}								
Rho-GDI (Arhgdia)		X	X					
Gdi1	X							
Gdi2	X	X		X				
Activated in obesity ²³⁸								
CAMK2		X	X			X	X	
Can regulate ion channels ²⁴¹								
Sgk2		X	X			X	X	

x = enriched on affinity matrix or pulled down from affinity matrix directly or indirectly

4.9.1 Effect of PDE4 and PDE5 inhibitors in RIN-5AH and TC6 cells

Some of the PDEs (cyclic nucleotide phosphodiesterases) were identified by MS as interactors for compounds, therefore they looked interesting target candidates to test. PDEs are enzymes that hydrolyze the phosphodiester bond of cyclic GMP (cGMP) or cyclic AMP (cAMP), which are important secondary messengers and play decisive role in the regulation of insulin release^{33,36,265-268}. PDEs can be classified into 11 different families and have several isoforms in each family that show different substrate specificities^{257,269}. By inhibition of certain PDEs in beta cells, cAMP level raises and insulin is secreted. On the other hand cGMP can also have a function in regulating PDE activity. During metabolism the produced nitric oxide (for example produced from L-Arginine) can increase cGMP level and augment insulin level, thus as a consequence the cGMP sensitive PDE3B is deactivated and thus cAMP concentration simultaneously increase. Expression pattern of different PDEs in INS-1 cells can correlate with their role played in insulin secretion²⁷⁰. Further research support the fact that in different beta cell lines different PDEs can be dominant. PDE1C was found to play the relevant role in TC3 beta cells, but in primary pancreatic islets both PDE1 and PDE3 inhibition stimulated the secretion. Zaprinast a PDE1/5A inhibitor with higher affinity to PDE1 potentiated insulin release only when co-administered with guanylyl cyclase activator YP-1, but not alone in BRIN-BD11 cells²⁷¹. Its inefficiency was confirmed on human beta cell islets in another study²⁷². PDE3B and PDE4C were found to play a major role in stimulation of insulin secretion by lowering the blood glucose level in INS-1 cells and in mice as well^{260,270,273,274}. Several PDE10A inhibitors could also effectively stimulate insulin secretion²⁵⁶. The PDE5 enzyme hydrolyzes cGMP and may have other favorable effects in diabetes. The chronic treatment with PDE5 inhibitors can be advantageous, because they reversed and improved the condition of oxidative stress in epithelial cells occurring in insulin resistance²⁷⁵⁻²⁷⁷ and could also improve the insulin sensitivity in mice on high fat diet, but did not increase the fasting insulin level²⁷⁸. Long term tadalafil treatment also improved fasting glucose level and reduce infarct size in db/db mice models²⁷⁹. By insulin ELISA assay we demonstrated that the acute treatment with some of the PDE5 inhibitors (sildenafil, vardenafil but not tadalafil) resulted in an enhanced insulin level in TC6 cells but not in RIN-5AH cells (*Figure 4.9.1*). Taken together PDE4C seems to be an important cyclic nucleotide phosphodiesterase enzyme in beta cells and putatively in pancreatic islets as well²⁷⁴. We could confirm this in our experiments by the treatment with selective PDE4 inhibitors (Roflumilast, CP 80633) in RIN-5AH and TC6 cells (*Figure 4.9.1*). Furthermore the knockdown of PDE4C in INS-1E cells caused a moderate but significant effect on insulin release (12%) as well (data not shown). The application of PDE

inhibitors can also suppress the transcription of iNOS and therefore may prevent beta cell dysfunction²⁷².

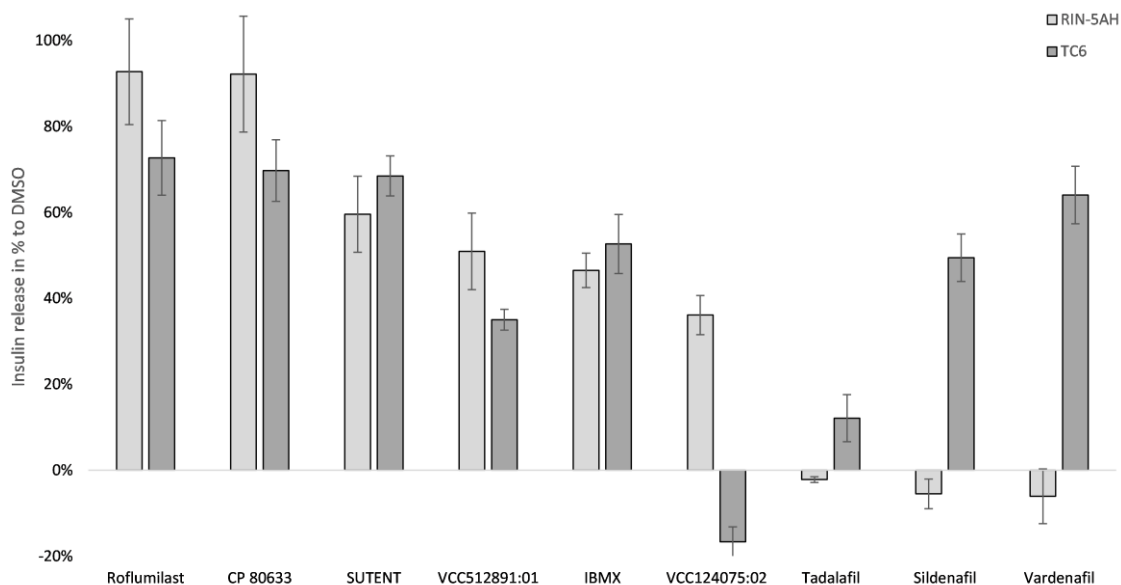


Figure 4.9.1 Effect of PDE4 and PDE5 inhibitors on insulin secretion in RIN-5AH (rat) and TC6 (mouse) cells (2h and 5uM treatment, SEM, n=4-6). Since PDEs were identified as hits for certain compounds (Sunitinib, VCC124075, VCC512891), officially available PDE4 (Roflumilast, CP 80633) and PDE5 (sildenafil, tadalafil, vardenafil) and PDE pan-inhibitors (IBMX) were tested. The importance of PDE4C could be confirmed in RIN-5AH and TC6 cells, that is in correlation with published data in other models. Interestingly PDE5 inhibitors affected insulin production in TC6 cells only. Furthermore it should be taken into account that tadalafil is structurally very much different compared to sildenafil and vardenafil. The expression level of PDE5 was not checked in the cells, therefore it is not clear whether the absence of PDE5 in RIN cells is the cause of the inefficiency of PDE5 inhibitors or is it an off-target effect.

4.10 Insulin secretion and GDIS in different beta cells

The potencies of the selected best compounds were tested in different beta cell line models. Many of them could maintain a generic insulinotropic effect, however one of the most effective compound in RIN-5AH cells (VCC981125:09 and other members from quinoline family) did not induce insulin release in TC6 and INS-1E cells (*Figure 4.10.1*). Only some of the VCC981125:09 derivatives were able to induce insulin secretion in BRIN-BD11 cells. (*see Appendix*). The cell line specific effect of some of the compounds (VCC981125:01, VCC124075:02 and VCC036051:03) can be explained with the heterogeneity of the different clonal insulinoma beta cell lines. The glucose sensitive INS-1E cell line provided a good model for testing the compounds in high (11.1mM) and low (1.1mM) glucose environments. Most of the compounds increased insulin release in high glucose but not in low glucose content buffer. Interestingly a compound from the thieno-pyrimidine family (VCC834153:01) showed a significant induction in low glucose compared to high glucose. On the other hand the bis-quinoline compound VCC405984:01 has produced an ideal result, it had negligible insulinotropic effect in buffer supplemented with 1.1mM glucose (*Figure 4.10.2*).

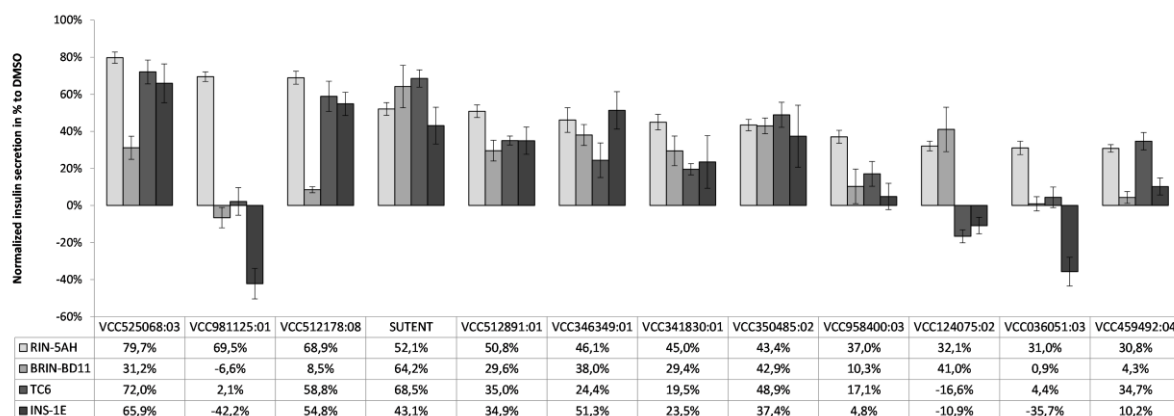


Figure 4.10.1 Efficacy of compounds in different beta cell lines. Most of the compounds maintained their potency and were effective on all beta cell lines. These compounds are probably targeting key regulators of insulin secretion which are present in all models. On the other hand VCC981125, VCC124075 and VCC036051 seem to have a cell line specific effect. ($n=5-6$; SE, 5 μ M; 2h treatment)

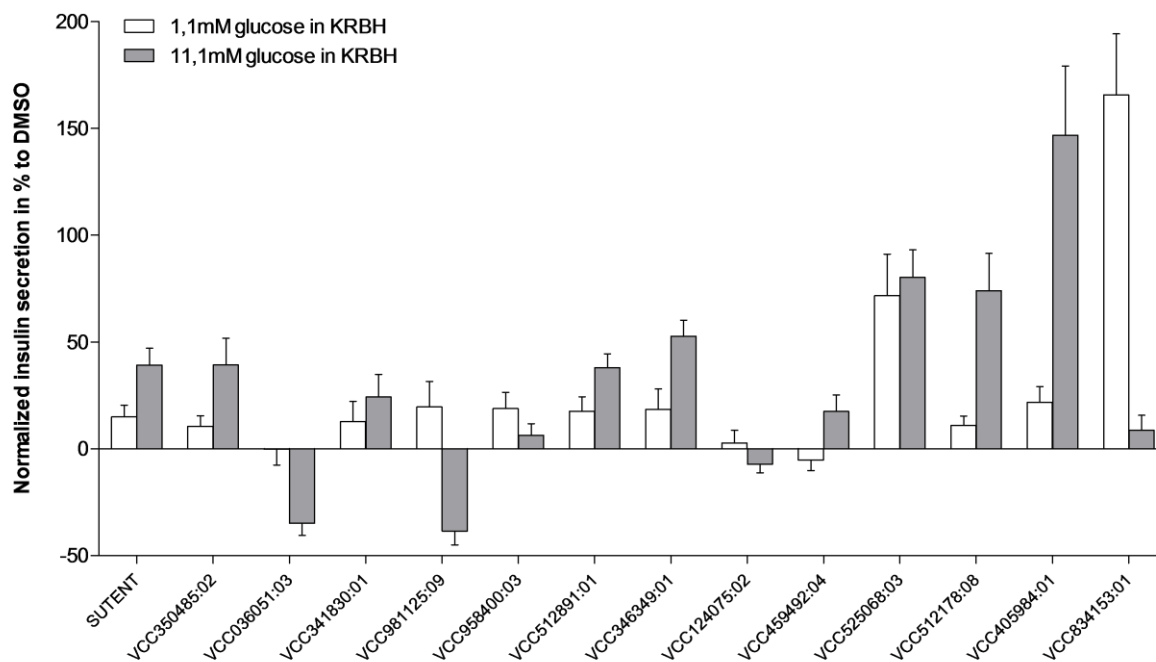


Figure 4.10.2 Glucose dependent insulin secretion (GDIS) by treatment of VCC compounds. Most of the compounds increased insulin in high glucose (11.1mM) but not in low glucose (1.1mM) environment. This property can be an important factor for an ideal treatment of diabetes as well, since most of the medicaments cause hypoglycaemia. Interestingly VCC981125 (quinoline) and VCC036051 (quinazoline) had an opposite effect in INS-1E cells. Nevertheless a bis-quinoline derivative VCC405984:01 had a massive impact on insulin secretion in INS-1E cells in high glucose compared to low glucose. It is worth to notice that its effect was not significant in low glucose compared to DMSO treatment. (n=5-8; SE; 2h and 5 μ M treatments)

4.11 Elevated cAMP levels can be a possible mechanism of action for some compounds

Intracellular cAMP level is one of the main driving mechanisms of insulin release. Certain GPCR ligands can activate the generation of cAMP. Upon activation of receptors a series of downstream signals stimulate the adenylyl cyclase enzymes which convert ATP to cAMP. Then cAMP can activate and/or phosphorylate effector proteins, i.e. PKA and Epac, which transmit several exocytotic stimulatory signals^{33,36}. Subsequently different enzymes that are regulating insulin secretion and/or cAMP sensitive transcriptional activators can be affected, e.g. CREB, CREM and ATF1. The breakdown of cAMP to AMP is mediated by PDEs as it was reviewed in the previous chapter, therefore Roflumilast a PDE4C inhibitor was also included in the cAMP assay. We found that after compound treatments (including not only those that bound PDEs in the affinity chromatography experiments) the intracellular cAMP level significantly increased in most cases (*Figure 4.11.1*), therefore supposedly this could be an important factor in the mode of action for the majority of tested VCC compounds.

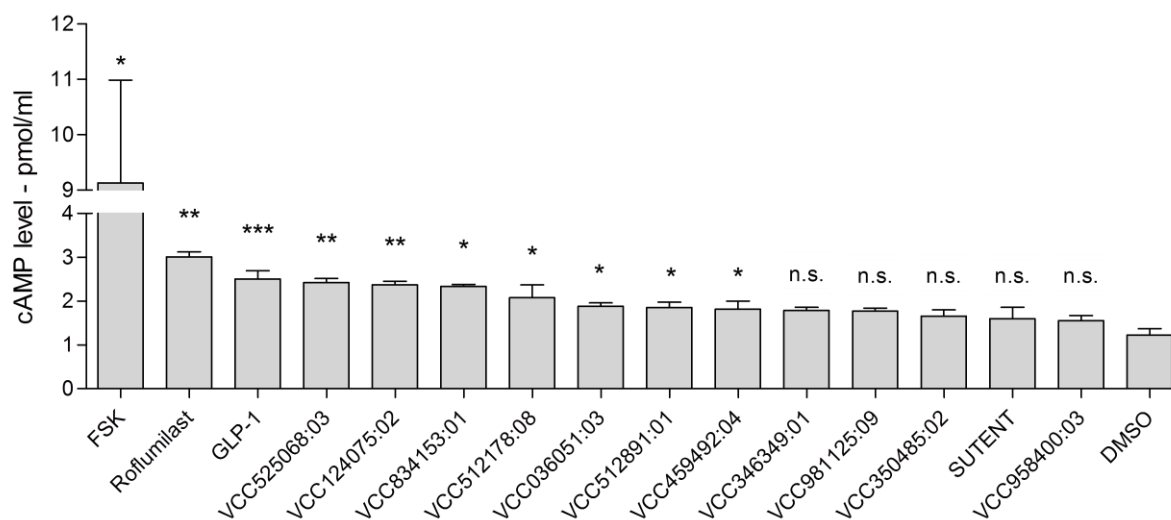


Figure 4.11.1 Changes in intracellular cAMP level in RIN-5AH cells. ($n=4$; 2h and 10 μ M treatment; paired t -test results: * $p<0.05$; ** $p<0.01$; *** $p<0.001$)

4.12 Increased Ca^{2+} influx is another mechanism of action for some compounds

Voltage dependent calcium channels play an important role in beta cell physiology and are critical regulators of insulin secretion in beta cells. Membrane depolarization or other stimuli that induce calcium channel opening and therefore calcium influx, triggers the exocytosis of insulin granules²¹. Several VDCCs are involved in this mechanism in human beta cells^{280,281}. In rat beta cells similarly to human beta cells the same set of calcium channels are also expressed (L-type, T-type, N-type and P/Q type Ca^{2+} channels), however it was found that P/Q type channels likely do not participate in insulin secretion in INS-1 cells^{282,283}. Interestingly in mouse beta cells the N-type and T-type Ca^{2+} currents are not present²⁸⁴⁻²⁸⁷. The L-, P/Q- and N- type currents are high voltage activated (HVA), while T-type current is considered as low voltage activated (LVA). Furthermore L-type channels inactivate slowly (500msec), the inactivation of T-type channels are faster (20-50msec). The involvement of the dihydropyridine (DHP) sensitive (nifedipine, efonidipine) L-type Ca^{2+} channels (Cav1.2 and Cav1.3) are probably the most crucial for GSIS secretion, they are responsible for ~80% of the Ca^{2+} current in human and rat beta cells as well²⁸⁸. Another important participant in Ca^{2+} influx is the T-type Ca^{2+} channel²⁸⁷. As VCC981125:01 was not hitting any kinases, it was suspected to have a direct effect on Ca^{2+} influx probably through ion channels or GPCRs. The Ca^{2+} influx measurements done by FACS have revealed that the compound and some of its derivatives rapidly increased calcium influx in RIN-5AH cells. Non-insulinotropic compounds from the same core family did not show any effect (*Figure 4.12.1*).

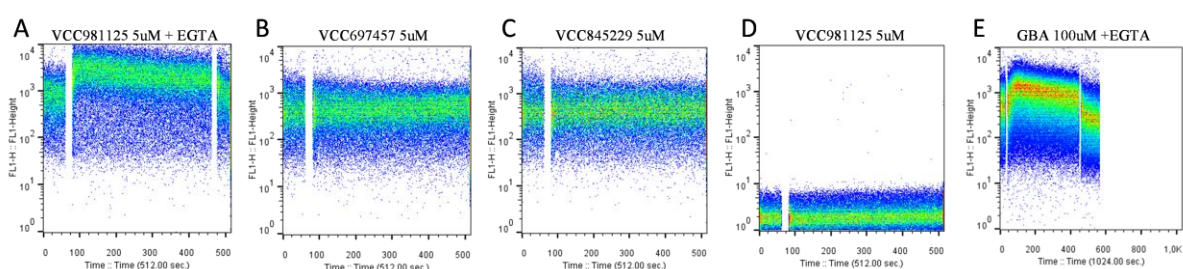


Figure 4.12.1 Calcium influx experiments by FACS. **A**, Addition of the compound VCC981125 (1st gap) induced Ca^{2+} influx in RIN-5AH cells when extracellular Ca^{2+} was present in the buffer. The long sustained signal could be quenched by EGTA (2nd gap). **B-C**, Non-insulinotropic compounds had no effect on Ca^{2+} influx. **D**, VCC981125 did not change the fluorescence signal in Fluo-4 unstained cells. **E**, Glibenclamide (GBA) effect.

It is important to notice that the effect of VCC981125:01 could only be observed in HBSS++ (HBSS with CaCl₂ and MgCl₂), which accounts for that the compound is unlikely to release Ca²⁺ from intracellular stores. Furthermore similarly to the insulinotropic effect Ca²⁺ inducing effect was also cell line specific. For positive control thapsigargin (SERCA inhibitor) was used, which increased [Ca²⁺]_i in HBSS-- (CaCl₂ and MgCl₂ free HBSS) as well as in HBSS++. The ionophore A23187 and thapsigargin (TG) showed a different characteristics for Ca²⁺ increase compared to VCC981125, furthermore they were not able to induce insulin secretion in the beta cells. The augmented Ca²⁺ influx could be attenuated by verapamil (L-type calcium channel blocker), efonidipine (L- and T-type inhibitor) and high concentration of NiCl₂ (T-Type inhibitor). Additionally some known drugs with quinoline cores (bosutinib, quinidine) were also investigated for Ca²⁺ level modulation (*Figure 4.12.2*).

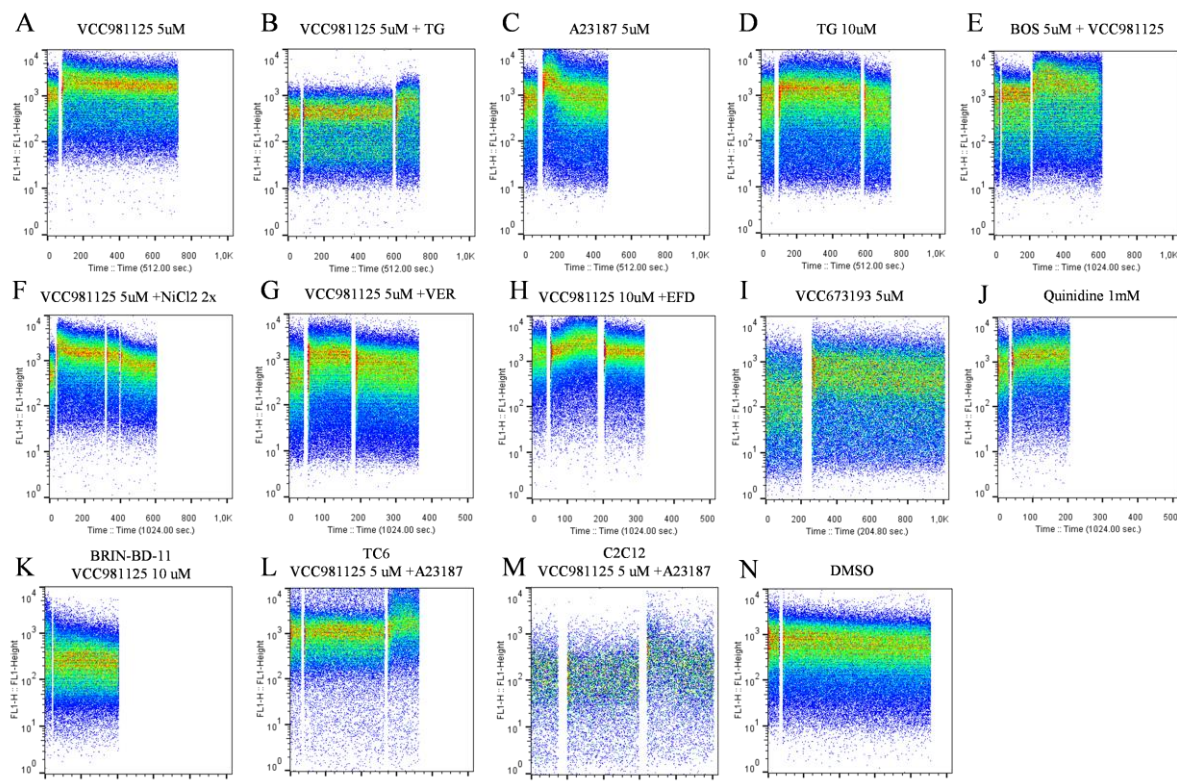


Figure 4.12.2 **A**, VCC981125 induces Ca^{2+} influx in HBSS++ buffer. **B**, In HBSS-- buffer it is unable to develop its effect. The addition of TG (2nd gap) confirms that cells were still healthy. **C-D**, Demonstrating the effect of positive control compounds A23187 and TG. The increased signal by TG could be quenched by EGTA (2nd gap). **E**, Bosutinib did not stimulate Ca^{2+} influx. **F-H**, The action of VCC981125 could be attenuated by Ca^{2+} channel blockers, $NiCl_2$, verapamil (VER) and efonidipine (EFD) respectively. **I-J**, Additional compounds sharing quinoline cores which induced Ca^{2+} influx in RIN-5AH cells. VCC673193 an analogous structure of VCC98112. Quinidine and VCC673193 have also induced insulin secretion in RIN-5H cells. **K-M**, The effect of VCC981125 seems to be cell line specific. **N**, DMSO control.

Ca²⁺ influx for the other selected VCC compounds was not detectable by FACS (data not shown). Effect on Ca²⁺ influx of quinoline molecules were confirmed in the same cells by spinning disc confocal microscope as well (*Figure 4.12.3a and 4.12.3b*). By using the Flexstation 3 microplate reader, additional relevant compounds were screened and the AUCs could be calculated for the Ca²⁺ influx curves (*Figure 4.12.4*).

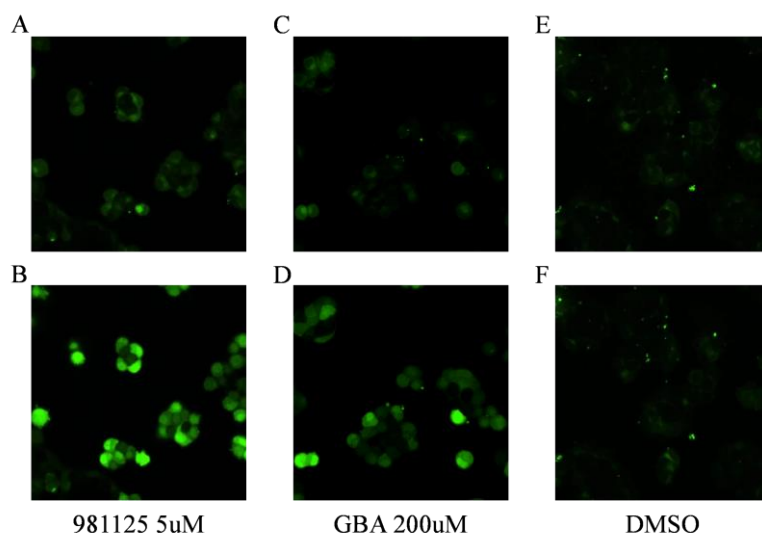


Figure 4.12.3a

Spinning disc confocal microscopy measurements in Fluo-4 AM loaded RIN-5AH beta cells. A-B, Before and after stimulation with 5uM VCC981125. C-D, Before and after stimulation with 200uM glibenclamide (GBA). E-F, Negative control with DMSO, before and after stimulation.

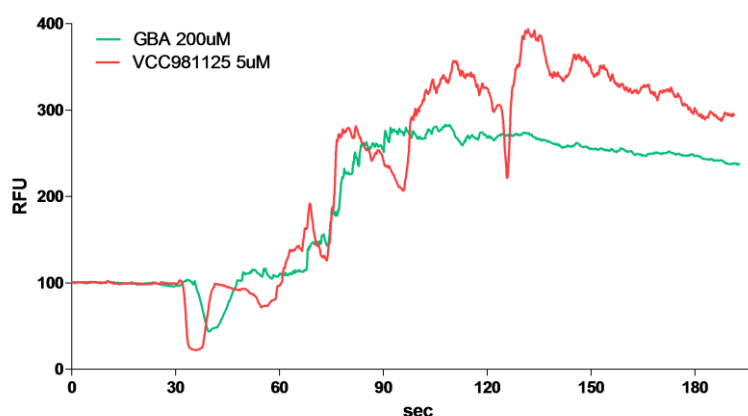


Figure 4.12.3b

Relative fluorescence signal registered by confocal microscope. Overlaid graphs for 200uM GBA and 5uM VCC981125. Compounds added at 30s. 6-9 cells were gated and their relative mean fluorescence values were averaged and plotted. The base line fluorescence level was calculated by taking the average fluorescence of the first unstimulated 20s.

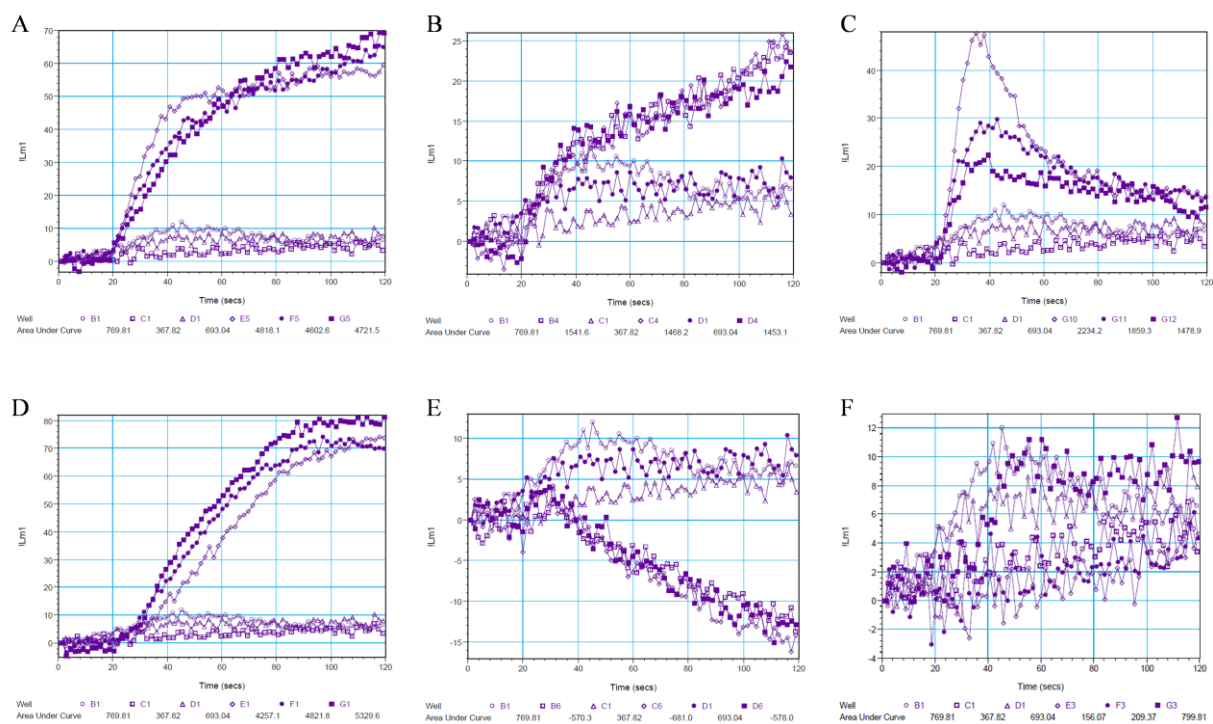


Figure 4.12.4 Confirmation of Ca^{2+} influx results on Flexstation 3 (demo instrument, Molecular Devices). Treatments with different compounds are displayed in comparison to DMSO ($n=3$) **A**, 5 μM VCC633768:01 (quinoline derivative); increased fluorescence **B**, 5 μM VCC981125 (quinoline); increased fluorescence **C**, 4.7 μM Glibenclamide; increased fluorescence **D**, 10 μM Thapsigargin; increased fluorescence **E**, 10 μM Verapamil; decreased fluorescence **F**, 1 $\mu\text{g/ml}$ Exendin-4; no change

4.12.1 Validation experiments with patch clamp for VCC981125

In order to validate if VCC981125 induces Ca^{2+} influx via membrane depolarization in RIN-5AH beta cells, whole cell patch clamp studies were performed under the supervision and help of Dr. Jana Hartmann (TUM, Institute of Neuroscience). 500 μM glibenclamide (GBA) was used as control compound in the experiments. After applying either 50 μM or 500 μM “puffs” for 30s of the quinoline compound on the cells, a shift in membrane potential was registered from -70mV up to -20mV in current clamp mode (CC). An increase in inward current could also be detected in voltage clamp mode (VC), which lasted longer compared to GBA stimulation. This effect correlated with the Ca^{2+} influx results seen on FACS. When comparing VC and CC curves for VCC981125 treatment, it was clear that the effect in VC is shorter than in CC, thus the compound keeps the membrane potential for a prolonged time in depolarized state even when it probably does not act on its target anymore. On the other hand treatment with VCC981125 has increased the inward current immediately, unlike GBA where a small delayed response could be observed. Interestingly lower concentration of the drug could generate almost the same rate of inward current as with higher concentration (*Figures 4.12.5-7*). We also experienced a change in the membrane capacitance after treatment with the compounds, which reflects to the exocytotic events happening in the cell²⁸⁹.

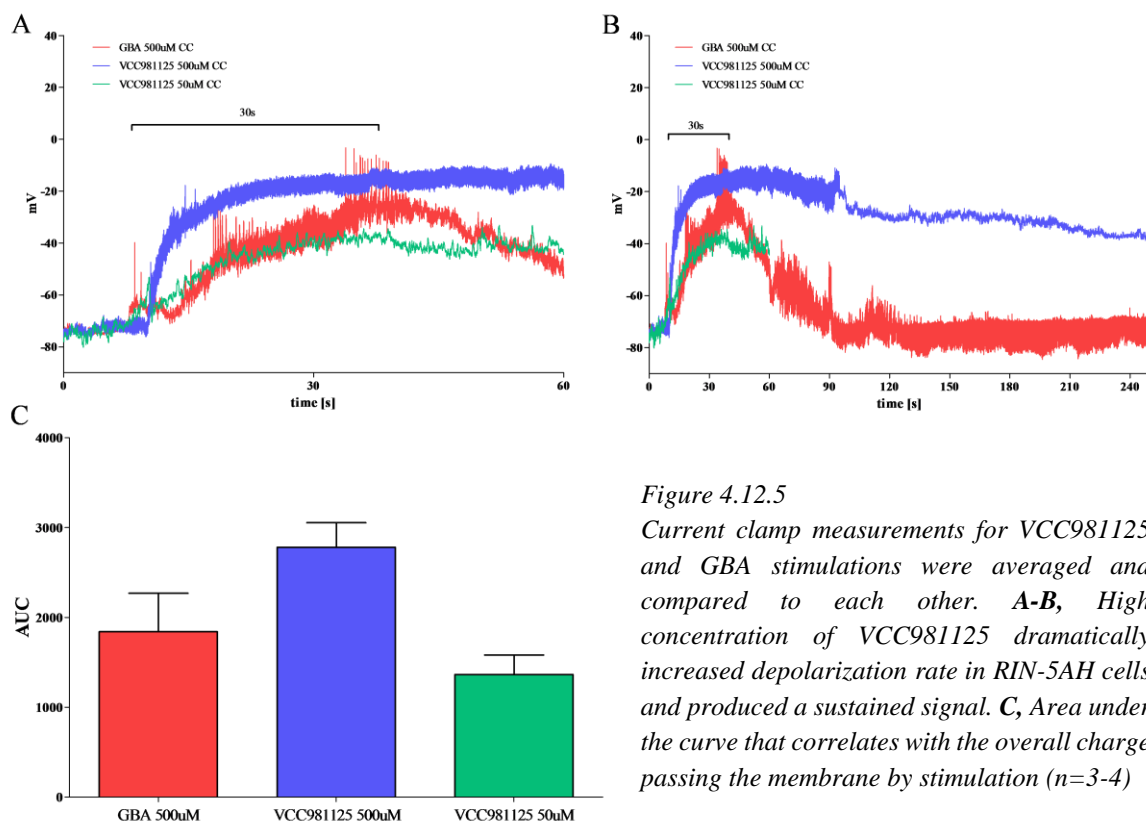


Figure 4.12.5

Current clamp measurements for VCC981125 and GBA stimulations were averaged and compared to each other. **A-B**, High concentration of VCC981125 dramatically increased depolarization rate in RIN-5AH cells and produced a sustained signal. **C**, Area under the curve that correlates with the overall charge passing the membrane by stimulation ($n=3-4$)

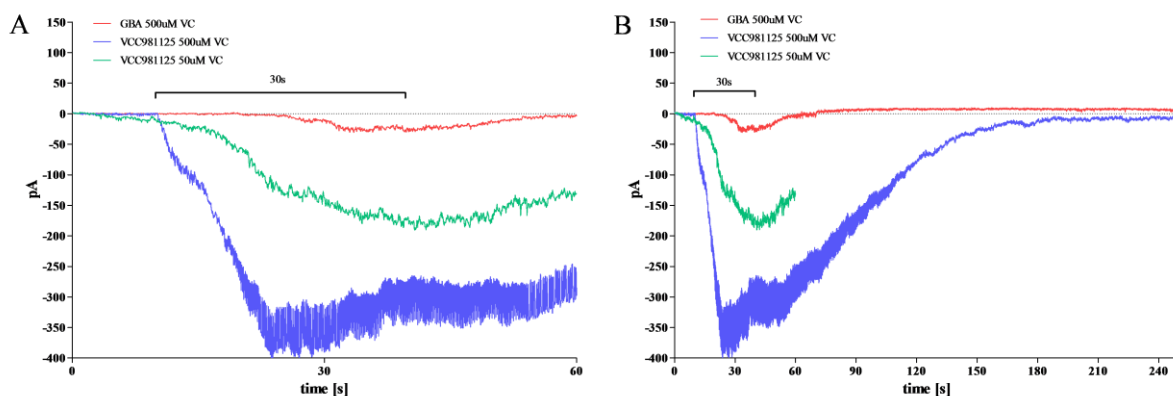


Figure 4.12.6 **A-B**, Averaged voltage clamp measurements. VCC981125 has markedly increased the inward current in RIN-5AH cells and flow returns back to baseline after 3 minutes. VCC981125 had a longer lasting effect compared to GBA. ($n=3-4$)

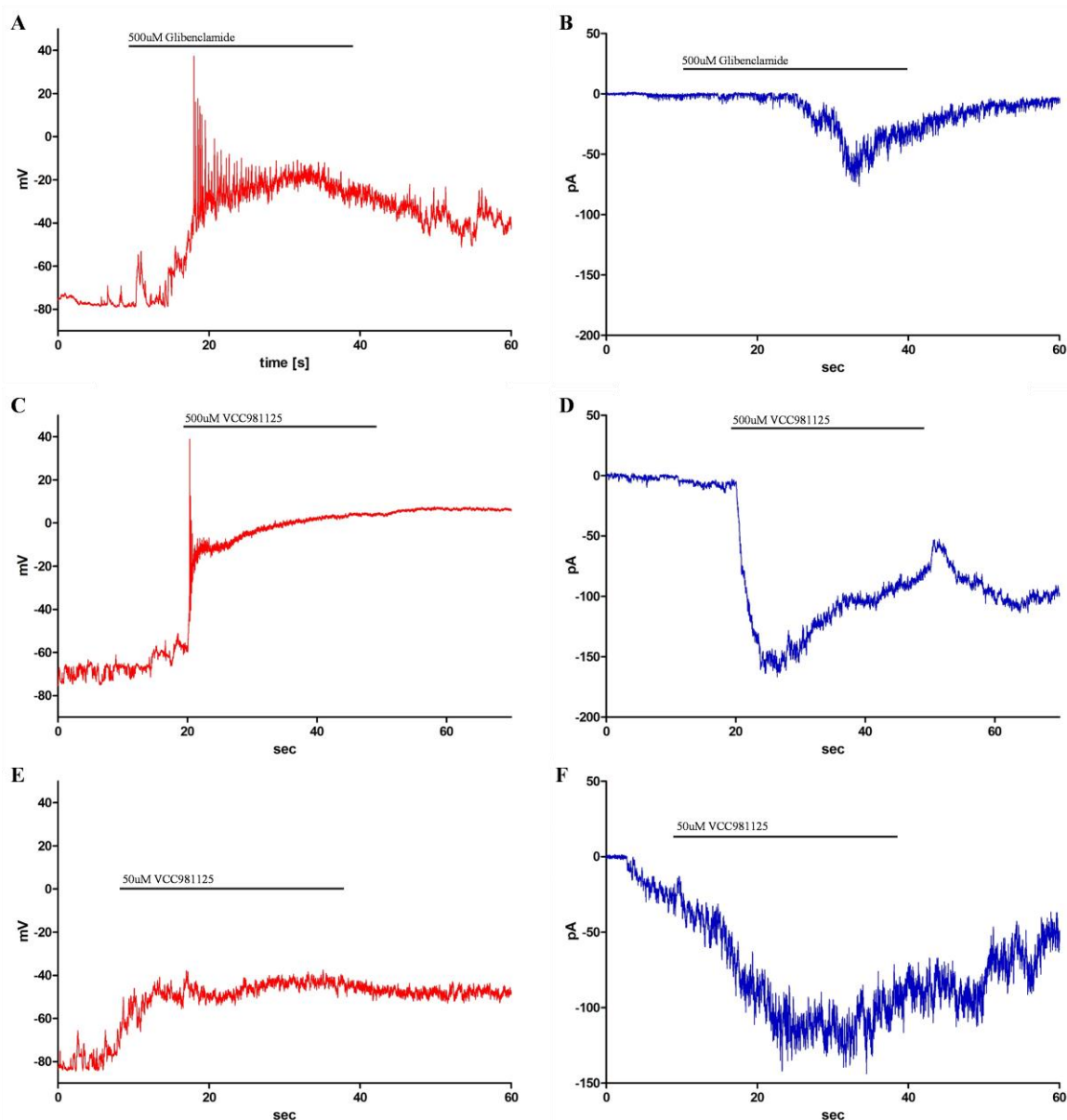


Figure 4.12.7 Representative non-averaged whole cell patch clamp curves of RIN-5AH cells. **A-B**, Current clamp and voltage clamp measurements respectively for 500uM glibenclamide was used as control in the experiments **C-D**, Current clamp and voltage clamp curves for 500uM VCC981125. It is worth to notice that the effect in voltage clamp is immediate and not delayed like at glibenclamide treatment **E-F**, Effect of 50uM VCC981125.

The exact target of VCC981125 is still unknown, however there is a high chance that it acts on any of the Ca^{2+} channels. Further possible targets could be other ion channels or maybe GPCRs that interact with ion channels²⁹⁰.

4.13 Combination treatments with ion channel modulators suggest different mechanism of actions for certain compounds

From previous experiments it turned out that Ca^{2+} signaling has a crucial role in the MOA of quinoline compounds in RIN-5AH cells. Therefore VCC981125 and Ca^{2+} channel inhibitors were combined together and checked for insulin secretion. Additionally the same combinations for sunitinib, glibenclamide (GBA), GLP-1 and Exendin-4 were done as well. All tested Ca^{2+} channel inhibitors could lower the VCC981125- or GBA-induced insulin secretion. Sunitinib, GLP-1 and Exendin-4 were not sensitive to verapamil and nifedipine, only to efonidipine. Furthermore, combinations with K_{ATP} channel openers diazoxide (DAO) and pinacidil (PIN) were also studied. DAO had no impact on GBA effect, which is probably due to the low K_{ATP} expression level in the cell line and therefore relatively low sensitivity to sulphonylureas (*see Appendix*) or because the affinity of GBA to the ion channel is higher than DAO. The K_{ATP} channel openers PIN and DAO should normally lower the insulin secretion, however PIN did not have any effect. It can be explained with the differences in selectivity of the compounds, since PIN has a much greater affinity to SUR2 subunit, which is expressed at a very low level compared to SUR1 in RIN-5AH cells (*see Appendix*). This correlates with published data also, where PIN did not influence insulin or calcium levels (along with diazoxide) in SUR1 knockout mice, presuming that no other isoforms of $\text{K}_{\text{ATP-S}}$ are expressed in the pancreatic islets²⁹¹. DAO targets both SUR1 and SUR2 subunits, therefore a diminished insulin level could be registered after treatment in RIN-5AH cells. DAO could significantly reduce the effect of VCC981125, sunitinib, GLP-1 and Exendin-4. These results revealed that Ca^{2+} (T-type) and K^{+} currents strongly modulate the potencies of VCC981125, glibenclamide, sunitinib, GLP-1 and exendin-4 in RIN-5AH cells (*Figure 4.13.1*).

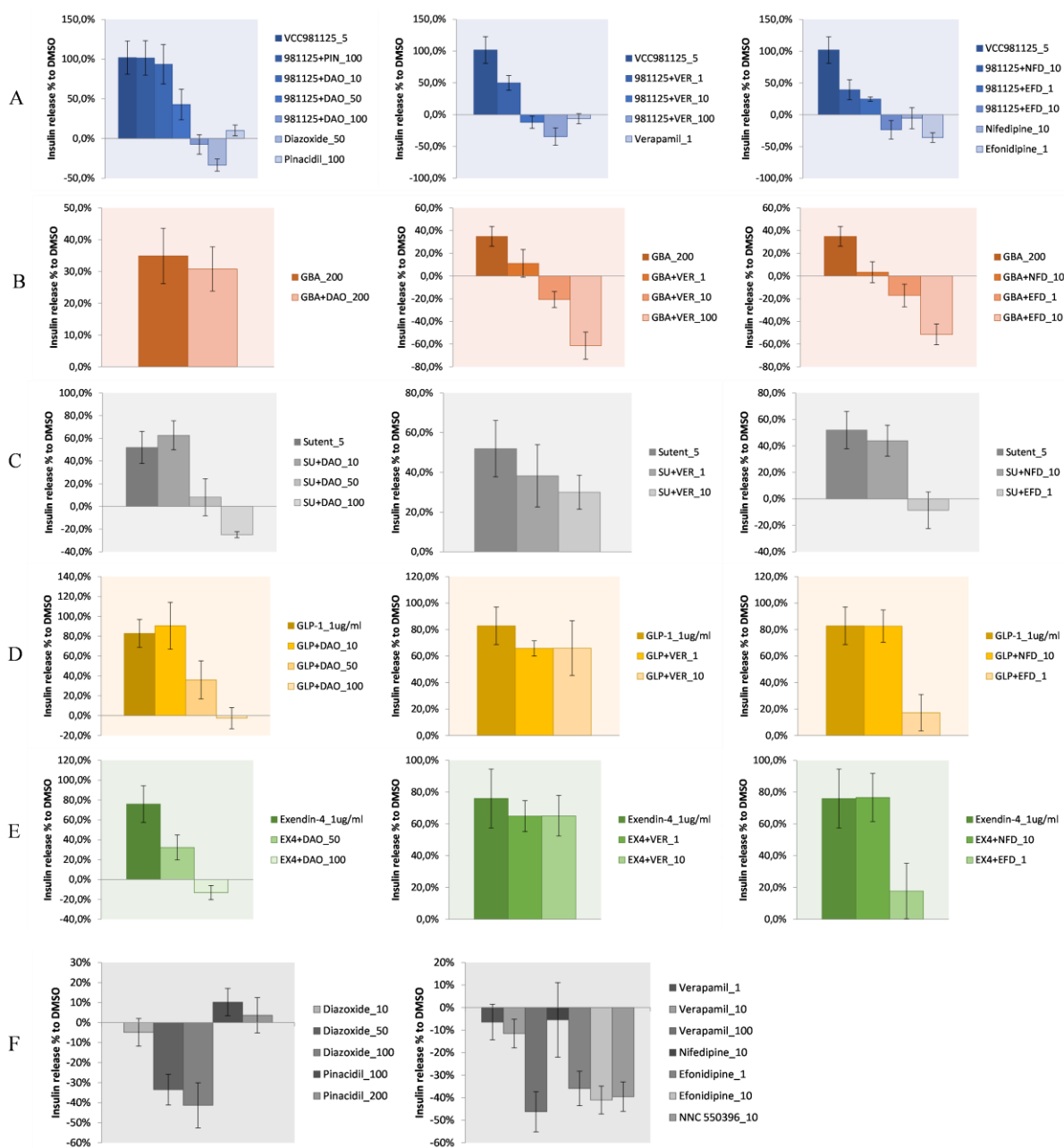


Figure 4.13.1 **A-B**, Combination treatment results for VCC981125 and glibenclamide are similar. They were both sensitive to L- and T-type Ca^{2+} channel inhibitors. The cell line shows low sensitivity to glibenclamide and probably due to the high concentration applied on the cells, its effect was not attenuated by DAO. **C**, Sunitinib treatment was sensitive to DAO and EFD. **D-E**, GLP-1 and Exendin-4 induced secretion was sensitive also to DAO and EFD. **F**, Effects of Ca^{2+} channel inhibitors and K^{+} channel openers on insulin secretion. PIN, pinacidil; DAO, diazoxide (K_{ATP} openers); VER, verapamil (L-type inhibitor); NFD, nifedipine (L-type inhibitor); EFD, efonidipine (L- and T-type inhibitor); EX-4, exendin-4

4.14 Compounds can increase glucose analog (2-NBDG) uptake in different cells

Glucose serves as one of the main energy source for the cells and is needed for their healthy functioning. In beta cells extracellular glucose is taken up particularly by the GLUT2 transporters. In healthy muscle cells and adipose tissue, insulin regulates glucose uptake by inducing the translocation of GLUT4 transporters to the plasma membrane. The failure or decreased utilization of glucose from the blood is one of the main issues in diabetic patients. The presence of excessive amount of glucose can lead to glucotoxicity and insulin resistance. We investigated how do the selected compounds influence glucose uptake in vitro in beta cells (RIN-5AH), myoblasts (C2C12) and differentiated adipocytes (3T3-L1). We utilized flow cytometry and the fluorescent glucose analogue, 2-NBDG for the measurements. Most of the compounds increased 2-NBDG uptake in C2C12 myoblasts. Four compounds significantly increased 2-NBDG uptake in differentiated 3T3-L1 cells together with insulin. This might suggest that they have an insulin independent mechanism for glucose uptake stimulation. In RIN-5AH cells three compounds caused a significant increase and the effect of VCC341830:01 could be alleviated by the GLUT4/2 inhibitor Cytochalasin B. By summarizing the results, VCC341830:01 and VCC346349:01 seem to be the most promising candidates for further investigation of their role played in the regulation of glucose uptake (*Figures 4.14.1-4*)

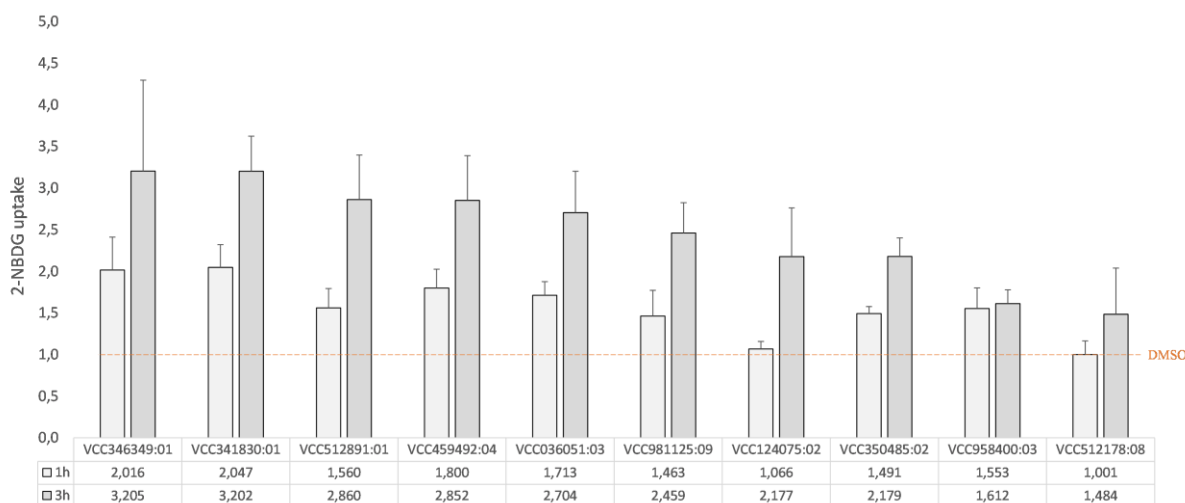


Figure 4.14.1 Normalized 2-NBDG uptake in C2C12 myoblasts. DMSO=1. All compounds had significantly increased 2-NBDG uptake after 1h stimulation, except VCC124075:02 and VCC512178:08. 2-NBDG uptake couldn't be measured for sunitinib and VCC525068:03, because of autofluorescence. ($n \geq 4$)

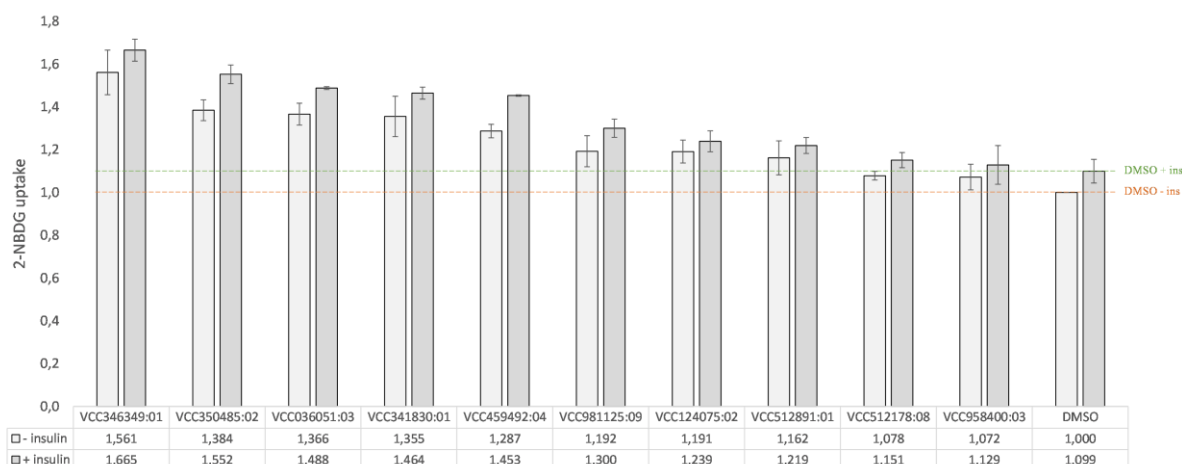


Figure 4.14.2 Normalized 2-NBDG uptake in differentiated 3T3-L1 adipocytes. DMSO=1. Five compounds produced a significant increase ($p < 0.05$) in 2-NBDG uptake with the addition of 0.5ug/ml insulin (VCC346349:01, VCC350485:02, VCC036051:03, VCC341830:01 and VCC459492:04) compared to non-treated samples (DMSO). It's likely that the compounds possess an insulin independent mechanism for the stimulation of 2-NBDG uptake. ($n=3$)

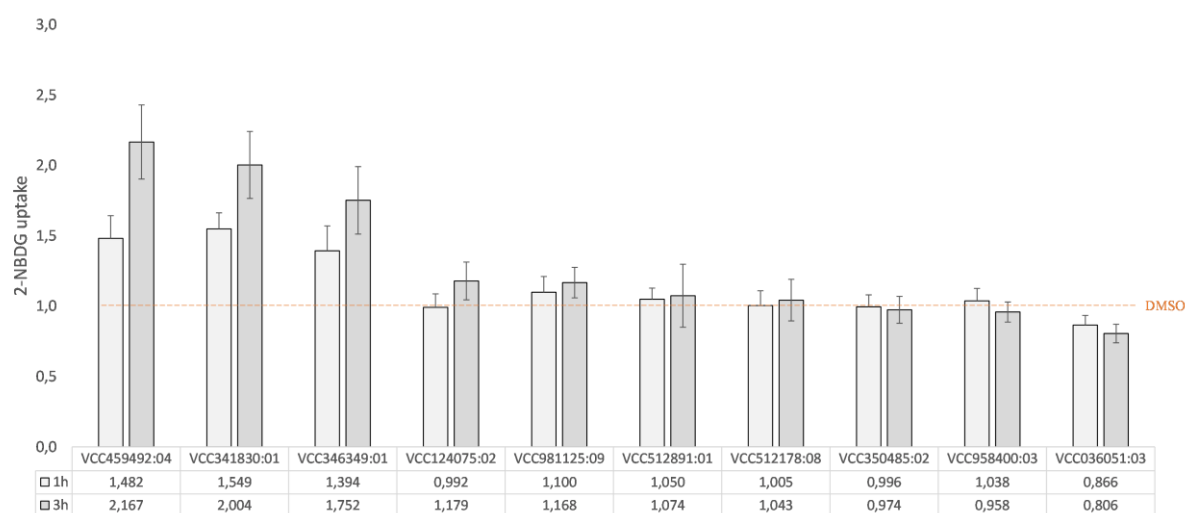


Figure 4.14.3 Normalized 2-NBDG uptake in RIN-5AH beta cells. DMSO=1. The 2-NBDG uptake was also checked in beta cells, since insulin secretion depends on glucose level. 3 compounds (VCC459492:04, VCC341830:01 and VCC346349:01) showed an increase in 2-NBDG uptake ($n=4$).

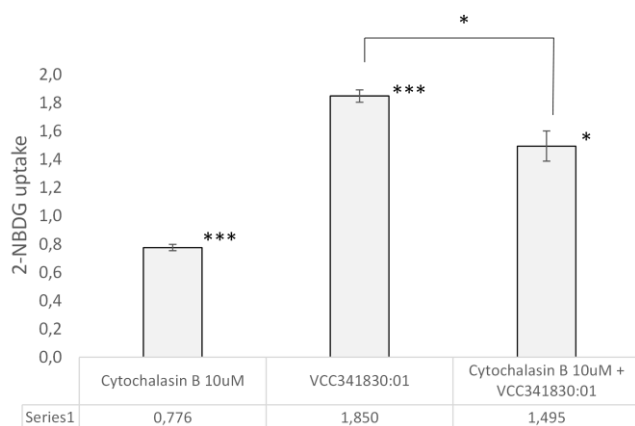


Figure 4.14.4

Normalized 2-NBDG uptake (DMSO=1). In RIN-5AH cells cytochalasin B significantly decreased 2-NBDG uptake compared to untreated DMSO control. It could also alleviate but not abolish the effect of VCC341830:01, which suggests that its action is partly dependent on glucose transporters (GLUT-2). (** $p < 0.001$; * $p < 0.05$ to DMSO or to combination treatment; $n=4-5$)

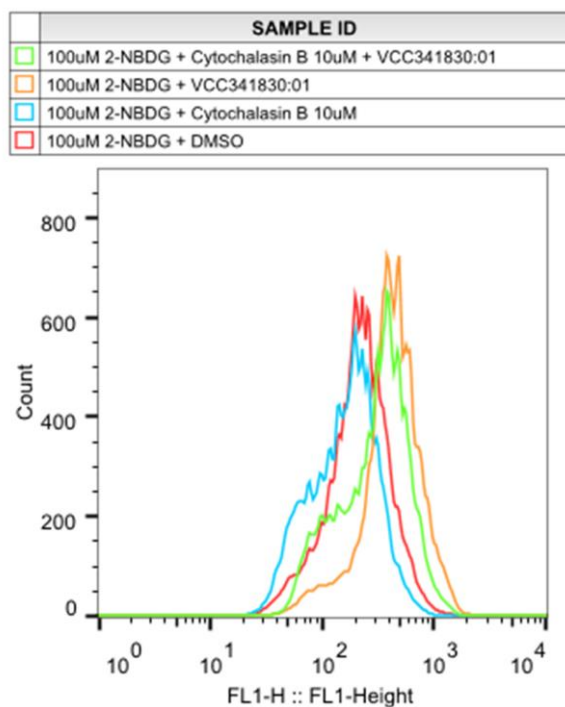


Figure 4.14.5

Representative histograms for 2-NBDG uptake assay. 5uM VCC341830 evoked a positive shift in FL-1 compared to DMSO treated cells, which could be attenuated by the co-treatment with 10uM Cytochalasin B.

4.15 Pathway analysis in RIN-5AH beta cells

AMPK, PKCs and ERK1/2 phosphorylation were tested for the seeded insulinotropic compounds and PKA, CREB, mTOR and ERK1/2 activities for the cAMP inducer compounds in RIN cells.

AMP-activated protein kinase (AMPK) plays central role in metabolic processes and its activated form negatively regulates nutrient-induced insulin secretion. By food uptake and metabolism, the AMP/ATP ratio is decreased, as a consequence AMPK activity is also lowered. It is thought that activated form negatively regulates insulin secretion from beta cells, thus its inhibition can be a MOA for insulin secretion in beta cells^{249,292}. On the other hand glucose starvation induced AMPK stimulation can be responsible for beta cell apoptosis²⁹³. It is important to notice that AMPK activation might be preferential in other tissues (in diabetes)¹⁹⁷ and blocking can produce cardio toxic effects²⁹⁴. The western blot results showed that AMPK phosphorylation was mildly induced by VCC036051:03 and markedly inhibited by sunitinib but not changed by the treatment of other compounds in RIN-5AH cells (*Figure 4.15.1*).

Protein kinase C (PKC) proteins can be classified into different subgroups: conventional PKCs (α, βI, βII and γ), novel PKCs (δ, ε, η and θ) and atypical PKCs (ζ, λ/ι). PKCs are often referred that they evoke exocytosis upon activation, they may induce a low rate Ca²⁺ influx as well²⁹⁵. I would like to highlight some of them which are associated with diabetes, insulin resistance or insulin release. PKCβ deletion or inhibition may be beneficial in the treatment of diabetic nephropathy; furthermore in PKCβ -/- mice GLUT-4 translocation was induced in different tissues and a slightly reduced blood glucose level was observed, however serum insulin level was not changed compared to PKCβ +/+ or +/- mice²⁹⁶. During exercise PKCs are regulated differentially, PKCβ was downregulated in mouse muscle and liver cells²⁹⁷ and upregulated PKCζ was detected in human muscle cells²⁹⁸. The atypical PKCs, PKC ζ and λ may regulate exercise-induced glucose mobilization through AMPK activation and interestingly can induce beta cell proliferation²⁹⁸⁻³⁰⁰. In beta cells the atypical PKCs regulate insulin secretion. Studies performed with selective PKC inhibitors and on knockout mice showed that atypical PKCs, most likely PKC λ plays an important role in insulin secretion. Down regulation of this isoform produced interesting results. It reduced the expression levels of GLUT2, Kir6.2 and SUR1, making the cells less sensitive to glucose and tolbutamide treatment, hexokinases (enzymes that initiate glycolysis) were unregulated. In PKC λ -/- mice showed impaired glucose tolerance and decreased insulin level. The involvement of atypical PKCs in insulin release was also shown in previous publications by using small molecule PKC

inhibitors^{301,302}. Additionally GLP-1 and PKC ζ is likely to share a common pathway, which induces beta cell proliferation³⁰³. PKC ζ activation could promote the proliferation of insulinoma cells and islets, indeed a transgenic mice model harboring the constitutively active PKC ζ showed an increased glucose tolerance and enhanced insulin secretion. This effect was concomitant with the activation of mTOR pathway^{304,305}. The conventional PKC α is necessary and plays an important role in GSIS. Interestingly beta cell stimulation with GLP-1 and GIP or glucose can also involve PKC α activation or its translocation to the membrane^{306,307}. Studies that investigated the cholinergic pathway or the effects of neurotensin or iduronate-2-sulfatase, also support the need of PKC α translocation or activation in the stimulation of exocytosis in beta cells³⁰⁸⁻³¹¹. The PKC α/β , PKC ζ/λ and unspecific PKC (PKC-pan) phosphorylation were tested after compound treatments in RIN-5AH cells (*Figure 4.15.1*).

It is known that activation of MEK/ERK1/2 pathway and the phosphorylation of ERK1/2 is implicated by the treatment of various insulinotropic drugs including GLP-1 and GIP. The beta cell proliferative effects of incretins might happen partly due to the activation of this signaling pathway^{92,312,313}. The clear correlation and the full mechanism of this process is not clear and numerous pathways were associated with the increased ERK phosphorylation. In MIN6 beta cells stimulated by GLP-1 or carbachol ERK activation was found to be dependent on L-type calcium channels or IP3Rs^{314,315}. An interesting study revealed that ERK2 activation may directly regulate PDE4 activity. Upon stimulation with EGF, Erk2 was able to bind and inhibit the long isoforms of PDE4C and PDE4B enzymes, thus increased the cAMP level in transfected COS-1 cells³¹⁶. A positive feedback mechanism is also possible for Erk1/2 activation via secreted insulin³¹⁷. ERK1/2 phosphorylation could also be stimulated through increased calcium level and PKA activation in INS-1 cells³¹⁸. However a recent study done with different MEK inhibitors on MIN6 cells revealed that ERK1/2 phosphorylation might not be necessary for insulin secretion³¹⁹. In overall the phosphorylation of ERK1/2 is always a stable consequence of most of the insulinotropic drug treatments and it is associated with insulin secretion as well. The p-ERK1/2 activity was markedly increased after treatment with the selected VCC compounds in RIN-5AH cells, although VCC124075:01 was an exception (*Figures 4.15.1-2*). Unfortunately the upstream signaling elements of ERK1/2 couldn't be completely unveiled so far.

The cyclic AMP-dependent protein kinase (PKA) is one of the key proteins that regulate the process of insulin exocytosis when intracellular cAMP is elevated. The protein is composed of two catalytic (PKA_C) and two regulatory (PKA_R) domains. When cAMP molecules bind to the regulatory domain, the catalytic domains dissociate and exert their effects by phosphorylating

different targets, including a lot of proteins that are associated with exocytosis as well. PKA_R may also mediate biological action apart from modulating the catalytic subunits activity. The PKA_C can be phosphorylated at two highlighted sites, Ser338 and Thr197. The p-Thr197 which is located at the activation loop of PKA_C is required for its enzymatic activity^{33,320}. This phosphorylation site is considered very stable, since it resists strongly to phosphatases. Interestingly, in mammals the phosphorylation of Thr197 is likely to happen by PDK-1 and it is not an autophosphorylation process as in bacteria^{321,322}. Taken together the detection of PKA activity by looking at p-PKA_C levels might be difficult due to its persistent phosphorylated state. This was also revealed for some compound treatments in western blot. Nevertheless testing the phosphorylation of one of its substrate (e.g. CREB Ser133) can be a good indicator for this purpose (*Figure 4.15.2*).

The cAMP response element binding protein (CREB) is a nuclear factor, which is a phosphorylation target for multiple kinases. When phosphorylated it binds to the conserved gene promoter element CRE (cAMP response element) and regulates the expression of many genes. It can be phosphorylated and activated by many kinases³²³. The cyclic AMP-dependent protein kinase (PKA) is one of them which is able to activate CREB when intracellular cAMP level is increased; furthermore CAMK-II and CAMK-IV are also important regulators for CREB, which activity depends on Ca²⁺ level³²⁴. Additional CREB kinases are e.g. the p90RSK, MAPKAP K2 and MSK via p38 kinase³²⁵. It was described by others that ERKs are also able to phosphorylate CREB through the Rap1-Raf-MEK-ERK pathway in PC12 cells, when Ca²⁺ level is increased³²⁶. In beta cells CREB provides an anti-apoptotic signal, it contributes for the preservation of normal beta cell mass and it also prevents beta cell dysfunction associated with glucotoxicity by stimulating the transcription of different pro-survival genes^{324,327-330}. Based on these data, I suspected that CREB might be concerned in the mechanism of action of the compounds, especially the ones that increased intracellular cAMP level. It was shown that some of the compounds induced CREB phosphorylation at Ser133, which provided further information in the understanding of the mechanism of action of the compounds that elevated cAMP or Ca²⁺ levels in RIN-5AH cells (*Figure 4.15.2*).

The mammalian target of rapamycin (mTOR) is a key metabolic regulator protein in the body and its impaired or loss of function can cause significant phenotypic changes in different tissues³³¹. In beta cells it senses ATP level; furthermore promotes proliferation signals through activation of S6K1. Upstream it can be inhibited by AMPK probably indirectly involving the Tsc1/2 - Rheb-GTP pathway. The normal functioning of mTOR is necessary for beta cell mass prevention and for insulin synthesis as well^{332,333}. Another potential regulator of mTOR activity

is cAMP. In the endocrine thyroid³³⁴ and beta cells cAMP activates the mTOR pathway. In beta cells this process was described by the treatment with GLP-1, thus it indicates another link for the proliferative effect of incretins³³⁵. Compound treatment in RIN-5AH cells, did not change mTOR activity, however a mild effect was detected for some compounds on mTOR phosphorylation (*Figure 4.15.2*). α -tubulin was used for loading control and are included in the Appendix.

The summarized western blot results and qualitative evaluation is displayed in *Table 4.15.1*.

VCC Compounds Phosphorylation	VCC525068:03	VCC512178:08	VCC981125:01	SUTENT	VCC512891:01	VCC350485:02	VCC346349:01	VCC341830:01	VCC834153:01	VCC958400:03	VCC036051:03	VCC124075:02	VCC459492:04	Forskolin	Roflumilast	GLP-1	Effects When Activated	Effects When Inactivated/ Knockdown / Knock out
AMPK (2h)	/	/	/	-	/	/	/	/	/	+	/	/					Suppression of IS	Induction of IS
PKC a/b (2h)	/	+	/	+	+	+	+	+		+	+	/	/				PKCa: may induce IS	PKCb: no effect on IS?
PKC z/la (2h)	-	+	/	/	/	/	/	/		/	+	/	/				PKCz: induced IS	PKCa: decreased IS PKCz: decreased proliferation
PKC-pan (2h)	-	+	/	+	/	+	+	/		/	+	/	/					
ERK (2h)	+	+	+	+	+	+	+	+	+	+	+	+	+				Proliferation	Suppressed proliferation
MEK (30min)	+	+		+	+		/		+			/		+	+	+	Proliferation	Suppressed proliferation
ERK (30min)	+	+		+	+		/		+			/	+	+	+	+	Proliferation	Suppressed proliferation
PKAc (30min)	+	/		+	+		+		+			+		+	+	+	Induction of IS	Suppression of IS
CREB (30min)	+	/		+	+		+		+			+		+	+	+	Anti-apoptotic	Beta cell dysfunction
mTOR (30min)	+	/		+	+		+		+			+		/	/	+	Proliferation	Decreased insulin synthesis, loss of beta cell mass

Table 4.15.1 Summarized results and qualitative evaluation of western blot results of treatment with VCC compounds and indicating the known effects in beta cells. Detailed description in the text. IS: insulin secretion; + : phosphorylated; - : dephosphorylated; / : no change

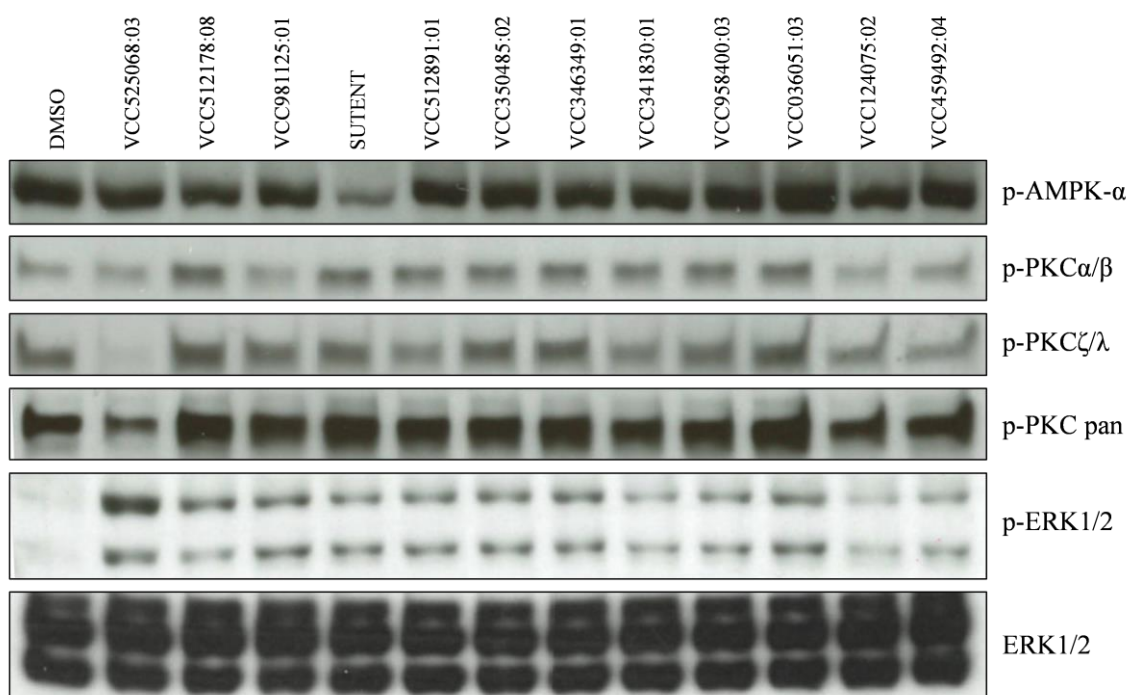


Figure 4.15.1 Western blot studies after compound treatments (5 μ M, 2h) in RIN-5AH cells.

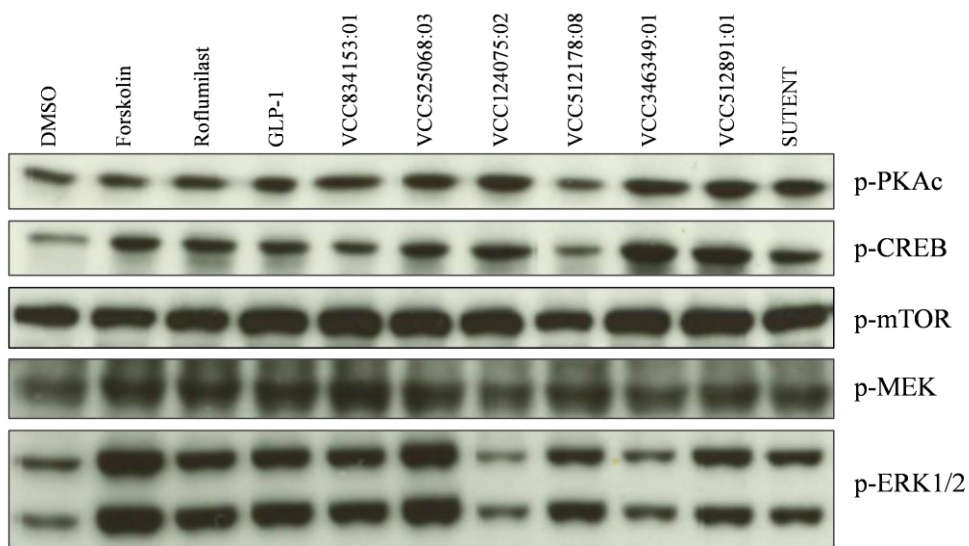


Figure 4.15.2 Western blot studies of cAMP inducer compounds in RIN-5AH cells (30min, 10 μ M). In order to confirm cAMP level stimulation, some of the "cAMP sensitive" proteins and pathways were studied.

5 **DISCUSSION**

According to human clinical data and experiments performed on different diabetic animal models, several TKIs were proven to have a capital role in improving the primary symptoms of diabetes. The following abilities were observed: they could restore normoglycemic state and treat hyperglycemia, they increased insulin sensitivity in peripheral tissues, also improved lipid metabolism and prevented beta cell loss by reducing the rate of apoptosis. Amongst these beneficial effects of TKIs, sunitinib was also able to elevate serum insulin level in vivo. We were focusing on this latter property of sunitinib and investigated the mechanisms that could be responsible for this phenomenon in in vitro systems. In the first instance the roles of kinases were investigated and for this purpose we composed a diverse compound library. The kinase inhibitor profiles of the members of this compound library were predicted to be analogous with the profile of sunitinib. These compounds were later on used as tools to identify kinases that may negatively regulate insulin secretion in beta cells. In RIN-5AH cells insulin secretion was induced by many of these compounds achieving a 10% hit rate in the insulin ELISA assay and the acutely toxic compounds were eliminated by MTT. The 55 active compounds could be clustered into different core structure families and kinase selectivity/affinity were tested for one member from each compound family. However there were differences in compound selectivity, a pool of common targets could be established. Moreover for VCC981125:09 (quinoline) and VCC958400:03 (quinoxaline) no kinase targets could be assigned (using threshold %Ctrl<35). 14 kinases could be validated by MS affinity chromatography of four substances, these were also identified in the kinase affinity panel test. I would also like to note, that in spite of the powerful capabilities of the target profiling done by MS, it has limitations and the synthesis of a proper and active linker derivative in cellular assays for these experiments is indispensable.

The results of the siRNA knockdown (KD) experiments performed in RIN-5AH and INS-1E beta cells lead to the identification of three kinases (STK16, CSNK2A1 and MARK2) that possibly negatively regulate insulin secretion in their active state in both cell lines. STK16 shares structure homology with Env7 a protein identified in yeast that negatively regulates membrane/vacuole fusion. In this regard it can't be excluded that it plays a role in insulin exocytosis as well. CSNK2A1 was already described as a regulator of insulin secretion, here we could validate this property by targeted KD in beta cells. KD effect of MARK2 in beta cells was not studied before, although in knockout mice experiments it improved insulin sensitivity and reduced high fat-induced weight gain. According to beta cell KD experiments it can be

concluded that MARK2 might have a short term effect on inhibiting insulin secretion, as longer KD has attenuated the insulin secretagogue effect. Double KD experiments and compound + KD combinations would be necessary for further validation of these targets.

By mass spectrometry additional non-kinase proteins were also identified as potential targets. Out of these PDE4C were studied in more detail and its importance was confirmed by selective PDE4 inhibitors (Roflumilast, CP 80633). As another family of PDE inhibitors (PDE5) proved to be advantageous in chronic applications in several experiments, we were curious to see whether these inhibitors can regulate insulin release in beta cells. It turned out that sildenafil and vardenafil but not tadalafil could increase insulin secretion from TC6 cells. The inefficiency of PDE5 inhibitor compounds on RIN-5AH cells can be explained with the different heterogeneity of these clonal beta cell lines.

The dissimilarity of the beta cell lines could be an important factor for the mode of action for the VCC compounds, therefore they were tested in different cell lines. Three compounds showed cell line specific insulinotropic effect (VCC981125:01, VCC124075:02 and VCC036051:03).

The cAMP molecules have crucial role in the transmission of insulinotropic signals. The cAMP level can be elevated by diverse impacts, including PDE inhibition, induction of AC enzymes e.g. by receptor signaling, and of course as a result of metabolism and conversion from ATP. In our assay the intracellular cAMP level was increased by several compounds in RIN-5AH cells. This additional effect seem to contribute to the mode of action of VCC compounds.

Another important criteria for stimulation of insulin secretion is the increased Ca^{2+} influx into the cells. Short term experiments with VCC compounds done in Fluo-4 stained cells revealed that several derivatives from the quinoline family (including VCC981125:09) induced Ca^{2+} influx in RIN-5AH cells. I hypothesized that the rapid Ca^{2+} influx might be a consequence of membrane depolarization. This idea was confirmed with whole cell patch clamp measurements. The application of higher concentration from VCC981125:09 may open the high voltage activated L-type Ca^{2+} channels, which get activated at -30mV. Moreover the 10-fold lower concentration which also depolarized the membrane, was probably enough to activate the T-type currents (threshold: between positive and -70mV). Most likely both L-type and T-type channels are involved in insulin secretion and this hypothesis was supported by other measurements: efonidipine (L- and T-type channel blocker), NiCl_2 (blocks T-type current) and verapamil (L-type channel blocker) could attenuate VCC981125-induced Ca^{2+} influx and/or insulin secretion. However the direct target of VCC981125:09 is yet unknown but most likely

it interacts with ion channels that are differently expressed in RIN-5AH (and maybe in BRIN-BD11) cells compared to TC6 and INS-1E cells.

The VCC compounds may exert some effect on peripheral tissues as well, since many of them could induce 2-NBDG uptake in myoblasts or differentiated adipocytes and they did it apparently independently to insulin. However it would be worth to check whether they can induce GLUT4 translocation in differentiated myoblasts or adipocytes, since the GLUT4/GLUT2 inhibitor Cytochalasin B could significantly attenuate the effect of VCC341830:01 in RIN-5AH cells.

In order to extend the knowledge about the mode of action of the VCC compounds in RIN-5AH cells, western blot studies were performed, which revealed some additional information. These results will be reviewed separately for each substance. The complete summarized data about the substances is displayed in *Table 5.1*.

Highlighted VCC compounds	SUTENT	VCC350485-02	VCC036051-03	VCC341830-01	VCC834153-01	VCC981125-01	VCC405984-01	VCC958400-03	VCC346349-01	VCC124075-02	VCC459492-04	VCC525068-03	VCC512178-08	VCC161829-02
Compound family	Indolines/ oxindoles	Styryl quinazolines	Other quinazolines	Thieno pyrimidines	Quinolines	Bis-quinolines	Quinoxalines	2-Amino- pyrimidines I.	2-Amino- pyrimidines II.	2-Amino- pyrimidines II.	1,6- Naphthyridines	Misc.	Misc.	Misc.
Kinase selectivity panel	+	+	+	+	+	+	+	+	+	+	+			
MS affinity chromatography	+	only binders		unsuccessful	unsuccessful	unsuccessful	unsuccessful							
RIN-5AH cells	/	/	+	+	/	/	/	+	/	+	+	+	+	+
RIN-5AH cells			+	+				+		+	+	+	+	+
RIN-5AH cells	/	/	/	/	/	/	/	/	/	/	/	/	/	/
RIN-5AH cells		/	/	+	/	/	/	/	+	/	+	/	/	/
RIN-5AH cells			+	+	/	/	/	?	?					
C2C12 cells		+	+	+	/	+	+	+	+	/	+	+	/	/
3T3L1 cells		++	++	++	+	+	/	/	++	+	++	/	/	/
RIN-5AH cells	+	+	+	+	+	+	+	+	+	+	+	+	+	+
BRIN-BD11 cells	+	+	/	+	/	/	/	+	+	+	/	+	/	/
TC6 cells	+	+	/	+	/	/	+	+	+	-	+	+	+	+
INS-IE cells	+	+	-	+	/	+	/	+	+	-	/	+	+	+
INS-IE cells	+	+	+	+	-	+	+	+	+	+	+	/	+	+
RIN-5AH cells	2,3	4,32	8,54	2,84	6,19	>1,67	2,51	2,16	4,6	3,13	3,4	>1,67	>1,67	
RIN-5AH cells		+		+	+									
ADME prediction (QRP-Prop)	198,789	1423,62	2609,734	1381,72	4540,374	336,759	918,284	69,798	459,745	135,273	3246,84	117,319	66,625	66,625
	3,907	5,668	6,338	3,374	4,721	4,505	4,899	2,585	3,51	2,538	4,125	4,299	2,495	0,993
No. of tested CPPDs	17	51	3	29	25	2	7	20	20	5	5			
	14	3	12	46	22	0	8	22	22	11	11			
	31	54	15	75	47	2	15	42	42	16	16			
Proposed mechanism	kinases	enzymes? / FLT3?	kinases	kinases	ion channel?	GPCR	?	kinases	kinases	kinases	kinases	kinases	kinases	kinases

+: positive effect; -: negative effect; /: no change
 *: ** analogues structures (difference is one functional group or substituent)
 ? ambiguous

Table 5.1

Sunitinib (oxindole). Several studies confirmed that sunitinib has clearly the potential to efficiently lower the blood glucose level. Although its main targets are already known, there is a lack of evidence underlying the complete mechanism. It was proposed that c-Kit and PDGFR is responsible for the glucose concentration lowering effect, but we hypothesized that this is a more complex effect. Since sunitinib was our primary tool compound, a comprehensive target profiling was performed. Not surprisingly it was shown binding affinity to many kinases and other proteins (MS), making it difficult to select the relevant targets responsible for insulin secretion. Nevertheless some of its targets (CSNK2A1, STK16, and MARK2) could be validated by siRNAs. The sunitinib-induced insulin secretion in RIN-1AH cells may also involve the inhibition of AMPK. AMPK was identified as a target for sunitinib in the affinity assays and it also inhibited the phosphorylation of AMPK in RIN-5AH cells. Sunitinib activated the MEK/ERK pathway in RIN-5AH cells, furthermore it has induced PKC-pan phosphorylation, notably most likely PKC α phosphorylation. However we couldn't demonstrate a significant increase in cAMP level, a slight activation of CREB was also detected. Sunitinib effectively increased the insulin level in TC6, BRIN-BD11 and INS-1E beta cells as well, which means that it has a "general effect" independently from their heterogeneity. In the glucose sensitive INS-1E cells it raised insulin level in a glucose dependent manner, similarly to other compounds. Combination treatments done with Ca²⁺ channel inhibitors showed that its insulinotropic effect could be significantly reduced only by efonidipine, the L- and T-type Ca²⁺ channel inhibitor DHP drug. Combinations with verapamil and nifedipine (blocking the L-type currents) couldn't alleviate the insulin secretion, similarly to GLP-1 and Exendin-4 treatments. In conclusion it seems that T-type channels are critical for sunitinib-induced insulin secretion in RIN-5AH cells. Moreover application of high concentration diazoxide could also reduce the effect of sunitinib, same way as incretin treatments. Since sunitinib is a multi-TKI with remarkable side effects in clinic, it is proposed that the same complex mechanisms are also present which contribute to its insulinotropic effect in beta cells.

VCC341830:01 and VCC834153:01 (thieno-pyrimidine). This compound family was originally designed to inhibit EGFR. Compound VCC341830:01 showed a high selectivity for EGFR, HER2, MKNK2 and KIT in the kinase affinity assay. Numerous kinator derivatives were tested (data not shown) by silver stained gel electrophoresis, but none of them produced any affinity to proteins. Furthermore these linker derivatives have also lost their efficiency in cellular assays. Therefore MS affinity chromatography was not performed. Nevertheless, the detection of membrane proteins by MS is one of the limitations of this technique (and needs

special protocols), which could also explain the negative results. Later on by testing more compounds from this family, the structure activity relationship data showed that most likely it is not the EGFR inhibition that is responsible for increased secretion. Some substances (e.g. VCC855801:01 and VCC321171:07) did not inhibit EGFR, but had significant insulinotropic effect (see Appendix) in RIN-5AH. The VCC834153:01 significantly increased cytoplasmic cAMP level in RIN-5AH cells and activated PKA, CREB and mTOR. It also had a great impact on ERK1/2 phosphorylation. The VCC834153:01 produced an extraordinary effect in INS-1E cells compared to the other compounds. It strongly increased insulin level in low glucose buffer, but interestingly not in high glucose buffer. The other derivative VCC341830:01 showed no glucose dependent effect but it was active in the insulin ELISA assay of all four beta cell line models. In 2-NBDG uptake assay VCC341830:01 was one of the most efficient compound and its effect was Cytochalasin B dependent. Thus it might be possible that it facilitates glucose metabolism. The VCC341830:01 and VCC834153:01 showed very low toxicity on C2C12, 3T3-L1, HepG2, TC6 and RIN-5AH cells.

VCC981125 and derivatives (quinoline). The VCC981125:09 is one of the most efficient compounds in RIN-5AH cells which exerts its effect by enhancing Ca^{2+} influx. Although VCC981125:09 shares the same core structure with bosutinib, the chemical modification in the molecule has resulted in a loss of affinity to kinases. This was confirmed by the kinase affinity screen, by MS pre-experiments and silver gel staining (data not shown), where no targets could be identified. There were numerous linker derivatives designed, but unfortunately none of them were potent enough in the cellular assay to perform an MS experiment using the target deconvolution technique. The compound did not affect p-Tyr, p-Ser and p-Thr levels (see Appendix); this further confirms that it is not a kinase inhibitor. Other officially available drugs that resemble to VCC981125:09 are quinidine, chloroquine and fluoroquinolones. Quinidine was shown to inhibit K_{ATP} channels in MIN6 cells³³⁶ and it also increased insulin level in our assay in RIN-5AH cells (data not shown). Reported data suggests that fluoroquinolones also inhibit K_{ATP} channels and can induce Ca^{2+} release from internal stores as well, dependently on ryanodine receptors³³⁷. These data supports the fact that VCC981125:09 and close derivatives may also influence ion channel or Ca^{2+} signaling. Nevertheless, the mechanism of this substance couldn't be compared to any of these drugs, neither to the action of glibenclamide, since it needs extracellular calcium to exert its stimulatory effect, furthermore glibenclamide which is targeting K_{ATP} channels, was effective on both TC6 and RIN-5AH cells, while VCC981125:09 wasn't (see Appendix). Thapsigargin a drug which works by emptying intracellular calcium

stores through inhibition of SERCA and the ionophore drug A23187 had an inhibitory effect on insulin secretion, therefore VCC981125:09 does not possess any of these mechanisms. Bosutinib did not induce Ca^{2+} influx as expected. Combinatorial treatments with calcium channel blockers and K_{ATP} opener diazoxide proved that its potency is dependent on L-type and T-type currents, furthermore the repolarizing effect of diazoxide could abrogate its activity. The influx of calcium is most likely the consequence of membrane depolarization that was validated by whole cell patch clamp measurements. By patch clamp, we could also register the changes in membrane capacitance, which reflects to an increased insulin exocytosis^{289,338}. Although a clear structure activity relationship could be established for this family of compounds in RIN-5AH cells, unfortunately these compounds were ineffective in INS-1E and TC6 cells, indeed in INS-1E cells it produced a negative shift. Conversely in BRIN-BD11 cells some of its derivatives could potentiate insulin secretion (see Appendix). The VCC981125:09 did not have any significant impact on 2-NBDG uptake. It activated ERK1/2 and did not change PKC phosphorylation.

VCC405984:01 (bis-quinoline). This compound increased insulin secretion in RIN-5AH and in INS-1E cells. In INS-1E cells the activity was highly dependent on glucose concentration and more importantly in low glucose buffer it had no significant effect compared to DMSO. This property could be very important in the treatment of diabetes and this is characteristic resembles to GPCR agonist drugs. Moreover it produced a significantly better response compared to sunitinib treatment. Since it did not inhibit p-Tyr, p-Ser and p-Thr, we can assume that it's not a kinase inhibitor. By the treatment of RIN-5AH cells the ERK1/2 phosphorylation was upregulated similarly to other efficient compounds (see Appendix). Preliminary data suggests that it is a GPCR antagonist coupled to a Gq/Gi mechanism however it did not increase Ca^{2+} influx by acute treatment. More research is needed to identify and validate the GPCR target and to discover whether this compound or its derivatives could be relevant candidates for the treatment of diabetes.

VCC350485:02 (Styryl-quinazoline) is a derivative of a compound that induces p53 activation³³⁹. It is a very potent compound in RIN-5AH cells with the lowest EC_{50} for insulin, but the lowest IC_{50} as well. By utilizing the target deconvolution method we couldn't pull down any targets, but several specific binders were detected, which could be correlated with insulin secretion or insulin gene transcription. The compound was effective on four different beta cell lines and a structure activity relationship could be prepared based on RIN-5AH insulin ELISA results. In differentiated adipocytes it increased 2-NBDG uptake significantly but not in RIN-5AH or C2C12 cells. The p-ERK1/2 level was upregulated and slightly the p-PKC α as well.

Taken together the substance showed a general insulin secretagogue effect however we should reckon with the increased toxicity, but this property can be likely eliminated by the synthesis of new derivatives.

VCC036051:03 (quinazoline) shares core structure with the EGFR inhibitor gefitinib, erlotinib or lapatinib, although it has no EGFR inhibitory feature (see Appendix). Anyway as it was proposed for the thieno-pyrimidine family, the EGFR inhibition is not feasible for the enhanced insulin release. The compound had the highest “in vitro therapeutic index”, thus it proved to be the least toxic in RIN-5AH cells (and other cells too). On the other hand along with VCC981125 it decreased secretion from INS-1E cells and was inactive on other beta cells. In mouse myoblasts (C2C12) and differentiated adipocytes (3T3-L1) it increased 2-NBDG uptake. The decreased insulin secretion could be associated with its activating effect on AMPK but on the other hand if this property is also present in peripheral tissues (liver, muscle or fat) this could give an explanation for its glucose uptake inducing effect. In overall AMPK activation is preferable and advantageous in the treatment of diabetes¹⁹⁷.

VCC459492:04 (1,6-Naphthyridine) was active for insulin secretion in RIN-5AH and TC6 cells, and less efficient on INS-1E cell. It was a strong 2-NBDG uptake inducer in RIN-5AH beta cells, myoblasts and differentiated adipocytes.

VCC346349:01 (2-Amino-pyrimidine II.) is also a highly effective 2-NBDG uptake inducer and possess a general insulinotropic effect on all four beta cell lines. It produced a delayed effect on ERK1/2 phosphorylation, compared to other compounds (VCC834153, VCC525068, VCC512178, VCC512891 and sunitinib) that already stimulated ERK1/2 activation after 30min treatment. The postliminary effect might be attributed to the positive feedback of insulin. On the other hand it raised the intracellular cAMP level in RIN-5AH cells and activated the PKA/CREB pathway, including mTOR.

VCC512891:01 (2-Amino-pyrimidine Ia.) shares kinase targets with sunitinib and was used as a tool to identify negative regulators of insulin release. It contains the core structure of imatinib, however it was more potent insulin secretion inducer in RIN-5AH cells. It significantly increased insulin secretion from all four beta cell lines, it slightly elevated cAMP level in RIN-5AH cells and activated PKA/CREB and mTOR.

VCC124075:02 (2-Amino-pyrimidine Ib.) was used as the fourth tool compound in the target deconvolution MS experiment. According to its kinases selectivity panel it was the least selective compound after sunitinib and showed a cell line specific effect for RIN-5AH and BRIN-BD11 cells in insulin ELISA assay. The slight negative effect achieved on TC6 and INS-1E cells can be attributed to the different expression patterns and heterogeneity of the clonal

beta cells. In RIN-5AH cells it activated PKA/CREB and mTOR, which correlates with the increased cAMP level caused by the drug.

VCC958400:03 (Quinoxaline) was a moderately active compound in insulin assay, although it showed some activity on p-PKC α/β . It has no, or very low affinity to kinases.

VCC512178:08 and VCC161829:02 (Misc. I.) are analogous structures. VCC512178:08 is a potent insulin secretagogue molecule which is known to inhibit PAK. It was active in RIN-5AH, TC6 and INS-1E cells too. It increased insulin secretion in a glucose dependent manner in INS-1E cells. Treatment with this compound caused a slightly increased cAMP level in RIN-5AH, however interestingly it seems that VCC512178:08 did not affect the PKA/CREB pathway, but involved the activation of ERK1/2. One possibility for ERK1/2 phosphorylation could be the Epac/Rap1/Raf/MEK/ERK pathway activation³⁴⁰, but other factors may play role as well.

VCC525068:03 (Misc. II.) is a PKC inhibitors molecule, but in spite of that it markedly induced insulin secretion in all cell lines. In RIN-5AH cells we demonstrated that PKA/CREB and mTOR, respectively the MEK/ERK pathway was strongly activated. It is worth to notice that despite its high activity it did not regulate the secretion glucose dependently from INS-1E cells.

In this study numerous small molecule kinase inhibitors and their derivatives were investigated for their insulinotropic effect. We found that not only Sutent but other kinase inhibitors stimulated the insulin secretion in beta cells and therefore may lower blood glucose level as well. The utilized VCC compounds in our assays provided efficient tools to investigate beta cell function and other mechanisms related to diabetes. Hopefully these data will also contribute to the development of novel therapies and to a better understanding of how TKIs can modulate beta cell function.

SUMMARY

We found that sunitinib increased insulin secretion *in vitro* in different beta cell lines. Based on this observation we prepared a compound library consisting of 558 members, which were predicted to overlap with the kinase inhibition profile of sunitinib. Using this library we performed a phenotypic screen for insulin secretion, utilizing an insulin ELISA assay. Then the compounds were clustered into different core structure families and from each family one compound was further investigated in different assays.

Summarizing our results, the following conclusions were made:

- We identified compounds that stimulated insulin secretion and were less toxic compared to sunitinib. The action of most of the compounds was dependent on glucose concentration in INS-1E cells
- Structure activity relationships could be set up for quinoline, styryl-quinazoline and thienopyrimidine compound families in RIN-5AH cells, therefore it seems to be possible that TKI compounds can be optimized for insulinotropic effects
- We could define and validate kinases (MARK2, STK16 and CSNK2A1) by siRNA that negatively regulate insulin secretion in RIN-5AH and INS-1E cells, however we can't rule out multitarget effects of compounds
- We could assign partial mechanisms of actions for most of the compounds, these involve the activation of cAMP and Ca²⁺ pathways
- Some VCC compounds were also able to increase 2-NBDG (glucose analogue) uptake into beta-cells, myoblasts and differentiated adipocytes, which could be also an attractive viewpoint in the treatment of diabetes

In conclusion we found potential lead candidates that should be further investigated. Amongst these, there are also compounds with a more selective kinase profile compared to sunitinib. An interesting group of compounds are the quinolines/bis-quinolines that are not targeting kinases, but can cause a rapid Ca²⁺ influx (quinoline) in RIN-5AH cells or act glucose dependently (bis-quinoline) in INS-1E cells. On the other hand, since many of the tested compounds are kinase inhibitors, our results further attract the attention to the insulinotropic effect of TKIs used in clinical treatments and this should be taken into account in clinical practice as well.

ZUSAMMENFASSUNG

Wir haben festgestellt, dass das Krebsmedikament Sutent die Insulinsekretion in vitro in verschiedenen pankreatischen beta-Zelllinien erhöhte. Basierend auf dieser Beobachtung wurde eine chemische Substanzbibliothek erstellt, die aus 558 Verbindungen bestand die mit dem Kinase Inhibitions Profil von Sunitinib korrelierte. Diese Bibliothek wurde mit einem „phänotypischen drug screen“ auf Insulin Induktion geprüft. Positive Verbindungen wurden nach Core-Struktur Familien geordnet und aus jeder Strukturgruppe wurde eine repräsentative Verbindung weiter untersucht.

Die Zusammenfassung unserer Ergebnisse erlaubten folgende Schlussfolgerungen:

- Es wurden mehrere Moleküle identifiziert, die in den verwendeten Zellen die Insulinsekretion induzierten und im Vergleich mit Sunitinib weniger toxisch waren. Die Wirkung der meisten Substanzen waren in INS-1E Zellen Glukosekonzentration-abhängig.
- Struktur-Aktivitäts-Beziehungen wurden bestimmt für die Qinolin, Styryl-quinazolin und Thieno-Pyrimidin Substanzfamilien nach den Insulin-ELISA Ergebnissen in RIN-5AH Zellen. Es scheint also möglich zu sein, dass Kinase Inhibitoren auf insulinotrope Wirkung optimiert werden können
- Wir konnten einige Ziel- Kinasen mit siRNA identifizieren und validieren (MARK2, STK16 and CSNK2A1), die die Insulinsekretion in RIN-5AH und INS-1E Zellen negativ regulierten, obwohl Multi-Target-Effekte der Verbindungen nicht ausgeschlossen werden können
- Für die meisten Substanzen konnten Wirkungsmechanismen etabliert werden welche, die Aktivierung von cAMP und Ca^{2+} Signalübertragungswegen betrafen.
- Einige Compounds konnten auch die Aufnahme von 2-NBDG (Glukose-Analog) in beta-Zellen, Myoblasten und differenzierte Adipozyten stimulieren was ein interessanter Aspekt bei der Behandlung von Diabetes sein könnte

Wir fanden auch potenzielle Substanzen, die weiteres Entwicklungspotenzial aufweisen. Darunter sind Moleküle, die im Vergleich zu Sunitinib selektivere Kinase-Profile aufweisen. Eine interessante Substanz Gruppe sind die Quinoline/Bis-quinoline die keine Kinase Bindung aufwiesen wurden, aber „ Ca^{2+} influx“ (Quinoline) in RIN-5AH Zellen oder Glukose-abhängige Wirkung in INS-1E Zellen stimulierten.

ACKNOWLEDGEMENTS

This study was performed at Max Planck Institute of Biochemistry, in the Department of Molecular Biology (Martinsried by Munich, Germany), under the supervision of Prof. Dr. Axel Ullrich.

First of all I would like to say thank you to my supervisor, Prof. Dr. Axel Ullrich that he gave me the opportunity to work on this very interesting project. I'm very thankful for his generous support and positive, motivating advices.

I would like to thank Prof. Dr. Bernhard Küster (Technical University Munich, Head of Proteomics and Bioanalytics) for accepting my request as doctor father and for promoting my doctoral thesis.

I would like to say thanks to all members of the Ullrich department, primarily Dr. Mathias Falckenberg who guided me in the beginning of the project and supported me with his ideas and discussions. I thank to Dr. Vijay K. Ulaganathan for not only the fruitful discussions about science but also for philosophical conversations, which helped me a lot to improve my skills. Thank to all technical assistants of the department for their helpful attitudes.

Moreover I really appreciated the collaborative talks and technical suggestions for the MS experiments from the people in Evotec. Thank to Dr. Stefan Müller, Dr. Christian Eckert and Dr. Klaus Godl.

I'm very thankful to Dr. Jana Hartmann (Technical University Munich, Institute of Neuroscience) for helping me to perform the patch clamp studies and I'm glad that she sacrificed her time and never gave up in order to produce successful experiments together. Moreover I'm very grateful to Prof. Dr. Bert Sakmann and Prof. Dr. Arthur Konnerth who recommended Dr. Hartmann for me to help.

Furthermore, I would like to extend my thanks to one of my best friend Bálint Nagy (University of Tübingen, Group of Neuron–Glia Interactions) for his helpful ideas to evaluate patch clamp results.

I acknowledge the medicinal chemistry support of Vichem Chemie Research Ltd. and say thanks to all the chemists who synthesized the customized compounds.

Finally I'm grateful to my family, my parents, my brother and my girlfriend for their continuous support and positive thoughts during hard times.

REFERENCES

- 1 Danaei, G. *et al.* National, regional, and global trends in fasting plasma glucose and diabetes prevalence since 1980: systematic analysis of health examination surveys and epidemiological studies with 370 country-years and 2.7 million participants. *Lancet* **378**, 31-40, doi:10.1016/s0140-6736(11)60679-x (2011).
- 2 Mannino, G. & Sesti, G. Individualized Therapy for Type 2 Diabetes. *Mol Diagn Ther* **16**, 285-302, doi:10.1007/s40291-012-0002-7 (2012).
- 3 www.who.int.
- 4 Kato, N. Insights into the genetic basis of type 2 diabetes. *Journal of diabetes investigation* **4**, 233-244, doi:10.1111/jdi.12067 (2013).
- 5 Brunetti, A., Chiefari, E. & Foti, D. Recent advances in the molecular genetics of type 2 diabetes mellitus. *World journal of diabetes* **5**, 128-140, doi:10.4239/wjd.v5.i2.128 (2014).
- 6 Busch, C. P. & Hegele, R. A. Genetic determinants of type 2 diabetes mellitus. *Clinical Genetics* **60**, 243-254, doi:10.1034/j.1399-0004.2001.600401.x (2001).
- 7 Marchetti, P., Bugliani, M., Boggi, U., Masini, M. & Marselli, L. The pancreatic beta cells in human type 2 diabetes. *Advances in experimental medicine and biology* **771**, 288-309 (2012).
- 8 Ferrannini, E., Gastaldelli, A. & Iozzo, P. Pathophysiology of prediabetes. *The Medical clinics of North America* **95**, 327-339, vii-viii, doi:10.1016/j.mcna.2010.11.005 (2011).
- 9 Knop, F. K. *et al.* Reduced Incretin Effect in Type 2 Diabetes: Cause or Consequence of the Diabetic State? *Diabetes* **56**, 1951-1959, doi:10.2337/db07-0100 (2007).
- 10 Zraika, S. *et al.* Toxic oligomers and islet beta cell death: guilty by association or convicted by circumstantial evidence? *Diabetologia* **53**, 1046-1056, doi:10.1007/s00125-010-1671-6 (2010).
- 11 Ma, Z. *et al.* Enhanced in vitro production of amyloid-like fibrils from mutant (S20G) islet amyloid polypeptide. *Amyloid* **8**, 242-249, doi:doi:10.3109/13506120108993820 (2001).
- 12 Maedler, K. *et al.* Glucose-induced beta cell production of IL-1beta contributes to glucotoxicity in human pancreatic islets. *J Clin Invest* **110**, 851-860, doi:10.1172/jci15318 (2002).
- 13 Newsholme, P. *et al.* Insights into the critical role of NADPH oxidase(s) in the normal and dysregulated pancreatic beta cell. *Diabetologia* **52**, 2489-2498, doi:10.1007/s00125-009-1536-z (2009).
- 14 Watson, J. D. Type 2 diabetes as a redox disease. *The Lancet* **383**, 841-843 (2014).
- 15 Bardy, G. *et al.* Quercetin induces insulin secretion by direct activation of L-type calcium channels in pancreatic beta cells. *British Journal of Pharmacology* **169**, 1102-1113, doi:10.1111/bph.12194 (2013).
- 16 Bhattacharya, S., Oksbjerg, N., Young, J. F. & Jeppesen, P. B. Caffeic acid, Naringenin and Quercetin enhance glucose stimulated insulin secretion and glucose sensitivity in INS-1E cells. *Diabetes, Obesity and Metabolism*, n/a-n/a, doi:10.1111/dom.12236 (2013).
- 17 Miki, T., Nagashima, K. & Seino, S. The structure and function of the ATP-sensitive K⁺ channel in insulin-secreting pancreatic beta-cells. *Journal of molecular endocrinology* **22**, 113-123 (1999).

- 18 Haider, S., Antcliff, J. F., Proks, P., Sansom, M. S. P. & Ashcroft, F. M. Focus on Kir6.2: a key component of the ATP-sensitive potassium channel. *Journal of Molecular and Cellular Cardiology* **38**, 927-936, doi:10.1016/j.yjmcc.2005.01.007 (2005).
- 19 Tucker, S. J., Gribble, F. M., Zhao, C., Trapp, S. & Ashcroft, F. M. Truncation of Kir6.2 produces ATP-sensitive K⁺ channels in the absence of the sulphonylurea receptor. *Nature* **387**, 179-183 (1997).
- 20 Craig, T. J., Ashcroft, F. M. & Proks, P. How ATP inhibits the open K(ATP) channel. *The Journal of general physiology* **132**, 131-144, doi:10.1085/jgp.200709874 (2008).
- 21 Wollheim, C. B., Blondel, B., Trueheart, P. A., Renold, A. E. & Sharp, G. W. Calcium-induced insulin release in monolayer culture of the endocrine pancreas. Studies with ionophore A23187. *J Biol Chem* **250**, 1354-1360 (1975).
- 22 Guinamard, R., Demion, M. & Launay, P. Physiological Roles of the TRPM4 Channel Extracted from Background Currents. *Physiology* **25**, 155-164, doi:10.1152/physiol.00004.2010 (2010).
- 23 Uchida, K. & Tominaga, M. The role of thermosensitive TRP (transient receptor potential) channels in insulin secretion [Review]. *Endocrine Journal* **58**, 1021-1028 (2011).
- 24 Nenquin, M., Szollosi, A., Aguilar-Bryan, L., Bryan, J. & Henquin, J.-C. Both Triggering and Amplifying Pathways Contribute to Fuel-induced Insulin Secretion in the Absence of Sulfonylurea Receptor-1 in Pancreatic β -Cells. *Journal of Biological Chemistry* **279**, 32316-32324, doi:10.1074/jbc.M402076200 (2004).
- 25 Gembal, M., Detimary, P., Gilon, P., Gao, Z. Y. & Henquin, J. C. Mechanisms by which glucose can control insulin release independently from its action on adenosine triphosphate-sensitive K⁺ channels in mouse B cells. *J Clin Invest* **91**, 871-880, doi:10.1172/jci116308 (1993).
- 26 Aizawa, T., Sato, Y. & Komatsu, M. Importance of nonionic signals for glucose-induced biphasic insulin secretion. *Diabetes* **51 Suppl 1**, S96-98 (2002).
- 27 Ahren, B. Islet G protein-coupled receptors as potential targets for treatment of type 2 diabetes. *Nature reviews. Drug discovery* **8**, 369-385, doi:10.1038/nrd2782 (2009).
- 28 Regard, J. B. *et al.* Probing cell type-specific functions of Gi in vivo identifies GPCR regulators of insulin secretion. *J Clin Invest* **117**, 4034-4043, doi:10.1172/jci32994 (2007).
- 29 Ahrén, B. Autonomic regulation of islet hormone secretion – Implications for health and disease. *Diabetologia* **43**, 393-410, doi:10.1007/s001250051322 (2000).
- 30 Ramos, L. S., Zippin, J. H., Kamenetsky, M., Buck, J. & Levin, L. R. Glucose and GLP-1 stimulate cAMP production via distinct adenylyl cyclases in INS-1E insulinoma cells. *The Journal of general physiology* **132**, 329-338, doi:10.1085/jgp.200810044 (2008).
- 31 Willoughby, D. & Cooper, D. M. F. *Organization and Ca²⁺ Regulation of Adenylyl Cyclases in cAMP Microdomains*. Vol. 87 (2007).
- 32 Hanoune, J. & Defer, N. REGULATION AND ROLE OF ADENYLYL CYCLASE ISOFORMS. *Annual Review of Pharmacology and Toxicology* **41**, 145-174, doi:doi:10.1146/annurev.pharmtox.41.1.145 (2001).
- 33 Seino, S. & Shibasaki, T. PKA-Dependent and PKA-Independent Pathways for cAMP-Regulated Exocytosis. *Physiological Reviews* **85**, 1303-1342, doi:10.1152/physrev.00001.2005 (2005).
- 34 Winzell, M. S. & Ahrén, B. G-protein-coupled receptors and islet function— Implications for treatment of type 2 diabetes. *Pharmacology & Therapeutics* **116**, 437-448, doi:<http://dx.doi.org/10.1016/j.pharmthera.2007.08.002> (2007).
- 35 Bos, J. L. Epac proteins: multi-purpose cAMP targets. *Trends in Biochemical Sciences* **31**, 680-686, doi:<http://dx.doi.org/10.1016/j.tibs.2006.10.002> (2006).

- 36 Tengholm, A. Cyclic AMP dynamics in the pancreatic beta-cell. *Upsala journal of medical sciences* **117**, 355-369, doi:10.3109/03009734.2012.724732 (2012).
- 37 Gloerich, M. & Bos, J. L. Epac: Defining a New Mechanism for cAMP Action. *Annual Review of Pharmacology and Toxicology* **50**, 355-375, doi:doi:10.1146/annurev.pharmtox.010909.105714 (2010).
- 38 Haber, E. P. *et al.* New insights into fatty acid modulation of pancreatic beta-cell function. *International review of cytology* **248**, 1-41, doi:10.1016/s0074-7696(06)48001-3 (2006).
- 39 Deeney, J. T. *et al.* Acute stimulation with long chain acyl-CoA enhances exocytosis in insulin-secreting cells (HIT T-15 and NMRI beta-cells). *J Biol Chem* **275**, 9363-9368 (2000).
- 40 Olofsson, C. S., Salehi, A., Holm, C. & Rorsman, P. Palmitate increases L-type Ca²⁺ currents and the size of the readily releasable granule pool in mouse pancreatic beta-cells. *J Physiol* **557**, 935-948, doi:10.1113/jphysiol.2004.066258 (2004).
- 41 Prentki, M. & Madiraju, S. R. Glycerolipid/free fatty acid cycle and islet beta-cell function in health, obesity and diabetes. *Mol Cell Endocrinol* **353**, 88-100, doi:10.1016/j.mce.2011.11.004 (2012).
- 42 C, L. *et al.* Mechanism of hyperinsulinism in short-chain 3-hydroxyacyl-CoA dehydrogenase deficiency involves activation of glutamate dehydrogenase. *J Biol Chem* **285**, 31806-31818. Epub 32010 Jul 31829 (2010).
- 43 GA, M. *et al.* Specificity in beta cell expression of L-3-hydroxyacyl-CoA dehydrogenase, short chain, and potential role in down-regulating insulin release. *J Biol Chem* **282**, 21134-21144. Epub 22007 May 21139 (2007).
- 44 E, P. *et al.* Short-chain 3-hydroxyacyl-CoA dehydrogenase is a negative regulator of insulin secretion in response to fuel and non-fuel stimuli in INS832/13 β -cells. *J Diabetes* **2**, 157-167 (2010).
- 45 N, S. *et al.* Role of medium- and short-chain L-3-hydroxyacyl-CoA dehydrogenase in the regulation of body weight and thermogenesis. *Endocrinology* **152**, 4641-4651. Epub 2011 Oct 4611 (2011).
- 46 Sandip B Bharate PhD, K. V. N. P. R. A. V. P. Progress in the discovery and development of small-molecule modulators of G-protein-coupled receptor 40 (GPR40/FFA1/FFAR1): an emerging target for type 2 diabetes. *Expert Opinion on Therapeutic Patents* **19**, 237-264, doi:10.1517/13543770802665717 (2009).
- 47 Doshi, L. S. *et al.* Acute administration of GPR40 receptor agonist potentiates glucose-stimulated insulin secretion in vivo in the rat. *Metabolism* **58**, 333-343, doi:<http://dx.doi.org/10.1016/j.metabol.2008.10.005> (2009).
- 48 Fahien, L. A. & MacDonald, M. J. The Complex Mechanism of Glutamate Dehydrogenase in Insulin Secretion. *Diabetes* **60**, 2450-2454, doi:10.2337/db10-1150 (2011).
- 49 Hsu, B. Y. *et al.* Protein-sensitive and fasting hypoglycemia in children with the hyperinsulinism/hyperammonemia syndrome. *J Pediatr* **138**, 383-389, doi:10.1067/mpd.2001.111818 (2001).
- 50 Kelly, A., Li, C., Gao, Z., Stanley, C. A. & Matschinsky, F. M. Glutaminolysis and insulin secretion: from bedside to bench and back. *Diabetes* **51 Suppl 3**, S421-426 (2002).
- 51 Heslegrave, A. *et al.* Leucine-sensitive hyperinsulinaemic hypoglycaemia in patients with loss of function mutations in 3-Hydroxyacyl-CoA Dehydrogenase. *Orphanet Journal of Rare Diseases* **7**, 25 (2012).

- 52 Kelly, A. *et al.* Acute insulin responses to leucine in children with the hyperinsulinism/hyperammonemia syndrome. *The Journal of clinical endocrinology and metabolism* **86**, 3724 - 3728 (2001).
- 53 Panten, U., Kriegstein, E., Poser, W., Schonborn, J. & Hasselblatt, A. Effects of L-leucine and alpha-ketoisocaproic acid upon insulin secretion and metabolism of isolated pancreatic islets. *FEBS Lett* **20**, 225-228 (1972).
- 54 Herchuelz, A., Lebrun, P., Boschero, A. C. & Malaisse, W. J. *Mechanism of arginine-stimulated Ca²⁺ influx into pancreatic B cell*. Vol. 246 (1984).
- 55 Sener, A. *et al.* Stimulus-secretion coupling of arginine-induced insulin release: comparison between the cationic amino acid and its methyl ester. *Endocr* **13**, 329-340, doi:10.1385/endo:13:3:329 (2000).
- 56 McClenaghan, N. H., Barnett, C. R. & Flatt, P. R. Na⁺ cotransport by metabolizable and nonmetabolizable amino acids stimulates a glucose-regulated insulin-secretory response. *Biochem Biophys Res Commun* **249**, 299-303, doi:10.1006/bbrc.1998.9136 (1998).
- 57 Brennan, L. *et al.* A nuclear magnetic resonance-based demonstration of substantial oxidative L-alanine metabolism and L-alanine-enhanced glucose metabolism in a clonal pancreatic beta-cell line: metabolism of L-alanine is important to the regulation of insulin secretion. *Diabetes* **51**, 1714-1721 (2002).
- 58 Dixon, G., Nolan, J., McClenaghan, N., Flatt, P. R. & Newsholme, P. A comparative study of amino acid consumption by rat islet cells and the clonal beta-cell line BRIN-BD11 - the functional significance of L-alanine. *The Journal of endocrinology* **179**, 447-454 (2003).
- 59 Seino, S. Cell signalling in insulin secretion: the molecular targets of ATP, cAMP and sulfonylurea. *Diabetologia* **55**, 2096-2108, doi:10.1007/s00125-012-2562-9 (2012).
- 60 Maedler, K. *et al.* Sulfonylurea induced beta-cell apoptosis in cultured human islets. *The Journal of clinical endocrinology and metabolism* **90**, 501-506, doi:10.1210/jc.2004-0699 (2005).
- 61 Gallagher, E. J. & LeRoith, D. Diabetes, cancer, and metformin: connections of metabolism and cell proliferation. *Ann N Y Acad Sci* **1243**, 54-68, doi:10.1111/j.1749-6632.2011.06285.x (2011).
- 62 Del Barco, S. *et al.* Metformin: multi-faceted protection against cancer. *Oncotarget* **2**, 896-917 (2011).
- 63 Ning, X., Shu, J., Du, Y., Ben, Q. & Li, Z. Therapeutic strategies targeting cancer stem cells. *Cancer biology & therapy* **14**, 295-303, doi:10.4161/cbt.23622 (2013).
- 64 Hirsch, H. A., Iliopoulos, D. & Struhl, K. Metformin inhibits the inflammatory response associated with cellular transformation and cancer stem cell growth. *Proceedings of the National Academy of Sciences* **110**, 972-977, doi:10.1073/pnas.1221055110 (2013).
- 65 Mihaylova, M. M. & Shaw, R. J. The AMPK signalling pathway coordinates cell growth, autophagy and metabolism. *Nat Cell Biol* **13**, 1016-1023 (2011).
- 66 Moffat, C. & Ellen Harper, M. Metabolic functions of AMPK: aspects of structure and of natural mutations in the regulatory gamma subunits. *IUBMB life* **62**, 739-745, doi:10.1002/iub.387 (2010).
- 67 Harrington, W. W. *et al.* The Effect of PPARalpha, PPARdelta, PPARgamma, and PPARpan Agonists on Body Weight, Body Mass, and Serum Lipid Profiles in Diet-Induced Obese AKR/J Mice. *PPAR research* **2007**, 97125, doi:10.1155/2007/97125 (2007).
- 68 Larsen, T. M., Toubro, S. & Astrup, A. PPARgamma agonists in the treatment of type II diabetes: is increased fatness commensurate with long-term efficacy? *International*

- journal of obesity and related metabolic disorders : journal of the International Association for the Study of Obesity* **27**, 147-161, doi:10.1038/sj.ijo.802223 (2003).
- 69 Spiegelman, B. M. PPAR-gamma: adipogenic regulator and thiazolidinedione receptor. *Diabetes* **47**, 507-514, doi:10.2337/diabetes.47.4.507 (1998).
- 70 Lenhard, J. M. PPAR gamma/RXR as a molecular target for diabetes. *Receptors Channels* **7**, 249-258 (2001).
- 71 Gastaldelli, A. *et al.* Decreased whole body lipolysis as a mechanism of the lipid-lowering effect of pioglitazone in type 2 diabetic patients. *American journal of physiology. Endocrinology and metabolism* **297**, E225-230, doi:10.1152/ajpendo.90960.2008 (2009).
- 72 Kramer, D., Shapiro, R., Adler, A., Bush, E. & Rondinone, C. M. Insulin-sensitizing effect of rosiglitazone (BRL-49653) by regulation of glucose transporters in muscle and fat of Zucker rats. *Metabolism* **50**, 1294-1300, doi:<http://dx.doi.org/10.1053/meta.2001.27202> (2001).
- 73 Solomon, S. S., Mishra, S. K., Cwik, C., Rajanna, B. & Postlethwaite, A. E. Pioglitazone and Metformin Reverse Insulin Resistance Induced by Tumor Necrosis Factor-Alpha in Liver Cells. *Hormone and metabolic research = Hormon- und Stoffwechselforschung = Hormones et metabolisme* **29**, 379-382, doi:10.1055/s-2007-979059 (1997).
- 74 Murase, K., Odaka, H., Suzuki, M., Tayuki, N. & Ikeda, H. Pioglitazone time-dependently reduces tumour necrosis factor-alpha level in muscle and improves metabolic abnormalities in Wistar fatty rats. *Diabetologia* **41**, 257-264 (1998).
- 75 Yang, W. S. *et al.* Synthetic peroxisome proliferator-activated receptor-gamma agonist, rosiglitazone, increases plasma levels of adiponectin in type 2 diabetic patients. *Diabetes care* **25**, 376-380 (2002).
- 76 Phillips, S. A. & Kung, J. T. Mechanisms of adiponectin regulation and use as a pharmacological target. *Current opinion in pharmacology* **10**, 676-683, doi:10.1016/j.coph.2010.08.002 (2010).
- 77 Kim, H. S. *et al.* PPAR-gamma activation increases insulin secretion through the up-regulation of the free fatty acid receptor GPR40 in pancreatic beta-cells. *PLoS One* **8**, e50128, doi:10.1371/journal.pone.0050128 (2013).
- 78 Bermudez, V. *et al.* PPAR-gamma agonists and their role in type 2 diabetes mellitus management. *American journal of therapeutics* **17**, 274-283, doi:10.1097/MJT.0b013e3181c08081 (2010).
- 79 Koffarnus, R. L., Wargo, K. A. & Phillippe, H. M. Rivoglitazone: a new thiazolidinedione for the treatment of type 2 diabetes mellitus. *The Annals of pharmacotherapy* **47**, 877-885, doi:10.1345/aph.1R754 (2013).
- 80 Duque, G. *et al.* Pharmacological inhibition of PPAR γ increases osteoblastogenesis and bone mass in male C57BL/6 mice. *Journal of Bone and Mineral Research* **28**, 639-648, doi:10.1002/jbmr.1782 (2013).
- 81 Charpentier, G., Riveline, J. P. & Varroud-Vial, M. Management of drugs affecting blood glucose in diabetic patients with renal failure. *Diabetes & metabolism* **26 Suppl 4**, 73-85 (2000).
- 82 Goyal, A. & Crook, E. D. Thiazolidinediones and progression of renal disease in patients with diabetes. *Journal of investigative medicine : the official publication of the American Federation for Clinical Research* **54**, 56-61 (2006).
- 83 Kintscher, U. & Goebel, M. INT-131, a PPAR γ agonist for the treatment of type 2 diabetes. *Current opinion in investigational drugs (London, England : 2000)* **10**, 381-387 (2009).

- 84 Taygerly, J. P. *et al.* Discovery of INT131: a selective PPARgamma modulator that enhances insulin sensitivity. *Bioorg Med Chem* **21**, 979-992, doi:10.1016/j.bmc.2012.11.058 (2013).
- 85 Lee, D. H., Huang, H., Choi, K., Mantzoros, C. & Kim, Y. B. Selective PPARgamma modulator INT131 normalizes insulin signaling defects and improves bone mass in diet-induced obese mice. *American journal of physiology. Endocrinology and metabolism* **302**, E552-560, doi:10.1152/ajpendo.00569.2011
10.1152/ajpendo.00569.2011 (2012).
- 86 Nicholls, S. J. & Uno, K. Peroxisome proliferator-activated receptor (PPAR α/γ) agonists as a potential target to reduce cardiovascular risk in diabetes. *Diabetes and Vascular Disease Research* **9**, 89-94, doi:10.1177/1479164112441477 (2012).
- 87 Munigoti, S. P. & Harinarayan, C. V. Role of Glitazars in atherogenic dyslipidemia and diabetes: Two birds with one stone? *Indian journal of endocrinology and metabolism* **18**, 283-287, doi:10.4103/2230-8210.131134 (2014).
- 88 Agrawal, R. The first approved agent in the Glitazar's Class: Saroglitazar. *Current drug targets* **15**, 151-155 (2014).
- 89 Jani, R. H., Kansagra, K., Jain, M. R. & Patel, H. Pharmacokinetics, safety, and tolerability of saroglitazar (ZYH1), a predominantly PPARalpha agonist with moderate PPARgamma agonist activity in healthy human subjects. *Clin Drug Investig* **33**, 809-816, doi:10.1007/s40261-013-0128-3 (2013).
- 90 Jani, R. H. *et al.* A multicenter, prospective, randomized, double-blind study to evaluate the safety and efficacy of Saroglitazar 2 and 4 mg compared with placebo in type 2 diabetes mellitus patients having hypertriglyceridemia not controlled with atorvastatin therapy (PRESS VI). *Diabetes Technol Ther* **16**, 63-71, doi:10.1089/dia.2013.0253 (2014).
- 91 Pai, V. *et al.* A Multicenter, Prospective, Randomized, Double-blind Study to Evaluate the Safety and Efficacy of Saroglitazar 2 and 4 mg Compared to Pioglitazone 45 mg in Diabetic Dyslipidemia (PRESS V). *Journal of diabetes science and technology* **8**, 132-141, doi:10.1177/1932296813518680 (2014).
- 92 Arnette, D. *et al.* Regulation of ERK1 and ERK2 by glucose and peptide hormones in pancreatic beta cells. *J Biol Chem* **278**, 32517-32525, doi:10.1074/jbc.M301174200 (2003).
- 93 Hartman, I., Rojas, E. & Rodriguez-Molina, D. Incretin-based therapy for type 2 diabetes mellitus: pancreatic and extrapancreatic effects. *American journal of therapeutics* **20**, 384-393, doi:10.1097/MJT.0b013e318235f27d (2013).
- 94 Jellinger, P. S. Focus on incretin-based therapies: targeting the core defects of type 2 diabetes. *Postgrad Med* **123**, 53-65, doi:10.3810/pgm.2011.01.2245 (2011).
- 95 Sauer, N., Reining, F., Schulze Zur Wiesch, C., Burkhardt, T. & Aberle, J. Off-Label Antiobesity Treatment in Patients without Diabetes with GLP-1 Agonists in Clinical Practice. *Hormone and metabolic research = Hormon- und Stoffwechselforschung = Hormones et metabolisme*, doi:10.1055/s-0034-1387793 (2014).
- 96 Giorda, C. B. *et al.* Incretin-based therapies and acute pancreatitis risk: a systematic review and meta-analysis of observational studies. *Endocr*, doi:10.1007/s12020-014-0386-8 (2014).
- 97 Li, X., Zhang, Z. & Duke, J. Glucagon-like peptide 1-based therapies and risk of pancreatitis: a self-controlled case series analysis. *Pharmacoepidemiology and drug safety* **23**, 234-239 (2014).
- 98 Li, L. *et al.* Incretin treatment and risk of pancreatitis in patients with type 2 diabetes mellitus: systematic review and meta-analysis of randomised and non-randomised studies. *Bmj* **348**, g2366, doi:10.1136/bmj.g2366 (2014).

- 99 Monami, M., Dicembrini, I., Nardini, C., Fiordelli, I. & Mannucci, E. Glucagon-like peptide-1 receptor agonists and pancreatitis: a meta-analysis of randomized clinical trials. *Diabetes research and clinical practice* **103**, 269-275, doi:10.1016/j.diabres.2014.01.010 (2014).
- 100 Funch, D., Gydesen, H., Tornøe, K., Major-Pedersen, A. & Chan, K. A. A prospective, claims-based assessment of the risk of pancreatitis and pancreatic cancer with liraglutide compared to other antidiabetic drugs. *Diabetes, obesity & metabolism* **16**, 273-275, doi:10.1111/dom.12230 (2014).
- 101 Yang, Y., Yu, X., Huang, L. & Yu, C. GLP-1R agonist may activate pancreatic stellate cells to induce rat pancreatic tissue lesion. *Pancreatology : official journal of the International Association of Pancreatology (IAP) ... [et al.]* **13**, 498-501, doi:10.1016/j.pan.2013.07.281 (2013).
- 102 Ryder, R. E. The potential risks of pancreatitis and pancreatic cancer with GLP-1-based therapies are far outweighed by the proven and potential (cardiovascular) benefits. *Diabet Med* **30**, 1148-1155, doi:10.1111/dme.12301 (2013).
- 103 Noyan-Ashraf, M. H. *et al.* GLP-1R Agonist Liraglutide Activates Cytoprotective Pathways and Improves Outcomes After Experimental Myocardial Infarction in Mice. *Diabetes* **58**, 975-983, doi:10.2337/db08-1193 (2009).
- 104 Bjerre Knudsen, L. *et al.* Glucagon-like Peptide-1 receptor agonists activate rodent thyroid C-cells causing calcitonin release and C-cell proliferation. *Endocrinology* **151**, 1473-1486, doi:10.1210/en.2009-1272 (2010).
- 105 Hegedus, L., Moses, A. C., Zdravkovic, M., Le Thi, T. & Daniels, G. H. GLP-1 and calcitonin concentration in humans: lack of evidence of calcitonin release from sequential screening in over 5000 subjects with type 2 diabetes or nondiabetic obese subjects treated with the human GLP-1 analog, liraglutide. *The Journal of clinical endocrinology and metabolism* **96**, 853-860, doi:10.1210/jc.2010-2318 (2011).
- 106 Gallo, M. Thyroid safety in patients treated with liraglutide. *Journal of endocrinological investigation* **36**, 140-145 (2013).
- 107 Petrie, J. The cardiovascular safety of incretin-based therapies: a review of the evidence. *Cardiovascular Diabetology* **12**, 130 (2013).
- 108 M. Monami, I. Dicembrini, S. Zannoni, C. Lamanna, E. Mannucci; Dipeptidyl peptidase-4 inhibitors and risk of cancer: myth or reality? *Diabetologia* 2011;54: S310. (2011).
- 109 Lamanna C, Monami M, Bartoli N, Zannoni S, Mannucci E. Dipeptidyl peptidase-4 inhibitors and cardiovascular events: a prospective effect? *Diabetologia* 2011;54: S109. (2011).
- 110 White, W. B. *et al.* Alogliptin after Acute Coronary Syndrome in Patients with Type 2 Diabetes. *N. Engl. J. Med.* **369**, 1327-1335, doi:10.1056/NEJMoa1305889 (2013).
- 111 Ussher, J. R. & Drucker, D. J. Cardiovascular Actions of Incretin-Based Therapies. *Circulation research* **114**, 1788-1803, doi:10.1161/circresaha.114.301958 (2014).
- 112 Ussher, J. R. & Drucker, D. J. Cardiovascular Biology of the Incretin System. *Endocrine reviews* **33**, 187-215, doi:10.1210/er.2011-1052 (2012).
- 113 White, W. B. *et al.* Alogliptin after Acute Coronary Syndrome in Patients with Type 2 Diabetes. *N. Engl. J. Med.* **369**, 1327-1335, doi:10.1056/NEJMoa1305889 (2013).
- 114 Scirica, B. M. *et al.* Saxagliptin and Cardiovascular Outcomes in Patients with Type 2 Diabetes Mellitus. *N. Engl. J. Med.* **369**, 1317-1326, doi:10.1056/NEJMoa1307684 (2013).
- 115 Kim, G. & Chung, S. Clinical implication of SGLT2 inhibitors in type 2 diabetes. *Arch. Pharm. Res.*, 1-10, doi:10.1007/s12272-014-0419-0 (2014).

- 116 Aylsworth, A., Dean, Z., VanNorman, C. & Nkemdirim Okere, A. Dapagliflozin for the Treatment of Type 2 Diabetes Mellitus. *Annals of Pharmacotherapy*, doi:10.1177/1060028014540450 (2014).
- 117 Perkins, B. A. *et al.* Sodium-Glucose Cotransporter 2 Inhibition and Glycemic Control in Type 1 Diabetes: Results of an 8-Week Open-Label Proof-of-Concept Trial. *Diabetes care* **37**, 1480-1483, doi:10.2337/dc13-2338 (2014).
- 118 Lamos, E. M., Younk, L. M. & Davis, S. N. Empagliflozin, a sodium glucose co-transporter 2 inhibitor, in the treatment of type 1 diabetes. *Expert opinion on investigational drugs* **23**, 875-882, doi:doi:10.1517/13543784.2014.909407 (2014).
- 119 Shah, U. & Kowalski, T. J. in *Vitamins & Hormones* Vol. Volume 84 (ed Litwack Gerald) 415-448 (Academic Press, 2010).
- 120 Jones, R. M., Leonard, J. N., Buzard, D. J. & Lehmann, J. GPR119 agonists for the treatment of type 2 diabetes. *Expert Opinion on Therapeutic Patents* **19**, 1339-1359, doi:doi:10.1517/13543770903153878 (2009).
- 121 Lan, H. *et al.* Agonists at GPR119 mediate secretion of GLP-1 from mouse enteroendocrine cells through glucose-independent pathways. *British Journal of Pharmacology* **165**, 2799-2807, doi:10.1111/j.1476-5381.2011.01754.x (2012).
- 122 Zhu, X., Huang, W. & Qian, H. *GPR119 Agonists: A Novel Strategy for Type 2 Diabetes Treatment*. (2013).
- 123 Ohishi, T. & Yoshida, S. The therapeutic potential of GPR119 agonists for type 2 diabetes. *Expert opinion on investigational drugs* **21**, 321-328, doi:10.1517/13543784.2012.657797 (2012).
- 124 Kim, S. R. *et al.* In vivo efficacy of HD0471953: a novel GPR119 agonist for the treatment of type 2 diabetes mellitus. *Journal of diabetes research* **2013**, 269569, doi:10.1155/2013/269569 (2013).
- 125 Mo, X.-L., Yang, Z. & Tao, Y.-X. in *Progress in Molecular Biology and Translational Science* Vol. Volume 121 (ed Tao Ya-Xiong) 95-131 (Academic Press, 2014).
- 126 Sato, K. *et al.* Discovery of a novel series of indoline carbamate and indolinylpyrimidine derivatives as potent GPR119 agonists. *Bioorganic & Medicinal Chemistry* **22**, 1649-1666, doi:<http://dx.doi.org/10.1016/j.bmc.2014.01.028> (2014).
- 127 Alper, P. *et al.* Discovery of structurally novel, potent and orally efficacious GPR119 agonists. *Bioorganic & Medicinal Chemistry Letters* **24**, 2383-2387, doi:<http://dx.doi.org/10.1016/j.bmcl.2014.03.023> (2014).
- 128 Kang, S.-U. GPR119 agonists: a promising approach for T2DM treatment? A SWOT analysis of GPR119. *Drug discovery today* **18**, 1309-1315, doi:<http://dx.doi.org/10.1016/j.drudis.2013.09.011> (2013).
- 129 Nunez, D. J. *et al.* Gut Hormone Pharmacology of a Novel GPR119 Agonist (GSK1292263), Metformin, and Sitagliptin in Type 2 Diabetes Mellitus: Results from Two Randomized Studies. *PLoS One* **9**, e92494, doi:10.1371/journal.pone.0092494 (2014).
- 130 Clin.Trial. <https://clinicaltrials.gov/ct2/show/NCT01512368>. (2013).
- 131 Emanuelli, B. *et al.* Interplay between FGF21 and insulin action in the liver regulates metabolism. *J Clin Invest* **124**, 515-527, doi:10.1172/jci67353 (2014).
- 132 Goetz, R. Metabolism: Adiponectin---a mediator of specific metabolic actions of FGF21. *Nature reviews. Endocrinology* **9**, 506-508, doi:10.1038/nrendo.2013.146 (2013).
- 133 Kharitononkov, A. & Adams, A. C. Inventing new medicines: The FGF21 story. *Molecular metabolism* **3**, 221-229, doi:10.1016/j.molmet.2013.12.003 (2014).
- 134 Gaich, G. *et al.* The effects of LY2405319, an FGF21 analog, in obese human subjects with type 2 diabetes. *Cell Metab* **18**, 333-340, doi:10.1016/j.cmet.2013.08.005 (2013).

- 135 Matschinsky, F. M. Assessing the potential of glucokinase activators in diabetes therapy. *Nature reviews. Drug discovery* **8**, 399-416 (2009).
- 136 Matschinsky, F. M. *et al.* Research and development of glucokinase activators for diabetes therapy: theoretical and practical aspects. *Handbook of experimental pharmacology*, 357-401, doi:10.1007/978-3-642-17214-4_15 (2011).
- 137 Matschinsky, F. M. *et al.* Glucokinase Activators for Diabetes Therapy: May 2010 status report. *Diabetes care* **34**, S236-S243, doi:10.2337/dc11-s236 (2011).
- 138 Oh, Y. S. *et al.* Treatment with glucokinase activator, YH-GKA, increases cell proliferation and decreases glucotoxic apoptosis in INS-1 cells. *European Journal of Pharmaceutical Sciences* **51**, 137-145, doi:<http://dx.doi.org/10.1016/j.ejps.2013.09.005> (2014).
- 139 Kiyosue, A., Hayashi, N., Komori, H., Leonsson-Zachrisson, M. & Johnsson, E. Dose-ranging study with the glucokinase activator AZD1656 as monotherapy in Japanese patients with type 2 diabetes mellitus. *Diabetes, Obesity and Metabolism* **15**, 923-930, doi:10.1111/dom.12100 (2013).
- 140 Meininger, G. E. *et al.* Effects of MK-0941, a Novel Glucokinase Activator, on Glycemic Control in Insulin-Treated Patients With Type 2 Diabetes. *Diabetes care* **34**, 2560-2566, doi:10.2337/dc11-1200 (2011).
- 141 Gude, D. Red carpeting the newer antidiabetics. *Journal of pharmacology & pharmacotherapeutics* **3**, 127-131, doi:10.4103/0976-500x.95507 (2012).
- 142 Louvet, C. *et al.* Tyrosine kinase inhibitors reverse type 1 diabetes in nonobese diabetic mice. *Proceedings of the National Academy of Sciences*, doi:10.1073/pnas.0810246105 (2008).
- 143 Stanley, C. *et al.* Molecular basis and characterization of the hyperinsulinism/hyperammonemia syndrome: predominance of mutations in exons 11 and 12 of the glutamate dehydrogenase gene. *Diabetes* **49**, 667 - 673 (2000).
- 144 Trial, C. <http://clinicaltrials.gov/show/NCT01781975>.
- 145 Templeton, A., Brandle, M., Cerny, T. & Gillessen, S. Remission of diabetes while on sunitinib treatment for renal cell carcinoma. *Annals of oncology : official journal of the European Society for Medical Oncology / ESMO* **19**, 824-825, doi:10.1093/annonc/mdn047 (2008).
- 146 Billefont, B. *et al.* Blood glucose levels in patients with metastatic renal cell carcinoma treated with sunitinib. *British journal of cancer* **99**, 1380-1382, doi:10.1038/sj.bjc.6604709 (2008).
- 147 Karaman, M. W. *et al.* A quantitative analysis of kinase inhibitor selectivity. *Nat Biotech* **26**, 127-132, doi:http://www.nature.com/nbt/journal/v26/n1/supinfo/nbt1358_S1.html (2008).
- 148 Prada, P. O. & Saad, M. J. Tyrosine kinase inhibitors as novel drugs for the treatment of diabetes. *Expert opinion on investigational drugs* **22**, 751-763, doi:10.1517/13543784.2013.802768 (2013).
- 149 Agostino, N. M. *et al.* Effect of the tyrosine kinase inhibitors (sunitinib, sorafenib, dasatinib, and imatinib) on blood glucose levels in diabetic and nondiabetic patients in general clinical practice. *Journal of oncology pharmacy practice : official publication of the International Society of Oncology Pharmacy Practitioners* **17**, 197-202, doi:10.1177/1078155210378913 (2011).
- 150 Mokhtari, D. & Welsh, N. Potential utility of small tyrosine kinase inhibitors in the treatment of diabetes. *Clinical science (London, England : 1979)* **118**, 241-247, doi:10.1042/cs20090348 (2010).
- 151 Fitter, S. *et al.* Plasma adiponectin levels are markedly elevated in imatinib-treated chronic myeloid leukemia (CML) patients: a mechanism for improved insulin

- sensitivity in type 2 diabetic CML patients? *The Journal of clinical endocrinology and metabolism* **95**, 3763-3767, doi:10.1210/jc.2010-0086 (2010).
- 152 Szalek, E. *et al.* The pharmacokinetics and hypoglycaemic effect of sunitinib in the diabetic rabbits. *Pharmacological reports : PR* **66**, 892-896, doi:10.1016/j.pharep.2014.05.011 (2014).
- 153 Mukai, E. *et al.* Enhanced vascular endothelial growth factor signaling in islets contributes to beta cell injury and consequential diabetes in spontaneously diabetic Torii rats. *Diabetes research and clinical practice*, doi:10.1016/j.diabres.2014.08.023 (2014).
- 154 Falckenberg, M. SUTENT-SENSITIVE KINASES AS TARGETS FOR ANTI-DIABETIC THERAPY DEVELOPMENT - PhD Thesis.
- 155 Brewis, I. A., Morton, I. E., Mohammad, S. N., Browes, C. E. & Moore, H. D. M. Measurement of Intracellular Calcium Concentration and Plasma Membrane Potential in Human Spermatozoa Using Flow Cytometry. *Journal of andrology* **21**, 238-249, doi:10.1002/j.1939-4640.2000.tb02101.x (2000).
- 156 Vines, A., McBean, G. J. & Blanco-Fernández, A. A flow-cytometric method for continuous measurement of intracellular Ca²⁺ concentration. *Cytometry Part A* **77A**, 1091-1097, doi:10.1002/cyto.a.20974 (2010).
- 157 Schepers, E., Glorieux, G., Dhondt, A., Leybaert, L. & Vanholder, R. Flow cytometric calcium flux assay: Evaluation of cytoplasmic calcium kinetics in whole blood leukocytes. *Journal of Immunological Methods* **348**, 74-82, doi:<http://dx.doi.org/10.1016/j.jim.2009.07.002> (2009).
- 158 Ong, S. E. & Mann, M. A practical recipe for stable isotope labeling by amino acids in cell culture (SILAC). *Nature protocols* **1**, 2650-2660, doi:10.1038/nprot.2006.427 (2006).
- 159 Ong, S.-E. *et al.* Stable Isotope Labeling by Amino Acids in Cell Culture, SILAC, as a Simple and Accurate Approach to Expression Proteomics. *Molecular & Cellular Proteomics* **1**, 376-386, doi:10.1074/mcp.M200025-MCP200 (2002).
- 160 Evotec. <http://www.evotec.com/article/en/Products-Services/Cellular-Target-Profilng/2255>.
- 161 Ong, S. E. & Mann, M. Mass spectrometry-based proteomics turns quantitative. *Nature chemical biology* **1**, 252-262, doi:10.1038/nchembio736 (2005).
- 162 Sharma, K. *et al.* Proteomics strategy for quantitative protein interaction profiling in cell extracts. *Nature methods* **6**, 741-744, doi:10.1038/nmeth.1373 (2009).
- 163 Cheng, Y. & Prusoff, W. H. Relationship between the inhibition constant (K₁) and the concentration of inhibitor which causes 50 per cent inhibition (I₅₀) of an enzymatic reaction. *Biochem Pharmacol* **22**, 3099-3108 (1973).
- 164 <http://www.discoverx.com/services/drug-discovery-development-services/kinase-profilng/kinomescan>.
- 165 Guo-Parke, H. *et al.* Configuration of electrofusion-derived human insulin-secreting cell line as pseudoislets enhances functionality and therapeutic utility. *The Journal of endocrinology* **214**, 257-265, doi:10.1530/joe-12-0188 (2012).
- 166 Berridge, M. V., Herst, P. M. & Tan, A. S. in *Biotechnology Annual Review* Vol. Volume 11 (ed M. R. El-Gewely) 127-152 (Elsevier, 2005).
- 167 Berridge, M. V. & Tan, A. S. Characterization of the Cellular Reduction of 3-(4,5-dimethylthiazol-2-yl)-2,5-diphenyltetrazolium bromide (MTT): Subcellular Localization, Substrate Dependence, and Involvement of Mitochondrial Electron Transport in MTT Reduction. *Archives of Biochemistry and Biophysics* **303**, 474-482, doi:<http://dx.doi.org/10.1006/abbi.1993.1311> (1993).
- 168 Berridge M., T. A., McCoy K., Wang R. . The Biochemical and Cellular Basis of Cell Proliferation Assays that Use Tetrazolium Salts. *Biochemica* **4:14-19** (1996).

- 169 Capdeville, R., Buchdunger, E., Zimmermann, J. & Matter, A. Glivec (STI571, imatinib), a rationally developed, targeted anticancer drug. *Nature reviews. Drug discovery* **1**, 493-502, doi:10.1038/nrd839 (2002).
- 170 Klebl, B. M. & Müller, G. Second-generation kinase inhibitors. *Expert Opinion on Therapeutic Targets* **9**, 975-993, doi:doi:10.1517/14728222.9.5.975 (2005).
- 171 Breccia, M., Muscaritoli, M., Aversa, Z., Mandelli, F. & Alimena, G. Imatinib mesylate may improve fasting blood glucose in diabetic Ph+ chronic myelogenous leukemia patients responsive to treatment. *Journal of clinical oncology : official journal of the American Society of Clinical Oncology* **22**, 4653-4655, doi:10.1200/jco.2004.04.217 (2004).
- 172 Veneri, D., Franchini, M. & Bonora, E. Imatinib and regression of type 2 diabetes. *The New England journal of medicine* **352**, 1049-1050, doi:10.1056/nejm200503103521023 (2005).
- 173 Arnaud Merglen, S. T., Blanca Rubi, Gaelle Chaffard, Claes B. Wollheim, and Pierre Maechler. Glucose Sensitivity and Metabolism-Secretion Coupling Studied during Two-Year Continuous Culture in INS-1E Insulinoma Cells. *Endocrinology* **145**, 667-678, doi:doi:10.1210/en.2003-1099 (2004).
- 174 McClenaghan, N. H. *et al.* Characterization of a novel glucose-responsive insulin-secreting cell line, BRIN-BD11, produced by electrofusion. *Diabetes* **45**, 1132-1140 (1996).
- 175 McClenaghan, N. H. & Flatt, P. R. Engineering cultured insulin-secreting pancreatic B-cell lines. *Journal of molecular medicine (Berlin, Germany)* **77**, 235-243 (1999).
- 176 Rosnet, O., Marchetto, S., deLapeyriere, O. & Birnbaum, D. Murine Flt3, a gene encoding a novel tyrosine kinase receptor of the PDGFR/CSF1R family. *Oncogene* **6**, 1641-1650 (1991).
- 177 M, H. *et al.* Cardiac ATP-sensitive K⁺ channel associates with the glycolytic enzyme complex. *FASEB J* **25**, 2456-2467. Epub 2011 Apr 2411 (2011).
- 178 BS, J., H, L., ZG, J. & Y, Y. Glucose stimulation induces dynamic change of mitochondrial morphology to promote insulin secretion in the insulinoma cell line INS-1E. *PLoS One* **8**, e60810. Epub 62013 Apr 60812 (2013).
- 179 D, R. *et al.* Transfection and overexpression of the calcium binding protein calbindin-D28k results in a stimulatory effect on insulin synthesis in a rat beta cell line (RIN 1046-38). *Proc Natl Acad Sci U S A* **94**, 1961-1966 (1997).
- 180 K, S. *et al.* Calbindin-D(28k) controls [Ca(2+)](i) and insulin release. Evidence obtained from calbindin-d(28k) knockout mice and beta cell lines. *J Biol Chem* **274**, 34343-34349 (1999).
- 181 L, V. *et al.* Delineation of glutamate pathways and secretory responses in pancreatic islets with β -cell-specific abrogation of the glutamate dehydrogenase. *Mol Biol Cell* **23**, 3851-3862. Epub 2012 Aug 3858 (2012).
- 182 MC, H. *et al.* SIRT4 inhibits glutamate dehydrogenase and opposes the effects of calorie restriction in pancreatic beta cells. *Cell* **126**, 941-954 (2006).
- 183 C, L. *et al.* Effects of a GTP-insensitive mutation of glutamate dehydrogenase on insulin secretion in transgenic mice. *J Biol Chem* **281**, 15064-15072. Epub 12006 Mar 15030 (2006).
- 184 C, L. *et al.* Green tea polyphenols control dysregulated glutamate dehydrogenase in transgenic mice by hijacking the ADP activation site. *J Biol Chem* **286**, 34164-34174. Epub 32011 Aug 34163 (2011).
- 185 Kosuga, S. *et al.* GSK-3 β Directly Phosphorylates and Activates MARK2/PAR-1. *Journal of Biological Chemistry* **280**, 42715-42722, doi:10.1074/jbc.M507941200 (2005).

- 186 GSK-3 β Function in Bone Regulates Skeletal Development, Whole-Body Metabolism, and Male Life Span. *Endocrinology* **154**, 3702-3718, doi:doi:10.1210/en.2013-1155 (2013).
- 187 Tanabe, K. *et al.* Genetic Deficiency of Glycogen Synthase Kinase-3 β Corrects Diabetes in Mouse Models of Insulin Resistance. *PLoS Biol* **6**, e37, doi:10.1371/journal.pbio.0060037 (2008).
- 188 Hurov, J. B. *et al.* Loss of the Par-1b/MARK2 polarity kinase leads to increased metabolic rate, decreased adiposity, and insulin hypersensitivity in vivo. *Proc Natl Acad Sci U S A* **104**, 5680-5685, doi:10.1073/pnas.0701179104 (2007).
- 189 Jansson, D. *et al.* Glucose controls CREB activity in islet cells via regulated phosphorylation of TORC2. *Proceedings of the National Academy of Sciences* **105**, 10161-10166, doi:10.1073/pnas.0800796105 (2008).
- 190 Lennerz, J. K. *et al.* Loss of Par-1a/MARK3/C-TAK1 Kinase Leads to Reduced Adiposity, Resistance to Hepatic Steatosis, and Defective Gluconeogenesis. *Molecular and Cellular Biology* **30**, 5043-5056, doi:10.1128/mcb.01472-09 (2010).
- 191 Hamilton, S. R. *et al.* An activating mutation in the γ 1 subunit of the AMP-activated protein kinase. *FEBS Letters* **500**, 163-168, doi:10.1016/S0014-5793(01)02602-3 (2001).
- 192 Prentki, M., Matschinsky, Franz M. & Madiraju, S. R. M. Metabolic Signaling in Fuel-Induced Insulin Secretion. *Cell Metabolism* **18**, 162-185, doi:<http://dx.doi.org/10.1016/j.cmet.2013.05.018> (2013).
- 193 Tsuboi, T., da Silva Xavier, G., Leclerc, I. & Rutter, G. A. 5'-AMP-activated Protein Kinase Controls Insulin-containing Secretory Vesicle Dynamics. *Journal of Biological Chemistry* **278**, 52042-52051, doi:10.1074/jbc.M307800200 (2003).
- 194 Sajan, M. P. *et al.* AICAR and metformin, but not exercise, increase muscle glucose transport through AMPK-, ERK-, and PDK1-dependent activation of atypical PKC. *American Journal of Physiology - Endocrinology And Metabolism* **298**, E179-E192, doi:10.1152/ajpendo.00392.2009 (2010).
- 195 Fischer, M. *et al.* Metformin induces glucose uptake in human preadipocyte-derived adipocytes from various fat depots. *Diabetes, Obesity and Metabolism* **12**, 356-359, doi:10.1111/j.1463-1326.2009.01169.x (2010).
- 196 Langelueddecke, C. *et al.* Effect of the AMP-Kinase Modulators AICAR, Metformin and Compound C on Insulin Secretion of INS-1E Rat Insulinoma Cells under Standard Cell Culture Conditions. *Cellular Physiology and Biochemistry* **29**, 75-86 (2012).
- 197 Coughlan, K. A., Valentine, R. J., Ruderman, N. B. & Saha, A. K. AMPK activation: a therapeutic target for type 2 diabetes? *Diabetes, metabolic syndrome and obesity : targets and therapy* **7**, 241-253, doi:10.2147/dms0.s43731 (2014).
- 198 Conner, S. D. & Schmid, S. L. Identification of an adaptor-associated kinase, AAK1, as a regulator of clathrin-mediated endocytosis. *The Journal of Cell Biology* **156**, 921-929, doi:10.1083/jcb.200108123 (2002).
- 199 Ricotta, D., Conner, S. D., Schmid, S. L., von Figura, K. & Höning, S. Phosphorylation of the AP2 μ subunit by AAK1 mediates high affinity binding to membrane protein sorting signals. *The Journal of Cell Biology* **156**, 791-795, doi:10.1083/jcb.200111068 (2002).
- 200 Henderson, D. M. & Conner, S. D. A novel AAK1 splice variant functions at multiple steps of the endocytic pathway. *Mol Biol Cell* **18**, 2698-2706, doi:10.1091/mbc.E06-09-0831 (2007).
- 201 Molinete, M., Dupuis, S., Brodsky, F. M. & Halban, P. A. Role of clathrin in the regulated secretory pathway of pancreatic β -cells. *Journal of Cell Science* **114**, 3059-3066 (2001).

- 202 Korolchuk, V. I. & Banting, G. CK2 and GAK/auxilin2 are major protein kinases in clathrin-coated vesicles. *Traffic (Copenhagen, Denmark)* **3**, 428-439 (2002).
- 203 Greener, T., Zhao, X., Nojima, H., Eisenberg, E. & Greene, L. E. Role of cyclin G-associated kinase in uncoating clathrin-coated vesicles from non-neuronal cells. *J Biol Chem* **275**, 1365-1370 (2000).
- 204 Meng, R., Götz, C. & Montenarh, M. The role of protein kinase CK2 in the regulation of the insulin production of pancreatic islets. *Biochemical and Biophysical Research Communications* **401**, 203-206, doi:<http://dx.doi.org/10.1016/j.bbrc.2010.09.028> (2010).
- 205 Al Quobaili, F. & Montenarh, M. CK2 and the regulation of the carbohydrate metabolism. *Metabolism* **61**, 1512-1517, doi:<http://dx.doi.org/10.1016/j.metabol.2012.07.011> (2012).
- 206 Wu, D. *et al.* Stable knockdown of protein kinase CK2- α (CK2 α) inhibits migration and invasion and induces inactivation of hedgehog signaling pathway in hepatocellular carcinoma Hep G2 cells. *Acta Histochemica*, doi:<http://dx.doi.org/10.1016/j.acthis.2014.06.001> (2014).
- 207 Gray, G. K., McFarland, B. C., Rowse, A. L., Gibson, S. A. & Benveniste, E. N. *Therapeutic CK2 inhibition attenuates diverse prosurvival signaling cascades and decreases cell viability in human breast cancer cells.* (2014).
- 208 Montenarh, M. Protein kinase CK2 and angiogenesis. *Advances in clinical and experimental medicine : official organ Wroclaw Medical University* **23**, 153-158 (2014).
- 209 Burakov, A. V. *et al.* Ste20-related protein kinase LOSK (SLK) controls microtubule radial array in interphase. *Mol Biol Cell* **19**, 1952-1961, doi:10.1091/mbc.E06-12-1156 (2008).
- 210 Roovers, K. *et al.* The Ste20-like kinase SLK is required for ErbB2-driven breast cancer cell motility. *Oncogene* **28**, 2839-2848, doi:10.1038/onc.2009.146 (2009).
- 211 Wagner, S. M. & Sabourin, L. A. A novel role for the Ste20 kinase SLK in adhesion signaling and cell migration. *Cell adhesion & migration* **3**, 182-184 (2009).
- 212 Chaar, Z., O'Reilly, P., Gelman, I. & Sabourin, L. A. v-Src-dependent Down-regulation of the Ste20-like Kinase SLK by Casein Kinase II. *Journal of Biological Chemistry* **281**, 28193-28199, doi:10.1074/jbc.M605665200 (2006).
- 213 Bright, N. J., Thornton, C. & Carling, D. The regulation and function of mammalian AMPK-related kinases. *Acta physiologica (Oxford, England)* **196**, 15-26, doi:10.1111/j.1748-1716.2009.01971.x (2009).
- 214 Edwards, P. A. & Howarth, K. D. Are breast cancers driven by fusion genes? *Breast cancer research : BCR* **14**, 303, doi:10.1186/bcr3122 (2012).
- 215 Robinson, D. R. *et al.* Functionally recurrent rearrangements of the MAST kinase and Notch gene families in breast cancer. *Nat Med* **17**, 1646-1651, doi:10.1038/nm.2580 (2011).
- 216 Ranganathan, R. & Ross, E. M. PDZ domain proteins: Scaffolds for signaling complexes. *Current Biology* **7**, R770-R773, doi:[http://dx.doi.org/10.1016/S0960-9822\(06\)00401-5](http://dx.doi.org/10.1016/S0960-9822(06)00401-5) (1997).
- 217 De Graeve, F. *et al.* Role of the ATF α /JNK2 complex in Jun activation. *Oncogene* **18**, 3491-3500, doi:10.1038/sj.onc.1202723 (1999).
- 218 Shaulian, E. AP-1 — The Jun proteins: Oncogenes or tumor suppressors in disguise? *Cellular signalling* **22**, 894-899, doi:<http://dx.doi.org/10.1016/j.cellsig.2009.12.008> (2010).

- 219 Tomlinson, V. *et al.* JNK phosphorylates Yes-associated protein (YAP) to regulate apoptosis. *Cell Death and Dis* **1**, e29, doi:<http://www.nature.com/cddis/journal/v1/n2/supinfo/cddis20107s1.html> (2010).
- 220 Oleinik, N. V., Krupenko, N. I. & Krupenko, S. A. Cooperation between JNK1 and JNK2 in activation of p53 apoptotic pathway. *Oncogene* **26**, 7222-7230, doi:<http://www.nature.com/onc/journal/v26/n51/supinfo/1210526s1.html> (2007).
- 221 Prause, M., Christensen, D. P., Billestrup, N. & Mandrup-Poulsen, T. JNK1 Protects against Glucolipotoxicity-Mediated Beta-Cell Apoptosis. *PLoS ONE* **9**, e87067, doi:10.1371/journal.pone.0087067 (2014).
- 222 Zhang, X. *et al.* Selective Inactivation of c-Jun NH2-Terminal Kinase in Adipose Tissue Protects Against Diet-Induced Obesity and Improves Insulin Sensitivity in Both Liver and Skeletal Muscle in Mice. *Diabetes* **60**, 486-495, doi:10.2337/db10-0650 (2011).
- 223 Abdelli, S. *et al.* JNK3 is abundant in insulin-secreting cells and protects against cytokine-induced apoptosis. *Diabetologia* **52**, 1871-1880, doi:10.1007/s00125-009-1431-7 (2009).
- 224 Jaeschke, A. *et al.* Disruption of the Jnk2 (Mapk9) gene reduces destructive insulinitis and diabetes in a mouse model of type I diabetes. *Proceedings of the National Academy of Sciences of the United States of America* **102**, 6931-6935, doi:10.1073/pnas.0502143102 (2005).
- 225 Berson, A. E. *et al.* Identification and Characterization of a Myristylated and Palmitylated Serine/Threonine Protein Kinase. *Biochemical and Biophysical Research Communications* **259**, 533-538, doi:<http://dx.doi.org/10.1006/bbrc.1999.0811> (1999).
- 226 Ligos, J. M., Gerwin, N., Fernandez, P., Gutierrez-Ramos, J. C. & Bernad, A. Cloning, expression analysis, and functional characterization of PKL12, a member of a new subfamily of ser/thr kinases. *Biochemical and Biophysical Research Communications* **249**, 380-384, doi:10.1006/bbrc.1998.9163 (1998).
- 227 Manandhar, S. P., Ricarte, F., Cocca, S. M. & Gharakhanian, E. *Saccharomyces cerevisiae* Env7 Is a Novel Serine/Threonine Kinase 16-Related Protein Kinase and Negatively Regulates Organelle Fusion at the Lysosomal Vacuole. *Molecular and Cellular Biology* **33**, 526-542, doi:10.1128/mcb.01303-12 (2013).
- 228 Gharakhanian, E., Manandhar, S., Cocca, S. & Ricarte, F. S. *Saccharomyces cerevisiae* ENV7 encodes a novel vacuolar membrane kinase involved in delivery or function at the vacuole and is an ortholog of human ser/thr kinase STK16. *Faseb J.* **26** (2012).
- 229 Stairs, D., Notarfrancesco, K. & Chodosh, L. The Serine/Threonine Kinase, Krct, Affects Endbud Morphogenesis during Murine Mammary Gland Development. *Transgenic Res* **14**, 919-940, doi:10.1007/s11248-005-1806-6 (2005).
- 230 Guinea, B. *et al.* Nucleocytoplasmic shuttling of STK16 (PKL12), a Golgi-resident serine/threonine kinase involved in VEGF expression regulation. *Experimental cell research* **312**, 135-144, doi:10.1016/j.yexcr.2005.10.010 (2006).
- 231 In, J. G., Striz, A. C., Bernad, A. & Tuma, P. L. Serine/threonine kinase 16 and MAL2 regulate constitutive secretion of soluble cargo in hepatic cells. *Biochem J*, doi:10.1042/bj20140468 (2014).
- 232 Verma, M. K. *et al.* Activation of GPR40 attenuates chronic inflammation induced impact on pancreatic beta-cells health and function. *BMC cell biology* **15**, 24, doi:10.1186/1471-2121-15-24 (2014).
- 233 Eason, R. A. CaM kinase II: a protein kinase with extraordinary talents germane to insulin exocytosis. *Diabetes* **48**, 675-684, doi:10.2337/diabetes.48.4.675 (1999).
- 234 Kline, C. F. *et al.* betaIV-Spectrin and CaMKII facilitate Kir6.2 regulation in pancreatic beta cells. *Proc Natl Acad Sci U S A* **110**, 17576-17581, doi:10.1073/pnas.1314195110 (2013).

- 235 Wei, J., Wayman, G. & Storm, D. R. Phosphorylation and inhibition of type III adenylyl cyclase by calmodulin-dependent protein kinase II in vivo. *J Biol Chem* **271**, 24231-24235 (1996).
- 236 Wei, J. *et al.* Phosphorylation and inhibition of olfactory adenylyl cyclase by CaM kinase II in Neurons: a mechanism for attenuation of olfactory signals. *Neuron* **21**, 495-504 (1998).
- 237 Leech, C. A., Castonguay, M. A. & Habener, J. F. Expression of adenylyl cyclase subtypes in pancreatic beta-cells. *Biochem Biophys Res Commun* **254**, 703-706, doi:10.1006/bbrc.1998.9906 (1999).
- 238 Ozcan, L. *et al.* Activation of Calcium/Calmodulin-Dependent Protein Kinase II in Obesity Mediates Suppression of Hepatic Insulin Signaling. *Cell Metabolism* **18**, 803-815, doi:10.1016/j.cmet.2013.10.011 (2013).
- 239 Ardestani, A. *et al.* MST1 is a key regulator of beta cell apoptosis and dysfunction in diabetes. *Nat Med*, doi:10.1038/nm.3482 (2014).
- 240 Lang, F. & Shumilina, E. Regulation of ion channels by the serum- and glucocorticoid-inducible kinase SGK1. *The FASEB Journal* **27**, 3-12, doi:10.1096/fj.12-218230 (2013).
- 241 Ullrich, S. *et al.* Dexamethasone increases Na⁺/K⁺ ATPase activity in insulin secreting cells through SGK1. *Biochemical and Biophysical Research Communications* **352**, 662-667, doi:<http://dx.doi.org/10.1016/j.bbrc.2006.11.065> (2007).
- 242 Bohmer, C. *et al.* The serum and glucocorticoid inducible kinases SGK1-3 stimulate the neutral amino acid transporter SLC6A19. *Cellular physiology and biochemistry : international journal of experimental cellular physiology, biochemistry, and pharmacology* **25**, 723-732, doi:10.1159/000315092 (2010).
- 243 Embark, H. M., Bohmer, C., Vallon, V., Luft, F. & Lang, F. Regulation of KCNE1-dependent K(+) current by the serum and glucocorticoid-inducible kinase (SGK) isoforms. *Pflugers Archiv : European journal of physiology* **445**, 601-606, doi:10.1007/s00424-002-0982-y (2003).
- 244 Friedrich, B. *et al.* The serine/threonine kinases SGK2 and SGK3 are potent stimulators of the epithelial Na⁺ channel alpha,beta,gamma-ENaC. *Pflugers Archiv : European journal of physiology* **445**, 693-696, doi:10.1007/s00424-002-0993-8 (2003).
- 245 Gamper, N. *et al.* K⁺ channel activation by all three isoforms of serum- and glucocorticoid-dependent protein kinase SGK. *Pflugers Archiv : European journal of physiology* **445**, 60-66, doi:10.1007/s00424-002-0873-2 (2002).
- 246 He, P. *et al.* Serum- and glucocorticoid-induced kinase 3 in recycling endosomes mediates acute activation of Na⁺/H⁺ exchanger NHE3 by glucocorticoids. *Mol Biol Cell* **22**, 3812-3825, doi:10.1091/mbc.E11-04-0328 (2011).
- 247 Henke, G., Maier, G., Wallisch, S., Boehmer, C. & Lang, F. Regulation of the voltage gated K⁺ channel Kv1.3 by the ubiquitin ligase Nedd4-2 and the serum and glucocorticoid inducible kinase SGK1. *Journal of cellular physiology* **199**, 194-199, doi:10.1002/jcp.10430 (2004).
- 248 Henke, G., Setiawan, I., Bohmer, C. & Lang, F. Activation of Na⁺/K⁺-ATPase by the serum and glucocorticoid-dependent kinase isoforms. *Kidney & blood pressure research* **25**, 370-374, doi:68699 (2002).
- 249 da Silva Xavier, G. *et al.* Role for AMP-activated protein kinase in glucose-stimulated insulin secretion and preproinsulin gene expression. *Biochem J* **371**, 761-774, doi:10.1042/bj20021812 (2003).
- 250 Herrero, L. *et al.* Alteration of the malonyl-CoA/carnitine palmitoyltransferase I interaction in the beta-cell impairs glucose-induced insulin secretion. *Diabetes* **54**, 462-471 (2005).

- 251 Pound, L. D. *et al.* G6PC2: a negative regulator of basal glucose-stimulated insulin secretion. *Diabetes* **62**, 1547-1556, doi:10.2337/db12-1067 (2013).
- 252 Li, C. *et al.* Mechanism of hyperinsulinism in short-chain 3-hydroxyacyl-CoA dehydrogenase deficiency involves activation of glutamate dehydrogenase. *J Biol Chem* **285**, 31806 - 31818 (2010).
- 253 Clayton, P. *et al.* Hyperinsulinism in short-chain L-3-hydroxyacyl-CoA dehydrogenase deficiency reveals the importance of beta-oxidation in insulin secretion. *J Clin Invest* **108**, 457 - 465 (2001).
- 254 MacDonald, M. J. *et al.* Knockdown of both mitochondrial isocitrate dehydrogenase enzymes in pancreatic beta cells inhibits insulin secretion. *Biochimica et biophysica acta* **1830**, 5104-5111, doi:10.1016/j.bbagen.2013.07.013 (2013).
- 255 Guay, C. *et al.* A role for cytosolic isocitrate dehydrogenase as a negative regulator of glucose signaling for insulin secretion in pancreatic ss-cells. *PLoS One* **8**, e77097, doi:10.1371/journal.pone.0077097 (2013).
- 256 Cantin, L.-D. *et al.* PDE-10A inhibitors as insulin secretagogues. *Bioorganic & Medicinal Chemistry Letters* **17**, 2869-2873, doi:<http://dx.doi.org/10.1016/j.bmcl.2007.02.061> (2007).
- 257 Bender, A. T. & Beavo, J. A. Cyclic Nucleotide Phosphodiesterases: Molecular Regulation to Clinical Use. *Pharmacological Reviews* **58**, 488-520, doi:10.1124/pr.58.3.5 (2006).
- 258 Furman, B., Ong, W. K. & Pyne, N. J. Cyclic AMP signaling in pancreatic islets. *Advances in experimental medicine and biology* **654**, 281-304, doi:10.1007/978-90-481-3271-3_13 (2010).
- 259 Han, P., Werber, J., Surana, M., Fleischer, N. & Michaeli, T. The calcium/calmodulin-dependent phosphodiesterase PDE1C down-regulates glucose-induced insulin secretion. *J Biol Chem* **274**, 22337-22344 (1999).
- 260 Harndahl, L. *et al.* Important role of phosphodiesterase 3B for the stimulatory action of cAMP on pancreatic beta-cell exocytosis and release of insulin. *J Biol Chem* **277**, 37446-37455, doi:10.1074/jbc.M205401200 (2002).
- 261 Pyne, N. J. & Furman, B. L. Cyclic nucleotide phosphodiesterases in pancreatic islets. *Diabetologia* **46**, 1179-1189, doi:10.1007/s00125-003-1176-7 (2003).
- 262 Aoyagi, K., Ohara-Imaizumi, M. & Nagamatsu, S. Regulation of resident and newcomer insulin granules by calcium and SNARE proteins. *Frontiers in bioscience (Landmark edition)* **16**, 1197-1210 (2011).
- 263 Nevins, A. K. & Thurmond, D. C. A direct interaction between Cdc42 and vesicle-associated membrane protein 2 regulates SNARE-dependent insulin exocytosis. *J Biol Chem* **280**, 1944-1952, doi:10.1074/jbc.M409528200 (2005).
- 264 Regazzi, R., Kikuchi, A., Takai, Y. & Wollheim, C. B. The small GTP-binding proteins in the cytosol of insulin-secreting cells are complexed to GDP dissociation inhibitor proteins. *J Biol Chem* **267**, 17512-17519 (1992).
- 265 Leech, C. A., Holz, G. G. & Habener, J. F. Signal Transduction of PACAP and GLP-1 in Pancreatic β Cells. *Annals of the New York Academy of Sciences* **805**, 81-92, doi:10.1111/j.1749-6632.1996.tb17475.x (1996).
- 266 Landa, L. R., Jr. *et al.* Interplay of Ca²⁺ and cAMP signaling in the insulin-secreting MIN6 beta-cell line. *J Biol Chem* **280**, 31294-31302, doi:10.1074/jbc.M505657200 (2005).
- 267 Smukler, S. R., Tang, L., Wheeler, M. B. & Salapatek, A. M. F. Exogenous Nitric Oxide and Endogenous Glucose-Stimulated β -Cell Nitric Oxide Augment Insulin Release. *Diabetes* **51**, 3450-3460, doi:10.2337/diabetes.51.12.3450 (2002).

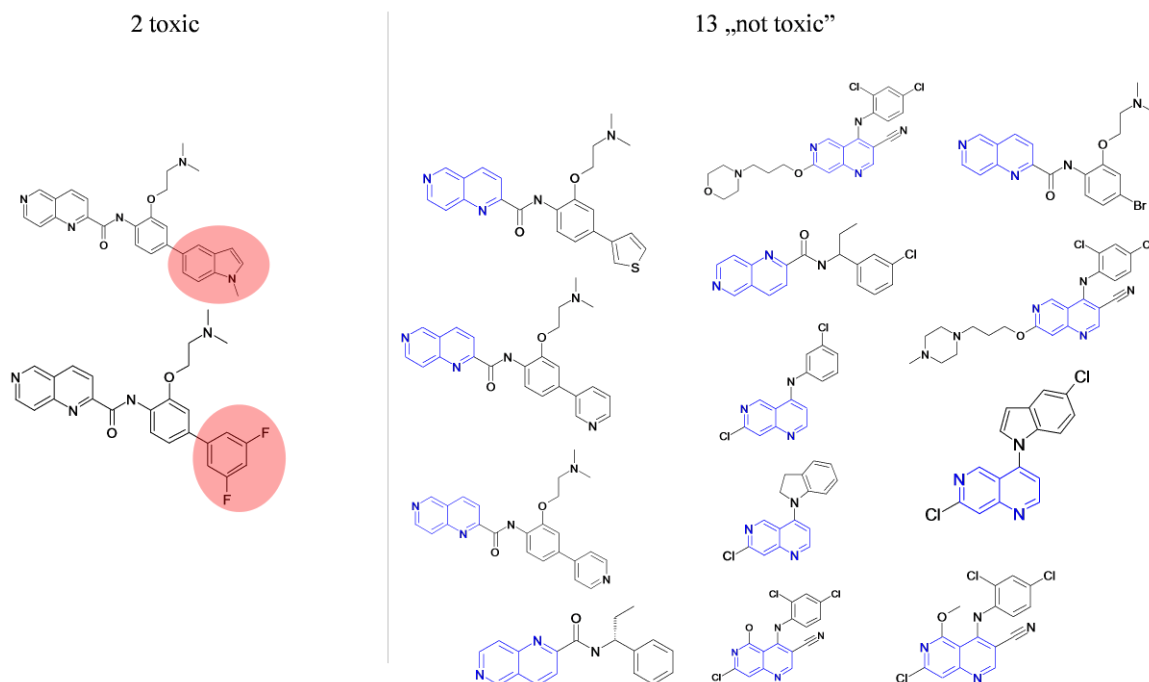
- 268 Kaneko, Y., Ishikawa, T., Amano, S. & Nakayama, K. Dual effect of nitric oxide on cytosolic Ca²⁺ concentration and insulin secretion in rat pancreatic beta-cells. *Am J Physiol Cell Physiol* **284**, C1215-1222, doi:10.1152/ajpcell.00223.2002 (2003).
- 269 Keravis, T. & Lugnier, C. Cyclic nucleotide phosphodiesterases (PDE) and peptide motifs. *Current pharmaceutical design* **16**, 1114-1125 (2010).
- 270 Waddleton, D. *et al.* Phosphodiesterase 3 and 4 comprise the major cAMP metabolizing enzymes responsible for insulin secretion in INS-1 (832/13) cells and rat islets. *Biochem Pharmacol* **76**, 884-893, doi:10.1016/j.bcp.2008.07.025 (2008).
- 271 Russell, M. A. & Morgan, N. Expression and functional roles of guanylate cyclase isoforms in BRIN-BD11 β -cells. *Islets* **2**, 374-382 (2010).
- 272 Muhammed, S. J., Lundquist, I. & Salehi, A. Pancreatic beta-cell dysfunction, expression of iNOS and the effect of phosphodiesterase inhibitors in human pancreatic islets of type 2 diabetes. *Diabetes, obesity & metabolism* **14**, 1010-1019, doi:10.1111/j.1463-1326.2012.01632.x (2012).
- 273 Ahmad, M. *et al.* Effect of type-selective inhibitors on cyclic nucleotide phosphodiesterase activity and insulin secretion in the clonal insulin secreting cell line BRIN-BD11. *Br J Pharmacol* **129**, 1228-1234, doi:10.1038/sj.bjp.0703165 (2000).
- 274 Vollert, S. *et al.* The glucose-lowering effects of the PDE4 inhibitors roflumilast and roflumilast-N-oxide in db/db mice. *Diabetologia* **55**, 2779-2788, doi:10.1007/s00125-012-2632-z (2012).
- 275 Mammi, C. *et al.* Sildenafil reduces insulin-resistance in human endothelial cells. *PLoS One* **6**, e14542, doi:10.1371/journal.pone.0014542 (2011).
- 276 Oudot, A. *et al.* How does chronic sildenafil prevent vascular oxidative stress in insulin-resistant rats? *J Sex Med* **7**, 79-88, doi:10.1111/j.1743-6109.2009.01551.x (2010).
- 277 Schäfer, A. *et al.* Improvement of vascular function by acute and chronic treatment with the PDE-5 inhibitor sildenafil in experimental diabetes mellitus. *British Journal of Pharmacology* **153**, 886-893, doi:10.1038/sj.bjp.0707459 (2008).
- 278 Ayala, J. E. *et al.* Chronic Treatment With Sildenafil Improves Energy Balance and Insulin Action in High Fat-Fed Conscious Mice. *Diabetes* **56**, 1025-1033, doi:10.2337/db06-0883 (2007).
- 279 Varma, A. *et al.* Anti-inflammatory and cardioprotective effects of tadalafil in diabetic mice. *PLoS One* **7**, e45243, doi:10.1371/journal.pone.0045243 (2012).
- 280 Horvath, A. *et al.* Voltage dependent calcium channels in adrenal glomerulosa cells and in insulin producing cells. *Cell Calcium* **23**, 33-42 (1998).
- 281 Braun, M. *et al.* Voltage-Gated Ion Channels in Human Pancreatic β -Cells: Electrophysiological Characterization and Role in Insulin Secretion. *Diabetes* **57**, 1618-1628, doi:10.2337/db07-0991 (2008).
- 282 Ashcroft, F. M., Kelly, R. P. & Smith, P. A. Two types of Ca channel in rat pancreatic beta-cells. *Pflugers Archiv : European journal of physiology* **415**, 504-506 (1990).
- 283 Taylor, J. T. *et al.* Role of high-voltage-activated calcium channels in glucose-regulated β -cell calcium homeostasis and insulin release. Vol. 289 (2005).
- 284 Vignali, S., Leiss, V., Karl, R., Hofmann, F. & Welling, A. Characterization of voltage-dependent sodium and calcium channels in mouse pancreatic A- and B-cells. *The Journal of Physiology* **572**, 691-706, doi:10.1113/jphysiol.2005.102368 (2006).
- 285 Sher, E. *et al.* Voltage-operated calcium channel heterogeneity in pancreatic beta cells: physiopathological implications. *Journal of bioenergetics and biomembranes* **35**, 687-696 (2003).
- 286 Rorsman, P., Ashcroft, F. M. & Trube, G. Single Ca channel currents in mouse pancreatic B-cells. *Pflugers Arch - Eur J Physiol* **412**, 597-603, doi:10.1007/BF00583760 (1988).

- 287 Zhuang, H. *et al.* Cloning of a T-type Ca²⁺ channel isoform in insulin-secreting cells. *Diabetes* **49**, 59-64, doi:10.2337/diabetes.49.1.59 (2000).
- 288 Pollo, A. *et al.* Sensitivity to dihydropyridines, omega-conotoxin and noradrenaline reveals multiple high-voltage-activated Ca²⁺ channels in rat insulinoma and human pancreatic beta-cells. *Pflugers Archiv : European journal of physiology* **423**, 462-471 (1993).
- 289 Neher, E. & Marty, A. Discrete changes of cell membrane capacitance observed under conditions of enhanced secretion in bovine adrenal chromaffin cells. *Proc Natl Acad Sci U S A* **79**, 6712-6716 (1982).
- 290 Altier, C. & Zamponi, G. W. Analysis of GPCR/ion channel interactions. *Methods in molecular biology (Clifton, N.J.)* **756**, 215-225, doi:10.1007/978-1-61779-160-4_11 (2011).
- 291 Szollosi, A., Nenquin, M. & Henquin, J. C. Pharmacological stimulation and inhibition of insulin secretion in mouse islets lacking ATP-sensitive K⁺ channels. *British Journal of Pharmacology* **159**, 669-677, doi:10.1111/j.1476-5381.2009.00588.x (2010).
- 292 Fu, A., Eberhard, C. E. & Sreaton, R. A. Role of AMPK in pancreatic beta cell function. *Mol Cell Endocrinol* **366**, 127-134, doi:10.1016/j.mce.2012.06.020 (2013).
- 293 Van de Casteele, M. *et al.* Prolonged culture in low glucose induces apoptosis of rat pancreatic beta-cells through induction of c-myc. *Biochem Biophys Res Commun* **312**, 937-944 (2003).
- 294 Kerkela, R. *et al.* Sunitinib-Induced Cardiotoxicity Is Mediated by Off-Target Inhibition of AMP-Activated Protein Kinase. *Clinical and Translational Science* **2**, 15-25, doi:10.1111/j.1752-8062.2008.00090.x (2009).
- 295 Ammala, C. *et al.* Activation of protein kinases and inhibition of protein phosphatases play a central role in the regulation of exocytosis in mouse pancreatic beta cells. *Proc Natl Acad Sci U S A* **91**, 4343-4347 (1994).
- 296 Standaert, M. L. *et al.* Effects of knockout of the protein kinase C beta gene on glucose transport and glucose homeostasis. *Endocrinology* **140**, 4470-4477, doi:10.1210/endo.140.10.7073 (1999).
- 297 Rao, X. *et al.* Exercise protects against diet-induced insulin resistance through downregulation of protein kinase Cbeta in mice. *PLoS One* **8**, e81364, doi:10.1371/journal.pone.0081364 (2013).
- 298 Perrini, S., Henriksson, J., Zierath, J. R. & Widegren, U. Exercise-induced protein kinase C isoform-specific activation in human skeletal muscle. *Diabetes* **53**, 21-24 (2004).
- 299 Rose, A. J., Michell, B. J., Kemp, B. E. & Hargreaves, M. Effect of exercise on protein kinase C activity and localization in human skeletal muscle. *J Physiol* **561**, 861-870, doi:10.1113/jphysiol.2004.075549 (2004).
- 300 Chen, H. C. *et al.* Activation of the ERK pathway and atypical protein kinase C isoforms in exercise- and aminoimidazole-4-carboxamide-1-beta-D-ribose (AICAR)-stimulated glucose transport. *J Biol Chem* **277**, 23554-23562, doi:10.1074/jbc.M201152200 (2002).
- 301 Furukawa, N. *et al.* Possible involvement of atypical protein kinase C (PKC) in glucose-sensitive expression of the human insulin gene: DNA-binding activity and transcriptional activity of pancreatic and duodenal homeobox gene-1 (PDX-1) are enhanced via calphostin C-sensitive but phorbol 12-myristate 13-acetate (PMA) and Go 6976-insensitive pathway. *Endocr J* **46**, 43-58 (1999).
- 302 Harris, T. E., Persaud, S. J. & Jones, P. M. Atypical isoforms of pKc and insulin secretion from pancreatic beta-cells: evidence using Go 6976 and Ro 31-8220 as Pkc

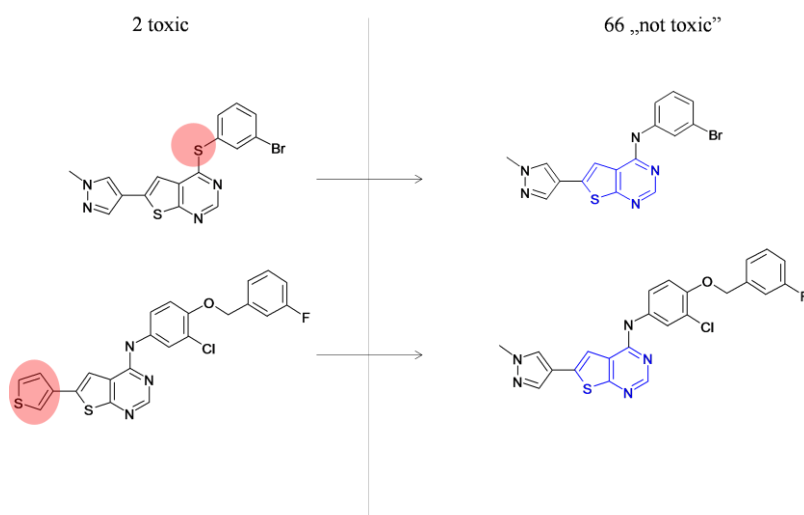
- inhibitors. *Biochem Biophys Res Commun* **227**, 672-676, doi:10.1006/bbrc.1996.1567 (1996).
- 303 Buteau, J. *et al.* Protein kinase Czeta activation mediates glucagon-like peptide-1-induced pancreatic beta-cell proliferation. *Diabetes* **50**, 2237-2243 (2001).
- 304 Velazquez-Garcia, S. *et al.* Activation of protein kinase C-zeta in pancreatic beta-cells in vivo improves glucose tolerance and induces beta-cell expansion via mTOR activation. *Diabetes* **60**, 2546-2559, doi:10.2337/db10-1783 (2011).
- 305 Vasavada, R. C. *et al.* Protein kinase C-zeta activation markedly enhances beta-cell proliferation: an essential role in growth factor mediated beta-cell mitogenesis. *Diabetes* **56**, 2732-2743, doi:10.2337/db07-0461 (2007).
- 306 Suzuki, Y. *et al.* Glucagon-like peptide 1 activates protein kinase C through Ca²⁺-dependent activation of phospholipase C in insulin-secreting cells. *J Biol Chem* **281**, 28499-28507, doi:10.1074/jbc.M604291200 (2006).
- 307 Warwar, N. *et al.* Dynamics of glucose-induced localization of PKC isoenzymes in pancreatic beta-cells: diabetes-related changes in the GK rat. *Diabetes* **55**, 590-599 (2006).
- 308 Ferreira, F. *et al.* Decreased cholinergic stimulation of insulin secretion by islets from rats fed a low protein diet is associated with reduced protein kinase calpha expression. *The Journal of nutrition* **133**, 695-699 (2003).
- 309 Beraud-Dufour, S. *et al.* Neurotensin is a regulator of insulin secretion in pancreatic beta-cells. *Int J Biochem Cell Biol* **42**, 1681-1688, doi:10.1016/j.biocel.2010.06.018 (2010).
- 310 Angelini, N., Rafacho, A., Boschero, A. C. & Bosqueiro, J. R. Involvement of the cholinergic pathway in glucocorticoid-induced hyperinsulinemia in rats. *Diabetes research and clinical practice* **87**, 184-191, doi:10.1016/j.diabres.2009.11.008 (2010).
- 311 Piquer, S. *et al.* Role of iduronate-2-sulfatase in glucose-stimulated insulin secretion by activation of exocytosis. *American journal of physiology. Endocrinology and metabolism* **297**, E793-801, doi:10.1152/ajpendo.90878.2008 (2009).
- 312 Bocker, D. & Verspohl, E. J. Role of protein kinase C, PI3-kinase and tyrosine kinase in activation of MAP kinase by glucose and agonists of G-protein coupled receptors in INS-1 cells. *International journal of experimental diabetes research* **2**, 233-244 (2001).
- 313 Quoyer, J. *et al.* GLP-1 Mediates Antiapoptotic Effect by Phosphorylating Bad through a β -Arrestin 1-mediated ERK1/2 Activation in Pancreatic β -Cells. *Journal of Biological Chemistry* **285**, 1989-2002, doi:10.1074/jbc.M109.067207 (2010).
- 314 Selway, J. *et al.* Evidence that Ca²⁺ within the microdomain of the L-type voltage gated Ca²⁺ channel activates ERK in MIN6 cells in response to glucagon-like peptide-1. *PLoS One* **7**, e33004, doi:10.1371/journal.pone.0033004 (2012).
- 315 Selway, J. L., Moore, C. E., Mistry, R., John Challiss, R. A. & Herbert, T. P. Molecular mechanisms of muscarinic acetylcholine receptor-stimulated increase in cytosolic free Ca(2+) concentration and ERK1/2 activation in the MIN6 pancreatic beta-cell line. *Acta diabetologica* **49**, 277-289, doi:10.1007/s00592-011-0314-9 (2012).
- 316 Baillie, G. S., MacKenzie, S. J., McPhee, I. & Houslay, M. D. Sub-family selective actions in the ability of Erk2 MAP kinase to phosphorylate and regulate the activity of PDE4 cyclic AMP-specific phosphodiesterases. *British Journal of Pharmacology* **131**, 811-819, doi:10.1038/sj.bjp.0703636 (2000).
- 317 Rhodes, C. J. & White, M. F. Molecular insights into insulin action and secretion. *European journal of clinical investigation* **32 Suppl 3**, 3-13 (2002).
- 318 Briaud, I., Lingohr, M. K., Dickson, L. M., Wrede, C. E. & Rhodes, C. J. Differential Activation Mechanisms of Erk-1/2 and p70S6K by Glucose in Pancreatic β -Cells. *Diabetes* **52**, 974-983, doi:10.2337/diabetes.52.4.974 (2003).

- 319 Wauson, E. M., Guerra, M. L., Barylko, B., Albanesi, J. P. & Cobb, M. H. Off-Target Effects of MEK Inhibitors. *Biochemistry* **52**, 5164-5166, doi:10.1021/bi4007644 (2013).
- 320 Taylor, S. S. *et al.* PKA: a portrait of protein kinase dynamics. *Biochimica et Biophysica Acta (BBA) - Proteins and Proteomics* **1697**, 259-269, doi:<http://dx.doi.org/10.1016/j.bbapap.2003.11.029> (2004).
- 321 Cauthron, R. D., Carter, K. B., Liauw, S. & Steinberg, R. A. Physiological Phosphorylation of Protein Kinase A at Thr-197 Is by a Protein Kinase A Kinase. *Molecular and Cellular Biology* **18**, 1416-1423 (1998).
- 322 Cheng, X., Ma, Y., Moore, M., Hemmings, B. A. & Taylor, S. S. Phosphorylation and activation of cAMP-dependent protein kinase by phosphoinositide-dependent protein kinase. *Proceedings of the National Academy of Sciences* **95**, 9849-9854, doi:10.1073/pnas.95.17.9849 (1998).
- 323 Johannessen, M., Delghandi, M. P. & Moens, U. What turns CREB on? *Cellular signalling* **16**, 1211-1227, doi:10.1016/j.cellsig.2004.05.001 (2004).
- 324 Liu, B., Barbosa-Sampaio, H., Jones, P. M., Persaud, S. J. & Muller, D. S. The CaMK4/CREB/IRS-2 cascade stimulates proliferation and inhibits apoptosis of beta-cells. *PLoS One* **7**, e45711, doi:10.1371/journal.pone.0045711 (2012).
- 325 Lonze, B. E. & Ginty, D. D. Function and Regulation of CREB Family Transcription Factors in the Nervous System. *Neuron* **35**, 605-623, doi:[http://dx.doi.org/10.1016/S0896-6273\(02\)00828-0](http://dx.doi.org/10.1016/S0896-6273(02)00828-0) (2002).
- 326 Grewal, S. S. *et al.* Calcium and cAMP signals differentially regulate cAMP-responsive element-binding protein function via a Rap-1-extracellular signal-regulated kinase pathway. *Journal of Biological Chemistry* **275**, 34433-34441 (2000).
- 327 Inada, A. *et al.* Overexpression of Inducible Cyclic AMP Early Repressor Inhibits Transactivation of Genes and Cell Proliferation in Pancreatic β Cells. *Molecular and Cellular Biology* **24**, 2831-2841, doi:10.1128/mcb.24.7.2831-2841.2004 (2004).
- 328 Kim, S.-J., Nian, C., Widenmaier, S. & McIntosh, C. H. S. Glucose-Dependent Insulinotropic Polypeptide-Mediated Up-Regulation of β -Cell Antiapoptotic Bcl-2 Gene Expression Is Coordinated by Cyclic AMP (cAMP) Response Element Binding Protein (CREB) and cAMP-Responsive CREB Coactivator 2. *Molecular and Cellular Biology* **28**, 1644-1656, doi:10.1128/mcb.00325-07 (2008).
- 329 Hussain, M. A. *et al.* Increased Pancreatic β -Cell Proliferation Mediated by CREB Binding Protein Gene Activation. *Molecular and Cellular Biology* **26**, 7747-7759, doi:10.1128/mcb.02353-05 (2006).
- 330 Costes, S. *et al.* Degradation of cAMP-Responsive Element-Binding Protein by the Ubiquitin-Proteasome Pathway Contributes to Glucotoxicity in β -Cells and Human Pancreatic Islets. *Diabetes* **58**, 1105-1115, doi:10.2337/db08-0926 (2009).
- 331 Polak, P. & Hall, M. N. mTOR and the control of whole body metabolism. *Current opinion in cell biology* **21**, 209-218, doi:10.1016/j.ceb.2009.01.024 (2009).
- 332 Hamada, S. *et al.* Upregulation of the mammalian target of rapamycin complex 1 pathway by Ras homolog enriched in brain in pancreatic beta-cells leads to increased beta-cell mass and prevention of hyperglycemia. *Diabetes* **58**, 1321-1332, doi:10.2337/db08-0519 (2009).
- 333 Shigeyama, Y. *et al.* Biphasic response of pancreatic beta-cell mass to ablation of tuberous sclerosis complex 2 in mice. *Mol Cell Biol* **28**, 2971-2979, doi:10.1128/mcb.01695-07 (2008).
- 334 Blancquaert, S. *et al.* cAMP-Dependent Activation of Mammalian Target of Rapamycin (mTOR) in Thyroid Cells. Implication in Mitogenesis and Activation of CDK4. *Molecular Endocrinology* **24**, 1453-1468, doi:doi:10.1210/me.2010-0087 (2010).

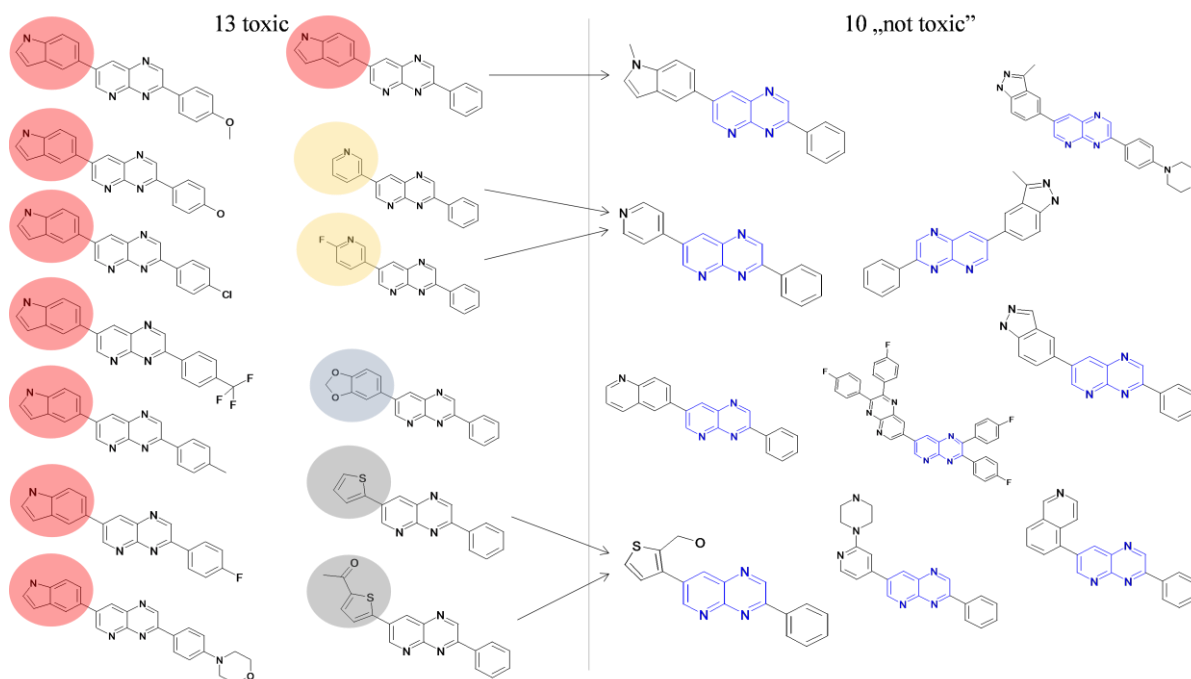
- 335 Van de Velde, S., Hogan, M. F. & Montminy, M. mTOR links incretin signaling to HIF induction in pancreatic beta cells. *Proc Natl Acad Sci U S A* **108**, 16876-16882, doi:10.1073/pnas.1114228108 (2011).
- 336 Nishida, A. *et al.* Inhibition of ATP-sensitive K⁺ channels and L-type Ca²⁺ channels by amiodarone elicits contradictory effect on insulin secretion in MIN6 cells. *Journal of pharmacological sciences* **116**, 73-80 (2011).
- 337 Bito, M. *et al.* The Mechanisms of Insulin Secretion and Calcium Signaling in Pancreatic β -Cells Exposed to Fluoroquinolones. *Biological and Pharmaceutical Bulletin* **36**, 31-35 (2013).
- 338 Gopel, S. *et al.* Capacitance measurements of exocytosis in mouse pancreatic alpha-, beta- and delta-cells within intact islets of Langerhans. *J Physiol* **556**, 711-726, doi:10.1113/jphysiol.2003.059675 (2004).
- 339 Sutherland, H. S. *et al.* Therapeutic reactivation of mutant p53 protein by quinazoline derivatives. *Investigational new drugs* **30**, 2035-2045, doi:10.1007/s10637-011-9744-z (2012).
- 340 Trumper, J. *et al.* The Rap-B-Raf signalling pathway is activated by glucose and glucagon-like peptide-1 in human islet cells. *Diabetologia* **48**, 1534-1540, doi:10.1007/s00125-005-1820-5 (2005).
- 341 Fukaya, M. *et al.* Protective effects of a nicotinamide derivative, isonicotinamide, against streptozotocin-induced β -cell damage and diabetes in mice. *Biochemical and Biophysical Research Communications* **442**, 92-98, doi:<http://dx.doi.org/10.1016/j.bbrc.2013.11.024> (2013).
- 342 Soni, A., Amisten, S., Rorsman, P. & Salehi, A. GPRC5B a putative glutamate-receptor candidate is negative modulator of insulin secretion. *Biochem Biophys Res Commun* **441**, 643-648 (2013).

APPENDIX**Toxic compounds**

1,6-Naphtyridine derivatives (core structure highlighted in blue). To the left: Two derivatives that decreased viability in MTT assay, after 2h treatment, probably because of the highlighted differences in their structures. To the right: 13 derivatives that were not toxic in the RIN-5AH cells. These structures include effective and non-effective compounds as well.

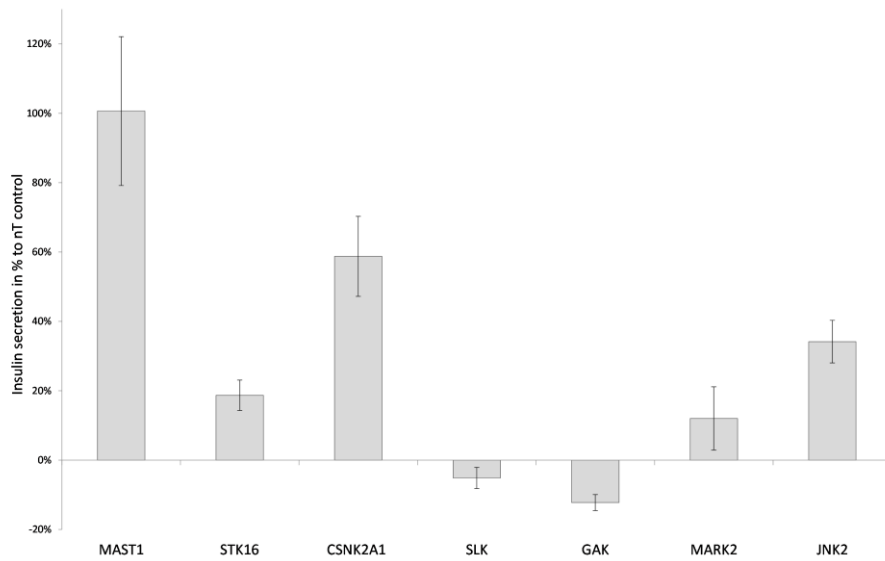


Structure activity relationships of toxic derivatives on RIN-5AH cells. Modifications in the cores structures decreased cell viability (to the left). Within the same core structure 66 non-toxic compounds were found. The displayed structures include effective and non-effective compounds as well.



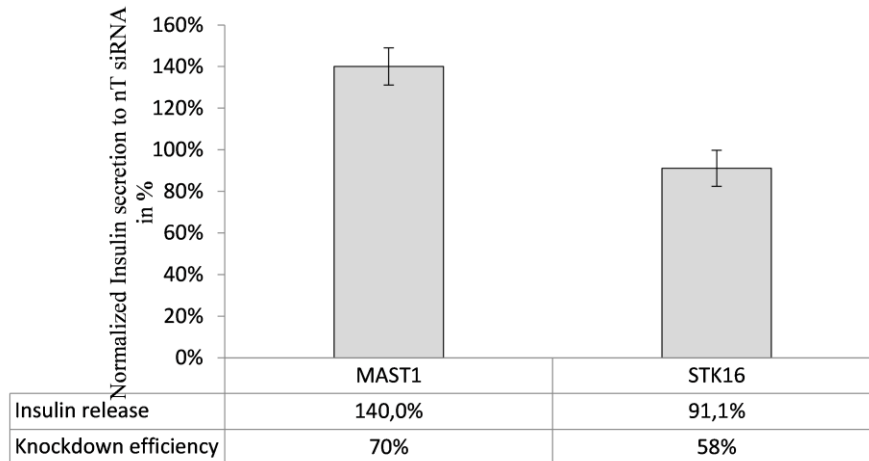
Structure activity relationships of toxic derivatives on RIN-5AH cells. Modifications in the cores structures decreased cell viability (to the left). Within the same core structure 10 non-toxic compounds were found. The displayed structures include effective and non-effective compounds as well.

Supplementary info for knockdown experiments



The 72h knockdown effect with DharmaFECT ON-TARGETplus in INS-1E cells

Accell siRNA knockdown - RIN-5AH cells



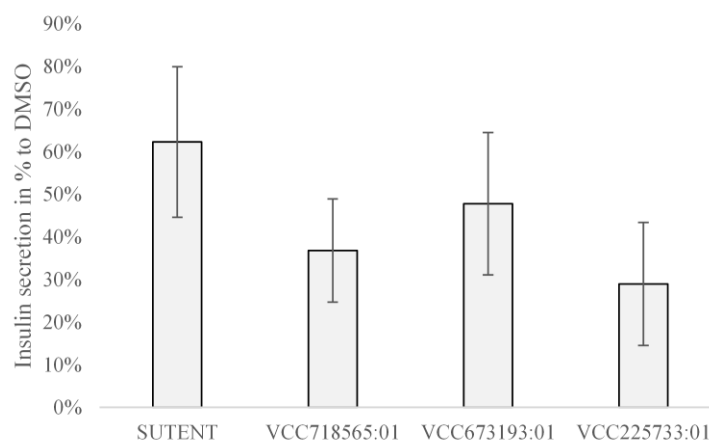
The siRNA effect of MAST1 and STK16 on insulin release and knockdown efficiency by Accell siRNA in RIN-5AH cells

RIN-5AH KD efficiencies with Accell siRNA

knockdown	sample	primer	Ct	Ct2	AV_Ct	SD_Ct	delta Ct	dd Ct	2 ⁻ -(dd Ct)	% KD
MAST1	KD_spl_MAST1	MAST1	30,75922012	31,21061897	30,98491955	0,319187187	9,165354729	1,747289658	0,297860835	70,2%
STK16	KD_spl_STK16	STK16	25,47702599	25,55031586	25,51367092	0,051823765	5,858898163	1,243083954	0,422468607	57,8%

RIN-5AH KD efficiencies with ON-TARGETplus siRNA

Sample Name	Target Name	Ct Mean	Ct SD	Δ Ct Mean	Δ Ct SE	$\Delta\Delta$ Ct	RQ Min	RQ Max	RQ	% KD
KD_MAST1	MAST1	28,69954681	0,362191826	9,129863739	0,245223388	2,188987017	0,14468357	0,332414031	0,219305381	78%
KD_STK16	STK16	24,78972435	0,296184301	5,326443195	0,205360219	2,313143969	0,142038867	0,285063326	0,201221451	80%
KD_CSNK2A1	CSNK2A1	31,7316227	0,197242051	11,7581234	0,147837013	1,920359373	0,205597773	0,339476764	0,264188707	74%
KD_SLK	SLK	28,49589729	0,519297957	8,879658699	0,329549074	2,697406292	0,088156834	0,269614756	0,154169977	85%
KD_GAK	GAK	26,33444405	0,37216711	7,08211565	0,261951506	1,6872859	0,199124381	0,484203815	0,310510516	69%
KD_MARK2	MARK2	24,42905617	0,450565636	5,135225773	0,322582752	1,707970977	0,177107528	0,529007673	0,306090266	69%
KD_JNK2	JNK2	26,56005859	0,023358146	7,083334923	0,024443628	2,518489122	0,16743806	0,181913212	0,174525633	83%

Efficient quinoline derivatives in BRIN-BD11 cells

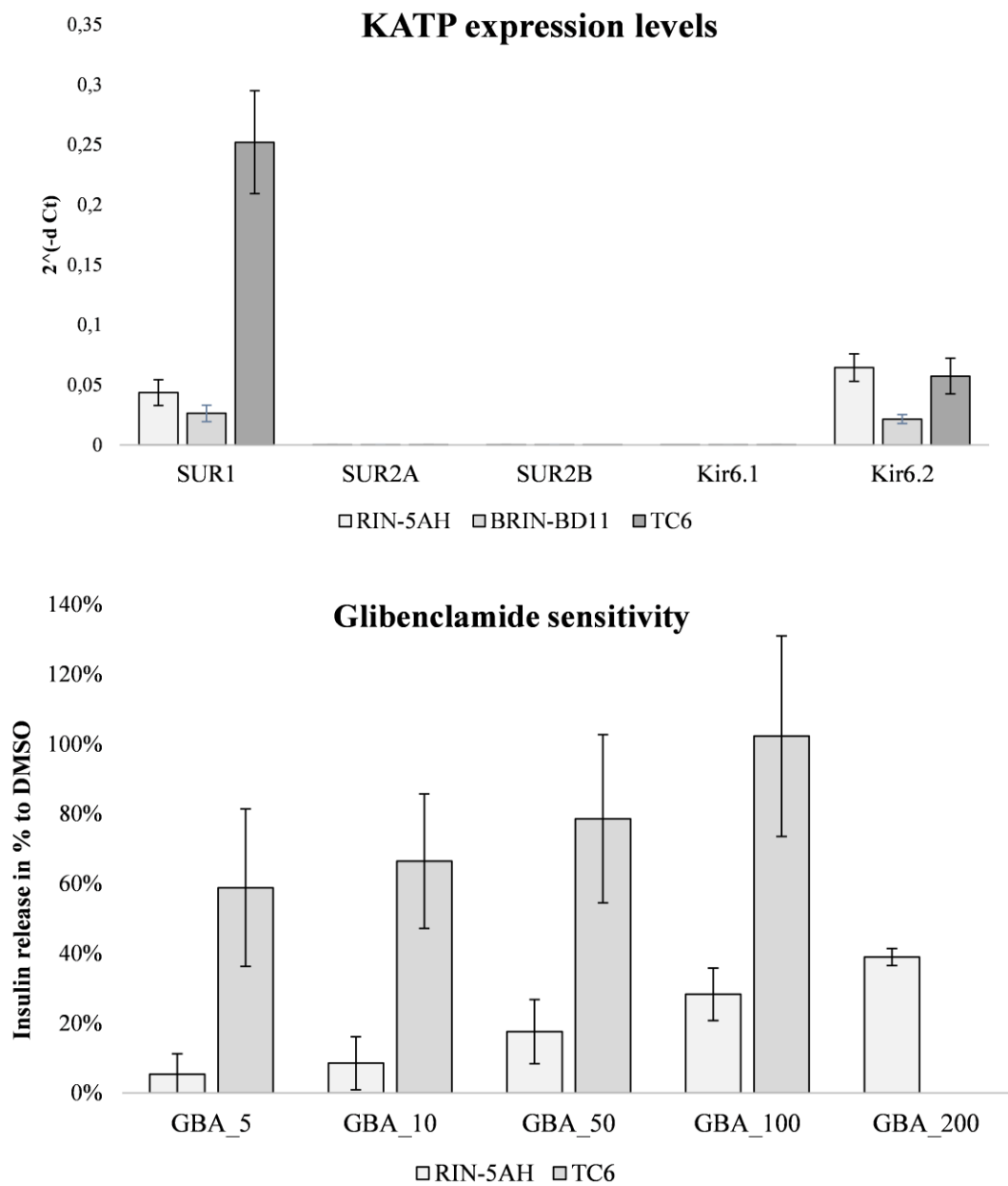
In BRIN-BD11 cells some derivatives of VCC981125 increased insulin secretion. (n=2)

Thieno-pyrimidines supplementary data

ID	Insulin RIN-5AH	Kinase inhibition		
		EGFR	HER2	KIT
VCC613596:10	80,7%	86,4%	55,7%	18,1%
VCC855801:01	60,5%	10,9%	-0,9%	1,8%
VCC919477:01	37,7%	64,8%	17,9%	-10,0%
VCC341830:01	35%	87%	40%	74%
VCC912492:01	31,7%	95,4%	62,4%	86,1%
VCC321171:07	30,4%	11,8%	-13,4%	-15,5%
VCC045928:01	22,7%	-10,3%	1,9%	-11,3%
VCC212350:01	22,0%	-7,1%	2,4%	-23,4%
VCC921037:01	15,9%	3,8%	0,3%	4,9%
VCC786494:01	5,2%	4,1%	4,6%	4,8%

Highlighted values above 30%. All compounds from the same family, but different selectivities for kinases. Data provided by Vichem Chemie Ltd. for kinase inhibition

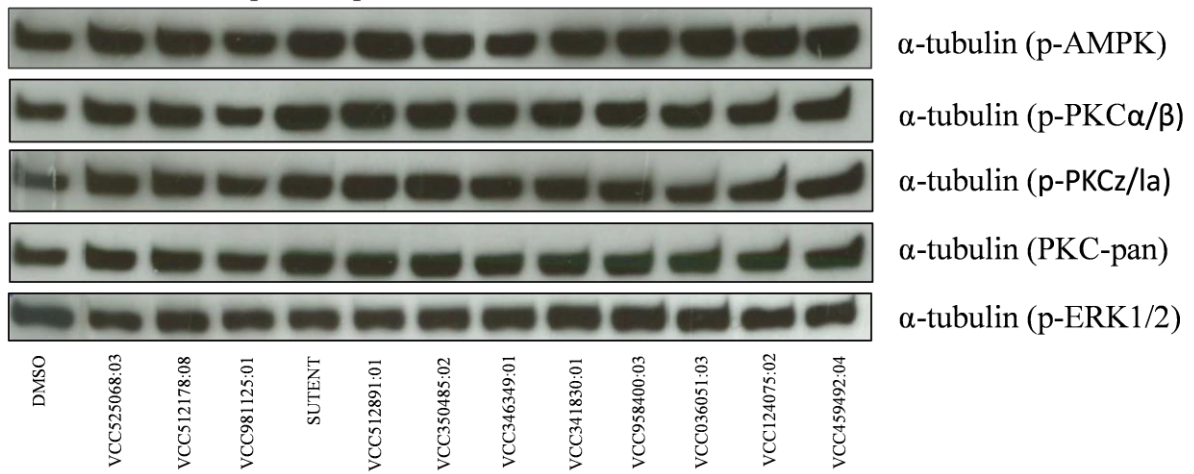
Altered K_{ATP} expression levels in different beta cell lines and the correlation with GBA sensitivity



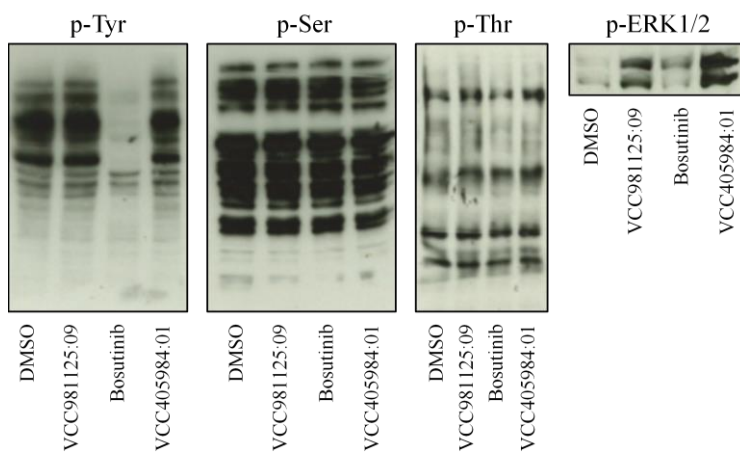
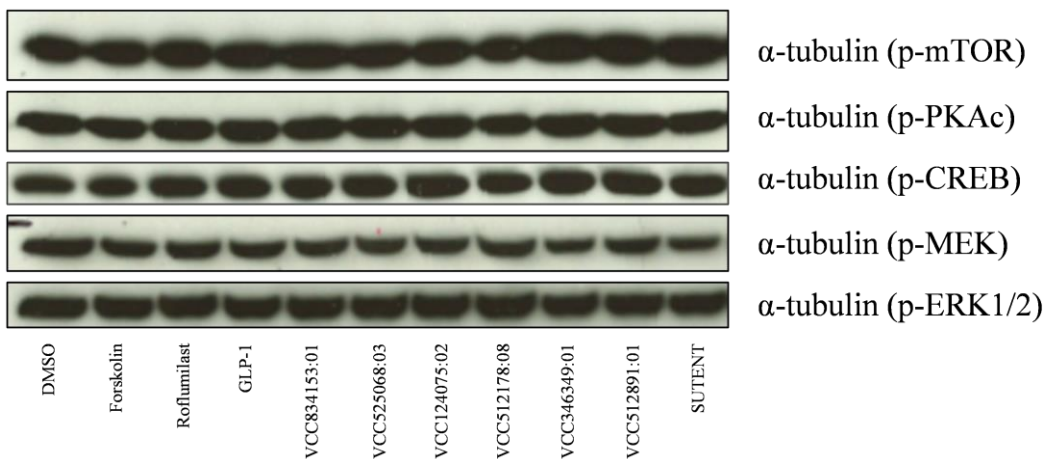
K_{ATP} subunits are expressed differentially in beta cells, which correlates with altered sensitivity of glibenclamide treatment as well. ($n=3$; housekeeping genes: *b-actin*, *GAPD*, *Cyclophilin B*)

Western blot supplementary info

„VCC insulinotropic compounds”



„cAMP inducer VCC compounds”



Top and middle: α-tubulin loading controls for VCC compound treatments and cAMP inducer compounds.

Bottom: Quinoline, bosutinib and bis-quinoline treatments.

ADME QikProp (Schrödinger)

ID	VCC350485:02 - mother compound	VCC350485:02 - acetyl protected	VCC350485:02 - dimethyl endgroup	VCC350485:02 - kinator	SUNITINIB	SUNITINIB linker	VCC512891:01 - mother compound	VCC512891:01 - linker	VCC512891:01 - BOC protected linker	VCC124075:02 - kinator/mother compound	VCC124075:02 - formyl protected linker
tautomer probability	1,00	1,00	1,00	1,00	1,00	1,00	1,00	1,00	1,00	1,00	1,00
mol MW	469,42	455,35	362,47	413,32	398,48	398,48	437,93	461,57	561,69	396,45	438,49
dipole	2,59	4,15	3,25	4,06	7,16	8,31	5,74	2,90	3,29	7,08	9,16
SASA	742,15	767,46	719,43	702,31	740,85	763,85	791,64	868,97	998,74	718,87	764,31
FOSA	362,75	300,82	339,80	231,16	403,90	365,61	259,35	352,28	502,50	334,64	405,74
FISA	25,25	100,51	46,17	82,42	112,81	174,18	105,70	162,46	161,45	133,04	130,63
PISA	276,85	290,57	333,47	311,42	177,23	177,16	352,57	354,24	334,79	251,19	227,94
WPSA	77,31	75,56	0,00	77,31	46,91	46,91	74,01	0,00	0,00	0,00	0,00
volume	1379,2	1331,9	1262,3	1207,5	1311,9	1329,8	1383,7	1523,5	1817,7	1261,8	1372,9
donorHB	1,00	2,00	1,00	3,00	2,00	4,00	2,00	5,00	4,00	4,00	3,00
acctptHB	5,25	5,75	5,25	4,25	6,00	5,00	10,00	11,50	13,00	7,25	8,75
dip ² /V	0,00	0,01	0,01	0,01	0,04	0,05	0,02	0,01	0,01	0,04	0,06
ACxDN [^] ,5/SA	0,01	0,01	0,01	0,01	0,01	0,01	0,02	0,03	0,03	0,02	0,02
glob	0,81	0,76	0,79	0,78	0,78	0,77	0,76	0,74	0,72	0,79	0,78
QPpolrz	44,62	44,14	41,77	39,37	42,91	42,34	48,74	51,78	62,72	40,32	44,55
QPlogPC16	13,95	14,54	12,93	13,51	12,71	13,84	15,53	17,63	20,24	13,64	14,30
QPlogPoct	18,85	20,74	17,64	19,73	20,66	23,16	25,00	30,69	33,80	23,27	24,36
QPlogPw	7,80	13,29	8,68	10,71	10,57	12,54	16,22	21,77	21,74	14,86	16,74
QPlogPo/w	5,67	4,36	4,54	4,23	3,92	3,57	2,56	1,16	3,00	2,54	2,71
QPlogS	-5,16	-5,78	-4,75	-4,80	-5,14	-5,13	-3,87	-2,33	-5,10	-3,61	-4,41
CIQPlogS	-6,59	-6,42	-4,40	-5,61	-4,65	-4,80	-3,20	-1,91	-4,37	-4,23	-4,99
QPlogHERG	-6,70	-5,38	-7,33	-7,29	-6,63	-6,90	-8,57	-9,66	-9,09	-6,93	-4,78
QPlogCaco	1423,62	604,71	901,48	408,51	210,40	55,09	61,28	4,43	18,14	135,27	354,29
QPlogBB	0,23	-0,95	-0,08	-0,29	-0,63	-1,51	-0,04	-1,24	-1,37	-1,08	-1,47
QPlogMDCK	2125,88	1427,34	489,27	551,43	183,44	43,10	75,30	1,91	7,94	62,98	270,29
QPlogKp	-2,02	-1,48	-2,39	-3,14	-4,27	-5,21	-5,78	-6,43	-6,39	-4,19	-2,16
IP(eV)	8,33	8,44	8,31	8,35	8,72	8,71	8,40	8,14	8,21	8,20	8,14
EA(eV)	1,02	1,20	0,98	1,02	1,30	1,30	1,08	0,51	0,61	0,66	0,65
#metab	2,00	1,00	2,00	3,00	3,00	4,00	7,00	9,00	7,00	7,00	5,00
QPlogKhsa	0,87	0,33	0,63	0,51	0,61	0,55	0,11	-0,10	0,34	0,05	-0,18

HumanOralAbsorption	3,00	3,00	3,00	3,00	3,00	3,00	2,00	2,00	2,00	2,00	3,00
PercentHumanOralAbsorption	100,00	100,00	100,00	100,00	91,47	79,02	73,89	45,28	41,11	79,95	88,43
SAfluorine	0,00	0,00	0,00	0,00	46,91	46,91	0,00	0,00	0,00	0,00	0,00
SAamideO	0,00	32,82	0,00	0,00	0,00	0,00	0,00	0,00	0,00	0,00	26,10
PSA	41,55	82,18	47,96	65,76	89,50	112,42	89,23	126,09	141,07	104,42	117,04
#NandO	5	6	5	5	6	6	8	10	12	9	10
RuleOffFive	1	0	0	0	0	0	0	0	2	0	0
RuleOfThree	0	1	0	0	0	0	1	2	2	1	0
#ringatoms	16	16	16	16	14	14	24	24	24	18	18
#in34	0	0	0	0	0	0	0	0	0	0	0
#in56	16	16	16	16	14	14	24	24	24	18	18
#noncon	0	0	0	0	0	0	4	4	4	0	0
#nonHatm	30	29	27	26	29	29	31	34	41	29	32

Descriptors predicted:

mol_MW Molecular weight of the molecule. 130.0 – 725.0

dipole† Computed dipole moment of the molecule. 1.0 – 12.5

SASA Total solvent accessible surface area (SASA) in square angstroms using a probe with a 1.4 Å radius. 300.0 – 1000.0

FOSA Hydrophobic component of the SASA (saturated carbon and attached hydrogen). 0.0 – 750.0

FISA Hydrophilic component of the SASA (SASA on N, O, and H on heteroatoms). 7.0 – 330.0

PISA π (carbon and attached hydrogen) component of the SASA. 0.0 – 450.0

WPASA Weakly polar component of the SASA (halogens, P, and S). 0.0 – 175.0

volume Total solvent-accessible volume in cubic angstroms using a probe with a 1.4 Å radius. 500.0 – 2000.0

donorHB Estimated number of hydrogen bonds that would be donated by the solute to water molecules in an aqueous solution. Values are averages taken over a number of configurations, so they can be non-integer. 0.0 – 6.0

acceptHB Estimated number of hydrogen bonds that would be accepted by the solute from water molecules in an aqueous solution. Values are averages taken over a number of configurations, so they can be non-integer. 2.0 – 20.0

dip²/V† Square of the dipole moment divided by the molecular volume. This is the key term in the Kirkwood-Onsager equation for the free energy of solvation of a dipole with volume V. 0.0 – 0.13

ACxDN⁵/SA Index of cohesive interaction in solids. This term represents the relationship; see Ref. [2]. 0.0 – 0.05

glob Globularity descriptor, $\frac{V}{4\pi r^3}$, where r is the radius of a sphere with a volume equal to the molecular volume. Globularity is 1.0 for a spherical molecule. 0.75 – 0.95

QPpolarz Predicted polarizability in cubic angstroms. 13.0 – 70.0

QPlogPC16 Predicted hexadecane/gas partition coefficient. 4.0 – 18.0

QPlogPoct‡ Predicted octanol/gas partition coefficient. 8.0 – 35.0

QPlogPw Predicted water/gas partition coefficient. 4.0 – 45.0

QPlogPo/w Predicted octanol/water partition coefficient. –2.0 – 6.5; should be <5 according to Lipinski rules

QPlogS Predicted aqueous solubility, log S. S in mol dm⁻³ is the concentration of the solute in a saturated solution that is in equilibrium with the crystalline solid. –6.5 – 0.5;

CIQPlogS Conformation-independent predicted aqueous solubility, log S. S in mol dm⁻³ is the concentration of the solute in a saturated solution that is in equilibrium with the crystalline solid. –6.5 – 0.5

QPlogHERG Predicted IC₅₀ value for blockage of HERG K⁺ channels. concern below –5 (*acceptHB*(*donorHB*)) / (SA) $4\pi r^2$ / (SASA)

QPPCaco Predicted apparent Caco-2 cell permeability in nm/sec. Caco-2 cells are a model for the gut-blood barrier. QikProp predictions are for non-active transport.

<25 poor,

>500 great

QLogBB Predicted brain/blood partition coefficient. Note: QikProp predictions are for orally delivered drugs so, for example, dopamine and serotonin are CNS negative because they are too polar to cross the blood-brain barrier
-3.0 – 1.2

QPPMDCK Predicted apparent MDCK cell permeability in nm/sec. MDCK cells are considered to be a good mimic for the bloodbrain barrier. QikProp predictions are for non-active transport.

<25 poor,

>500 great

QLogKp Predicted skin permeability, log K_p . -8.0 – -1.0

IP(ev)† PM3 calculated ionization potential. 7.9 – 10.5

EA(eV)† PM3 calculated electron affinity. -0.9 – 1.7

#metab‡ Number of likely metabolic reactions

QLogKhsa Prediction of binding to human serum albumin. -1.5 – 1.5

HumanOralAbsorption

Predicted qualitative human oral absorption: 1, 2, or 3 for low, medium, or high. The text version is reported in the output. The assessment uses a knowledge-based set of rules, including checking for suitable values of PercentHumanOralAbsorption, number of metabolites, number of rotatable bonds, logP, solubility and cell permeability.

PercentHuman-OralAbsorption

Predicted human oral absorption on 0 to 100% scale. The prediction is based on a quantitative multiple linear regression model. This property usually correlates well with HumanOral-Absorption, as both measure the same property.

>80% is high

<25% is poor

SAFluorine Solvent-accessible surface area of fluorine atoms. 0.0 – 100.0

SAamideO Solvent-accessible surface area of amide oxygen atoms. 0.0 – 35.0

PSA Van der Waals surface area of polar nitrogen and oxygen atoms. 7.0 – 200.0

#NandO Number of nitrogen and oxygen atoms. 2 – 15

RuleOfFive: Number of violations of Lipinski's rule of five [3]. The rules are: mol_MW < 500, QLogPo/w < 5, donorHB ≤ 5, accptHB ≤ 10. Compounds that satisfy these rules are considered druglike (The "five" refers to the limits, which are multiples of 5.) maximum is 4

RuleOfThree: Number of violations of Jorgensen's rule of three. The three rules are: QLogS > -5.7, QP PCaco > 22 nm/s, # Primary Metabolites < 7. Compounds with fewer (and preferably no) violations of these rules are more likely to be orally available. maximum is 3

#ringatoms: Number of atoms in a ring

#in34: Number of atoms in 3- or 4-membered rings

#in56: Number of atoms in 5- or 6-membered rings

#noncon: number of ring atoms not able to form conjugated aromatic systems (e.g. sp³ C).

#nonHatm: Number of heavy atoms (nonhydrogen atoms)

Kinase affinity assay results

Binding affinities for kinases at 5 μ M in Ctrl%.

Kinase	VCC036051:03	VCC124075:02	VCC341830:01	VCC346349:01	VCC350485:02	VCC459492:04	VCC512891:01	VCC553231:16	VCC958400:03	VCC981125:01
AAK1	89	2,9	66	14	100	76	3,8	0,85	97	94
ABL1(E255K)-phosphorylated	70	0,85	100	39	84	11	10	1,3	98	70
ABL1(F317I)-nonphosphorylated	69	47	94	72	64	74	35	17	100	80
ABL1(F317I)-phosphorylated	82	28	80	78	67	51	46	12	92	85
ABL1(F317L)-nonphosphorylated	57	30	75	58	64	44	17	17	81	78
ABL1(F317L)-phosphorylated	48	7,3	88	48	76	21	23	3,1	70	47
ABL1(H396P)-nonphosphorylated	71	0,1	65	9,1	69	4	1,6	0,2	100	100
ABL1(H396P)-phosphorylated	67	0,25	80	39	81	13	7,6	1,8	100	84
ABL1(M351T)-phosphorylated	65	1,1	65	31	88	21	15	0,2	77	69
ABL1(Q252H)-nonphosphorylated	85	1,2	100	17	98	13	2,6	0,65	94	64
ABL1(Q252H)-phosphorylated	74	1,2	100	37	100	21	10	2,4	100	100
ABL1(T315I)-nonphosphorylated	56	1,7	87	35	85	69	3,6	0,05	91	69
ABL1(T315I)-phosphorylated	51	0,8	100	29	85	70	10	0	82	61
ABL1(Y253F)-phosphorylated	61	0,4	92	30	97	15	7,8	1,2	99	75
ABL1-nonphosphorylated	58	2,2	85	26	89	21	3,9	1,4	95	70
ABL1-phosphorylated	56	0,3	97	41	79	14	5,8	1,6	100	76
ABL2	92	30	100	84	95	60	47	67	100	82
ACVR1	100	40	100	14	100	7,8	6,2	71	87	100
ACVR1B	100	100	100	100	100	89	100	100	100	100
ACVR2A	100	55	100	46	100	16	58	98	71	84
ACVR2B	94	76	76	32	96	1,8	43	100	73	88
ACVRL1	97	100	100	100	100	12	91	100	93	92
ADCK3	100	49	71	9,8	85	62	75	87	86	88
ADCK4	98	57	96	3,4	100	24	96	95	100	88
AKT1	77	62	73	75	78	91	91	65	51	64
AKT2	87	100	100	100	100	98	71	38	91	100
AKT3	100	100	86	100	83	97	100	100	76	98
ALK	99	45	46	19	60	55	100	0,15	87	82
AMPK-alpha1	100	12	100	96	100	90	57	0,75	92	100
AMPK-alpha2	100	17	100	86	100	87	50	0,75	81	98
ANKK1	98	1,6	98	91	100	85	46	1,5	94	90
ARK5	74	1,4	98	53	100	98	59	0,95	87	80
ASK1	92	100	97	94	87	76	85	100	69	82
ASK2	77	50	100	100	100	96	100	51	95	81
AURKA	77	0,05	100	4	95	68	7,7	14	100	87
AURKB	68	1,4	100	18	100	55	18	1,9	77	69

AURKC	100	1,2	97	11	93	51	5,6	1,9	100	88
AXL	100	2,4	84	19	84	78	54	0	100	100
BIKE	100	0,05	83	41	65	67	0,15	0	100	80
BLK	93	3,6	78	54	65	41	69	0,45	76	73
BMPR1A	100	100	100	100	100	100	100	100	100	100
BMPR1B	31	1,4	36	11	41	8	0,25	24	37	38
BMPR2	100	16	100	91	100	100	13	2	100	100
BMX	100	72	77	81	72	75	64	74	77	92
BRAF	100	29	100	36	100	16	64	100	100	100
BRAF(V600E)	75	25	100	27	100	11	57	93	100	100
BRK	91	78	82	57	98	53	64	68	93	86
BRSK1	100	64	69	83	96	8,5	100	26	100	100
BRSK2	98	59	58	63	100	11	63	12	66	88
BTK	100	47	100	100	100	90	60	39	100	100
BUB1	100	0	100	41	100	19	39	12	100	100
CAMK1	100	15	100	18	100	89	41	11	91	100
CAMK1D	99	9,2	98	59	87	91	16	5,2	84	100
CAMK1G	100	47	100	42	100	92	59	7	100	100
CAMK2A	88	16	94	74	100	96	49	2,8	92	100
CAMK2B	100	40	97	75	100	98	66	16	100	100
CAMK2D	96	19	100	71	100	100	76	12	100	100
CAMK2G	93	57	100	91	100	83	71	11	100	100
CAMK4	100	100	100	100	100	100	100	2	99	89
CAMKK1	95	81	100	60	100	100	38	11	100	100
CAMKK2	96	76	100	47	100	98	13	22	100	100
CASK	83	95	100	100	100	100	100	100	100	93
CDC2L1	98	99	100	100	100	84	74	91	100	87
CDC2L2	89	81	96	100	85	77	77	79	100	89
CDC2L5	88	99	93	61	99	99	65	90	94	99
CDK11	68	100	98	100	100	64	100	100	100	100
CDK2	100	100	98	58	100	100	100	100	95	100
CDK3	72	100	100	84	98	93	96	82	87	73
CDK4-cyclinD1	92	97	100	43	99	85	63	48	97	98
CDK4-cyclinD3	43	76	84	36	94	95	33	46	85	70
CDK5	98	100	100	88	100	95	100	86	100	94
CDK7	86	13	100	71	100	88	26	0,2	100	86
CDK8	70	100	85	68	100	80	99	66	98	97
CDK9	100	99	100	83	100	84	83	100	100	86
CDKL1	94	18	100	83	100	100	28	75	100	82
CDKL2	83	62	97	9,5	100	87	2,6	20	95	100
CDKL3	97	100	91	100	100	82	6,2	83	100	84
CDKL5	69	100	100	27	98	100	5,8	97	80	82
CHEK1	100	23	100	100	100	100	100	2,7	100	100
CHEK2	75	1,4	73	59	91	79	46	0,05	76	82
CIT	100	0,1	64	70	100	34	20	22	94	92

CLK1	96	2,6	86	5,4	100	93	0,75	0,65	67	100
CLK2	90	1,4	85	9,2	100	93	1	0,2	98	100
CLK3	100	18	100	14	100	88	30	82	76	100
CLK4	100	2	51	3,6	94	81	0,75	0,6	74	91
CSF1R	100	2,1	100	63	100	100	24	0	100	77
CSF1R-autoinhibited	69	55	93	79	85	94	20	0,35	83	77
CSK	93	61	100	75	100	79	85	69	89	86
CSNK1A1	79	1,8	100	5	23	52	58	0,35	91	89
CSNK1A1L	97	17	100	3,8	55	69	100	5,7	100	100
CSNK1D	100	10	76	0,55	51	30	100	0,05	84	90
CSNK1E	98	19	90	0	48	5,9	100	0,1	74	97
CSNK1G1	80	46	74	5,4	81	60	73	7,1	70	78
CSNK1G2	100	96	100	0,6	100	92	100	1,6	100	100
CSNK1G3	100	89	100	1,4	86	74	85	2,2	64	94
CSNK2A1	100	0,9	100	62	100	100	34	16	100	100
CSNK2A2	71	0,05	64	7,4	51	81	2,9	2,8	77	69
CTK	89	24	89	74	78	69	92	6,1	100	82
DAPK1	100	6,1	68	73	91	93	13	1,2	100	100
DAPK2	100	8,8	75	76	100	84	19	0,95	84	100
DAPK3	85	1,4	67	55	89	85	4,4	0,7	87	82
DCAMKL1	62	20	74	72	61	71	40	3,9	76	64
DCAMKL2	100	98	100	100	100	95	86	40	100	98
DCAMKL3	92	19	68	100	100	84	100	0,25	95	83
DDR1	99	100	100	54	100	24	42	43	100	73
DDR2	90	24	100	69	92	54	44	15	100	87
DLK	95	68	100	94	100	100	77	4,2	97	96
DMPK	100	34	90	88	90	83	74	100	80	100
DMPK2	91	73	76	14	96	36	85	73	95	98
DRAK1	99	0	40	44	94	74	0,1	0	99	93
DRAK2	92	0,15	81	80	100	80	2	1	91	83
DYRK1A	64	5,7	48	8,2	91	90	3,2	3,4	81	79
DYRK1B	100	49	64	12	100	82	25	24	100	96
DYRK2	100	3	100	12	100	100	37	17	100	100
EGFR	91	79	7,1	96	100	33	98	75	89	85
EGFR(E746-A750del)	93	38	4	78	100	13	83	74	74	100
EGFR(G719C)	93	15	1,8	84	77	33	56	46	96	91
EGFR(G719S)	100	57	1,4	95	100	24	86	62	97	100
EGFR(L747-E749del, A750P)	100	30	0,9	75	96	12	84	79	88	83
EGFR(L747-S752del, P753S)	100	43	3,7	92	84	12	80	94	82	100
EGFR(L747-T751del,Sins)	100	52	2,2	81	100	12	72	67	89	100
EGFR(L858R)	100	68	5,6	100	100	34	100	73	89	87
EGFR(L858R,T790M)	83	23	71	84	66	79	71	48	90	83
EGFR(L861Q)	100	63	4,7	89	100	32	78	68	99	100
EGFR(S752-I759del)	100	27	4,4	92	82	16	78	75	100	100
EGFR(T790M)	62	5,1	18	45	44	29	37	17	61	62

EIF2AK1	100	63	100	79	100	77	100	91	100	100
EPHA1	95	19	83	7,3	100	19	25	62	78	68
EPHA2	100	70	87	36	91	53	61	62	78	71
EPHA3	55	15	59	40	69	7,2	45	22	58	60
EPHA4	100	73	89	64	100	49	90	69	98	79
EPHA5	89	93	100	81	100	55	92	81	90	87
EPHA6	100	50	87	51	100	22	100	47	100	100
EPHA7	100	70	100	89	100	95	92	77	100	98
EPHA8	92	98	100	100	100	60	88	96	100	91
EPHB1	96	54	100	25	100	66	67	52	100	93
EPHB2	100	93	100	42	100	68	81	62	100	91
EPHB3	95	100	100	53	100	72	100	91	99	99
EPHB4	83	72	100	32	100	25	85	56	100	92
EPHB6	80	1,8	84	0,8	100	37	2,7	16	100	70
ERBB2	83	75	8,4	88	100	60	86	85	100	98
ERBB3	93	78	87	79	100	15	92	80	100	80
ERBB4	100	100	100	100	100	84	100	100	100	100
ERK1	100	100	100	100	100	93	89	100	100	100
ERK2	84	100	100	100	100	89	86	91	87	85
ERK3	88	16	73	11	100	95	3,6	75	98	100
ERK4	100	95	100	100	100	83	28	100	100	87
ERK5	89	89	100	100	98	96	97	81	100	83
ERK8	90	34	100	0,95	91	92	3,7	80	70	98
ERN1	74	61	100	66	100	77	71	6,6	80	76
FAK	99	44	100	59	98	100	76	11	86	92
FER	100	100	100	99	100	100	95	38	98	100
FES	70	63	99	44	100	79	39	53	84	95
FGFR1	100	35	94	7,4	100	69	61	8,2	87	100
FGFR2	80	31	85	2,4	72	74	54	14	85	80
FGFR3	89	44	70	1,4	88	76	69	7,3	84	84
FGFR3(G697C)	90	72	79	1,6	100	87	71	8,8	78	73
FGFR4	96	88	84	9,1	100	76	82	60	95	91
FGR	86	19	92	51	87	49	86	8,8	100	93
FLT1	92	17	100	22	89	77	32	0	88	80
FLT3	78	0,1	64	4	19	90	14	0	98	99
FLT3(D835H)	79	0,05	45	5,4	2,9	72	2,7	0	91	71
FLT3(D835Y)	84	0,1	52	8,6	5,4	68	4,8	0	100	93
FLT3(ITD)	98	0	72	10	4,2	85	14	0	96	96
FLT3(K663Q)	100	0,35	64	8,4	20	82	13	0,05	82	90
FLT3(N841I)	98	0	75	16	5	92	2,2	0	100	95
FLT3(R834Q)	80	2,5	100	90	48	86	26	1,5	88	87
FLT3-autoinhibited	54	1,4	94	100	66	83	32	0	70	59
FLT4	88	0,45	100	16	94	96	26	0,1	100	83
FRK	99	78	95	47	93	34	58	20	86	83
FYN	100	8,5	95	52	71	43	53	24	100	88

GAK	97	0,7	34	2,8	35	1,5	10	0,45	88	100
GCN2(Kin.Dom.2,S808G)	85	0,2	100	77	100	82	31	0,55	82	100
GRK1	59	46	81	70	68	71	72	7,3	75	63
GRK4	100	0,6	100	77	100	100	2,2	0,95	100	100
GRK7	76	39	100	100	85	94	42	2,5	100	99
GSK3A	91	100	100	2	100	100	29	95	100	100
GSK3B	52	54	100	9,6	100	65	23	56	67	61
HASPIN	88	15	38	41	81	84	34	1,8	100	100
HCK	100	27	100	85	96	43	100	2,9	100	100
HIPK1	68	1	62	28	100	94	3,4	0,45	98	73
HIPK2	100	1,5	86	40	100	88	5,4	0,25	100	100
HIPK3	66	0,5	100	37	100	65	8,8	0,2	100	100
HIPK4	98	6,6	61	4,6	100	85	3,2	2,5	98	100
HPK1	96	9	96	28	96	90	51	2,3	100	88
HUNK	90	100	100	84	83	55	99	1,6	71	72
ICK	100	100	100	61	100	100	35	44	100	100
IGF1R	100	100	100	100	100	93	100	64	100	100
IKK-alpha	57	0,3	88	67	100	73	6,2	46	92	72
IKK-beta	92	0	100	83	100	100	7,4	91	100	79
IKK-epsilon	54	4	89	61	57	80	29	0	93	75
INSR	58	35	62	40	62	64	54	1,8	78	66
INSRR	79	100	100	100	100	97	100	4,8	84	72
IRAK1	100	0,3	100	1,2	100	100	3,4	0,05	100	100
IRAK3	97	4,2	28	14	100	47	17	18	100	100
IRAK4	100	3,6	100	100	100	100	100	2,4	100	100
ITK	87	100	100	100	92	94	87	3,8	100	82
JAK1(JH1domain-catalytic)	85	22	100	72	100	95	100	63	90	100
JAK1(JH2domain-pseudokinase)	69	0,25	100	99	100	100	0,3	0	98	84
JAK2(JH1domain-catalytic)	69	0,1	69	21	82	61	0,7	0,05	75	72
JAK3(JH1domain-catalytic)	96	0	83	30	100	76	0,1	0	100	85
JNK1	76	0,35	69	3,4	81	7,1	0,85	68	96	93
JNK2	65	23	100	11	100	1,2	7,4	39	97	86
JNK3	58	1,1	91	3,4	91	0,9	0,7	47	78	69
KIT	100	0,7	16	0,15	72	79	1,2	0	91	89
KIT(A829P)	75	0	55	57	40	63	11	0,35	88	84
KIT(D816H)	77	2,2	100	78	85	74	15	7	87	75
KIT(D816V)	86	0,15	62	12	57	64	3,4	2,4	70	75
KIT(L576P)	100	0	20	0,9	69	69	1,6	0	100	100
KIT(V559D)	90	0,05	9,7	0,1	54	70	0,35	0	88	86
KIT(V559D,T670I)	100	3,1	80	4,1	100	100	19	0	100	89
KIT(V559D,V654A)	100	23	17	22	100	82	24	1	92	98
KIT-autoinhibited	85	71	100	80	100	100	15	0	100	77
LATS1	100	10	96	100	100	97	100	4	100	100
LATS2	63	4,2	75	77	92	68	61	0,35	73	66
LCK	100	23	100	85	100	21	33	2,4	89	100

LIMK1	100	71	97	20	100	95	55	100	86	100
LIMK2	91	62	73	5,7	87	100	39	76	100	80
LKB1	70	1,5	73	78	85	63	12	0,9	66	86
LOK	100	8,3	85	87	100	23	74	3,8	96	79
LRRK2	95	2,6	98	74	100	100	65	2,4	100	100
LRRK2(G2019S)	64	0,75	80	85	100	92	75	1,1	82	83
LTK	100	32	35	67	100	83	100	16	99	100
LYN	100	36	92	38	100	29	86	13	100	95
LZK	100	52	100	100	100	100	83	11	100	97
MAK	100	100	100	100	100	100	100	100	100	95
MAP3K1	37	26	100	43	93	42	42	35	48	56
MAP3K15	100	21	100	78	100	100	79	9,8	100	100
MAP3K2	59	0,9	58	60	71	63	16	0,1	64	63
MAP3K3	75	2,5	83	83	100	61	52	0,1	100	78
MAP3K4	97	36	92	54	100	87	46	59	84	84
MAP4K2	61	0,05	38	23	74	32	1,1	0,3	61	64
MAP4K3	95	20	100	36	100	61	34	0,4	100	100
MAP4K4	87	6,2	93	30	100	38	4,2	0,85	94	87
MAP4K5	95	89	99	52	100	54	54	0,6	91	94
MAPKAPK2	100	100	100	100	100	100	100	100	94	100
MAPKAPK5	81	48	82	93	88	96	80	59	96	94
MARK1	100	37	69	69	100	65	46	11	73	100
MARK2	55	5,6	65	37	69	56	24	5,1	62	45
MARK3	100	14	100	100	100	100	69	5,8	100	100
MARK4	100	15	82	71	100	76	47	7,8	76	96
MAST1	100	19	96	80	100	79	17	3,2	100	100
MEK1	92	4,8	70	98	89	68	64	0,25	98	100
MEK2	94	4	84	94	100	70	56	0,1	100	100
MEK3	81	1	67	31	100	41	12	38	89	99
MEK4	50	1,9	67	29	56	19	3,6	11	66	64
MEK5	100	0,1	36	11	36	3,8	4,6	0,15	100	100
MEK6	76	28	77	41	80	55	51	42	73	94
MELK	100	16	86	56	79	52	20	1,2	76	63
MERTK	100	1,6	91	2,2	78	76	46	0	89	84
MET	100	68	97	100	100	77	73	58	86	92
MET(M1250T)	100	27	100	100	100	100	100	24	100	100
MET(Y1235D)	100	65	100	100	100	75	47	49	74	100
MINK	100	1,8	100	54	100	27	17	0,65	93	91
MKK7	85	71	83	73	72	82	50	78	87	79
MKNK1	99	0,55	42	100	100	99	82	44	100	87
MKNK2	100	0	10	51	60	55	5,8	56	100	100
MLCK	100	0	86	75	100	80	7,5	0,15	100	90
MLK1	100	0,3	100	100	100	92	73	56	97	100
MLK2	100	1,6	100	69	100	91	48	57	86	87
MLK3	100	3,1	100	62	100	99	50	15	94	100

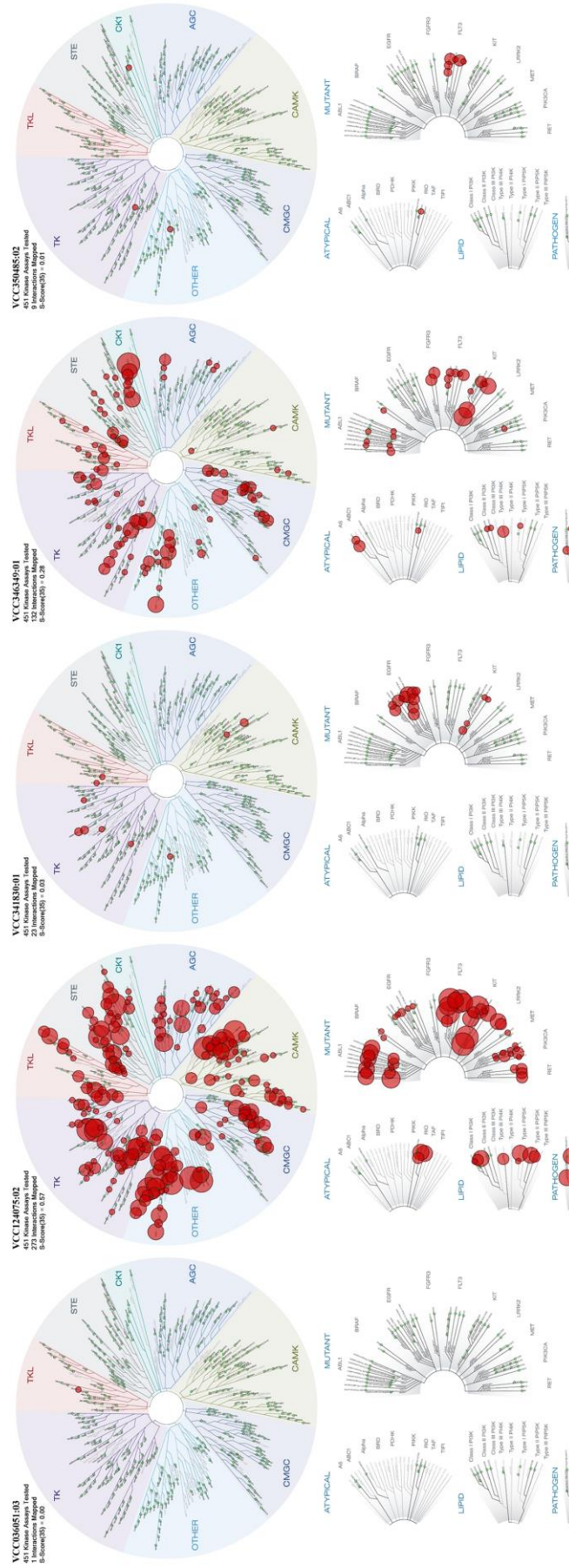
MRCKA	100	97	78	4,4	100	83	100	100	100	90
MRCKB	89	78	99	22	100	71	98	87	85	87
MST1	100	100	100	100	100	91	100	2,2	100	100
MST1R	97	15	100	100	100	91	100	100	90	95
MST2	78	3,2	100	100	100	69	100	0	82	73
MST3	95	57	99	88	89	88	80	0,8	90	98
MST4	67	17	100	89	100	91	82	2,4	100	76
MTOR	100	65	100	71	100	100	98	91	100	100
MUSK	81	99	100	100	100	98	33	4,4	89	78
MYLK	85	6,8	78	75	74	87	21	0	100	74
MYLK2	100	0,75	100	100	100	100	20	5,6	100	100
MYLK4	100	0	100	56	100	100	17	0	100	90
MYO3A	100	70	96	100	100	52	93	50	100	100
MYO3B	84	100	96	100	100	87	100	56	100	100
NDR1	100	4,8	100	83	100	100	100	12	100	100
NDR2	100	15	100	61	86	78	96	36	100	100
NEK1	100	9,2	70	46	90	56	30	74	100	100
NEK11	100	49	100	95	100	95	39	100	98	100
NEK2	86	14	96	55	92	60	50	24	87	97
NEK3	100	0,15	100	31	100	94	0,6	87	100	100
NEK4	100	15	100	46	95	91	73	82	100	91
NEK5	100	0,2	61	0,45	89	83	0,5	87	100	92
NEK6	88	1,4	100	0,25	97	100	0,2	91	93	94
NEK7	88	43	100	55	100	85	52	83	100	100
NEK9	97	15	100	1,6	100	100	1	100	100	100
NIM1	100	3,6	100	100	100	100	100	45	100	100
NLK	93	86	100	31	100	30	53	87	99	96
OSR1	81	28	84	61	82	89	98	10	96	100
p38-alpha	100	100	99	90	100	66	100	86	96	88
p38-beta	100	100	100	83	100	90	100	100	100	100
p38-delta	81	100	100	100	90	98	100	100	85	83
p38-gamma	73	42	68	56	60	86	62	38	67	61
PAK1	84	5,8	100	86	100	100	81	96	100	85
PAK2	95	34	97	76	99	100	79	71	100	96
PAK3	90	2,7	89	65	83	76	29	0,45	67	100
PAK4	82	3,6	100	34	100	90	67	32	89	73
PAK6	100	15	89	8,4	100	77	77	65	100	100
PAK7	68	0,35	78	24	89	69	53	18	78	75
PCK1	65	95	100	33	100	100	82	14	78	82
PCK2	100	82	100	73	99	100	100	69	100	93
PCK3	100	100	100	94	100	84	91	36	100	90
PDGFRA	100	1,2	68	51	88	100	10	0	100	100
PDGFRB	100	0	37	0,2	55	75	2,8	0	89	89
PDPK1	97	28	68	76	62	76	60	23	58	68
PFCDPK1(P.falciparum)	80	0,35	43	8,8	50	40	34	24	83	79

PFPK5(P.falciparum)	100	100	100	100	100	100	100	100	100	100
PFTAIRE2	97	97	100	100	100	90	100	79	100	100
PFTK1	95	98	100	86	93	97	89	38	100	87
PHKG1	100	17	100	73	100	100	67	1	100	100
PHKG2	99	22	90	55	100	100	13	0,6	100	100
PIK3C2B	100	40	100	35	64	49	100	100	100	100
PIK3C2G	78	94	95	21	80	44	84	100	97	97
PIK3CA	100	30	100	91	89	100	88	100	100	89
PIK3CA(C420R)	93	30	74	70	69	96	76	100	99	96
PIK3CA(E542K)	100	32	95	100	100	100	100	100	100	100
PIK3CA(E545A)	100	30	74	90	61	100	98	100	100	100
PIK3CA(E545K)	100	21	100	81	100	100	69	100	100	99
PIK3CA(H1047L)	96	4,3	100	64	100	100	16	92	100	100
PIK3CA(H1047Y)	71	30	69	89	59	87	52	54	73	60
PIK3CA(I800L)	85	3,2	62	14	91	72	22	42	88	98
PIK3CA(M1043I)	75	15	62	62	58	88	56	95	98	100
PIK3CA(Q546K)	67	21	92	71	74	93	64	87	76	81
PIK3CB	100	100	100	100	100	100	100	100	100	100
PIK3CD	95	1,4	100	43	65	87	21	90	100	100
PIK3CG	91	0,6	100	40	92	75	0,6	86	100	95
PIK4CB	100	2,2	36	3,2	100	92	52	100	100	100
PIM1	99	100	67	100	95	100	100	71	100	96
PIM2	61	100	37	69	54	53	56	61	37	37
PIM3	85	85	60	91	100	100	65	27	94	82
PIP5K1A	95	0,75	100	31	71	73	6,2	0,15	78	67
PIP5K1C	86	13	100	65	100	90	100	2,1	95	100
PIP5K2B	100	0,45	97	74	100	100	2,6	0,15	100	100
PIP5K2C	78	4,7	93	48	98	55	50	50	83	85
PKAC-alpha	78	24	75	83	69	80	76	66	58	71
PKAC-beta	91	25	100	100	91	80	100	84	71	99
PKMYT1	88	62	90	52	100	58	100	93	79	76
PKN1	97	1,2	100	100	92	90	61	15	100	100
PKN2	100	4,7	100	58	100	87	36	14	85	100
PKNB(M.tuberculosis)	79	0,8	100	29	80	100	4,8	0,2	100	100
PLK1	90	100	100	100	100	100	96	100	96	98
PLK2	69	1,6	77	74	80	92	29	46	74	67
PLK3	68	0,75	81	74	78	90	16	87	77	79
PLK4	69	0,35	99	13	87	96	40	3,2	80	81
PRKCD	100	12	74	68	100	82	77	58	79	100
PRKCE	100	3,2	70	92	100	98	66	56	100	100
PRKCH	100	37	73	59	100	91	100	97	78	96
PRKCI	100	42	100	87	100	88	100	66	100	90
PRKCQ	100	9,6	100	100	94	98	100	52	100	100
PRKD1	100	40	100	100	100	100	30	3,6	100	100
PRKD2	76	26	100	100	91	87	60	2,6	82	100

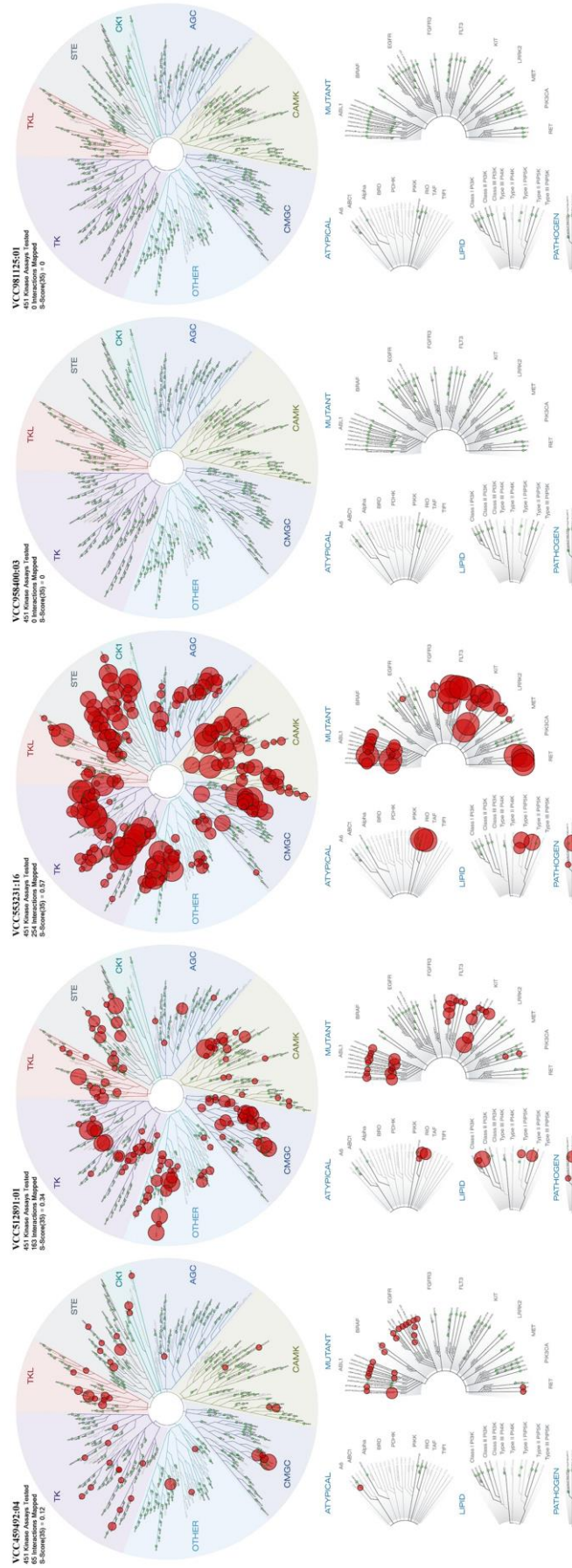
PRKD3	100	33	100	100	100	91	20	3,8	100	100
PRKG1	98	53	100	77	84	87	92	42	90	97
PRKG2	84	0,95	100	69	100	89	97	57	94	79
PRKR	80	7,7	78	27	93	71	22	4,6	66	73
PRKX	90	36	100	92	100	100	100	74	100	100
PRP4	100	1,2	100	100	100	100	6,4	0,3	100	95
PYK2	92	37	100	60	100	93	69	4,4	100	100
QSK	67	8,2	100	100	100	93	77	56	79	66
RAF1	100	76	99	38	100	38	69	96	100	92
RET	90	4,6	68	98	96	33	89	0	94	100
RET(M918T)	75	1,4	51	80	85	21	67	0	92	80
RET(V804L)	77	4,8	95	85	88	90	82	0	91	84
RET(V804M)	95	6,3	100	98	99	87	77	0	77	84
RIOK1	80	0,65	89	75	37	91	1,8	0	83	88
RIOK2	81	2,5	92	12	78	79	15	47	97	83
RIOK3	100	0,2	54	66	26	81	1,3	0,05	93	78
RIPK1	81	73	82	11	91	90	8	5,6	100	85
RIPK2	87	5,3	32	40	93	7,6	31	54	100	75
RIPK4	69	0,3	80	73	80	85	4,8	52	84	83
RIPK5	80	20	73	77	84	82	63	14	91	99
ROCK1	100	7,4	100	100	94	100	52	13	100	100
ROCK2	100	1,4	90	100	80	100	40	5	100	100
ROS1	100	33	100	4,6	100	88	47	100	92	100
RPS6KA4(Kin.Dom.1-N-terminal)	84	71	99	77	100	89	100	0,65	69	91
RPS6KA4(Kin.Dom.2-C-terminal)	56	1,4	8,7	57	58	63	1,8	5,1	67	64
RPS6KA5(Kin.Dom.1-N-terminal)	98	100	82	93	100	94	100	12	73	88
RPS6KA5(Kin.Dom.2-C-terminal)	100	7,6	100	99	98	90	39	22	100	99
RSK1(Kin.Dom.1-N-terminal)	93	88	100	84	100	100	100	0,2	100	90
RSK1(Kin.Dom.2-C-terminal)	93	59	48	36	79	18	60	38	90	94
RSK2(Kin.Dom.1-N-terminal)	64	8,8	72	28	63	58	68	0,1	69	65
RSK2(Kin.Dom.2-C-terminal)	100	79	100	100	100	95	100	100	100	100
RSK3(Kin.Dom.1-N-terminal)	78	65	100	74	81	74	100	0,5	100	96
RSK3(Kin.Dom.2-C-terminal)	100	92	100	99	100	85	90	28	78	92
RSK4(Kin.Dom.1-N-terminal)	55	1,5	60	46	88	65	70	1	72	61
RSK4(Kin.Dom.2-C-terminal)	98	74	83	75	86	17	64	58	87	93
S6K1	100	19	100	71	100	97	100	1	100	100
SBK1	93	7,2	100	95	100	94	69	8,2	100	100
SGK	76	9,6	72	11	56	58	30	0,2	92	88
SgK110	100	1,7	98	100	100	92	26	18	98	100
SGK3	72	24	100	21	100	78	69	2,8	81	86
SIK	88	44	100	92	92	85	48	58	100	91
SIK2	86	9	78	33	100	53	32	14	92	88
SLK	97	0,9	77	55	100	7,2	14	0,95	91	98
SNARK	87	0,95	100	28	100	83	13	1,1	86	95
SNRK	78	55	100	84	100	77	76	22	93	76

SRC	80	1,4	80	58	68	49	38	10	56	69
SRMS	59	34	42	34	38	52	46	33	54	51
SRPK1	100	0,45	94	100	100	84	11	0	92	75
SRPK2	100	2	100	89	100	84	9	0,8	100	88
SRPK3	100	0,35	100	67	100	84	1,8	0	100	98
STK16	98	0,75	100	1,2	100	79	5,4	5,8	97	95
STK33	82	1,4	97	29	76	71	40	0,4	50	81
STK35	100	3,6	100	31	89	15	68	20	100	100
STK36	92	80	100	20	100	92	37	76	100	88
STK39	100	16	99	51	100	79	50	8,2	97	87
SYK	100	2,4	100	100	98	91	16	49	89	100
TAK1	78	1,2	100	25	97	66	14	0	100	85
TAOK1	48	7,4	51	1,7	59	36	1,6	9,4	45	48
TAOK2	100	69	100	37	96	100	44	94	100	100
TAOK3	64	20	54	2	57	71	5,7	8,2	64	64
TBK1	77	3	100	53	88	100	19	4,6	90	70
TEC	88	100	94	100	100	100	100	100	100	91
TESK1	95	42	92	63	100	91	88	86	85	84
TGFBR1	84	94	100	47	100	43	55	68	94	78
TGFBR2	100	100	100	3	100	17	37	100	100	84
TIE1	89	4,4	100	18	100	81	20	51	84	85
TIE2	100	84	100	57	100	100	100	100	100	100
TLK1	85	51	97	90	82	95	87	3,9	90	96
TLK2	90	59	97	72	100	85	85	1,4	94	96
TNIK	61	0,3	51	34	69	15	7,6	0,9	61	57
TNK1	100	10	94	13	100	90	43	37	83	100
TNK2	100	54	100	53	100	80	62	57	81	100
TNNI3K	100	19	82	57	97	59	31	90	98	95
TRKA	79	25	93	91	74	100	57	0,25	100	97
TRKB	100	8	100	75	100	96	28	0,6	84	50
TRKC	61	28	93	65	64	83	43	2,2	72	63
TRPM6	100	94	100	100	100	100	100	80	100	90
TSSK1B	100	33	100	92	100	100	45	9,3	100	100
TTK	91	11	90	28	96	62	41	2,6	94	99
TXK	91	42	81	40	100	37	90	75	90	75
TYK2(JH1domain-catalytic)	57	0	63	21	40	36	3,6	0	70	60
TYK2(JH2domain-pseudokinase)	100	91	34	100	100	100	0,6	6,6	100	100
TYRO3	89	84	100	32	100	79	81	17	79	100
ULK1	46	0,1	62	69	44	66	42	0	70	66
ULK2	100	1,9	100	100	100	100	87	0,1	100	100
ULK3	48	0	65	33	61	49	2,8	0,05	62	58
VEGFR2	73	10	100	35	100	85	34	0	100	80
VRK2	89	45	83	51	53	19	52	51	89	87
WEE1	99	98	100	53	100	100	64	29	82	87
WEE2	95	76	100	100	100	94	81	14	100	100

WNK1	100	100	100	94	100	84	92	100	100	100
WNK3	100	100	100	100	100	100	9,2	100	100	100
YANK1	94	19	100	59	100	68	65	77	95	92
YANK2	99	100	95	37	100	76	100	100	70	90
YANK3	74	100	90	60	100	84	64	100	85	100
YES	100	36	100	70	100	83	72	2,7	88	98
YSK1	100	25	88	63	100	91	100	2,4	93	98
YSK4	100	0,05	100	12	100	46	0,2	0,25	100	100
ZAK	100	61	85	12	100	35	24	100	98	98
ZAP70	100	3,1	92	96	97	89	45	59	94	100



Kinome-trees depicting compound selectivities in kinase affinity assay. (Threshold set to 35)



Kinome-trees depicting compound selectivities in kinase affinity assay. (Threshold set to 35)

Cellular Target Profiling results (MS-affinity chromatography)

Binding/competition Affinity matrix:	Binders		Competed off, direct from SUTENT matrix		Competed off, indirect from VCC512891 matrix		Competed off, direct from VCC512891 matrix		Competed off, indirect from SUTENT matrix		Competed off, from direct from VCC124075 matrix	
	VCC350485 linker	SUTENT	K _d free [μM]	SUTENT	K _d free [μM]	VCC512891	K _d free [μM]	VCC512891	K _d free [μM]	VCC124075:02	K _d free [μM]	
A7VJC2	Q66HA4	0,0001	Q924I2	0,1376	P0C0R5	0,0881	F1LR17	0,0314	P63170	0,0053		
B0BN93	Q91Z96	0,0048	P54645	0,3735	O88763	0,0891	F1LZD9	0,0461	P97874	0,0179		
B0K020	P05532	0,0101	O35346	0,4073	Q91XJ1	0,0939	D4A4B2	0,0577	Q9R1U5	0,0674		
B2RYG6	Q3UEI1	0,0212	P80386	0,4286	Q6P6T4	0,1000	P18266	0,1272	P57760	0,0687		
O35303	P52332	0,0318	P80385	0,4451	Q78P75	0,2075	G3V9W2	0,2117	O08678	0,0755		
O35509	Q8BWJ3	0,0335	P14644	0,5575	P63170	0,2241	P57760	0,2687	P80386	0,1367		
O35567	Q7TSH2	0,0367	P57760	0,5921	Q6AY80	0,2813	F1LN52	0,4331	P54645	0,1375		
O35763	Q8BGM7	0,0556	P97874	0,6258	P18266	0,3451	F1M7R9	0,6638	P0C1X8	0,1378		
O35814	O08576	0,0570	F1LP90	0,6672	Q6AYG3	0,4027	D3ZFU9	0,6738	Q9QY78	0,1493		
O55096	P14644	0,0595	Q8VHF0	0,8515	P57760	0,7977	D4A355	0,6849	P80385	0,1580		
O88767	P0C1X8	0,0652	Q9ESV1	0,9665	O88370	0,8815	P49186	0,7066	Q8VHF0	0,1959		
O88989	Q9QX05	0,0665	P11275	0,9754	P53670	1,0588	O55099	0,7152	O88850	0,2448		
P00406	Q1HKZ5	0,0771	O08815	1,0057	Q8VHF0	1,1111	F1LMD9	0,7256	O08679	0,2477		
P00507	F1LM93	0,0786	Q810W7	1,0552	Q9ESV1	1,2006	F1LUY7	0,7287	P59241	0,3164		
P00787	Q09137	0,0793	O08679	1,3563	Q99N14	1,3199	F1M7M4	0,7314	Q4KMA0	0,3275		
P02793	Q8R4Y4	0,0798	O88764	1,3989	P49185	1,4261	D4A7D3	0,7835	Q62925	0,3959		
P04256	Q4QR82	0,0808	Q62844	1,4675	O08679	1,4594	F1LQ89	0,8036	Q6DG50	0,4620		
P04642	Q9WUN2	0,0833	Q5XIS9	1,6063	O88377	1,5395	D3ZG78	0,8076	P49185	0,6345		
P04764	P54645	0,0846	P11730	1,6923	Q9R0I8	1,5802	P16446	0,9454	Q6AY80	1,6180		
P04785	Q80UK8	0,0864	P08413	1,7298	P59241	1,7910	D3ZHP7	0,9475	P18266	2,2193		
P04961	O88370	0,0866	Q4KMA0	1,8581	P97874	1,8449	G3V8Y3	0,9503	P49186	2,4916		
P05065	P80386	0,0869	P15791	1,9910	P0C1X8	1,8557	Q6DG50	0,9887	Q78P75	3,1978		
P05197	Q9QZH4	0,0873	Q9WUD9	2,3062	O88764	1,8712	F1M836	1,0267	P18265	5,0766		
P05369	P52633	0,0876	O55099	2,3513	Q5XIS9	1,9167	D3ZW27	1,0457	Q02974	6,7750		
P05765	P80385	0,0896	Q91ZN7	2,3867	O35346	3,0296	D3Z8I4	1,0987	P53670	7,9065		
P06302	Q91WG5	0,0914	P0C1X8	2,5041	P49186	3,0321	D3ZSB7	1,1126	Q01062	8,1267		
P06761	Q9QUL0	0,0976	P59241	4,1354	Q5CZZ9	3,2337	F1M101	1,1175	Q6MGA9	12,2176		
P07171	Q924I2	0,1008	P09759	5,1688	Q924I2	3,3254	F1LQJ7	1,1576	Q01066	12,3303		
P07335	P17426	0,1078	Q63802	5,6399	P86172	3,3796	G3V715	1,1808				
P07632	O35643	0,1093	Q63450	5,8399	Q53UA7	3,9528	G3V8J8	1,2588				
P07943	Q6DG50	0,1095	P54759	6,1219	F1LP90	4,6596	Q66HA1	1,2795				
P09527	Q07014	0,1256	Q03114	10,7503	Q4KMA0	5,6177	P09760	1,2934				
P10111	Q8BMK0	0,1282	Q62868	11,6294	P39951	5,8611	F1LNP9	1,2991				
P10719	Q4KMA0	0,1307	Q06486	12,3763	A0JPM9	7,1118	F1LQL4	1,3679				
P10760	P84091	0,1312	P18266	13,3582	Q3ZAV8	7,7006	F1LR34	1,4002				
P10860	P70347	0,1344	O35331	15,9230	P11275	7,9634	D3ZUD6	1,5032				
P11348	Q9QYP6	0,1420	Q63644	15,9963	P68255	8,0107	Q66H82	1,7156				
P11598	Q04736	0,1434	Q78P75	16,0720	P63102	8,0359	F1LUM8	1,7317				
P11980	Q8BPB0	0,1546	A0JPM9	16,5459	Q810W7	8,1427	D3ZJ71	1,7376				

P13084	P57760	0,1677	P35213	16,6105	P67874	8,2006	F8WFI7	1,9256
P13383	Q3T1J9	0,1683	P67874	18,3442	P62260	8,9855	D3ZPU9	2,1184
P13596	P31325	0,1704	P61983	18,4355	Q6MGB6	9,3643	B5DF62	2,2389
P13668	Q61846	0,1714	P84092	19,6090	P35213	9,5302	D3ZIC0	2,2567
P13803	O35346	0,1720	Q6MGB6	21,9513	P68511	9,5861	E9PT20	2,4885
P14668	P62743	0,1850	P49186	25,7620	P19139	9,7418	Q6AY80	2,5509
P15865	P97874	0,1865	Q9ESW0	26,0064	Q516B8	10,1568	Q61FZ5	2,5763
P16617	Q3B7D5	0,1899	O54874	26,2248	Q510H5	10,9356	F1LR45	2,6442
P16638	Q8BYR2	0,1961	Q7TT49	29,4974	P11730	10,9876	D3ZID5	2,6640
P17074	Q9J111	0,2101	P97633	30,0000	P70486	11,1378	D4A1V7	2,7056
P17220	P17427	0,2141			P21708	11,2426	D3ZYV4	2,8988
P18297	A2A9T0	0,2239			P08413	11,3812	D4A280	3,2272
P18298	O08815	0,2333			P09759	11,8640	F1MAJ0	3,4006
P18418	P36506	0,2519			P15791	12,5323	O08678	3,4166
P18421	P83510	0,2522			P54645	12,6111	Q3T1J9	3,9441
P19804	Q8C0P0	0,2574			P63086	12,6992	F1M2K4	4,2434
P21670	O35832	0,2685			Q63802	12,8654	G3V9X3	4,4079
P22734	Q06486	0,2688			P52303	12,8799	D3ZZQ0	4,5763
P24155	Q8BPM2	0,2731			P53676	13,2436	Q924I2	4,7869
P24368	Q9Z2B9	0,2846			Q9JIX5	13,3438	F1M0N1	4,8958
P25113	Q810W7	0,2889			P14644	13,5722	P80386	4,9335
P26772	Q8VHF0	0,2983			Q9WUD9	13,7636	Q810W7	5,0443
P28075	O55099	0,3108			P80386	13,7673	P54645	5,0503
P29410	O08678	0,3261			O08815	13,8882	Q9JJ10	5,1618
P31044	P08413	0,3466			P54759	13,9325	F1LQC5	5,1726
P34058	P16879	0,3503			P80385	14,0964	D3ZMG0	5,2512
P34064	P09760	0,3539			Q68H95	14,5536	P80385	5,2577
P35213	O08679	0,4032			Q6TQE1	15,4695	F1LM93	5,5213
P35565	Q9R117	0,4267			Q64725	15,6545	P31325	5,7239
P37199	P11275	0,4588			Q62844	16,4681	F1LLY5	5,8771
P37285	Q3U214	0,4627			P46892	17,5497	P63086	5,9757
P37996	Q8VE70	0,5052			Q9R1Q2	19,6394	D4A7E4	6,4885
P38983	BOLT89	0,5093			Q63450	20,0855	D4AE19	7,2877
P40112	Q91ZN7	0,5445			Q6TMG5	21,0496	P21708-2	8,0439
P40307	O35942	0,5858			Q9QY78	21,1995	P54759	9,6970
P41498	Q8R4U9	0,6188			Q5RK09	21,3863	P35739	9,7766
P41562	Q63531	0,6326			P18484	22,7378	F1M7W0	9,9408
P42123	P05480	0,6626			P62944	23,0470	Q8R4U9	10,3352
P45592	Q8R4K2	0,6951			P84092	23,1050	F1M801	11,2750
P46462	Q3U3Q1	0,7618			Q1JU68	24,1540	P50297	11,3575
P47942	P18654	0,7819			Q6P9U8	24,5975	D3ZHL6	11,4904
P48004	P15127	0,7901			Q9ESW0	24,6805	F1M778	11,5145
P48500	O54748	0,8013			B5DFC8	25,2247	Q62862	12,8546
P48508	Q4KSH7	0,8878			Q6AYK8	25,4211	Q5XIF0	16,0433
P49088	Q01986	0,9870			Q4G061	25,4556	Q06486-2	18,4259
P50137	O35099	0,9972			Q641X8	26,1392		
P50398	P15791	1,0531			BOBNA7	28,4073		
P50399	Q66HA1	1,1004			Q7TT49	29,4974		
P52555	P00520	1,1072			Q63644	30,0000		
P52925	Q9QYR9	1,1253						
P54313	B2GUY1	1,1276						
P55053	A2AQW0	1,1313						
P56574	P35739	1,2089						
P60881	Q61083	1,2395						
P61459	Q62689	1,2867						
P61765	O88831	1,3034						
P61980	O55047	1,3222						
P61983	Q61084	1,3312						
P62083	P59241	1,6140						

P62161	D3ZML2	1,6447
P62260	Q62862	1,7684
P62744	Q8C050	1,7736
P62752	P54759	1,8365
P62815	P54763	1,8797
P62870	Q3U1V8	1,9782
P62898	O55173	2,0491
P62902	Q8K1R7	2,1077
P62963	Q9WU61	2,6252
P62994	P63017	3,0354
P63029	Q60629	3,5052
P63036	P50297	3,5284
P63039	Q4JIM5	3,6040
P63102	O35607	3,7123
P63159	P63168	3,7851
P63259	Q02974	4,0635
P63324	Q99ML2	4,5662
P68101	Q8C015	4,7651
P68255	Q8BK63	5,1482
P68511	Q8BTW9	5,8363
P81795	Q62925	6,2128
P82995	Q9JKY5	6,8749
P83868	Q29RW1	7,3977
P83941	P18266	7,7715
P84245	P22315	12,3765
P85968	Q9WTU6	17,9270
P85970		
P97852		
Q00981		
Q05982		
Q08163		
Q27W01		
Q2PQA9		
Q3KRD8		
Q3TIJ1		
Q4KM49		
Q4KM73		
Q5EGY4		
Q5FVL2		
Q5I034		
Q5I0G4		
Q5M7U6		
Q5M819		
Q5RJR2		
Q5RJR8		
Q5RKI1		
Q5SGE0		
Q5U300		
Q5XFX0		
Q5XHY5		
Q5XHZ0		
Q5XI73		
Q5XIA9		
Q5XIM9		
Q5XIT1		
Q62636		
Q62658		
Q62724		
Q63009		

Q63081
Q63396
Q63413
Q63524
Q63525
Q63584
Q63598
Q63610
Q63617
Q63945
Q64057
Q64270
Q64537
Q66HD0
Q66HD3
Q66HR2
Q66X93
Q68FQ0
Q68FR9
Q68FS4
Q68FU3
Q68FY0
Q68G31
Q6AXX6
Q6AY80
Q6AYK8
Q6DGG1
Q6MG08
Q6MG61
Q6P502
Q6P6V0
Q6P799
Q6P7B0
Q6P7Q4
Q6PCU2
Q6R556
Q6URK4
Q71UF4
Q794F9
Q7M0E3
Q7M767
Q7TPB1
Q8VHF5
Q920D2
Q920J4
Q924S5
Q99NA5
Q99PF5
Q9EPB1
Q9EQS0
Q9EQX9
Q9ER34
Q9JHB5
Q9JHW0
Q9JLZ1
Q9JMB5
Q9QUL6
Q9QXQ0
Q9R063

Q9WVK7
Q9Z0V6
Q9Z0W7
Q9Z1P2

Excel macro for the analysis of overlapping targets

```

Sub CALC_ALL()
'
' Remove duplicates from each of original max. of 10 col. and 5000 rows (Needed for displaying
the right overlap number)
'
    Sheets("Set1").Select
    Columns("A:A").Select
    ActiveSheet.Range("$A$1:$A$5000").RemoveDuplicates Columns:=1, Header:=xlNo
    Columns("B:B").Select
    ActiveSheet.Range("$B$1:$B$5000").RemoveDuplicates Columns:=1, Header:=xlNo
    Columns("C:C").Select
    ActiveSheet.Range("$C$1:$C$5000").RemoveDuplicates Columns:=1, Header:=xlNo
    Columns("D:D").Select
    ActiveSheet.Range("$D$1:$D$5000").RemoveDuplicates Columns:=1, Header:=xlNo
    Columns("E:E").Select
    ActiveSheet.Range("$E$1:$E$5000").RemoveDuplicates Columns:=1, Header:=xlNo
    Columns("F:F").Select
    ActiveSheet.Range("$F$1:$F$5000").RemoveDuplicates Columns:=1, Header:=xlNo
    Columns("G:G").Select
    ActiveSheet.Range("$G$1:$G$5000").RemoveDuplicates Columns:=1, Header:=xlNo
    Columns("H:H").Select
    ActiveSheet.Range("$H$1:$H$5000").RemoveDuplicates Columns:=1, Header:=xlNo
    Columns("I:I").Select
    ActiveSheet.Range("$I$1:$I$5000").RemoveDuplicates Columns:=1, Header:=xlNo
    Columns("J:J").Select
    ActiveSheet.Range("$J$1:$J$5000").RemoveDuplicates Columns:=1, Header:=xlNo
'
'.....
'Macro to copy columns of variable length'
'into 1 continuous column in a new sheet '
'Modified 17 Feb 2006 by Bernie Dietrick
'.....

Dim iLastcol As Long
Dim iLastRow As Long
Dim jLastrow As Long
Dim ColNdx As Long
Dim ws As Worksheet
Dim myRng As Range
Dim ExcludeBlanks As Boolean
Dim mycell As Range

ExcludeBlanks = (MsgBox("Exclude Blanks", vbYesNo) = vbYes)
Set ws = ActiveSheet
iLastcol = ws.Cells(1, ws.Columns.Count).End(xlToLeft).Column
On Error Resume Next

Application.DisplayAlerts = False
Worksheets("Calculation").Delete
Application.DisplayAlerts = True

Sheets.Add.Name = "Calculation"

For ColNdx = 1 To iLastcol

iLastRow = ws.Cells(ws.Rows.Count, ColNdx).End(xlUp).Row

Set myRng = ws.Range(ws.Cells(1, ColNdx), _
ws.Cells(iLastRow, ColNdx))

If ExcludeBlanks Then
For Each mycell In myRng
If mycell.Value <> "" Then
jLastrow = Sheets("Calculation").Cells(Rows.Count, 1) _
.End(xlUp).Row
mycell.Copy
Sheets("Calculation").Cells(jLastrow + 1, 1) _
.PasteSpecial xlPasteValues
End If
Next mycell
Else
myRng.Copy

```

```
jLastrow = Sheets("Calculation").Cells(Rows.Count, 1) _
.End(xlUp).Row
mycell.Copy
Sheets("Calculation").Cells(jLastrow + 1, 1) _
.PasteSpecial xlPasteValues
End If
Next

Sheets("Calculation").Rows("1:1").EntireRow.Delete

ws.Activate

With ActiveWorkbook.Sheets("Calculation").Tab
    .Color = 65535
    .TintAndShade = 0
End With

' Remove Duplicates from combined list

    Sheets("Calculation").Select
    ActiveSheet.Range("A:A").RemoveDuplicates Columns:=1, Header:=xlNo
    Sheets("Set1").Select

'
' Counts matching names for each of all lists
'

    Sheets("Calculation").Select
    Range("B1").Select
    ActiveCell.FormulaR1C1 = "=COUNTIF('Set1'!R1C[-1]:R5000C[-1],Calculation!RC1)"
    Range("B1").Select
    Selection.AutoFill Destination:=Range("B1:B5000"), Type:=xlFillDefault
    Range(Selection, Selection.End(xlDown)).Select
    Selection.AutoFill Destination:=Range("B1:K5000"), Type:=xlFillDefault
    Range("B1:K5000").Select
    Sheets("Set1").Select

'
' Calculates overlaps / The intersections of the different datasets
'

    Sheets("Calculation").Select
    Range("L1").Select
    ActiveCell.FormulaR1C1 = "=SUM(RC[-10]:RC[-1])"
    Range("L1").Select
    Selection.AutoFill Destination:=Range("L1:L5000"), Type:=xlFillDefault
    Range("L1:L5000").Select
    Sheets("Set1").Select

'
' Displays Overlapping Compounds
'

    Sheets("Calculation").Select
    Range("M1").Select
    ActiveCell.FormulaR1C1 = "=IF(RC[-11]>0,'CPD List'!R1C[-12],\"\")"
    Range("M1").Select
    Selection.AutoFill Destination:=Range("M1:M5000"), Type:=xlFillDefault
    Range("M1:M5000").Select
    Selection.AutoFill Destination:=Range("M1:V5000"), Type:=xlFillDefault
    Sheets("Set1").Select

'
' Copies and sorts by overlapping numbers
'

    Application.DisplayAlerts = False
    Worksheets("RESULT").Delete
    Application.DisplayAlerts = True

    Sheets.Add.Name = "RESULT"

    Sheets("Calculation").Select
```

```

Columns("A:V").Select
Selection.Copy
Sheets("RESULT").Select
Selection.PasteSpecial Paste:=xlPasteValues, Operation:=xlNone, SkipBlanks _
:=False, Transpose:=False
Application.CutCopyMode = False
ActiveWorkbook.Worksheets("RESULT").Sort.SortFields.Clear
ActiveWorkbook.Worksheets("RESULT").Sort.SortFields.Add Key:=Range("L1:L5000") _
, SortOn:=xlSortOnValues, Order:=xlDescending, DataOption:=xlSortNormal
With ActiveWorkbook.Worksheets("RESULT").Sort
.SetRange Range("A1:V5000")
.Header = xlGuess
.MatchCase = False
.Orientation = xlTopToBottom
.SortMethod = xlPinYin
.Apply
End With
Sheets("RESULT").Select
Columns("L:L").Select
Selection.FormatConditions.Add Type:=xlCellValue, Operator:=xlBetween, _
Formula1:="=5", Formula2:="=10"
Selection.FormatConditions(Selection.FormatConditions.Count).SetFirstPriority
With Selection.FormatConditions(1).Font
.Color = -16383844
.TintAndShade = 0
End With
With Selection.FormatConditions(1).Interior
.PatternColorIndex = xlAutomatic
.Color = 13551615
.TintAndShade = 0
End With
Selection.FormatConditions(1).StopIfTrue = False
Selection.FormatConditions.Add Type:=xlCellValue, Operator:=xlBetween, _
Formula1:="=2", Formula2:="=4"
Selection.FormatConditions(Selection.FormatConditions.Count).SetFirstPriority
With Selection.FormatConditions(1).Font
.Color = -16751204
.TintAndShade = 0
End With
With Selection.FormatConditions(1).Interior
.PatternColorIndex = xlAutomatic
.Color = 10284031
.TintAndShade = 0
End With
Selection.FormatConditions(1).StopIfTrue = False
Sheets("RESULT").Select
With ActiveWorkbook.Sheets("RESULT").Tab
.Color = 5287936
.TintAndShade = 0
End With
Sheets("Set1").Select

'
' Inserts headers + "Overlap %"
'

Sheets("RESULT").Select
Rows("1:1").Select
Selection.Insert Shift:=xlDown, CopyOrigin:=xlFormatFromLeftOrAbove
Range("A1").Select
ActiveCell.FormulaR1C1 = "ID"
Range("B1:K1").Select
With Selection
.HorizontalAlignment = xlCenter
.VerticalAlignment = xlBottom
.WrapText = False
.Orientation = 0
.AddIndent = False
.IndentLevel = 0
.ShrinkToFit = False
.ReadingOrder = xlContext
.MergeCells = False
End With
Selection.Merge
ActiveCell.FormulaR1C1 = "Matching Ids"
Range("L1").Select
ActiveCell.FormulaR1C1 = "Overlaps"

```

```
Range("M1").Select
ActiveCell.FormulaR1C1 = "'CPD List'!RC[-12]"
Range("M1").Select
Selection.AutoFill Destination:=Range("M1:V1"), Type:=xlFillDefault
Range("M1:V1").Select
Columns("A:W").EntireColumn.AutoFit
Rows("1:1").Select
Selection.Font.Bold = True
With Selection
    .HorizontalAlignment = xlCenter
    .VerticalAlignment = xlBottom
    .WrapText = False
    .Orientation = 0
    .AddIndent = False
    .IndentLevel = 0
    .ShrinkToFit = False
    .ReadingOrder = xlContext
End With

Columns("L:L").Select
With Selection
    .HorizontalAlignment = xlCenter
    .VerticalAlignment = xlCenter
    .WrapText = False
    .Orientation = 0
    .AddIndent = False
    .IndentLevel = 0
    .ShrinkToFit = False
    .ReadingOrder = xlContext
    .MergeCells = False
End With
Selection.Font.Bold = True
Range("W1").Select

Range("W1").Select
ActiveCell.FormulaR1C1 = "% Overlap"
Range("W2").Select
ActiveCell.FormulaR1C1 = "=RC[-11]/'CPD List'!R3C1"
Range("W2").Select
Selection.Style = "Percent"
Range("W1").Select
Selection.AutoFilter
Range("W2").Select
Selection.AutoFill Destination:=Range("W2:W5000"), Type:=xlFillDefault

End Sub
```